The Interaction of Transforming Growth Factor Beta and Pro-inflammatory signalling in Peritoneal Fibrosis

Tanya Jayne Bodenham

Thesis presented for degree of Philosophiae Doctor

2015

Institute of Molecular of Molecular and Experimental Medicine
Institute of Nephrology
School of medicine
Cardiff University
Heath Park
CF14 4XN

Dedication

In loving memory of my dear Granny, Jean Short who sadly passed away during the amendment process of this thesis. Thank you for your love and support throughout this thesis. You are always in my thoughts.

Acknowledgments

I would first like to thank the Sir Jules Thorn charitable trust for providing me with the resources to undertake my PhD and make this project possible. It was a wonderful opportunity and I am ever grateful for the experience that was provided.

I would like to express my appreciation to my supervisor Dr Donald Fraser, who has been exceptionally patient and supportive throughout my PhD even when I have struggled with the writing of this thesis! I am indebted to his support and supervision and am extremely grateful to have had such a fabulous supervisor.

My family have always supported me throughout my education and life in general. I am ever indebted to them for continuing to support me through this project. Thank you for the wise words Gramp "no one can take your education away from you."

To the Institute of Nephrology past and present you made the three years of my PhD so enjoyable. The help and advice and the banter I will always remember and be thankful for. Many thanks to Dr Bob Steadman, Dr Soma Meeran, Dr Aled Philips and Dr Tim Bowen for the help and advice along the way. I am extremely grateful to the talented Dr John Martin who has supported and guided me through various scientific techniques and provided so much help and advice thank you! Many thanks to Dr Adam Midgely and Dr Cristina Beltrami for their constant friendship and support for the duration of my PhD. Thank you to Emma Woods and Melisa Lopez-Anton for always brightening my day during the last 18 months of my PhD, I have made some true friends. A huge thank you to Kim Abberley and Cheryl Ward for their support and assistance and for making me smile every day, you keep the institute of nephrology running smoothly. Many thanks to Dr Alexa Wonnacott, Chantal Colman, Dr Chris Carrington, Dr Usman Khalid, Dr Ruth MacKenzie, Dr Kate Rodgers and Dr Robert Jenkins.

Last but by no means least I would like to say thank you to my fiancé Daniel Court. Thank you for supporting me for the three years and the writing up period, giving me a nudge when my progress was slow. You have always encouraged me and helped me persevere throughout this project and made sure I didn't "overwork" myself. Thank you so much and here's to a bright future!

Thesis Summary

Peritoneal fibrosis is a significant problem for peritoneal dialysis patients resulting in a loss in membrane dialysing capacity ultimately leading to technique failure. The development of peritoneal fibrosis is attributed to recurrent peritonitis infections and bio-incompatible dialysate fluid, both of which contribute to a chronic inflammatory state within the peritoneum. Transforming growth factor beta 1 (TGF-β1) is a cytokine with a central role in peritoneal fibrosis. However, this cytokine has multiple key roles, including development, wound healing cell proliferation and differentiation and regulation of the immune response. Cellular response to TGF- β1 can vary depending on cellular context and phenotype. Factors governing responses to TGF-β1 within the peritoneum are poorly characterised. Previous research through a murine model representing inflammation driven fibrosis has identified Interferon gamma (IFN-γ) having a central role in inflammation driven fibrosis. Therefore examination of the interaction between TGF-β1 and IFN-γ were undertaken in both murine samples and primary human peritoneal cells (HPMC).

Within the SES murine model differences in TGF-β1 responses were observed between WT and IL6KO mice, with WT mice displaying significant increase in expression of TGF-β1 and matrix genes. There was increased expression of matrix metalloproteinases 3 and 10 (MMP3 and MMP10) in IL6KO mice, suggesting that these mice are protected against scarring and fibrosis through enhanced tissue remodelling. Similar findings were observed in HPMC treated with TGF-β1 alone resulting in significant increased MMP3 expression, which was inhibited in the presence of IFN-γ. IFN-γ did not affect any other TGF-β1 induced responses thus suggesting a specific fibrotic effect of IFN-γ within this system by inhibiting matrix degradation.

Analysis of the mechanism of MMP3 regulation by TGF-β1 and IFN-γ revealed that SMAD and MAPK pathways are involved in the induction of MMP3 by TGF-β1 and are not inhibited by IFN-γ. Analysis of the AP-1 promoter site in the MMP3 revealed that this site may be involved in basal MMP3 expression but is not modulated by TGF-β1 and IFN-γ. Further examination of MMP3 regulation may provide a potential target in helping protect against peritoneal fibrosis, thus helping reduce technique failure in peritoneal dialysis.

Publications and Presentations arising from this thesis

Publications

Bodenham T, Topley N and Fraser D (2012) Peritoneal fibrosis is mouse strain dependent. *Nephrology Dialysis Transplant* pp1-3

Presentations

Bodenham T, Topley N, Fielding C and Fraser D, Developing *in vitro* and *in vivo* models to study Transforming growth factor beta 1 and pro-inflammatory signalling in peritoneal fibrosis. 1st Inaugural South West Regional Regenerative Medicine Meeting, Bristol, UK, 2011 (Poster runner up prize awarded)

Bodenham T, Topley N, Fielding C and Fraser D, Developing *in vitro* and *in vivo* models to study Transforming growth factor beta 1 and pro-inflammatory signalling in peritoneal fibrosis. 26th Annual Life Sciences Post Graduate Research Day, Cardiff, UK, 2011 (Poster)

Bodenham T, Topley N, Fielding C and Fraser D, Regulation of matrix metalloproteinase 3 expression by Transforming Growth Factor Beta 1 and Interferon Gamma I human peritoneal mesothelial cells. 2nd Inaugural South West Regional Regenerative Medicine Meeting, Bristol, UK, 2012 (Oral 1st prize awarded)

Bodenham T, Topley N, Fielding C and Fraser D, Regulation of matrix metalloproteinase 3 expression by Transforming Growth Factor Beta 1 and Interferon Gamma I human peritoneal mesothelial cells. 27th Annual Life Sciences Post Graduate Research Day, Cardiff, UK, 2012 (Oral 3rd prize awarded)

Bodenham T, Topley N, Fielding C, Bowen T and Fraser D, Interferon gamma alters mesothelial cell response to Transforming growth factor beta 1, promoting peritoneal fibrosis. Renal Association 2013 (Poster)

Bodenham T, Topley N, Fielding C, Bowen T and Fraser D, The role of pro-inflammatory signalling in peritoneal fibrosis. Peritoneal Dialysis Research Day Sheffield, 2013 (Oral)

Table of Contents

Glossary of Abbreviations

ALK	Activin-receptor-like-kinase
AP-1	Activator protein 1
APD	Automated peritoneal dialysis
αSMA	Alpha smooth muscle actin
BM	Basement membrane
BMP	Bone morphogenetic protein
CAPD	Continuous ambulatory peritoneal dialysis
CKD	Chronic Kidney Disease
Col1a1	Collagen type 1 alpha 1
Col1a2	Collagen type 1 alpha 2
CTGF	Connective tissue growth factor
DNA	Deoxribose nucleic acid
ECM	Extracellular matrix
EMT	Epithelial-mesenchymal transition
EPS	Encapsulating peritoneal sclerosis
EPSA	Effective peritoneal surface
ESRD	End stage renal disease
GRF	Glomerular filtration rate
HA	Hyaluronic acid/ hyaluronan
HAS	Hyaluronan synthase
HPMC	Human peritoneal mesothelial cells
ICAM-1	Intracellular adhesion molecule-1
IFN-γ	Interferon gamma
IL1β	Interleukin 1 beta

IL6	Interleukin 6
JAK	Janus kinase
LAP	Latency associated peptide
MAPK	Mitogen activated protein kinase
MCP-1	Monocyte chemoattractant protein 1
MMP	Matrix metalloproteinases
PAI-1	Plasminogen activator inhibitor protein 1
PCR	Polymerase chain reaction
PD	Peritoneal dialysis
PDF	Peritoneal dialysis fluid
PDGF	Platelet derived growth factor
SIS3	Specific inhibitor of Smad 3
SMC	Submesothelial compact zone
STAT	Signal transducer and activators of transcription
TGF-β1	Transforming growth factor beta 1
TIMP	Tissue inhibitor of metalloproteinases
TNF-α	Tumour necrosis factor alpha
UFF	Ultrafiltration failure
VEGF	Vascular endothelial growth factor
ZBP-89	Zinc binding protein 8

Chapter 1: General Introduction

1.1 Chronic Kidney disease and End Stage Renal Disease

Chronic kidney disease (CKD) is the term used to describe heterogenous disorders that affect the structural and functional capacity of the kidney. The National Kidney Foundation (NKF) defines CKD by a reduction in glomerular filtration rate (GFR) (<60ml/min per 1.73 m^2) for a sustained period of time (≥ 3 months) or by the presence of kidney damage[1]. The prevalence of CKD is increasing globally and varies between countries. In the UK CKD prevalence is estimated at 4.3-6.76%, compared to 13.1% in the USA[2-4]. CKD is associated with old age, hypertension, diabetes, smoking, obesity and cardiovascular disease[5-7]. Therefore with an ever increasing aging population and an obesity epidemic further increases in CKD prevalence are predicted, potentially having a significant impact on health and economic costs.

The NKF's Kidney Disease Outcomes Quality Initiative has classified CKD into five stages. These stages are based on the patient's Glomerular Filtration Rate (GFR), indicative of the extent to which excretory function of the kidneys is preserved. Unfortunately CKD is generally asymptomatic until the disease has advanced and therefore many patients are diagnosed in the later stages of CKD such as the onset of End stage renal disease (ESRD). ESRD is defined as stage V of CKD with a GFR of <15/min per 1.73 m^2, indicative of kidney failure and irreversible damage[1]. Stage V CKD is the point at which renal replacement therapy with haemodialysis, peritoneal dialysis or kidney transplantation is considered likely to be necessary. In some patients, typically of advanced age and with multiple other illnesses and/or frailty, non-dialytic (conservative) management may be deemed more appropriate.

1.2 Peritoneal dialysis

1.2.1 Background

Peritoneal dialysis (PD) is an established form of renal replacement therapy used in the management of end stage renal disease (ESRD). The establishment of PD as a renal replacement therapy has taken many years of research. In 1959 a technique employing “intermittent dialysis” of the peritoneal cavity was developed by Maxwell and colleagues, which involved the use of commercially prepared PD solution and a catheter within a “closed system of infusion and drainage”[8]. Five years later in 1964 Fred Boen described two patients treated with the first automatic cycling PD machine, reporting a long-term survival of 2 years[9]. The popularity of PD as a form of renal replacement therapy increased with the development of continuous ambulatory peritoneal dialysis (CAPD) by Popovich and Moncrief and the development of continuous cyclical PD, a form of automated peritoneal dialysis (APD) in 1981[10, 11].

1.2.2 The Technique

In the UK patients are offered the choice between Haemodialysis or PD therapy in the form of CAPD or APD when commencing renal replacement therapy. CAPD involves manual exchange of dialysis fluid. Patients or carers perform 4-5 exchanges daily. APD is a general term used to describe the forms of PD that use a mechanical device for dialysis. Forms of APD include: continuous cyclical PD, nightly intermittent PD, intermittent PD and tidal PD[12].

To commence PD therapy, a catheter is inserted into the peritoneal cavity, this is achieved by different techniques such as open surgery or laparoscopic technique[13]. Following successful placement of the catheter dialysis can be initiated straight away. PD fluid is instilled into the cavity and allowed to dwell for variable periods of time before subsequent removal. Generally PD fluids consist of glucose, lactate or bicarbonate, potassium, sodium and calcium[14]. The glucose within the PD fluid generates an osmotic gradient that enables water to be removed from the patient through transportation across the peritoneal membrane into the dialysate. Other solutes within the patient such as urea diffuse from the blood into the dialysate down a concentration gradient, again resulting in subsequent removal. Changing the volume of dialysate used and the glucose concentration and dwell time can enhance solute and water removal respectively[15].

PD is perceived to provide many advantages for the patients such as increased independence and mobility. The technique is simple to teach, enabling patients to be dialysed at home[13]. Rubin *et al,* (2004) reported that patients receiving peritoneal dialysis were more satisfied with their level of care and rated their level of care higher than those patients receiving haemodialysis[16]. This therapy has become a viable alternative to haemodialysis, with the number of patients using PD increasing progressively worldwide[17]. Currently in the UK 20% of patients starting dialysis use PD as the first choice of renal replacement therapy[15].

1.2.3 Limitations of PD therapy

PD therapy relies on the integrity of the patient's peritoneal membrane structure and functionality. Studies have shown that long term PD is associated with

morphological changes to the membrane such as thickening of the submesothelial compact zone, which compromise the functional efficiency of the peritoneum[18]. This leads to a loss of ultrafiltration and development of fibrosis. These changes are linked to bioincompatible dialysis solution components (pH and glucose) and peritonitis infections.

1.3 The Peritoneum

1.3.1 Anatomy

The peritoneal cavity is the largest cavity within the body, comprising a surface area of approximately $1.7m^2$ [19, 20]. The peritoneal cavity was first described in 3000 B.C. in Ebers papyrus as a "definitely outlined cavity in which the viscera are somehow suspended". The peritoneum is a complex serous membrane that forms a closed sac within males, however in females the peritoneum consists of an open sac due to the free ends of uterine tubes, which open directly into the peritoneal cavity[21].

The structure of the peritoneum is composed of two separate continuous layers; the parietal and visceral peritoneum. The parietal peritoneum is the layer that lines the abdominal wall and pelvic cavity, whereas the visceral peritoneum is a continuation of the parietal layer that covers the viscera and abdominal organs. The space between these two layers is referred to as the peritoneal cavity, which can also be subdivided into two regions, the greater sac that forms the largest region and the lesser sac. As well as this subdivision the peritoneal cavity can also be compartmentalised into interconnecting spaces, thus dividing the peritoneal cavity into the supramesocolic and inframesocolic spaces and the pelvic cavity[22].

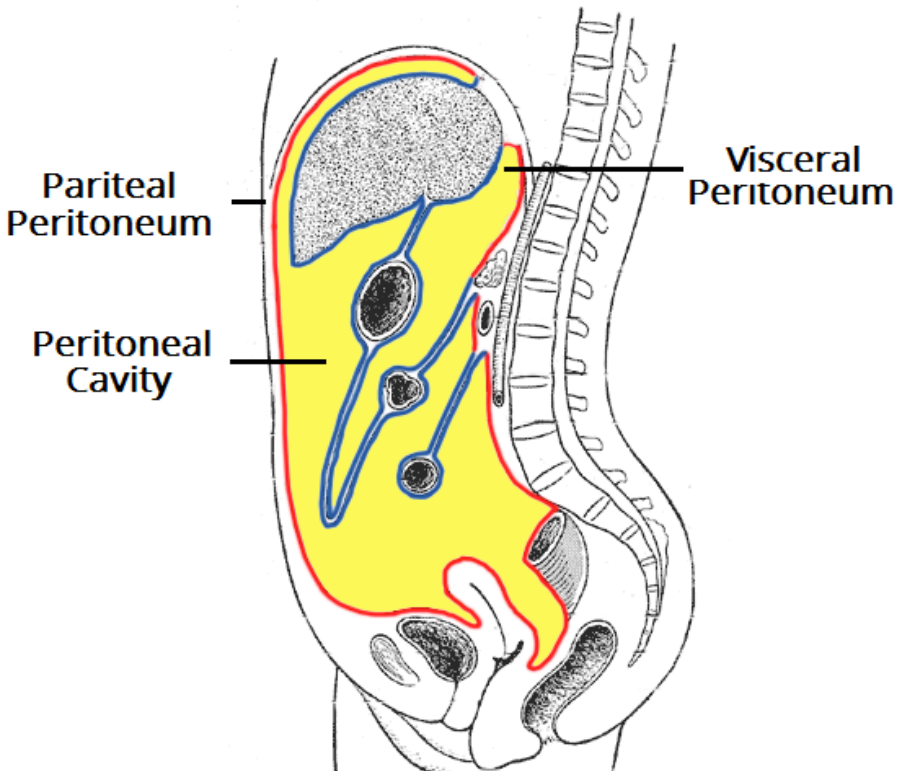

Figure 1.1 Schematic diagram of the peritoneal cavity sagittal section

The peritoneum is composed of two layers the parietal peritoneum (shown in red), which covers the abdominal wall and pelvic cavity and the visceral peritoneum (shown in blue) that covers the abdominal organs. The peritoneal cavity is the space between the parietal and visceral peritoneal layers (image taken from teachmeanatomy.info).

1.3.2 The peritoneal membrane

The peritoneal membrane acts as a dialyzing organ enabling the exchange of solutes between the peritoneal blood vessels and the peritoneal cavity. Before the late 19th

century the structure and function of the peritoneum was not well known. It was von Recklinghausen's work in the 1860's that provided the first histological description of the peritoneal membrane using silver nitrate reactions, which revealed that a membrane consisting of "thin flattened cells" lined the peritoneal cavity[23].

The peritoneal membrane is composed of two distinct layers: 1) a monolayer of epithelial-like cells known as the mesothelium, which under optimum conditions possess microvilli that increases their surface area and 2) an underlying layer of connective tissue known as the submesothelial compact zone. These two layers are separated by a discontinuous basement membrane (BM), which supports the mesothelium[24]. The mesothelium layer covers both the parietal and visceral peritoneal membrane and is made up of a single cell type known as mesothelial cells (MC)[25]. The MC lie on the BM, which is a thin laminar network that is composed mainly of type IV collagen but also consists of proteoglycans and laminin[26]. The BM appears to have two key functions; the first acting as a selective cellular barrier, allowing the movement of macrophages but preventing fibroblast trafficking, the second as a regulator of mesothelium regeneration following injury[24].

Beneath the BM lies the submesothelial compact zone. This region is highly vascularised, composed of various extracellular matrix (ECM) proteins, which include: collagen I, collagen III, fibronectin, laminin, elastin and hyaluronic acid as well as a cellular population of fibroblasts and intermittent macrophages[27, 28]. The submesothelial compact zone has a key function in regulating the trafficking of

cells and macromolecules across the peritoneal membrane. Proteoglycans within the ECM form gels containing pores of various sizes and charge density, thus regulating the movement of molecules by their size and charge[24].

1.3.3 The mesothelial cell layer

The mesothelium is a monolayer composed of a specialised singular population of cells known as mesothelial cells. Mesothelial cells were first described by Bichat in 1827, who observed that a single layer of cells lined the serous cavities. Bichat referred to this layer as the "epithelial lining of the mammalian mesodermic cavities" and subsequently in 1880 Minot termed it "the mesothelium"[29-31]. Mesothelial cells cover the three serosal cavities, which includes the peritoneal cavity. Studies have shown that the mesothelium in different anatomical sites and species does not differ in morphology and is considered "essentially similar"[32-34].

Approximately $1x10^9$ mesothelial cells, each with a diameter of 25μm covers the visceral and parietal surfaces within the peritoneum[24, 35]. These cells appear flattened and squamous, which makes the mesothelium have a cobble-stone appearance. The internal structure of these cells consists of a cytoplasm that is raised over a round nucleus. The organelles within the cell are located in the centre close to the nucleus. These consist of; a few mitochondria, poorly developed Golgi apparatus and little rough endoplasmic reticulum as well as microtubules and microfilaments[30, 36]. On the luminal surface of these cells is a well-developed microvillous border, which increases the functional surface area of the cells. The

number of microvilli present on the surface of these cells is changeable, depending on different physiological conditions[35, 37-39].

Mesothelial cells are often described as “epithelial-like cells” and do possess various epithelial characteristics such as their squamous shape and the expression of cytokeratin filaments 8 and 18[35, 40]. These cells also express E, N and P-cadherins, with N-cadherin being the dominant form[36]. However they are generated from mesodermal tissue during day 8-18 of gestation and express the mesenchymal markers vimentin and desmin[30, 41]. The mesothelial layer is a slow renewing tissue due to only a small percentage of cells (0.16-0.5%) undergoing mitosis at any time. The mitotic activity however can be increased following particular stimulation. Another feature that distinguishes these cells from typical epithelial cells is the repair process. Normally in epithelial cells healing occurs at the wound edges alone, whereas in mesothelial cells healing occurs diffusely across the injured surface[30].

1.3.4 Functions of the mesothelial layer

The mesothelial layer has various functions within the peritoneum. Initially it was believed that the primary function of the mesothelium was as a protective barrier, protecting against abrasion and invading microbes[30]. Mesothelial cells secrete surfactant glycosaminoglycans, which consist predominantly of hyaluronic acid and phosphatidylcholine[42, 43]. The secretion of phosphatidylcholine in particular is shown to lubricate the surface of the mesothelium lining the parietal and visceral

peritoneum and protecting against adhesion formation[44]. This secretion causes the mesothelial layer to become non-adhesive and is reported to protect against infection and adhesion formation, but may also be important in differentiation[45]. Along with this protective role, the mesothelial layer is involved in transport and movement of fluid and particulate matter across the peritoneal cavity. This can be via active transport through pinocytic vesicles, or through intracellular junctions and stomata although there is conflicting evidence concerning this method of transport[46-48].

Other functions of the mesothelium include roles in inflammation, host defence and antigen presentation. In the absence of antigen presenting cells, peritoneal mesothelial cells stimulated with IFN-γ induce $CD4^+$ Th cell proliferation[49]. Mesothelial cells also express the adhesion molecule ICAM-1, which is important in leukocyte recruitment[50]. In contrast to these defensive roles, the mesothelial layer promotes tumour growth and adhesion. Studies have shown that "traumatised mesothelial surfaces are privileged sites for tumour cell adhesion"[30, 51]. This may be due to inflammation stimulating an upregulation of adhesion molecules on mesothelial cell surface, thus facilitating anchorage of tumour cells[52]. Mesothelial cells also produce an array of growth factors, which may also promote tumour growth[36]. Other studies however, have shown that intact hyaluronic acid that covers the mesothelial cells, prevents adhesion of tumour cells to the mesothelium. This has been shown *in vitro* where treatment of cultured mesothelial cells with hyaluronidases resulted in increased adhesion[53].

1.4 Peritoneal Fibrosis: Functional changes to the membrane

1.4.1 Fibrosis

Fibrosis is a pathological process that results in scarring and loss of function within multiple organs and tissues including the peritoneum. This process is described as an "uncontrollable wound healing response"[54, 55]. The increased deposition of ECM components, which include fibronectin and collagen leads to scar formation and tissue dysfunction[56].

Fibrosis within the peritoneum of PD patients results in technique failure. The causes of peritoneal fibrosis are numerous: peritonitis, bioincompatible dialysate fluids, chronic inflammation and uremia[57-59]. The morphological changes that occur in the peritoneal membrane result in a loss of dialysing function and are a major problem for PD patients. In a small number of cases some patients develop an aggressive fibrotic response with severe alterations to the peritoneum, known as encapsulating peritoneal sclerosis[60].

1.4.2 Encapsulating peritoneal sclerosis

Encapsulating peritoneal sclerosis (EPS) is a rare but very serious complication of PD and can cause considerable morbidity and mortality. Mortality rates vary between studies from 42% up to 100%[61, 62] although the prevalence of this condition remains low within the PD population, ranging between 0.7% - 3.3%[63, 64]. EPS is an aggressive fibrotic condition, characterised by progressive thickening and sclerosis of the peritoneum with persistent, intermittent or recurrent intestinal obstruction in the presence or absence of inflammation[65]. The vast fibrosis of the

peritoneum leads to encapsulation of the bowel, which causes an impairment in gut motility. This leads to symptoms of nausea, vomiting, pain, bloating, diarrhoea, anorexia, weight loss and malnutrition[66].

Laparotomy provides the only method to make a definite diagnosis of EPS, however this is not frequently used due to risk of morbidity and mortality. Instead a combination of clinical features described above and radiological examinations are used to diagnose patients with EPS[67, 68]. Screening for EPS still remains elusive, with no consistent biochemical or radiological markers evident[69, 70]. Thus it remains difficult to diagnose this condition in the asymptomatic stage.

Some reports have suggested monitoring changes in the morphology of the peritoneal membrane and membrane efficiency[71]. However, this may not be effective as changes to the membrane are present within a significant proportion of patients on long term PD that do not develop EPS[72]. This has led to some researchers hypothesising that EPS may be part of a spectrum of peritoneal fibrosis, that in certain individuals an abnormal fibrotic response occurs to the stimuli present within all PD patients, resulting in EPS[73]. This suggests that potentially genetic variability may account for development of EPS in certain individuals[74].

The risk factors associated with causing EPS are multifactorial. There is a proposed "two-hit" theory that suggests the need for two factors in the development of EPS. This includes a predisposing factor such as disruption to normal peritoneal physiology as observed in long term PD patients, which makes the individual prone

to a second hit/initiation factor that initiates EPS. This initiation factor could include a peritonitis episode[60, 75]. The “two-hit” hypothesis supports evidence that PD duration is a validated risk factor for EPS as increased time on PD leads to greater deterioration in peritoneal membrane function in a significant proportion of PD patients. Various studies have shown an increased incidence of EPS with increased time on PD[76, 77], with one Australian study reporting an incidence of 19.4% in patients receiving PD therapy for 8 years[63].

Other potential factors include age of patient when commencing PD therapies, with studies reporting a greater incidence of EPS in younger patients[78, 79]. Inflammation through peritonitis infections may also be a potential trigger for EPS, with some studies finding an association between frequency of peritonitis episodes and the development of EPS[80, 81]. This has not been found in other studies however, and some PD patients develop EPS without experiencing a peritonitis episode[64, 78, 82].

Functional changes associated with peritoneal membrane failure such as increased solute transporter status and ultafiltration failure (UFF) are key changes observed in a significant proportion of patients on long-term PD therapy and in EPS sufferers[57]. High solute transporter status may be a risk factor for EPS with one study reporting a significant difference in EPS development in high transporter status patients[83]. Other studies have reported no difference in transport or UFF between non-EPS and EPS patients[84]. This is also supported by data showing that low transporter status PD patients can develop EPS[68]. These functional and morphological changes are

important in both EPS and non-EPS PD patients and are key in understanding the fibrotic process in the peritoneum.

1.4.3 Peritoneal membrane failure

During PD therapy solutes and fluids are exchanged between the peritoneal blood vessels and cavity across the peritoneal membrane through various pores via diffusion and convection[85, 86]. Dialysate fluid is perfused into the peritoneal cavity generating an osmotic gradient across the peritoneal membrane. Contact with the dialysate fluid and peritoneal membrane enables solute and fluid transport[14, 87]. Diffusion occurs in a bidirectional manner, depending on the concentration gradient. The main barrier to peritoneal transport is the interstitial capillaries, which lie beneath the mesothelial layer[88]. Transport across any membrane is dependent on surface area and permeability[89]. During PD only the areas of the peritoneal membrane exposed to dialysate solution are involved in the exchange of fluids and solutes. This is deemed the effective peritoneal surface area (EPSA)[87]. The number of capillaries and the number of vessels perfused affect EPSA. This can be altered by dialysis and various pathologies.

1.4.4 Solute transport

Peritoneal membrane failure is a term used to describe changes to the characteristics of the membrane that results in functional impairment of peritoneal solute and fluid transport across the membrane. This is evident by increased solute

transport and ultrafiltration failure[86]. It is a serious problem for PD patient causing an increase in morbidity and mortality, with approximately 50% of PD patients experiencing a progressive loss in membrane function within five years, resulting in technique failure[90].

Peritoneal membrane function is assessed using the peritoneal equilibration test (PET), which measures net ultrafiltration along with low molecular weigh solute transport[91]. Solute transport is determined through a dialysate/plasma creatinine ratio measured at the end of a four-hour dwell. This ratio enables patients to be classified on transporter status into four groups: low, low average, high average and high[86]. High transporters usually absorb glucose rapidly resulting in a loss of the osmotic gradient leading to reabsorption of fluid[92]. Studies have shown that patients with high transporter status are associated with poorer prognosis, with increased hospitalisation, mortality and increased technique failure[93-96]. Various studies have examined factors that may influence transporter status, such as gender, body mass, age and body surface area, with some modest effects reported[97-99].

Solute transport is also reported to increase with time on PD within a certain proportion of patients[100, 101]. Research suggests that the increase in solute transport relates to expansion of the EPSA through angiogenesis[102]. The expanded EPSA results in enhanced small solute transport due to changes in permeability and vessel wall thickening, which impairs the exchange of waste products[103]. In addition the increased vasculature decreases the osmotic pressure generated by the glucose within the PDF leading to ultrafiltration failure[104].

1.4.5 Angiogenesis and ultrafiltration failure

Angiogenesis is the process of blood vessel formation from existing vasculature[105]. Patients on long term PD display morphological evidence of increased angiogenic activity within the peritoneum including, increased vasculature and formation of vascular lesions along with increased production of the angiogenic cytokine vascular endothelial growth factor (VEGF)[18, 106, 107]. Angiogenesis within the peritoneum is strongly associated with peritoneal membrane function and hence ultrafiltration failure. Time on glucose based dialysate fluids is associated with increased VEGF production and ultrafiltration failure, along with an association between VEGF levels and solute transport[108, 109]. Margetts et al (2002) demonstrated in rats that inhibition of angiogenesis was more effective at preserving ultrafiltration and membrane function, then inhibition of the fibrotic cytokine transforming growth factor beta[110].

Ultrafiltration failure (UFF) is a common cause of technique failure in PD patients. The definition of UFF varies amongst studies, some use the PET to define UFF as a net ultrafiltration of less than 100ml after 4 hours using a 2.27% glucose solution[111]. Other studies define UFF as an inability to remain at a stable dry weight and retain fluid balance as well as the number of hypertonic bags used by the patient[112].

UFF is mainly associated with long term PD therapy, with one study reporting an incidence of 3% in the first year of PD therapy dramatically increasing to 31% in

patients receiving PD for more than 6 years[113]. The causes of UFF are attributed to an increase in solute transport and enhanced angiogenesis[114]. UFF is also linked to inflammation with IL6 levels alongside VEGF in plasma and dialysate samples correlating with impaired membrane function[109]. Following recurrent episodes of peritonitis ultrafiltration loss was accelerated compared to peritonitis free patients, with the authors of the study concluding that the degree of ultrafiltration failure was proportional to the amount of inflammation and number of infections[101].

1.5 The effects of peritoneal fibrosis on the morphology of the peritoneum

1.5.1 Overview

During PD therapy, the peritoneum is routinely exposed to components within the dialysate fluid and potentially peritonitis infections that lead to inflammation and fibrosis. The functional deterioration of the membrane as mentioned above is linked to the morphological changes that occur within it[115]. Fibrotic changes of the peritoneum are common in biopsies taken from PD patients and various studies have provided evidence linking the morphological changes that occur during PD treatment to functional impairment[86, 116, 117]. These changes include increased thickness of the submesothelial compact zone, myofibroblast presence, phenotypic changes to the mesothelial layer, loss of mesothelial layer, reduplication of capillary basement membrane and increased angiogenesis and vasculopathy[118].

1.5.2 Increase in the submesothelial compact zone thickness

A common feature of interstitial fibrosis in PD patients is increased thickness of the submesothelial compact zone (SMC). This occurs through excessive deposition of ECM components including laminin and collagen. In the largest PD biopsy study Williams et al (2002) collected 130 biopsies from PD patients and compared them to control, haemodialysis and uremic patients. The results showed an increase in thickness of the SMC in PD patients that was significantly associated with time on PD, from 50μm in control to 700μm in PD samples that had undergone therapy for over 8 years[18]. PD patients displaying functional changes such as membrane failure were found to have significantly thicker SMC. This was supported by a study that found increase in SMC was associated with increased solute transport, again linking peritoneal fibrosis with membrane failure[119]. Furthermore, research indicates that changes to the SMC correlate with loss of the mesothelial layer, potentially as a result of local ischemia[18].

1.5.3 Changes to the mesothelial layer

The mesothelium was originally reported to be a passive monolayer, however further research revealed that these cells have key roles in regulating the homeostasis of the peritoneum, including the fibrotic response. The loss of the mesothelial layer is frequently observed in fibrotic PD patients[18]. *In vivo* and *in vitro* studies have shown that exposure of mesothelial cells to fibrotic agents such as transforming growth factor beta 1 or glucose components within the dialysate fluid as well as inducing fibrosis also causes mesothelial damage and loss[120-122].

There is also evidence that suggests mesothelial cells actively contribute to the fibrotic response. During PD the mesothelium is exposed to various stimuli within the dialysate and through local inflammation. *In vitro* studies of HPMC exposed to glucose, a key component in conventional dialysate fluid, show increased production of fibrotic cytokines and ECM proteins such as fibronectin[123, 124]. This was also the case when HPMC were exposed to inflammatory cytokines, thus emphasising the contribution of HPMC to peritoneal injury and fibrosis[125, 126].

Fibrosis is characterised by the presence of myofibroblast cells and mesothelial cells appear to have a central involvement in this fibrotic process. The mesothelium has a central role in controlling the inflammatory response within the peritoneum, with cells able to release vasoactive prostaglandins and chemokines such as interleukin-8 (IL-8) and monocyte chemoattractant protein 1 (MCP-1)[127, 128]. This enables the recruitment of inflammatory cells to the peritoneum, which then through the release of further cytokines can activate resident fibroblasts within the peritoneum to undergo differentiation to myofibroblasts[129, 130]. In combination with this, studies show that during PD therapy mesothelial cells undergo phenotypic changes including a decrease in the expression of the cell surface protein E-cadherin and increase in αSMA and the development of a more migratory phenotype[131, 132]. This results in a transformation of the mesothelial cell to a myofibroblast.

1.5.4 Presence of myofibroblasts within the peritoneum

Myofibroblasts are activated fibroblast cells characterised by the expression of alpha smooth muscle actin (αSMA)[133]. Within all contexts of wound healing and

fibrosis, the myofibroblast is shown to have a central role, producing collagen and aiding in wound contraction[54]. In normal peritoneum tissue there is a resident fibroblast population but an absence of myofibroblasts[134]. In PD patients myofibroblasts are detected in the early stages, prior to the onset of fibrosis. Resident fibroblasts within the peritoneum express the cell surface marker CD34. Research has shown that the expression of CD34 decreases in PD patients during peritoneal fibrosis and appears to correlate to the appearance of myofibroblasts within the peritoneum[135].

The source of myofibroblasts within the peritoneum was originally believed to originate from the resident fibroblasts within the SMC layer, activated by stimuli such as inflammation and components of the dialysate fluid[136]. However *in vivo* and *in vitro* studies have shown that the mesothelial cells may also contribute to the myofibroblast population through the process of epithelilal-to-mesenchymal transition (EMT)[122, 137].

1.5.5 Epithelial to mesenchymal transition

EMT is a biological process that enables polarised epithelial cells to undergo differentiation that results in a phenotypic change becoming a mesenchymal cell[138]. This process was first described in chick embryos by Elisabeth Hay and was originally defined as a transformation process[139, 140]. During EMT various biochemical changes occur, the epithelial cell loses its polarity and key epithelial proteins such as E-cadherin, which are replaced with mesenchymal markers. There is a decrease in adherens and cytokeratin filaments, disruption of intercellular

junctions and the cytoskeleton of actin stress fibres is reorganised producing a cell with greater motility, increased resistance to apoptosis and enhanced ECM production[141].

EMT occurs in various physiological and pathological states. In development EMT is involved in embryogenesis, including implantation of the embryo and placenta formation. EMT is also activated in response to stimuli such as inflammation and is involved in wound healing, by increasing the number of mesenchymal cells to produce ECM required for wound contraction and tissue remodelling. Therefore EMT is also a key feature of pathological fibrosis, when wound healing becomes aberrant. Due to the increased invasive phenotype of mesenchymal cells, EMT also has an involvement in cancer progression and metastasis.

In fibrosis EMT contributes to the pathology by providing a source of fibroblasts. The main objective of EMT in this situation is to enhance tissue repair and aid wound healing, however this contributes to fibrogenesis resulting in excessive deposition of ECM. Studies have shown EMT is present in a number of organs including the kidney, liver and the peritoneum[134, 142, 143]. The conversion of mesothelial cells to fibroblasts is reported in both *in vivo* and *in vitro* settings[122, 131, 137]. Yanez-Mo et al (2003) demonstrated in HPMCs collected from dialysis effluent, that soon after the initiation of PD therapy mesothelial cells undergo a progressive loss of epithelial phenotype. This was apparent through the loss of E-cadherin and cytokeratins and the up-regulation of the E-cadherin transcriptional repressor Snail

and α2 integrin[131]. *In vitro* conversion of HPMC to myofibroblasts with various stimuli, such as glucose has also been reported[144].

There is still much debate surrounding the origin of myofibroblasts within fibrotic organs and the contribution through EMT to the fibroblast population. Within a mouse model of kidney fibrosis 36% of fibroblasts were attributed to EMT[145]. In immunohistochemical studies of peritoneal biopsies Jiménez-Heffernan et al (2004) reported that myofibroblasts originate from both activation of resident fibroblasts and transformation of mesothelial cells. This was evident by the expression of mesothelial markers on αSMA positive myofibroblasts[135].

The induction of EMT arises through a combination of various cytokines, the principal stimulus being the pro-fibrotic cytokine Transforming growth factor beta 1 (TGF-β1). This cytokine is reported to have a central role in driving fibrosis within PD. Reports show that over-expression of TGF-β1 correlates to worse PD outcomes and inhibition of this cytokine can prevent EMT and reverse fibrogenesis in the peritoneum[146].

1.6 Transforming Growth Factor Beta

1.6.1 Overview

TGF-β1 is a centrally important cytokine in numerous contexts of wound healing and pathological fibrosis. TGF-β1 belongs to the TGF-β family of cytokines, which consists of 33 proteins in vertebrates comprised of TGF-βs, activins and inhibins, bone morphogenetic proteins, and growth/differentiation proteins nodal and

myostatin[147, 148]. TGF-β1 is the most abundant of three isoforms (TGF-β1-3) expressed within mammals. These isoforms contain a high degree of homology, each containing a conserved cysteine knot structure and functional similarities[149]. The locus of these genes in humans lies on chromosomes 19, 1 and 14 respectively[150, 151]. Of the TGF-β isoforms, the effects of TGF-β1 in PD have been the most fully characterised, with Margetts et al demonstrating the significant effects of this cytokine alone on peritoneal morphology and fibrosis[152]. It is TGF-β1 that will be the focus of this thesis.

First isolated from platelets in 1981, TGF-β1 is ubiquitously expressed within mammalian cells and has a high degree of conservation in numerous organisms[153]. This isoform has been the most extensively studied of the TGF-β genes, with a key role in embryonic development, immunity and cancer as well as tissue homeostasis and fibrosis[154-156].

TGF-β1 is synthesised as an inactive proprotein homodimer, which is released from the cell as part of a latent complex. The latent complex consists of the TGF-β1 dimer non-covalently associated with a dimeric pro-peptide known as the latency associated peptide (LAP), which is then disulphide linked to a glycoprotein called the latent TGF-β1 binding protein (LTBP)[157]. The LAP and LTBP are essential for maintaining TGF-β1 in an inactive form[158]. Cleavage of TGF-β1 from this complex via thrombospondin-1 or plasmin allows the TGF-β1 to become active and bind to specific cell-surface receptors, resulting in activation of signalling pathways that mediate the biological effects of this peptide[159, 160].

1.6.2 Physiological functions of TGF-β1

TGF-β1 is a central regulator of various cellular processes, exerting pleiotropic effects throughout biology. This cytokine is essential for survival, as demonstrated within TGF-β1 null mice where more than 50% died in utero and the offspring that survived pregnancy died of multifocal inflammatory disease within 3-5 weeks[161]. Some of the actions that TGF-β1 exerts appear to be contradictory such as with cellular proliferation. Within epithelial cells TGF-β1 inhibits proliferation, whereas in certain cells of mesenchymal lineage TGF-β1 stimulation induces cellular proliferation[162].

TGF-β1 is a potent mediator of tissue repair and the contrary effects of this cytokine are also clear within the process. Following wounding, TGF-β1 initially promotes the inflammatory response, acting as a chemoattractant for neutrophils and monocytes and promoting angiogenesis[163, 164]. TGF-β1 stimulates the production of extracellular matrix (ECM) by myofibroblasts allowing closure of the wound and tissue remodelling to occur[165]. Later within the inflammatory process, TGF-β1 exerts immunosuppressant effects through inhibition of proliferation and activity of certain T cell subsets and suppression of natural killer cell activity, overall leading to a reduction in inflammation[155, 166, 167]. Therefore the varying responses that TGF-β1 can induce within different situations appear to depend on the cellular context and the cellular environment.

1.6.3 The role of TGF-β1 in Peritoneal Dialysis and Fibrosis

Aberrant regulation of TGF-β1 production and signalling are implicated in a multitude of disease states such as cardiovascular disease, cancer and fibrosis[168]. As mentioned in the previous section, TGF-β1 is a potent stimulus of ECM production and tissue repair. When this response is not regulated, excess deposition of ECM occurs leading to what is deemed an "uncontrollable wound healing response" that results in scar formation and ultimately fibrosis[54].

The role of TGF-β1 as a pro-fibrotic cytokine has been studied extensively in different systems. Within CKD TGF-β1 is implicated in the pathogenesis of diabetic nephropathy as well as being involved in the progress of fibrosis in the lung and liver[169-171]. In PD TGF-β1 is reported to be centrally involved in driving peritoneal membrane dysfunction and fibrosis[172]. This is evident in clinical studies that have correlated overexpression of TGF-β1 with worse PD outcome[173]. Following episodes of peritonitis TGF-β1 levels remain elevated compared to non-infected patients, for 6 weeks despite clinical remission providing a potential mechanism of peritonitis driven membrane failure[174]. Animal studies by Margetts et al (2001 and 2005) have highlighted the effects that overexpression of TGF-β1 alone in the rat peritoneum produces effects comparable to those of patients with peritoneal fibrosis[122, 152]. This includes thickening of the SMC zone, increase in collagen deposition within the interstitial region and increased vascularisation.

TGF-β1 is a major stimulus of EMT in various systems including the peritoneum. *In vitro* studies on HPMC incubated with 5 ng /ml of TGF-β1 showed a loss of E-cadherin and up-regulation of αSMA and a change to a spindle shape

phenotype[175]. This was also the case in rat peritoneum transiently transfected with adenoviruses overexpressing TGF-β1. Four days following infection increased mRNA expression of Snail and αSMA were recorded and the presence of αSMA positive cells were detected in the mesothelial layer[122]. These studies again emphasise the important role of TGF-β1 in driving fibrotic changes within the peritoneum, providing a source of fibroblasts and altering the morphology.

The importance of TGF-β1 in driving the fibrotic process within the peritoneum is further validated in studies investigating the effects of blocking TGF-β1 signalling. In a rat model of peritoneal fibrosis ultrasound delivery of Smad7 gene transfer caused a substantial inhibition of TGF-β1 activation, which resulted in a marked attenuation of peritoneal fibrosis, evident by significant decrease in mRNA and protein expression of collagen I and IV and αSMA[176]. In another rat PD model, treatment with BMP-7 resulted in a blockade of TGF-β1 induced EMT and resulted in a reduction in fibrosis and angiogenesis[177]. The effects of BMP-7 were further investigated in mesothelial cells collected from PD patient effluents. Following *ex vivo* treatment with TGF-β1 the mesothelial cells underwent EMT, which was reversed following treatment with BMP-7[178]. All these studies highlight that modulating TGF-β1 signalling may be a potential therapeutic prospect for peritoneal fibrosis in PD. The TGF-β1 signalling pathways may therefore become future therapeutic targets.

1.6.4 TGF-β1 Signalling

TGF-β1 exerts its effects through binding to TGF-β cell surface receptors. The TGF-β receptors are transmembrane glycoproteins that are classified into type I and II subsets according to their structure and function[179]. At present five type II and seven type I receptors have been identified. The type I receptors are also known as the Activin-receptor-like-kinases (ALK) and ALK-5 is the receptor that is used specifically by the TGF-βs[180]. Specific combinations of type I and type II receptors are required to bind to particular members of the TGF-β family.

The TGF-β receptors possess serine-threonine kinase activity that enables them to propagate the TGF-β1 signal through phosphorylation of various transcription factors. An active TGF-β1 dimer binds to two type II receptors, which then initiates receptor assembly. Type II and type I homodimers are brought together within close proximity to form a large ligand-receptor complex[181]. This conformational change enables the type II receptors to activate the type I receptors through phosphorylation of serine and threonine residues within the highly conserved "GS domain", a feature that is specific to type I receptor[182]. Activation of type I receptor dimer enables TGF-β1 signal transduction through activation of specific transcription factors.

Another subset of TGF-β1 receptors known as type III have also been identified through ligand crosslinking studies[183]. The type III receptors are transmembrane proteoglycans and the most abundant TGF-β1 receptor subtype. These receptors do not posses an intrinsic signalling function, but bind readily to the TGF-β isoforms. Therefore it has been deduced that these receptors do not have a signalling role but

rather act as "reservoir molecules" for TGF-β1, thereby aiding ligand presentation to the type II receptors[184, 185]. The type III receptors are identified as betaglycan, which are widely expressed heparan and chondroitin sulfate proteoglycan. The betaglycan molecule is composed of 853 amino acids and is approximately 200-300kDa in size. It binds to TGF-β1 with high affinity through its core protein[186].

1.6.5 The Smad signalling pathway

The Smad family of transcription factors are the principal mediators of the TGF-β family signalling within various organisms. Originally identified in *Drosophila* as Drosophila mothers against dpp (Mad) and *Caenorhabditis elegans* Sma, the Smad family consists of 8 members within mammals (Smad 1-8)[187-189]. Smads can be subdivided by function and structure into: receptor-phosphorylated Smads (R-Smads 1-3,5 and 8), common-partner Smads (Co-Smads; Smad 4) and inhibitory Smads (Smad 6 and 7)[190]. The R-Smads act as substrates for the TGF-β receptor family, with Smad 1,5 and 8 used as substrates for the BMP and anti-Muellerian receptors and Smads 2 and 3 serving as substrates for the TGF-β and actin receptors[189, 191].

The Smad proteins consist of two conserved domains, the N-terminal Mad Homology 1 (MH1) and the C-terminal Mad Homology 2 (MH2) domain. Between these two domains is a linker region that contains various phosphorylation sites and binding sites for Smurf and ubiquitin ligase[189]. The linker region varies in sequence and length between the different subgroups of Smads. In contrast, the MH1 domain is strongly conserved between the R-Smads and Co-Smads and is involved in DNA binding and import to the nucleus through the presence of a nuclear localisation

signal[192]. In the absence of receptor phosphorylation, this domain also inhibits the functional activity of the MH2 domain[193]. The MH2 is highly conserved among all the Smads and is involved in recognition by the TGF-β type I receptors, Smad oligomerisation and interaction with various transcription factors[190, 194].

The propagation of the TGF-β1 signal via Smads begins with the phosphorylation of the R-Smads by the type I receptor. Phosphorylation of Smad 2 or 3 occurs on two serine residues within a conserved SSXS motif at the C-terminal of the MH2 domain[195, 196]. This phosphorylation results in a conformational change that relieves the inhibition of MH2 and enables the formation of hetero-oligomers of the R-Smads with the Co-Smad. This interaction appears to be mediated through contact of the MH2 domains[197]. Following oligomerisation, the R-Smad-Co-Smad complexes translocate into the nucleus where their central function is to regulate the transcription of various genes.

Within the nucleus Smad complexes target specific gene promoters through direct binding to the DNA and association with various DNA binding proteins and transcriptional cofactors. Smads directly bind to CAGA sequence motifs, also known as Smad-binding elements (SBE) within DNA[198]. Binding to the DNA occurs through the MH1 domain via a β-hairpin structure that binds in the major groove of the DNA strand[199]. Not all Smad components can bind directly to the DNA as is the case with Smad 2, the most common splice variant of which lacks DNA binding activity due to a small extra exon-3-encoded insert located next to the β-hairpin[200,

201]. This emphasises the lack of necessity for all components of the Smad oligomer to be associated with the DNA.

The presence of SBEs appears to be required for genes to respond to TGF-β signals, however binding of Smad oligomers to the DNA alone is not sufficient to activate transcription. This is due to; the binding affinity of Smads to the CAGA motif, which is very low and would not be sufficient for successful binding, the frequency of the CAGA motif within the genome which would lead to mass induction of numerous genes and the lack of Smad specificity within the SBE, due to high conservation of the β-hairpin structure amongst all the R-Smads[201].

For specific transcriptional activation of target genes Smad oligomers associate with various DNA binding proteins. Such proteins include activating protein-1 (AP-1), Fast-1 and the histone acetyltransferases cAMP response element binding protein (CREB) binding protein (CBP) and p300, the latter two of which have been shown to be required for TGF-β Smad dependent COL1A2 transcription within fibroblasts[202, 203]. Smad complexes are shown to associate with transcriptional co-repressors including Sloan-Kettering Institute proto-oncogene (Ski) and Ski-related novel protein N (SnoN), which is believed to be part of a negative feedback system to control duration of the Smad response[204, 205].

1.6.6 Non-Smad Signalling Pathways

The Smad proteins are firmly established as the major mediators of TGF-β1 signalling. Despite this, increasing biochemical and developmental research has

shown that TGF-β1 signalling involves several non-Smad signalling pathways, which include the mitogen-activated protein kinase (MAPK), the Rho-like GTPases (Rac, RhoA and Cdc42) and the phosphatidylinositol 3-kinase (PI3K)[206, 207]. These non-Smad signalling pathways are reported to be involved in TGF-β1 dependent responses such as EMT and cell migration, cell proliferation, differentiation and apoptosis and in regulation of various ECM components[208, 209].

At present these pathways although activated via TGF-β1 receptors independently of Smad, are believed to function in conjunction with Smad pathways to mediate TGF-β1 responses, thus resulting in cross-talks between various signalling pathways[207]. The non-Smad pathways contribute to TGF-β1 responses through three general mechanism of cross-talks: (1) at the receptor level, the TGF-β receptors directly interact with or phosphorylate non-Smad proteins. This initiates parallel signalling that collaborates with the Smad pathway in inducing various responses; (2) non-Smad signalling pathways directly modify the Smad proteins activity, such as through phosphorylation resulting in regulation of the TGF-β1 signalling pathway; (3) Smads directly interact and modulate the other signalling proteins activities, thus enabling the transmission of Smad signals to other pathways[206].

1.6.7 Regulation of TGF-β1 Signalling

TGF-β1 signalling is regulated at numerous levels of the signalling pathways, through extracellular, cytoplasmic and nuclear mechanisms as well as modulation by other signalling pathways[210]. The TGF-β1 molecule is synthesised in a latent form, ensuring control of signal strength and the situation in which latent TGF-β1 becomes

activated. Activation of TGF-β1 usually occurs through cleavage of the LAP through proteases such as plasmin. Acidic cellular environment and exposure to reactive oxygen species also can activate TGF-β1 as can Thrombospondin-1 (TSP-1), which causes the LAP to undergo a conformational change resulting in TGF-β1 activation[211].

For the TGF-β1 signal to be propagated, the TGF-β1 ligand needs to bind to the TGF-β1 receptor complex. At the receptor level, regulation of TGF-β1 signalling occurs through access of the ligand to the receptor. This can be promoted or inhibited by various molecules. Decorin, a small proteoglycan is believed to be a natural inhibitor of TGF-β1, binding to circulating TGF-β1 and neutralising the effects. In fibrotic disease models, decorin was shown to produce a significant reduction in fibrosis[212]. Molecules such as the TGF-β type III receptor, betaglycan, act as co-receptors by enhancing binding of TGF-β1 to the type II receptor[185]. Connective tissue growth factor (CTGF) was also found *in vitro* to enhance the TGF-β1 signalling response through increasing the cross links between TGF-β1 and its three receptors[213].

The inhibitor Smads (I-Smads 6 and 7) are able to negatively regulate TGF-β signalling pathway at various levels via a negative feedback loop[214]. Smad 7 is the predominant antagonist in the TGF-β1 signalling pathway. Following receptor activation, the TGF-β1 receptors are negatively regulated by the inhibitor Smad Smad 7, which competes with R-Smads for binding to the activated receptor, thus inhibiting Smad phosphorylation and complex formation of R-Smads and

Smad4[215]. Binding of Smad 7 to the receptor also promotes ubiquitination and degradation of the receptor. This occurs through the interaction of Smad 7 and the Smad ubiquitination regulatory factors (Smurfs) E3 ligases Smurfs 1 and 2[216]. This interaction occurs in the nucleus, the complex is then translocated to the cytoplasm and interacts with the activated type I receptor, resulting in downregulation of TGF-β1 signalling.

In the nucleus, Smad 7 can prevent transcriptional factor recruitment and can bind directly to the DNA disrupting the generation of Smad-DNA complexes, resulting in transcriptional repression of TGF-β1 signalling[217].

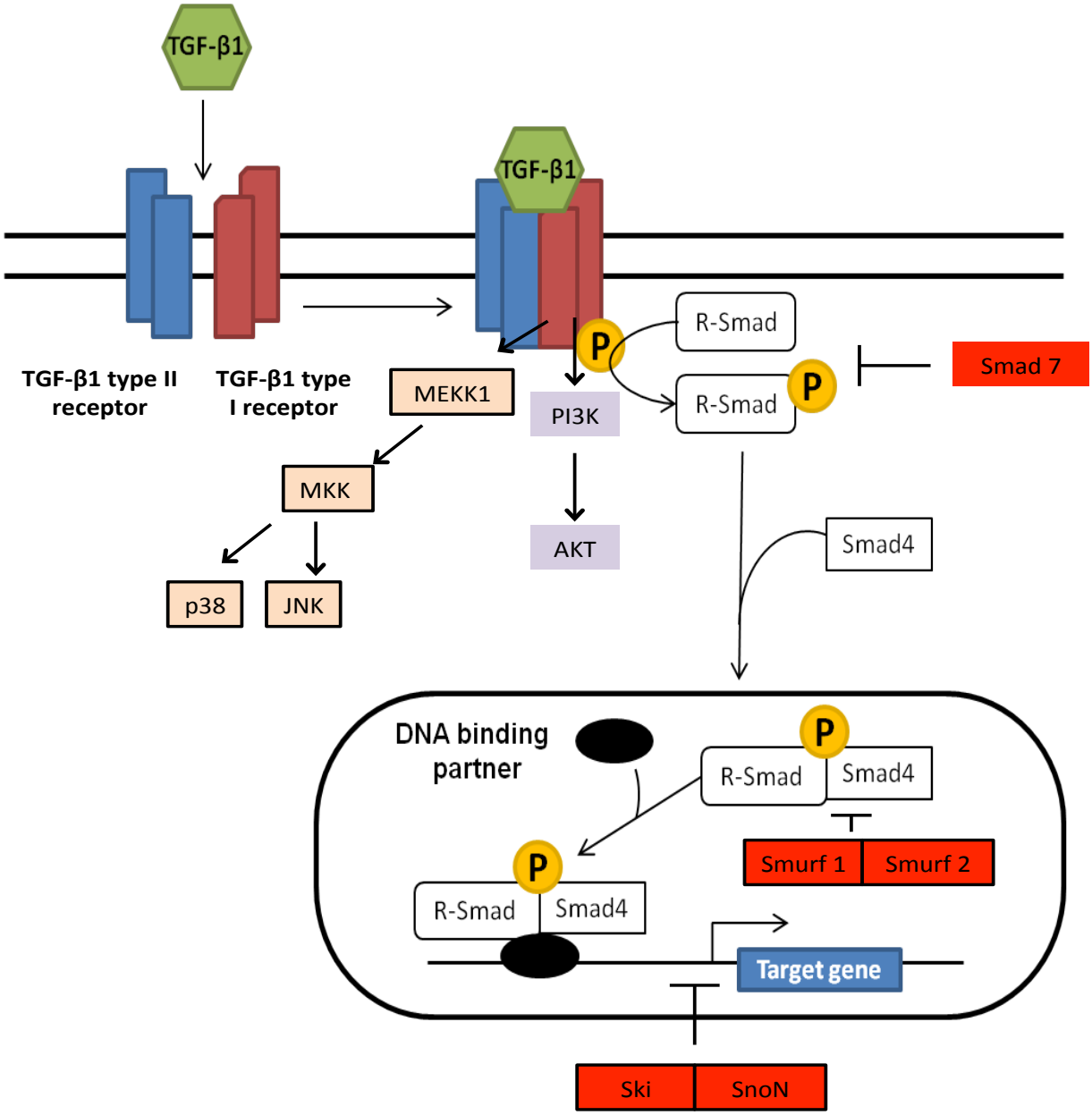

Figure 1.2 Overview of TGF-β1 signalling pathways

TGF-β1 mediates effects mainly through the SMAD dependent signalling pathway in conjunction with non-SMAD signalling pathways including PI3K and MAPK. SMAD signalling occurs through R-SMADS (SMAD2/3) which then associate with SMAD4 before being directed to the nucleus and interacting with co-activators to initiate transcription of target genes. Regulation of this pathway occurs at various levels with the main negative regulator being SMAD7, which can interact with the TGF-β1 receptor, preventing interaction with R-SMADS. SMAD7 also interacts with Smurf 1 and Smurf 2 to further negatively regulate the pathway. Co-repressors Ski and SnoN inhibit signalling by associating with SMAD complexes thus preventing transcription (adapted from Massague 1998[218] and Akhurst and Hata 2012[219])

1.7 Inflammation and peritoneal fibrosis

1.7.1 The inflammatory response

Inflammation is an adaptive response that is elicited in reaction to tissue injury or infection. The symptoms of inflammation include redness, heat, swelling and pain were described in the first century CE by Aulus Cornelius Celsus, a Roman academician[220]. This process is both physiological, a key phase in the wound healing process, but can also be pathological such as in autoimmune conditions and sepsis. Generally, inflammation is a controlled and self-limiting process, enabling clearance of pathogens and restoration to homeostasis[221].

An acute inflammatory response consists of a series of co-ordinated events including activation of resident macrophages, release of pro-inflammatory cytokines and chemokines, vasodilation and recruitment of leukocytes to the sight of injury[222]. The initial recruitment of leukocytes (predominantly neutrophils) to the injured tissue results in their activation, either by cytokines or contact with the infectious agent. This causes the release of toxic compounds such as reactive oxygen species (ROS), proteinase 3, cathepsin G and elastase, which not only damage the pathogen but also the host. Following clearance of the insult, the inflammatory response undergoes a phase of resolution, which is then followed by tissue repair[223].

The resolution phase involves the release of the lipoxin eicosanoids. The lipoxins promote resolution through inhibition of neutrophil recruitment to the site of injury and chemotaxis of nonphlogistic monocytes, which become activated macrophages.

This usually occurs within 2-3 days following injury provided the noxious stimuli is removed. This is followed by neutrophil apoptosis and the removal of the dead cells by macrophages through phagocytosis[224]. The macrophages then mediate the tissue repair response through the release of mediators including TGF-β1, which contributes to suppression of the inflammatory response, and also initiates tissue repair through production and deposition of extracellular matrix components[225].

1.7.2 Causes of inflammation within PD patients

1.7.2.1 Existing low-grade inflammation

Inflammation is an established risk factor of morbidity and mortality within CKD patients, with markers such as C-reactive protein (CRP) and IL6 production being linked to poor prognosis[226]. Prior to the commencement of dialysis therapy it was reported that 30-50% of patients with advanced CKD displayed serologic evidence of inflammation[227]. Numerous animal and human studies have linked inflammation with the progression of CKD, with reports that inflammation occurs during the early stages of kidney failure[228-230].

The causes of inflammation within CKD are multifactorial, with patient related factors such as age, gender, underlying comorbidities and residual renal function believed to contribute to the inflammatory state[231, 232]. Comorbidities such as obesity and diabetes are associated with inflammation, with some studies reporting a direct association between BMI, truncal fat and waist circumference and CRP in CKD patients[233-235]. Uremia also generates inflammation through increased production of advanced glycation end products (AGEs) and other carbonyl

compounds[236]. Loss of residual renal function may also contribute to the inflammatory process in dialysis patients. Some studies have found a link with cytokine clearance and renal function, with decrease in renal function leading to higher concentration of molecules such as IL-1β and TNF-α in nephrectomised rats[237, 238]. Decreased renal function may exacerbate the inflammatory response through increased oxidative stress. Conversely, inflammation can also affect residual renal function, suggesting a detrimental cycle.

1.7.2.2 Dialysis treatment increases inflammation

The presence of inflammation prior to the commencement of renal replacement therapy in CKD patients is well documented[239]. Some studies have reported no difference in inflammatory markers between ESRD patients and dialysed patients. However, the overall consensus is that dialysis therapy augments the inflammatory process[240, 241]. This is evident by the increased levels of inflammatory markers IL-1β and IL6 in the dialysate effluent, which increases with time on conventional dialysis fluid[242, 243]. PD patients displayed increased macrophage presence within the peritoneum even in the absence of infection, indicative of a chronically inflamed state. How PD therapy augments the inflammatory state within ESRD patients can be attributed to bio-incompatible dialysis fluids and peritonitis infections[244].

1.7.2.3 Bioincompatible peritoneal dialysate fluids

Conventional peritoneal dialysis fluids (PDF) are hyperosmolar, have an acidic pH (5 - 5.4), high glucose concentration and are buffered with high concentrations of lactate[245]. These components are deemed as bioincompatible and are believed to

contribute to inflammation morphological changes and technique failure observed in PD patients[246]. This has led to the development of alternative PDF with alterations in the composition, such as the removal of glucose or changes in the buffering system such as the use of bicarbonate and neutral pH. Studies have reported that more biocompatible PDF may provide benefit to the patient, with marked decrease in inflammatory markers such as IL6 and hyaluronic acid (HA) and increase in cancer antigen 125 (CA125), which is deemed a marker of mesothelial cell mass and mesothelial homeostasis[247-249].

Glucose is a component within conventional PDF that causes various detrimental effects to the peritoneal cavity, including cytotoxicity to the mesothelial layer, fibrotic changes to the membrane and modulation of the host's immune defence[250]. Stimulation of HPMCs for 7 days with glucose resulted in an increase in the expression of monocyte chemoattractant protein-1 (MCP-1) in cell supernatant[251]. This protein is involved in the recruitment of monocytes, suggesting that glucose enhances the chemotaxis of macrophages to the peritoneal cavity, thus contributing to the intraperitoneal inflammatory response. This is also supported by another study, which found exposure of HPMC to glucose-enriched PDF caused increased production of hydrogen peroxide, a potential mechanism of PDF induced peritoneal injury[252]. Exposure of HPMC to glucose also leads to the production of TGF-β1 and thus extracellular matrix deposition, which contribute to peritoneal fibrosis and ultimately treatment failure[253].

Conventional glucose containing PDF also generates glucose degradation products (GDP) following heat sterilization of PDF. At present research in animals and *in vitro* suggests that GDPs contribute to the local toxicity attributed to glucose. Prolonged exposure of HPMCs to various GDPs resulted in loss of cell viability and promoted apoptosis via a caspase-related mechanism[120, 254]. The presence of GDPs is also attributed to the formation of advanced glycosylation end products (AGE). AGEs are reported to predominantly accumulate in the vascular wall of the peritoneum and may account for increased membrane permeability, accounting for ultrafiltration failure observed in patients on CAPD[255, 256]. Binding of AGE to receptor of AGE expression (RAGE) on HPMC was reported to stimulate induction of vascular cell adhesion molecule 1 (VCAM-1), a structure involved in leukocyte adhesion and recruitment[257], thus potentially promoting local intra-peritoneal inflammation. This binding also stimulated the release of VEGF, a cytokine involved in angiogenesis, thus contributing to the vascular changes observed in patients on long-term PD.

1.7.2.4 Peritonitis

Peritonitis is a serious complication within PD therapy and remains the leading cause of treatment failure and subsequent transfer of patients to haemodialysis. Peritonitis infection becomes apparent through symptoms such as abdominal pain and the appearance of cloudy dialysis effluent or “cloudy bag”, indicative of a substantial influx of leukocytes into the peritoneal cavity[258]. The number of patients that have their catheter removed because of peritonitis varies between regions, ranging from 16% in Canada to 42.6% in Scotland[259, 260]. The microbiological causes of peritonitis include Gram-positive and Gram-negative

bacteria and fungi, with Gram-positive being the most common cause of infection, in particular *Staphylococcus epidermidis*[261].

Various studies have reported the effects of peritonitis on the inflammatory response within the peritoneum. Twenty-four hours prior to the onset of symptoms pro-inflammatory cytokines IL6 and tumour necrosis factor alpha (TNF-α) levels were elevated in the effluent of PD patients[262]. This was also the case with the inflammatory cytokine IL8, which was elevated in the dialysate between 4-12 hours before the onset of peritonitis infection[263]. Acute peritonitis infection is also shown to increase the EPSA and increase the peritoneal permeability in PD patients.

Studies have reported that following acute peritonitis episodes levels of inflammatory mediators return to control levels. However, the effects of peritonitis may remain despite apparent clinical remission. In a longitudinal study following peritonitis episodes the levels of pro-inflammatory cytokines were found to peak at day 1 of infection and gradually decrease over the six weeks following infection[174]. However, the levels of these cytokines were still significantly greater than those in non-infective patients, suggesting that peritonitis may contribute to morphological changes to the peritoneum despite clinical remission.

The enhanced inflammatory response generated from peritonitis may contribute to fibrotic changes within the peritoneum. Following clinical remission of peritonitis the fibrotic mediators TGF-β1 and fibroblast growth factor (FGF) remained elevated[264]. This is supported by studies reporting that peritonitis episodes are

linked to functional changes in the peritoneal membrane such as UFF[101]. Frequent peritonitis episodes are associated with higher TGF-β1 concentrations in the dialysate effluent of PD patients, further supporting the link between inflammation and fibrosis[173]. A key study that links recurrent inflammation and fibrosis is Fielding et al (2014) repeat hit murine model[265], which provided the focus for this thesis.

1.8 Murine model of inflammation driven fibrosis

Within Cardiff University a murine model of peritoneal inflammation was developed through intraperitoneal administration of a cell free supernatant prepared from a clinical isolate of *Staphylococcus epidermidis* (termed SES), which mimics the inflammatory response observed in acute bacterial peritonitis episodes[266]. This model was then adapted to examine changes in the mouse peritoneum following recurrent episodes of SES administration[265].

The mice were injected 4 sequential times with a cell free supernatant derived from a clinical isolate of SES, at weekly intervals for four weeks (day 0, 7, 14 and 21). Peritoneal biopsies were then collected at defined time points including four weeks after the final SES hit at day 49 and examined for histological changes. Different genotypes of mice including wild type (WT) and IL6 knock out (IL6KO) were used to determine the effect of pro-inflammatory cytokines within this process.

The work revealed that a singular injection of SES did not produce fibrosis, however following the fourth hit WT mice developed significant thickening of the

submesothelial compact zone and increased expression of collagen, changes similar to those reported in PD patients. The role of inflammation in driving this process was evident in the differences observed between the different mice genotypes.

The fibrotic response to repeat SES challenge was not observed in IL6KO mice, which presented with a peritoneal histology similar to control animals. Examination of signalling pathways between the mice genotypes showed a release of IFN-γ from TH1 cells following the fourth SES injection in WT mice that was absent in IL6KO mice. A change in the balance of STAT activation from a predominant STAT3 response during the first 3 SES hits to STAT1 response during the fourth hit in WT mice, further supported the involvement of IFN-γ in the fibrotic process. Examination of IFNKO mice response to recurrent SES challenge revealed a lack of fibrosis, indicating the central role of IFN-γ in promoting the fibrotic response within this model and potentially in PD patients.

It is apparent from the previous research that both TGF-β1 and pro-inflammatory cytokines have major roles in peritoneal fibrosis. Their interaction however, has not been well characterised in this context. The work of Fielding et al (2014) was suggestive that pro-inflammatory cytokines IL6 and IFN-γ played a predominant role in peritoneal fibrogenesis[265]. This is a novel finding and surprising finding as various studies have reported that IFN-γ is a potent anti-fibrotic cytokine, specifically in inhibiting TGF-β1 signalling and attenuating fibrogenic processes such as ECM deposition. Therefore this recent work developing a model of inflammation-driven fibrogenesis provided an ideal opportunity for me to study the interaction of TGF-β1

and pro-inflammatory cytokines in peritoneal fibrogenesis. The central role of IFN-γ in this mouse SES model and the novelty of this apparent pro-fibrotic effect provided the focus of my work to examine the interaction of IFN-γ on TGF-β1 responses.

1.9 Interferon gamma

1.9.1 Overview

The Interferons (IFNs) were first discovered by Issacs and Lindenmann (1957) as agents that provided resistance to cells from viral infection[267]. Further research into this group of proteins has revealed key roles in immunomodulation, apoptosis, cell cycle arrest, as well as anti-microbial activity[268-271]. The IFNs are classed into type I and type II on basis of sequence homology and receptor specificity. Type I consists of IFN-α and IFN-β (most documented) along with IFN-ε, IFN-κ, IFN-ο, IFN-δ, and IFN-τ. The sole type II IFN is IFN-γ, which is structurally distinct and encoded on a different chromosomal locus to that of type I IFNs[272, 273]. Unlike the type 1 IFNs, which are produced in most cells, IFN-γ is produced mainly by; natural killer cells (NK) CD8+ cytotoxic lymphocytes and CD4+ T helper cell type 1 (Th1) lymphocytes[274]. Hence IFN-γ is also known as immune IFN.

Encoded by the single IFNG gene located on chromosome 12 in humans and chromosome 10 in mice, IFN-γ shares no structural similarity and signals through different receptors to type I IFNs[275, 276]. It was classified as an IFN due to its ability to "interfere with viral infection"[267]. Unlike the type I IFNs, IFN-γ has a much lower specific antiviral activity (10-100 fold) but has greater immunomodulation activity[277]. The IFNG gene is 6kb in size and consists of four

exons and 3 introns. Transcription of this gene yields a 1.2kb mRNA sequence, which encodes a 166 amino acid polypeptide[278]. At the protein level IFN-γ exists as a noncovalent homodimer with a molecular weight of 34kDa. The 3D structure of the IFN-γ dimer was elucidated in 1991, which found the majority of the structure (62%) was helical, with each subunit comprised of six α helices attached by short nonhelical regions[279]. It is only the dimeric form of IFN-γ that is biologically active. Binding of the homodimer to the specific cell surface receptor initiates a signalling cascade, which enables IFN-γ to exert its effects on cells.

1.9.2 IFN-γ Signalling

1.9.2.1 IFN-γ Receptor

IFN-γ exerts its biological activity by signalling through the heterodimeric type II receptor (IFNγR). Characterisation of the IFNγR during the 1980s revealed that the receptor consisted of two subunit components IFNGR1 and IFNGR2. The IFNGR1 subunit is required for binding of the ligand to the receptor, whereas IFNGR2 is required for signal transduction and hence induction of response to IFN-γ[273, 277, 280]. This was highlighted in 1987 when a series of genetic experiments were undertaken which elucidated the genetic locus of the subunit components to chromosome 6 and chromosome 21 respectively[281].

Further studies revealed the specificity of the IFNγR for IFN-γ alone and that the receptor was species-specific[280]. IFNGR is widely expressed particularly in peripheral blood lymphocytes and macrophages. However, the expression patterns of the subunit components have been shown to differ. The IFNGR1 subunit is highly

expressed on the surface of nearly all human cells. The expression of IFNGR2 is typically the limiting factor, defining capability of the cell to respond to IFN-γ[273, 280, 282]. This subunit is usually expressed at low levels but can be positively and negatively regulated via stimuli in certain cell types, thus affecting total IFN- γ responsiveness.

1.9.2.2 JAK-STAT signalling pathway

The binding of the IFN-γ ligand to its specific IFNγR results in the activation of signalling pathways, predominantly the Janus kinase (JAK)- Signal transducer and activator of transcription (STAT) pathway. This was the first pathway discovered to be activated by the IFNs[283, 284]. The JAK kinases consist of a family of four protein tyrosine kinases (JAK 1-3 and tyrosine kinase 2). All these proteins are composed of seven regions (JH1-7), which are highly homologous. The JH1 region consists of a kinase domain whereas the JH2 encodes a pseudo-kinase domain that does not have catalytic activity but may be required for JH1 region to function.

STATs are a family of seven transcription factors (STAT1, STAT2, STAT3, STAT4, STAT 5a, STAT5b and STAT6) that reside in a latent state within the cytoplasm of cells until activated[285]. All the proteins within this family are similar in structure; they contain various domains the most conserved of which is a SRC homology 2 (SH2) domain. This domain is necessary for STAT signalling as it enables binding to specific phosphotyrosine motifs thus allowing recruitment of STAT to specific receptors allowing activation and dimerization[286, 287].

The JAK-STAT signalling pathway is employed by various cytokines and growth factors. IFN-γ signalling utilises specific JAK and STAT proteins to signal through, which include JAK1, JAK2 and STAT1. The IFNγR subunits do not possess catalytic activity, hence each subunit is pre-associated with an inactive JAK protein[273]. The IFNγR1 subunit is associated with JAK1 and IFNγR2 with JAK2 through their intracellular domains[288]. When a homodimer of IFN-γ binds to the IFNγR a conformational change of the receptor is induced resulting in the respective JAK kinases being brought into close proximity. This allows JAK1 and JAK 2 to activate each other by transphosphorylation[289].

Once activated, the JAK kinases then phosphorylate key tyrosine motifs within the cytoplasmic domains of the receptor. These phosphorylated motifs enable the recruitment of STAT1 to the receptor by providing docking sites for the SH2 domain[290, 291]. Upon docking at the receptor STAT1 becomes phosphorylated by JAK. The activated STAT1 proteins dissociate from the receptor and undergo dimerization. The phosphorylated STAT1 homodimer then translocates to the nucleus. Within the nucleus this homodimer binds to gamma activated sequences (GAS) within the promoter of specific genes, initiating transcription[273].

The JAK-STAT signalling mechanism described in this section is the most well characterised pathway of IFN-γ signalling. The importance of this pathway has been highlighted in various inhibitor and mouse knockout models[292, 293]. For example STAT1 knockout mice are incapable of generating any biologic response to IFN-γ. These mice display normal organ and tissue physiology but have impaired resistance

to microbial and viral infections[294, 295].

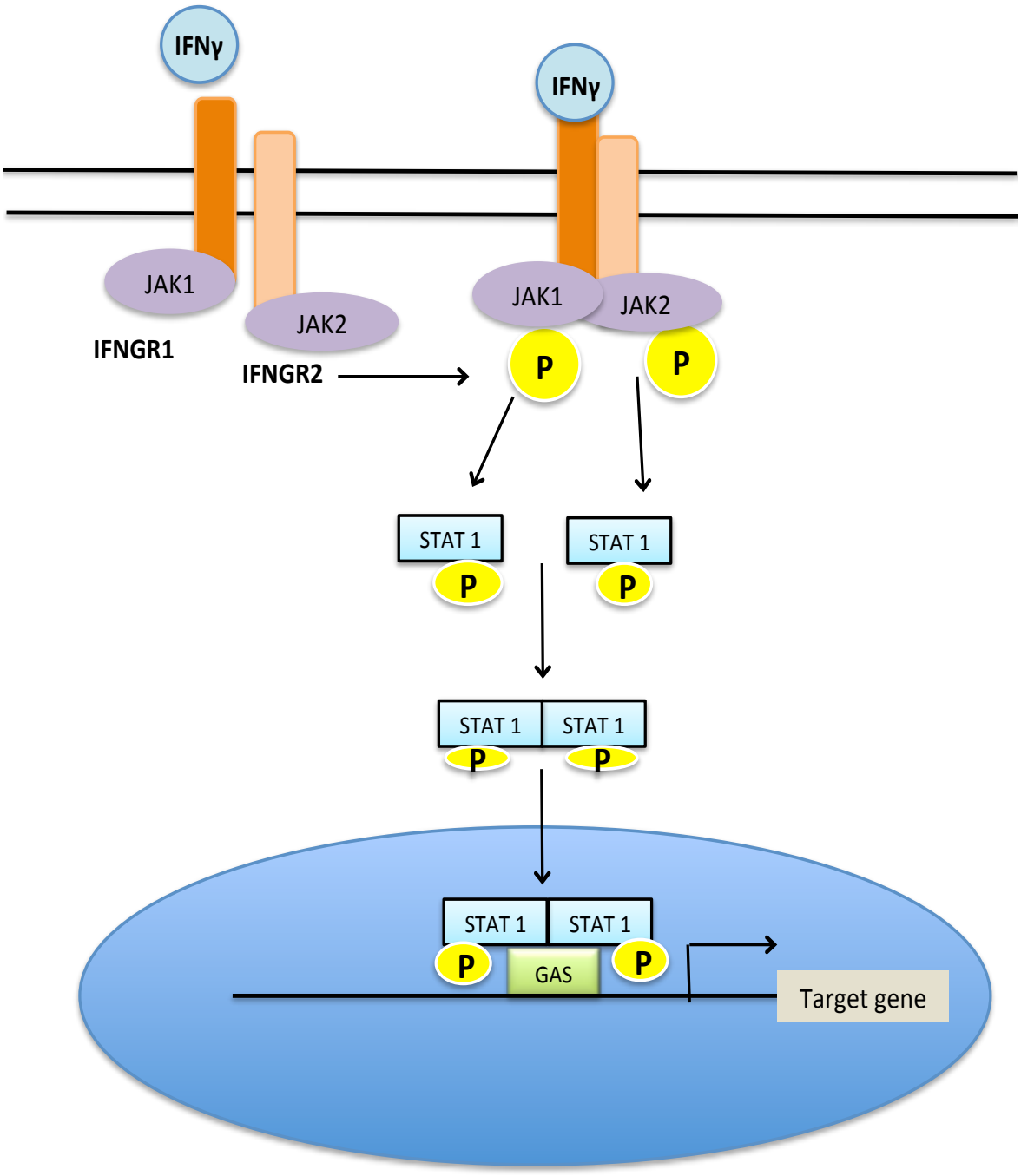

Figure 1.3 IFNγ signalling through the JAK-STAT pathway
IFNγ signals through receptor consisting of IFNGR1 subunit required for ligand binding and IFNGR2 subunit used for signal transduction. Each subunit is associated with a JAK protein. Binding of IFNγ to the receptor activates the JAK protein causing transphosphorylation. This results in recruitment of STAT1 proteins, which in turn are phosphorylated from dimers and translocate to the nucleus, initiating transcription of target genes (adapted from Baldridge et al 2011[296]).

1.9.3 Alternative signalling pathways

Although the JAK-STAT pathway is necessary for various cellular responses to IFN-γ, recent research suggests it may not be sufficient to elicit all of the actions of IFN-γ. In microarray analysis of murine bone marrow macrophages, activation of macrophage inflammatory proteins (MIP-1α and MIP-1β) occurred in both wild type and STAT1 null cells, indicating STAT1 independent regulation[297]. Another JAK-STAT independent mechanism was revealed in the induction of IL-27 by IFN-γ in human monocytes[298]. IFN-γ has profound anti-viral activity and STAT1 is important in this response. However there is still significant anti-viral activity in STAT1 null mice, again emphasising STAT1 independent mechanisms and implying that additional signalling pathways may have functionality in the generation of IFN-γ responses[297].

The binding of IFN-γ to its receptor can activate various downstream effector molecules in addition to JAK-STAT. These include the p38, Pyk2 and ERK1/2 branches of the MAPK signalling pathway[299-301], the G-protein-linked signalling molecules C3G and Ras GTPase-activating protein 1 (Rap-1)[302], PI3K and several isoforms of protein kinase C (PKC)[303-305]. These alternative signalling pathways appear mainly to work in conjunction with the JAK-STAT pathway by enhancing transcriptional activity of STAT1 through induction of serine phosphorylation. This is evident in studies showing PKC isoforms augmenting the transcription of MHC class II and ICAM by IFN-γ [306]‘[307]. This therefore provides a higher degree of control and regulation on the various responses IFN-γ elucidates.

1.9.4 IFN-γ and Peritoneal Dialysis

Within the context of PD research early studies revealed an important role of IFN-γ in PD patients' immune defence against bacterial peritonitis. IFN-γ was shown to enhance peritoneal macrophages process of phagocytosis and bactericidal activity in PD patients[308]. This was also supported in another study, which monitored the addition of IFN-γ to dialysis fluid and showed significant increase in peritoneal macrophage number and clearance of bacteria from the peritoneal cavity[309]. Comparisons of IFN-γ levels in PD patients with peritonitis and those without peritonitis revealed that IFN-γ expression increases following bacterial infection, which again emphasised the role of this cytokine in the immune response within the peritoneum[310].

Further roles of IFN-γ in the peritoneal host defence were reported in the regulation of neutrophils within the peritoneal cavity. IFN-γ was shown to regulate neutrophil migration across the peritoneum in both *in vivo* and *in vitro* systems through modulation of chemokine expression including IL8 and MCP-1[311]. Neutrophil recruitment and clearance in the peritoneal cavity also appears to be regulated by IFN-γ, with IFN-γ knockout mice displaying impaired neutrophil recruitment following inflammatory challenge. IFN-γ is also shown to promote neutrophil apoptosis through regulation of IL6 activity, thus promoting resolution of the immune response[312].

In the context of peritoneal fibrosis Fielding et al (2014) appear to be the only study to identify a potential fibrotic role of IFN-γ[265]. IFN-γ is identified as a marker of

tissue injury evident by its increased expression during peritonitis episodes[313]. However most studies have reported the anti-fibrotic effects of this cytokine and its potential as a therapy for fibrosis[314, 315]. Whether the fibrotic effect of IFN-γ is unique to the murine model developed by Fielding et al (2014) or unique to PD patients requires further elucidation. This includes the mechanism of how these fibrotic effects are mediated potentially through interaction with typical pro-fibrotic cytokines such as TGF-β1.

1.10 Aims of Thesis

The overall focus of this thesis will examine the interaction between pro-inflammatory signalling and TGF-β1 signalling within the context of peritoneal fibrosis. The main pro-inflammatory cytokine selected being IFN-γ. The interactions between these cytokines will be determined through use of *in vivo* and an *in vitro* system. The specific objectives being:

- To characterise the TGF-β1 response within the *in vivo* SES model and thus determine if TGF-β1 is involved in inflammation induced fibrosis
- To delineate the interaction between TGF-β1 and IFN-γ within primary human peritoneal mesothelial cells (HPMC) *in vitro* and identify any augmentation in the fibrotic response
- To study the mechanism undelying any modulation of pro-fibrotic responses by IFN-γ

Chapter 2: Materials and Methods

2.1 Materials

All general and tissue culture reagents were purchased from Sigma (Poole, Dorset, UK), Fisher Scientific (Leicestershire, UK) and GIBCO/BRL Life Technologies (Paisley, UK) unless otherwise stated. PCR and qPCR primers were purchased from Invitrogen Life Technologies (Paisley, UK) and Applied Biosystems (Cheshire, UK). Recombinant IFN-γ and TGF-β1 were purchased from R&D Systems (Oxford, UK). The MAPK kinase (MEK) inhibitor PD98059 and the p38 kinase inhibitor SB203580 were obtained from Calbiochem (Nottingham, UK). The SMAD3 inhibitor SIS3 was purchased from Santa Cruz Biotechnology (Heidelberg, Germany).

2.2 Generation of murine control and SES samples

The murine samples used in this thesis were generated and kindly donated by Dr Ceri Fielding. Briefly, inbred WT mice C57BL/6 were purchased from Charles River UK. IL6KO were bred in house from breeding pairs originally purchased from The Jackson Laboratory[316]. All mice were aged between 8 and 12 weeks and were weight matched for each experiment. Mice were injected with four sequential episodes of SES at 7 day intervals to generate peritoneal inflammation and were maintained for a maximum of 49 days before sacrifice[265]. SES was prepared as described in McLoughlin et al 2003[317]. I received peritoneal membrane samples collected by Fielding et al 2014 from mice at day 28, 35, 42 and 49 through which I generated RNA samples that were used in subsequent experiments in this thesis.

2.3 Cell culture

2.3.1 Isolation and culture of human peritoneal mesothelial cells

Human peritoneal mesothelial cells (HPMC) were isolated from greater omental tissue obtained with the consent from patients undergoing elective abdominal surgery. Small pieces of omentum tissue (5 cm^2) were washed in sterile PBS and transferred to 50 ml falcon containing 15 ml of trypsin/PBS (1X) mixture and incubated for 15 minutes at 37°C with continuous rotation. The digested tissue was centrifuged for 6 minutes at 1600 rpm causing a pellet of HPMC to form at the bottom of the falcon. The supernatant was removed by aspiration and cells were washed in 10 ml of serum supplemented growth medium. Pellet was re-suspended and centrifuged for a further 6 minutes at 1600 rpm, following which pelleted cells were suspended in growth medium and transferred to a T25 culture vessel[318].

Confirmation of HPMC identity and purity of culture obtained was determined using cell staining and observation using light microscopy. The cells cultured were identified as pure mesothelial cells by their uniform cobblestone appearance at confluence, by the presence of surface microvilli, by the lack of staining for factor VIII related antigen and the uniform positive staining for cytokeratins 8 and 1[319].

2.3.2 HPMC growth conditions

HPMC were grown in Earles salt medium M199 (Gibco) containing 10% foetal calf serum (FCS) supplemented with 100 μg/ml penicillin, 100 μg/ml streptomycin 100 μg/ml, 2 mM glutamine, 5 μg/ml insulin, 5 μg/ml transferrin and 0.4 μg/ml hydrocortisone. Cell monolayers were then grown (incubated at 37°C, 5% CO_2) in T25 Falcon culture flasks until confluent. Fresh growth medium was replaced every 2-3

days. HPMC cultures attained confluence in 3-5 days. All experiments were performed on cells of passage two.

2.3.3 Monolayer Sub-culture

On reaching confluence in the primary culture flask, cells were transferred into T75 culture flasks and then into the required experimental culture vessel. The growth medium was first aspirated and a 1:10 dilution (v/v) of trypsin in sterile PBS (2-4 ml) was added to the cells. Cell detachment was observed using light microscopy. Following detachment growth medium supplemented with 10% FCS (10 ml) was added to neutralise trypsin. The cell mixture was transferred to 50 ml falcon and centrifuged at 1600 rpm for 6 minutes. The supernatant was then removed and the pellet re-suspended in supplemented medium with 10% FCS which was then added into the new culture vessel. Confluent cells were split in a ratio of 1:4.

2.3.4 Growth Arrest

Before each experiment, the cells growth phase was synchronized via growth arresting the cells in serum free supplemented medium M199. Growth medium was removed and replaced with serum free medium. Cells were growth arrested for 24 hours prior to addition of experimental conditions. All experiments on HPMC were conducted in serum free medium.

2.3.5 Cell stimulation

HPMC at passage two were grown to 80% confluence within a culture vessel. Following growth arrest the serum free medium was removed and replaced with

fresh serum free medium containing the desired stimulus. Cells were incubated with the cytokine medium for varying times and concentrations depending on the experimental design.

2.4 Met5a cell culture and limitations

For subsequent transfection experiments HPMC were substituted for the transformed pleural mesothelial cell line Met5a[320]. Cell culture growth conditions for Met5a were the same as that described for HPMC except the experimental passage, with Met5a cells being used at experimental passage of 15 and 16 respectively. Met5a and HPMC responses were compared under experimental conditions described to ensure no variation in key responses investigated. However, this is a transformed cell line and the use of these cells was limited to transfection experiments only.

2.5 RNA Extraction and Analysis

2.5.1 Chloroform/Isopropanol RNA extraction

One millilitre of tri-reagent was added to 50-100 mg of tissue or per well of a 6 well plate and left for 5 minutes until total cell lysis. The lysate was collected in a 1.5 ml microcentrifuge tube to which 0.2 ml of chloroform was added per 1 ml of lysate. After mixing by inversion, samples were centrifuged at 13000 rpm for 15-30 minutes (4°C without braking). The colourless phase was transferred to a clean microcentrifuge tube and the lower phase discarded. RNA precipitation was achieved by addition of 0.5 ml ispropanol to each sample which were then stored overnight at -20°C. The samples were then centrifuged at 12000 rpm for 15-30

minutes at 4°C to form RNA pellet. The pellet was then washed twice with 1 ml of ice cold ethanol (75%) and then centrifuged at 12000 rpm for 10 minutes at 4°C following each wash. Ethanol was then removed and pellet allowed to air dry for 30 minutes before re-suspension in 10-20 μl of sterile H_2O.

2.5.2 Determination of RNA concentration

RNA concentrations were determined using the nanodrop (Henry Wellcome Building). Equal volume (1 μl) of sample was placed on nanodrop reader and absorbance measured at both 260 nm and 280 nm. A 260/280 ratio of above 1.8 was indicative of a sufficiently pure sample. Concentration was calculated as ng/μl.

2.5.3 Reverse Transcription

Reverse Transcription (RT) of mRNA to cDNA was carried out using the random primer method. Briefly, 1 μg of purified RNA dissolved in 10 μl sterile H_2O was combined with reagents from the high-capacity cDNA reverse transcriptase kit (Applied Biosystems). The RT was carried out in a final volume of 20 μl per reaction containing 1 μg of RNA sample, 2 μl of 10 x RT random primers, 2 μl of 10 x RT buffer, 0.8 μl of 25 mM dNTPs (deoxynucleoside triphosphates dATP, dCTP, dGTP and dTTP), 1 μl of Multiscribe® reverse transcriptase, and 1 μl of RNase inhibitor. Samples were then placed in an Applied Biosystems Gene Amp PCR System 9700 thermocycler. The RT reaction solution was first incubated at 25°C for 10 min, which allowed annealing of the random hexamer primers to the RNA. The primers were then extended by the reverse transcriptase in the presence of the four dNTPs through heating of the solution to 37°C for 2 h, thus generating cDNA. The RT

reaction solution was then heated to 85°C for 5 min, allowing separation of the hybridised RNA: cDNA hetro-duplexes and deactivating the reverse transcriptase. The resulting single stranded complementary DNA (cDNA) was stored at −80 °C. The 20 μl reaction was then diluted 1:4 by addition of 60 μl of sterile H_2O before the use of quantitative polymerase chain reaction.

2.5.4 Real-Time Quantitative Polymerase Chain Reaction (RT-qPCR)

Each RT-qPCR reaction was carried out in a final volume of 20 μl. For each 20 μl reaction 4 μl of the cDNA generated from RT was added to a 96 well plate with 10 μl of SYBR green mastermix reagent (2X), 0.6 μl of forward primer (10 μM) and 0.6 μl reverse primer (10 μM) for a given gene followed by 4.8 μl of sterile H_2O. 18S ribosomal RNA was used as an internal endogenous control to enable normalisation of the data according to the total amount of cDNA present in each sample.

RT-qPCR SYBR green assays were performed using ABI Prism 7000 sequence detection system (Applied Biosystems UK Ltd) according to manufacturer's instructions. Amplification was carried out using a cycle of 95°C for 1 second and 60°C for 1 minute for 40 cycles. A final dissociation stage was included to determine product purity and primer efficiency.

2.5.5 Primer Design

All primers for SYBR assays were designed using the internet based software UCSC genome and PrimerBlast. Primers were then purchased from Invitrogen Ltd. Primers were designed to have an annealing temperature (T_M) between approximately 55-

60°C and a GC content of 50-60%. All primers (lypholised upon arrival) were reconstituted in sterile H_2O to generate a stock concentration of 200 μM. The primer sequences are listed below.

Table 2.1 Murine SYBR qPCR primers

Gene		Primers
TGF-β1	F	TGAGTGGCTGTCTTTTGACG
	R	GCTGAATCGAAAGCCCTGTA
PAI-1	F	TCATCAATGACTGGGTGGAA
	R	GCGTGTCAGCTCGTCTACAG
CTGF	F	AGGGCCTCTTCTGCGATT
	R	GTACACCGACCCACCGAAG
E-cadherin	F	TGAAGGCGGGAATCGTGGCA
	R	AGGATCAGAATCAGCAGGGCGAGG
αSMA	F	AACTGGGACGACATGGAAA
	R	AGGGTGGGATGCTCTTCAG
Snail-1	F	TGAGAAGCCATTCTCCTGCT
	R	CTTCACATCCGAGTGGGTTT
Slug	F	CACATTAGAACTCACACTGGGGA
	R	TGATCTGTCTGCAAAAGCCCT
Zeb1	F	CCAGCCAAACGGAAACCAGGATG
	R	TGGGTGGCGTGGAGTCAGAGT
Zeb2	F	TTCTCCCCCACACTTCGCGG
	R	GCACGCAGGCTCGATCTGTGA
Col1a1	F	CCCTGGTCCCTCTGGAAATG
	R	GGACCTTTGCCCCCTTCTTT

Col1a2	F	AGTCGATGGCTGCTCCAAAA
	R	AGCACCACCAATGTCCAGAG
Fibronectin	F	TGTACCTGCTATGGAGGAAGC
	R	CCAGTGTATTTGTCAAAGCAAG
HAS2	F	GAGCAGGAGCTGAACAAGATGC
	R	TTCCGAGGAGGAGAGACACT
HAS3	F	TGGACTACATCCAGGTGTGTG
	R	CTCCAACACCTCCTACTTGGG
MMP3 and 10	F	TCAGTACCTTCCCAGGTTCG
	R	TTTCAATGGCAGAATCCACA
TIMP1	F	CATGGAAAGCCTCTGTGGAT
	R	AAGAAGCTGCAGGCACTGAT
SMAD7	F	TCTCAAACCAACTGCAGGCT
	R	TTGGGAATCTGAAAGCCCCC
ZBP89	F	GGAAAGGCACAAAAGAACTCA
	R	TCGTGATTTTCATGGCACATA

Table 2.2 Human SYBR qPCR primers

Gene		Primer
TGF-β1	F	CCTTTCCTGCTTCTCATGGC
	R	ACTTCCAGCCGAGGTCCTTG
PAI-1	F	TCTCTGCCCTCACCAACATTC
	R	CGGTCATTCCCAGGTTCTCT
MMP3	F	TCTGAGGGGAGAAATCCTGA
	R	GGAAGAGATGGCCAAAATGA
TIMP1	F	AGACGGCCTTCTGCAATTC
	R	TGGTATAAGGTGGTCTGGTTGA

Fibronectin	F	CCGAGGTTTTAACTGCGAGA
	R	TCACCCACTCGGTAAGTGTTC
MMP1	F	GCTCAGGATGACATTGATGG
	R	ACACGCTTTTGGGGTTTGT
Col1a1	F	CATGTTCAGCTTTGTGGACCTC
	R	TTGGTGGGATGTCTTCGTCT
Col1a2	F	GGCTCTGCGACACAAGGAGT
	R	TGTAAAGATTGGCATGTTGCTAGGC
SMAD7	F	AGATGCTGTGCCTTCCTCCGCT
	R	GAAGTTGGGAATCTGAAAGCCCCC
ZBP89	F	TGGAAAGGCATAAGAGAACTCA
	R	TGATTTTCATGGCACATACG

2.6 Western Blot

2.6.1 Protein extraction

Total protein was extracted from HPMC monolayers via cell lysis. Briefly, serum free medium was aspirated and replaced with appropriate volume of ice-cold PBS dependent on culture vessel. Cell lysis occurred via "scraping" of the culture vessel with a cell scraper or pipette tip. The cell lysates were transferred to clean eppendorf and centrifuged for 1 minute at 13000 rpm to form a pellet. Supernatant was removed and pellet was resuspended in appropriate volume (100 μl) of 1X RIPA lysis buffer (mix of 1X TBS, 0.5% NP-40, 0.5% sodium deoxycholate, 0.004% sodium azide) supplemented with PMSF solution (1 μl), sodium orthovanadate (1 μl) and protease cocktail inhibitor (1 μl).

2.6.2 Determination of protein concentration

Protein concentrations of samples were determined using the BioRad protein assay. Firstly, stock solution of BSA (10 mg/ml) was serially diluted with H_2O to produce standards ranging in concentration from 1000-15.625 μg/ml. Sample protein concentration was determined by direct comparison to these BSA standards. BSA standards and diluted protein samples (1:10) were loaded in triplicate into a clear flat bottomed 96 well plate (5 μl). BioRad protein assay (5X) was diluted 1:5 with H_20 and added to the wells (200 μl/well). Samples were incubated for 5 minutes at room temperature before absorbance was measured using FLUOSTAR OPTIMA.

2.6.3 Gel Preparation

SDS-polyacrylamide running gels were used for all Western blotting experiments, and the percentage of the gel was adjusted depending on the protein of interest (ranging from 7.5%-10%). Gels were made using a Gel Cassette apparatus (BioRad laboratories Ltd). An SDS-polyacrylamide running gel was poured into the apparatus leaving a 2 cm gap from the top. The gel was then overlaid with water to ensure that the gel set equally within the cassette. Once the running gel had polymerized (approximately 20-30 minutes), the water was removed and replaced with a stacking gel. A comb was inserted into the cassette to allow wells to form within the stacking gel. Gels were left to polymerise for 20 minutes or allowed to polymerise overnight depending on commencement of experiment.

2.6.4 Reduction of samples and electrophoresis

Following determination of concentration equal amounts of samples (20-30 μg) was added to clean eppendorf with equal volume of 1X reducing loading buffer (0.5 M

Tris-HCl (pH 6.8), glycerol, 10% SDS, 0.05% bromophenol blue and β-mercaptoethanol). Samples were then boiled at 95°C for 5 minutes, then vortexed and centrifuged briefly. Following this samples were then loaded onto the gel, which was submerged in 1X running buffer. Broad range molecular weight protein marker (20 μl) was also loaded onto the gel to enable confirmation of target protein size. The gel was then run at 100 V for 20 minutes and then 150 V until the loading buffer had migrated down 90% of the gel.

2.6.5 Transfer to nitrocellulose membrane

Following electrophoresis gel was removed from electrode apparatus and inserted into transfer apparatus with a nitrocellulose membrane. Both gel and membrane were placed between a layer of filter papers and plastic wool pads. The apparatus was then submerged in chilled 1X Transfer buffer. The transfer procedure was carried out at 100 V for 1 hour with cooling.

2.6.6 Blocking of nitrocellulose membrane

After transfer, the nitrocellulose membrane was blocked in 5% w/v skimmed powdered milk dissolved in PBS Tween-20 (0.1%) for 1 hour.

2.6.7 Incubation with Primary and Secondary Antibody

The nitrocellulose membrane was then incubated with the specific primary antibody, diluted according to manufacturer's instructions with PBS Tween 20 (0.1%) and bovine serum albumin (0.1-5%). The membrane was incubated overnight at 4°C with gentle rocking. After incubation, the membrane was washed with PBS-Tween

20 (0.1%) for 3 quick washes and 3 slow washes lasting 1 hour in total. Following these washes, the membrane was then incubated with the appropriate horseradish peroxidase-conjugated secondary antibody (diluted 1:10000) in 1% BSA and PBS Tween 20 (0.1%). Incubation occurred at room temperature for 1 hour with rocking.

2.6.8 ECL detection

After incubation with secondary antibody the membrane was again washed (3X quick and 3X slow) with PBS Tween 20 (0.1%) over a 1 hour period. The binding of the antibodies was visualised using the ECL chemiluminescence system. ECL reagents A and B were added dropwise to the membrane in a ratio of 40:1 and left for 1 minute. The blot was then developed on high performance autoradiography film, with exposure time varying depending on the experiment.

2.7 Immunohistochemistry (IHC)

HPMC were grown to 50-60% confluence on an 8-well glass chamber slide (Gibco) and were washed twice in PBS. The cells were then fixed and permeabilised using 4.5% paraformaldehyde for 30 min at room temperature. Following fixation, the paraformaldehyde was removed through PBS washes and the cultures subsequently stored in PBS at 4°C. The cells were then blocked using 1% bovine serum albumin (BSA) in PBS before addition of the primary antibody and overnight incubation at 4°C with rocking.

Following staining of the cells with the primary antibody, the cells were washed three times in 0.1% PBS/BSA before incubation with a FITC secondary antibody for 1

h at room temperature protected from light. This was followed by staining of the nuclei using Hoechst 3342 for 15 minutes at room temperature, again protected from light. Cells were then washed for a final time before mounted with Fluorsave mountant and then observed and photographed under a Leitz Orthoplan fluorescence microscope (Leica UK Ltd, Milton Keynes, UK).

2.8 Measurement of matrix metalloproteinase activity

2.8.1 Zymography

2.8.1.1 Supernatant collection and solubilisation

Following stimulation of HPMC monolayers in serum free medium, supernatant was collected from cells and transferred to clean eppendorfs before being stored at minus 80°C until use. Following collection 10 μl of sample was transferred to eppendorf along with an equal volume of non-reducing loading buffer (0.5 M Tris-HCL(pH 6.8), 10% SDS, glycerol, H_2O and 0.05% bromophenol blue). Samples were then incubated in solution at room temperature for at least 30 minutes.

2.8.1.2 Gel Preparation

SDS-polyacrylamide running gels were used for all zymography experiments, and the percentage of the gel was adjusted depending on the protein of interest (ranging from 7.5%-10%). Gels were made using a Gel Cassette apparatus (BioRad laboratories Ltd). An SDS-polyacrylamide running gel incorporated with the specific substrate was poured into the apparatus leaving a 2 cm gap from the top. The gel was then overlaid with water to ensure that the gel set equally within the cassette. Once the running gel had polymerized (approximately 20-30 minutes), the water was

removed and replaced with a stacking gel. A comb was inserted into the cassette to allow wells to form within the stacking gel. Gels were left to polymerise for 20 minutes

2.8.1.3 Electrophoresis

Once gels had polymerised samples were loaded onto gel, which was submerged in ice-cold 1X running buffer. Broad range molecular weight protein marker (20 μl) was also loaded onto the gel to enable confirmation of target protein size. Electrophoresis was carried out at 50-60 V at 4°C for approximately 3-4 hours until the loading dye had migrated down 90% of the gel.

2.8.1.4 Removal of SDS

Following electrophoresis, gel was removed from cassette and washed in 2.5% Triton solution (200-250 ml per gel). The gel was washed for 1 hour at room temperature with gentle rocking. Triton solution was then removed and replaced with 250 ml of 1X incubation buffer. The gel was incubated with the incubation buffer overnight at 37°C with gentle rocking.

2.8.1.5 Visualisation of Enzyme Activity

After incubation, gel was stained with PAGE stain for 3-4 hours with gentle rocking. Enzyme activity was visualised by the appearance of clear bands within the blue stained gel.

2.8.2 Fluorogenic Substrate assay

2.8.2.1 Substrate and sample preparation

Substrate M-2300 (Bachem) was reconstituted to 5 mM stock using 50% acetic acid and H_2O. Substrate M-2300 was then diluted (1:500) with 2X Substrate assay buffer (400 mM NaCl, 50 mM Tris, 10 mM $CaCl_2$, 40 μM $ZnSO_4$, 500 ml H_2O, 0.1% Brij). Supernatant was collected from stimulated HPMC growth arrested in serum free medium for 24 hours[321, 322].

2.8.2.2 Measurement of total MMP3 activity

To activate total MMP3 within sample, 50 μl of supernatant was added to 96 well plate suitable for fluorescence and incubated with 3.3 μl of PAMA for 1 hour at 37°C. Following incubation 50 μl of diluted M-2300 substrate was added to each well. Absorbance was measured at varying time intervals (15 minutes – 48 hours).

2.8.2.3 Measurement of active MMP3

To measure activity of the active enzyme 50 μl of supernatant was added to 96 well plate suitable for fluorescence along with 50 μl of diluted M-2300 substrate. Absorbance was measured at varying time intervals (15 minutes-48 hours).

2.9 Polymerase Chain Reaction (PCR)

The PCR was carried out in a final volume of 50 μl per reaction, containing 5 μl of 10x AccuPrimeTM (Invitrogen) PCR Buffer II, 1 μl each of 20 μM sense strand and antisense strand primers, 100 ng of gDNA, 1 μl of AccuPrime® Taq and the remaining volume was made up using sterile H_2O. The PCR amplification was

performed in a GeneAmp® PCR system 9700 Thermocycler (Applied Biosystems). Each reaction was heated to 94°C for 1 minute, and was then followed by 35 cycles of 94°C for 30 s, 55°C for 30 s and 68°C for 2 min ending with 68 °C for 7 min.

2.9.1 Sizing of PCR Products

All PCR products were run on a 2% 50 ml agarose gel. Each gel contained 2% (w/v) agarose, 50 ml 1x TAE and 5 μg/ml of ethidium bromide. Ten μl of PCR product was loaded onto the gel along with 2 μl of loading buffer (bioline) and 10 μl of a 100 bp ad 1 kb DNA ladder (New England Biolabs). Once the PCR products were loaded onto the gel, electrophoresis was undertaken using 75-90 V for 60-120 min until the products had migrated down 90% of the gel. The PCR products were then visualised and photographed using a ChemiDoc® Gel documentation system.

2.9.2 Purification of PCR Products

PCR products were gel purified using the QIAquick® Gel purification kit (Qiagen Ltd, Crawley, UK) in accordance with the manufacturers protocol. Briefly, bands were made visible on a UV transilluminator (GRI, Braintree, UK) where they were excised from the gel using a sterile scalpel and then melted in triple the volume of buffer PB (supplied in kit) at 50°C until the gel slice had completely dissolved. One gel volume of isopropanol was then added to the sample and each sample was transferred to a spin-column and centrifuged at 13,000 g for 1 min through a filter column, to bind the DNA. DNA bound to the column was then washed with 750 μl ethanol by centrifugation (13,000 g for 60 s) and eluted in 30 μl of sterile H_2O.

2.9.3 Generation of Luciferase Promoter Constructs

The Purified promoter constructs were ligated into a modified version of the pGL-3® Basic luciferase reporter vector (Promega Ltd) in which the multiple cloning site had been altered to include cleavage sites from other common restriction enzymes (supplied by Dr. P. Buckland, Department of Psychological Medicine, Cardiff University School of Medicine). Appendix IV shows the original and modified sequence of the pGL-3 multiple cloning sites. Using the restriction enzymes HindIII and Nco1, 5 μg of modified pGL-3 vector was digested for 2-3 h at 37°C in 50 μl of New England Biolabs Buffer 2. The digested vector was then analysed by electrophoresis on a 2% agarose gel before being extracted using the QIAquick gel extraction kit in accordance with the manufacturer's protocol. Two μg of the digested vector was then treated with 2 μl of shrimp alkaline phosphatase (Promega Ltd) in a total volume of 30 μl. The reaction was heated to 65°C for 60 min to ensure deactivation of the enzyme and prevent re-ligation of the vector.

As with the pGL3 basic modified vector, the purified promoter fragments were digested using 0.5 μl of HindIII and Nco1 in a 50 μl reaction of NEB buffer II and purified as described previously. The promoter fragments and pGL3 basic vector's DNA concentration were determined using the Nanodrop and converted into pica moles to enable an accurate molar ratio to be determined for the ligation reaction. The promoter constructs were ligated into the digested and dephosphorylated pGL-3 vector using a 3:1 ratio of insert to plasmid; 6 μl of promoter fragment, 2 μl of vector, 1 μl of 10 x ligase buffer and 1 μl of T4 DNA ligase (New England Biolabs (UK)

Ltd, Hitchin, UK) in a total volume of 10 μl. The reaction was then incubated at 16°C for 24 h.

2.9.4 Transformation

Following ligation 3 μl of each sample were added to 16 μl (10^8 cfu/μg) of *Escherichia coli* cells and incubated on ice for 30 min. The cells were then heat-shocked by incubating at 42°C for 30 s before being placed back on ice for 5 min. To the cells, 400 μl of SOC medium was added. The samples were then shaken and incubated at 37°C for 60 min in an orbital shaker (200 rpm). These cells were then plated on to LB Agar (see Appendix V) containing 100 μg/ml ampicillin and incubated at 37°C overnight.

2.9.5 Purification of Recombinant Vectors

From each plate 6 colonies were selected and transferred to a liquid culture consisting of 5 ml of LB broth and 100 μg/ml of ampicillin) and incubated in the orbital shaker at 37°C, overnight. Following incubation 1.5 ml aliquots of each cell culture were centrifuged at 13,000 g for 1 min to enable pelleting of the cells. The supernatant was then removed by decanting. Cell pellets were then purified using GenElute™ HP Plasmid Miniprep Kit according to manufacturer's protocol (Sigma-Aldrich, UK).

Briefly, the cell pellets were re-suspended in 200 μl of Resuspension solution containing RNase by pipetting up and down until solution was homogenous. This was followed by the addition of 200 μl of lysis buffer. The solutions were then mixed by

inversion and left to incubate at room temperature for a maximum of 5 min before the addition of 350 μl of neutralising buffer. Samples were then mixed by inversion and then centrifuged at 13,000 g for 10 min. The supernatants were loaded onto GenElute Miniprep Binding columns within clean eppendorfs and centrifuge again for 1 min at 13,000 g. The flow-through liquid was discarded and 500 μl of Wash Solution 1 was added to the columns followed again by another 1 min centrifugation at 13,000 g. Again, flow-through liquid was discarded and 750 μl of Wash solution 2 containing ethanol (95%) was loaded onto the column, again followed by a 1 min centrifugation at 13,000 g. After removal of the ethanol, the columns were transferred to fresh eppendorfs and promoter constructs were eluted in 100 μl of Elution solution by centrifugation at 13,000 g for 1 minute(10mM Tris-HCL, ph8.5) Samples were then centrifuged for a further 4 min at 13,000 g before being stored at -20°C.

2.9.6 Screening for Presence of Inserts

In order to confirm the presence of the desired insert, 5 μl of each sample was then digested with the appropriate restriction enzymes for 2 h, to excise the inserted fragments. These digested samples were then loaded onto a 2% agarose gel along with as previously mentioned a 100 bp and 1 kb DNA ladder. After visual inspection to ensure that the insert was present within the vectors, the colonies containing the promoter insert were then sequenced as described in section 2.4.11.

2.9.7 Sequence Analysis

In order to verify the integrity of the amplified target sequence, all promoter constructs were sent for sequence analysis to The DNA Sequencing Core, Main Building Cardiff University, Cardiff, UK. Promoter constructs were sequenced in the pGL-3 modified vector using the pGL3 forward and pGL reverse primers

2.10 Luciferase Analysis of MMP3 promoter constructs

2.10.1 Transient Transfection

Transient transfection of Met5a cells were performed using the lipofection agent Lipofectamine® LTX (Invitrogen). Confluent T75 flasks of Met5a cells were sub-cultured as described previously and plated into 12-well plates (1 ml per well). Cells were grown to a confluence of between 60-80% prior to transfection. When the cells reached the required confluence the growth medium was aspirated and replaced with M199 medium containing 10% FCS and all supplements described except for penicillin/streptomycin (Antibiotic-free medium). The cells were then transfected with 0.4 μg of the MMP3 promoter firefly luciferase constructs and 0.1 μg of Renilla luciferase vector (Promega Ltd) per well in accordance with the manufacturer's instructions. For each 12 well plate, 4.8 μg of promoter construct and 1.2 μg renilla DNA were diluted into 1.2 ml of Opti-MEM reduced serum medium (Gibco) and mixed, before addition of 6 μl of PLUS Reagent® (Invitrogen). This mixture was incubated at room temperature for 5 min. This was then followed by the addition of 30 μl of Lipofectamine® LTX reagent and a further incubation at room temperature for 30 min to allow transfection complexes to form. The transection complexes were then added drop-wise to the 12 well plate (100 μl per well). The cells were then

incubated in the transfection medium overnight (18-20 h) before the medium was aspirated and replaced with serum free medium. Cells were then growth arrested for 24h before addition of stimuli depending on experimental design for a further 24 h.

2.10.2 Reporter Gene Analysis in Met5a cells

At the end of the experiment the stimulation medium was removed and the cells were washed with PBS before the addition of 250 μl of cold 1X passive lysis buffer (Promega) per well. The cells were then incubated at room temperature for 15 min with gentle agitation to ensure cell lysis. Any remaining adhered cells were removed by scraping and the cell suspension was transferred to 1.5 ml micro-centrifuge tubes. Cells were then incubated overnight at -20°C to ensure complete cell lysis. The next day samples were thawed at room temperature for 15-30 minutes. Each sample was then vortexed for 10 s before the addition of 20 μl of cell lysate from each sample was transferred to a white luminometric 96-well plate (Thermo Life Sciences). Luciferase activity was then assayed using the Dual-Glo® luciferase assay kit as described in the manufacturer's protocol. Briefly, 50 μl of Luciferase Assay Reagent II (LARII) was added to each sample in the 96-well plate and gently mixed. Immediately after this the luminescence of each well was read for 10 s using a luminometer (FLUOSTAR® Optima, BMG Labtechnologies GmbH, Offenburg, Germany). Following the firefly luminescence reading, Stop and Glo reagent (50 μl) was then added and Renilla luminescence in each sample was recorded as before. The Renilla luciferase activity was measured in the same cell lysates as a measure of transfection efficiency.

2.11 Nuclear Protein Extraction

HPMCs and Met5a cells were cultured in T75 to passage 2 and 15 respectively until at least 80% confluence. Following growth arrest and experimental conditions, cell monolayers were washed in ice cold PBS at equal volume to the culture medium (15 ml). Following the first wash cells were submerged again in equal volume to the culture medium of ice cold PBS and placed on ice for 1-2 minutes. The PBS was removed and then replaced with 2 ml of ice-cold PBS to which the cell monolayers were scraped into using a cell scraper and transferred to a fresh 2 ml eppendorf. Samples were then centrifuged at 13000 rpm for 2 minutes at 4°C causing the cells to form a pellet at the bottom of the eppendorf. The cells were lysed in 40 μl of ice-cold cytoplasmic protein extraction buffer (10 mM HEPES pH8, 1.5 mM $MgCl_2$, 10 mM KCl, 0.5 mM DTT, 0.2 mM PMSF, 1 mM Na_3VO_4, 1 mM NaF and 20 μl of Protease inhibitor cocktail (Sigma)) and incubated on ice for 10 minutes. The samples were then vortexed for approximately 10 seconds and centrifuged at 4°C for 2 minutes at 13000 rpm. The supernatant (cytosolic extract) generated from this centrifugation was transferred to a clean eppendorf. The pellet was resuspended in 40 μl of nuclear protein buffer (20 mM HEPES, 1.5 mM $MgCl_2$, 25% glycerol, 420 mM NaCl, 0.2 mM EDTA, 0.5 mM DTT, 0.2 mM PMSF, 1 mM Na_3VO_4, 1 mM NaF and 20 μl of Protease inhibitor cocktail (Sigma)) and incubated on ice for 20 minutes with frequent vortexing. The samples were centrifuged at at 4°C for 5 minutes at 13000 rpm. The supernatant (nuclear extract) was then transferred to a clean eppendorf tube and stored at -80°C.

2.11.1 Determination of nuclear protein concentration

To quantify nuclear cell extract protein concentration the micro BCA™ Protein Assay Kit (Thermo Scientific) was used. A standard curve of Bovine Serum Albumin (Sigma) was prepared fresh for each assay, ranging from 100 μg to 1.5625 μg. Cell extracts were diluted typically 100-fold to ensure that the protein concentration fell within the range of the standards used for the assay. 150 μl aliquots of standards and sample were pipetted in duplicate into a clear 96-well plate along with 150 μl of micro BCA reagent (25 parts micro BCA reagent MA, 24 parts micro BCA reagent MB and 1 part micro BCA reagent MC). Wells were mixed thoroughly before being covered with Sealing Tape and incubated at 37°C for 2 hours. The plate was then cooled to room temperature before absorbance at 560 nm was measured using the OPTIMA-Flo Star plate reader. If the sample reading fell outside the standard curve, the dilution was adjusted and the assay repeated.

2.12 Non-Radioactive Electrophoretic Mobility Shift Assay

2.12.1 Annealing biotinylated probes

Sense and anti-sense biotinylated oligonucleotide primers (40 ng) were annealed in 50 μl reactions using Oligo annealing buffer (Promega). Samples were placed in a water bath (90°C) for 3 minutes. The samples were then cooled on a heating block at 37°C for 15 minutes before being stored at -80°C.

2.12.2 Binding reaction

Nuclear extracts collected from HPMC (3 μg) were incubated with 0.5 ng of annealed biotinylated oligonucleotides in a binding reaction solution of 20 μl. The binding reaction consisted of 4 μl of 5X Binding Buffer (89 μl of 5X reaction buffer stock (50μl 1 M HEPES pH8, 250 μl 1M KCl, 500 μl 100% Glycerol, 90 μl dH_2O), 10 μl 10 mg/ml Acetylated BSA, 0.5 μl 1 M DTT, 1.0 μl 0.1 M PMSF), 1 μl of Poly dIdC (1 mg/ml) and H_2O made up to a volume of 18 μl. The reaction was incubated at room temperature for 30 minutes. Following incubation 2 μl of DNA loading buffer was added to each binding reaction.

2.12.3 Gel preparation

Gels were made using a Gel Cassette apparatus (BioRad laboratories Ltd). Mini- gels were made with final concentration of 4% polyacrylamide to ensure optimal separation. Two mini gels were made using 29.5 ml of H_2O, 5 ml of Acrylamide (stock concentration 40%), 10 ml of 5X TBE (54 g Tris, 27.5 g Boric acid, 20 ml 0.5 M EDTA pH8 made up to 1 Litre with dH2O), 5 ml of glycerol (50%), 0.5 ml Ammonium Persulphate (10%) and 40 μl of TEMED. Gels were left to solidify for 30 minutes.

2.12.4 Electrophoresis

Samples (20 μl) were loaded onto gel. The gels were placed in electrophoresis cassette (BioRad laboratories Ltd), and submerged in 0.5X TBE running buffer. The cassette was placed in ice and the samples were run on the gel at 180 V for 30 minutes when the loading dye had migrated down 90% of the gel.

2.12.5 Transfer and blocking of nitrocellulose membrane

Following electrophoresis the gel was transferred into a transfer cassette and placed on top of filter paper and plastic gel pad. A Hybond-N+ membrane was then placed on top of the gel and then filter paper and gel pad placed on top of the membrane. The cassette was then placed into ice cold 0.5X TBE for 1 h at 400mA. Following transfer, the membrane was blocked with 15 ml of PBS-0.1% Tween-20 containing 1% BSA.

2.12.6 Incubation with Antibody

After the membranes were blocked, the membranes were incubated with 20 ml of PBS-0.1% Tween-20 containing 1% BSA mixed with 100 μl of streptavidin-HRP for 1-2 hours at room temperature on a rocker.

2.12.7 ECL detection

Antibody solution was removed and the membrane was washed 3X with PBS-0.1% Tween-20. The binding of the antibody was visualised using the ECL chemiluminescence system. ECL reagents A and B were added dropwise to the membrane in a ratio of 1:1 ensuring full coverage of the membranes and left for 1 minute. The blot was then developed on high performance autoradiography film, with exposure time from 1-3 minutes.

2.13 Statistical Analysis

All statistical analysis was performed using the software GraphPad Prism version 4. Data was generated from biological replicates for both mouse samples (≥3 different

mice per time point and genotype) and HPMC cultured separately (≥3 omental donors per experiment). Normality was determined using the Kolmogorov-Smirnov (KS) test to assess deviation from Guassian distribution. If data was determined to display normality parametric tests including one way and 2-way ANOVA were used with Bonferronni post-test ($p<0.05$*, $p<0.005$**, $p<0.0005$***). Results were deemed statistically significance at p-value of <0.05.

Chapter 3: Characterisation of the TGF-β1 response within the SES murine model of inflammation driven peritoneal fibrosis

3.1 Introduction

Inflammation is a key response within the body, enabling protection and subsequent removal of foreign pathogens that can elicit harm and damage[223]. The actions of TGF-β1 on the inflammatory response (as described in chapter one) can promote and suppress inflammation, thus suggesting an important balance in egulating the inflammatory response to ensure that it remains beneficial to the host and not pathogenic[155]. Inflammation involves a variety of signalling pathways and molecules and the overall summation of these interactions influences the duration and regulation of this process.

Chronic inflammation occurs when there is persistent stimulus or dysregulation in the inflammatory response. This is shown to be associated with the development of fibrosis, another process in which TGF-β1 has a central role[323]. The peritoneum within dialysis patients is deemed chronically inflamed, with causes being attributed to recurrent peritonitis infections and bio-incompatible dialysate solutions[57]. The SES murine model developed by Fielding et al (2014) replicates changes observed in dialysis patients that have suffered recurrent peritonitis infections by injecting mice with persistent SES infection (Figure 3.1). The development of fibrosis within the mice attributed to IL6 dependent release of IFN-γ[265].

The involvement of TGF-β1 and its response was not characterised within this model. This chapter will aim to elucidate the TGF-β1 response in both WT and IL6KO mice,

to determine whether TGF-β1 is involved in the fibrotic process observed in WT mice following persistent SES infection and to examine if the TGF-β1 response differs in IL6KO mice. Previous research has indicated that TGF-β1 exerts fibrotic effects within the peritoneum and blockade of TGF-β1 ameliorates these effects[152]. Interactions between inflammatory signalling and TGF-β1 signalling are still being elucidated, therefore this model provides an opportunity to determine if the absence of inflammatory signalling protects against fibrosis through modulation of the TGF-β1 response.

The aims of this chapter will be:

- To characterise the TGF-β1 response in WT and IL6KO mice between day 28-49
- To determine differences at the mRNA level in the fibrotic response between mice genotypes

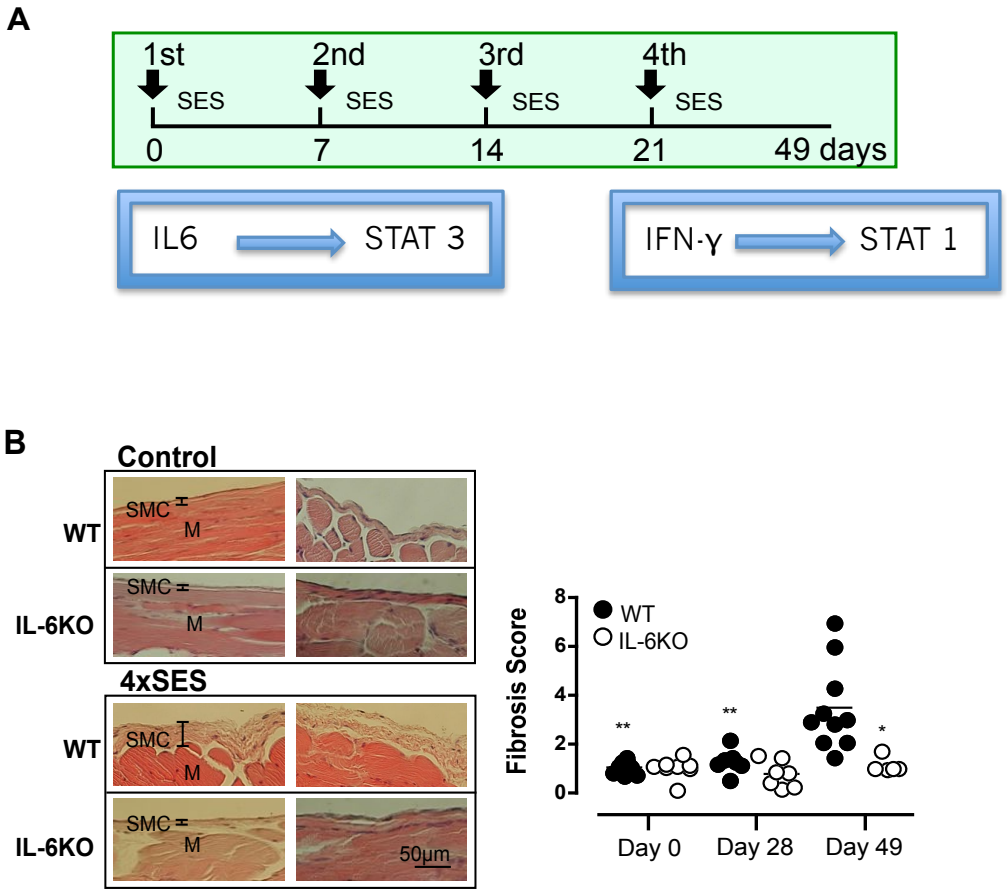

Figure 3.1 The *in vivo* model of inflammation driven peritoneal fibrosis
A model of SES-induced inflammation was developed by Fielding *et al* (2014) to investigate the role of inflammation in tissue fibrosis (A). WT and IL6KO mice were injected (i.p.) at weekly intervals with SES for 4 weeks and then left for a further 5 weeks at day 49 when the peritoneal membrane was histologically examined. The first 3 injections in WT mice generated a release of IL6 and activation of STAT 1 whereas the 4th hit stimulated a release of IFN-γ and activation of STAT 1. This switch was concluded to induce tissue fibrosis, which became evident at day 49 and was not apparent in IL6KO mice (B). 5µm sections of peritoneal membrane were taken from SES treated and age matched control mice on Day 49 were stained with haematoxylin/eosin and examined for thickening of the sub-mesothelial compact zone layer between the muscle and membrane surface. Representative fields are shown from two individual mice per group (x400 magnification). Scale bar, 50µM. Sub-mesothelial compact zone (SMC) and muscle layers (M) are indicated on representative WT sections. Sections were scored in terms of fibrotic development from WT and IL-6KO mice on Day 0, Day 28 and Day 49 as fold-change in sub-mesothelial zone thickness compared to the WT control group at Day 49 (n≥5 per group, unpaired t-test * P<0.05 or ** P<0.01 compared to WT Day 49). This data was generated and analysed by Fielding et al (2014).

3.2 Results

3.2.1 WT mice have a greater TGF-β1 response compared to IL6KO mice

The SES murine model of inflammation driven fibrosis reported a significant difference in fibrotic response (Figure 3.1). However, Fielding et al (2014) did not investigate differences in TGF-β1 responses between the different genotypes of mice[265]. Therefore to determine if TGF-β1 is a key mediator in facilitating the fibrosis observed in the murine model, I measured mRNA expression of TGF-β1 (Figure 3.2 A) after the final fourth hit of SES between days 28-49 at the time when fibrosis became histologically apparent. The qPCR analysis showed a significant difference in TGF-β1 expression between the genotypes, with WT mice producing double the amount at day 35 compared to IL6KO.

This led on to investigation of other fibrotic markers. I examined PAI-1 mRNA expression between day 28-49 in both genotypes and found no significant difference in production (Figure 3.2 B). I then measured the expression of Connective Tissue Growth Factor (CTGF), which has been shown to interact with TGF-β1 and maintain fibrosis (Figure 3.2 C). As with PAI-1 mRNA expression there was no difference in the mRNA expression of CTGF between WT and IL6KO mice.

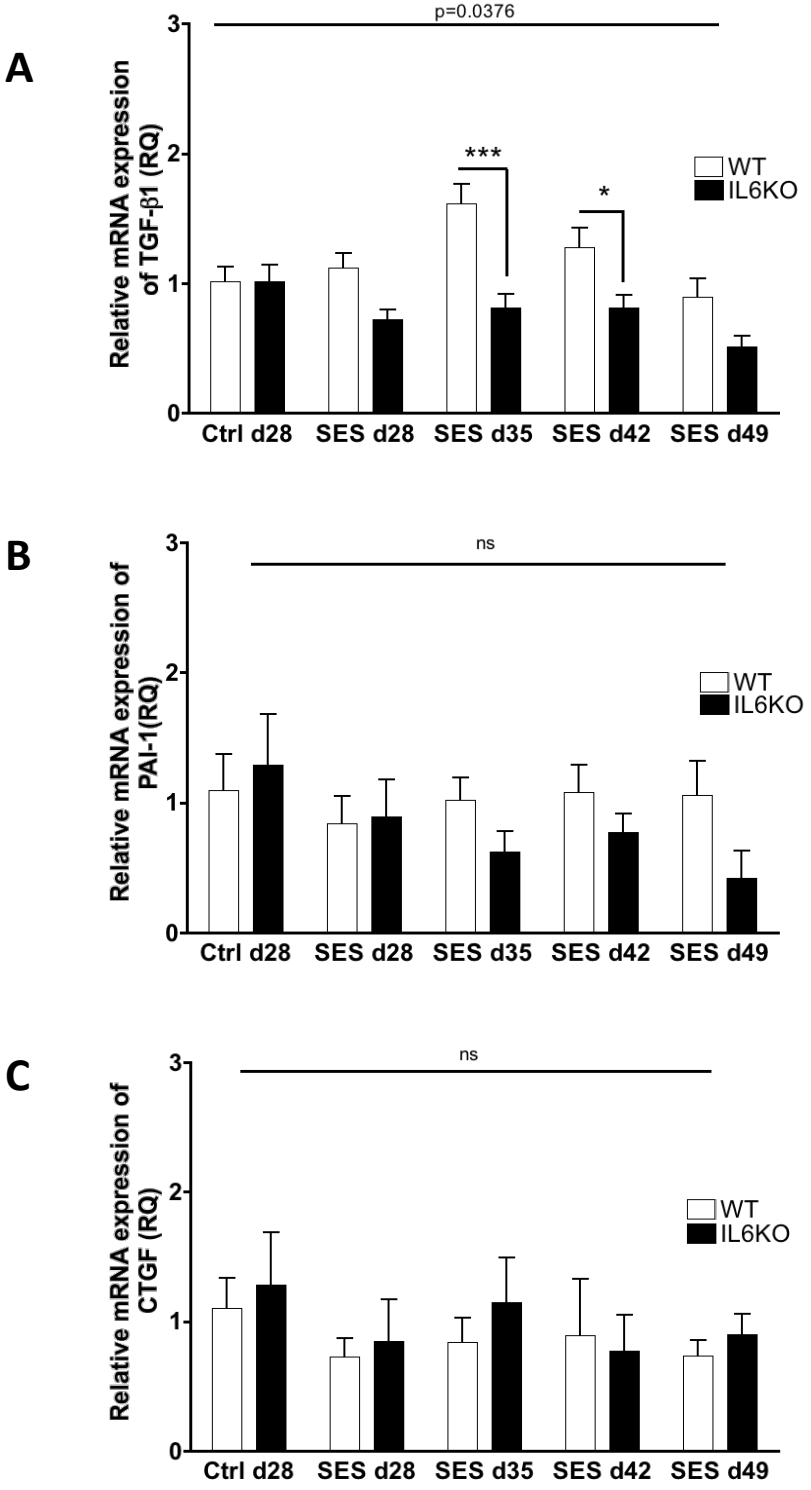

Figure 3.2 Characterisation of the fibrotic response in WT and IL6KO mice
The expression of pro-fibrotic genes in WT and IL6KO mice were determined at the mRNA level by quantitative PCR using cDNA prepared from the peritoneal membrane. The mRNA expression of TGF-β1 (A), PAI-1 (B) and CTGF (C) were measured to determine the degree of fibrogenesis between mice genotypes from day 28 to day 49. Results shown are from cDNA prepared from ≥3 different mice per time point and genotype, expressed relative to WT control. Statistical analysis was performed using 2-way ANOVA followed by Bonferroni post-test ($p<0.05$*,$p<0.0005$***), error bars represent SEM.

3.2.2 WT and IL6KO mice display similar expression of Epithelial-Mesenchymal markers

Epithelial-Mesenchymal Transition (EMT) is a process whereby epithelial cells lose their epithelial characteristics and gain a mesenchymal phenotype and is believed to be a potential source of fibroblasts and a hallmark of fibrosis. Recent data suggests that during PD HPMC undergo EMT, which contributes to the development and progression of peritoneal fibrosis. Overexpression of TGF-β1 has been shown to induce EMT in rat peritoneum. Therefore I examined various EMT markers mRNA expression to determine if EMT is present within the SES model.

I first measured the mRNA expression of E-cadherin (A) and alpha smooth muscle actin (B) (αSMA) (Figure 3.3). There was no difference in the expression of either marker between genotypes. This led me to examine changes in the expression of genes involved in the repression of E-cadherin (Figure 3.4 and Figure 3.5). I found no difference in the expression of Snail-1 between genotypes (Figure 3.4 A). However, there was a significant increase in the mRNA expression of Slug in WT mice at day 35 and 49 (Figure 3.4 B). This was not the case when I measured the expression of Zeb1 (A) and Zeb2 (B) (Figure 3.5), which revealed no difference between the mouse genotypes.

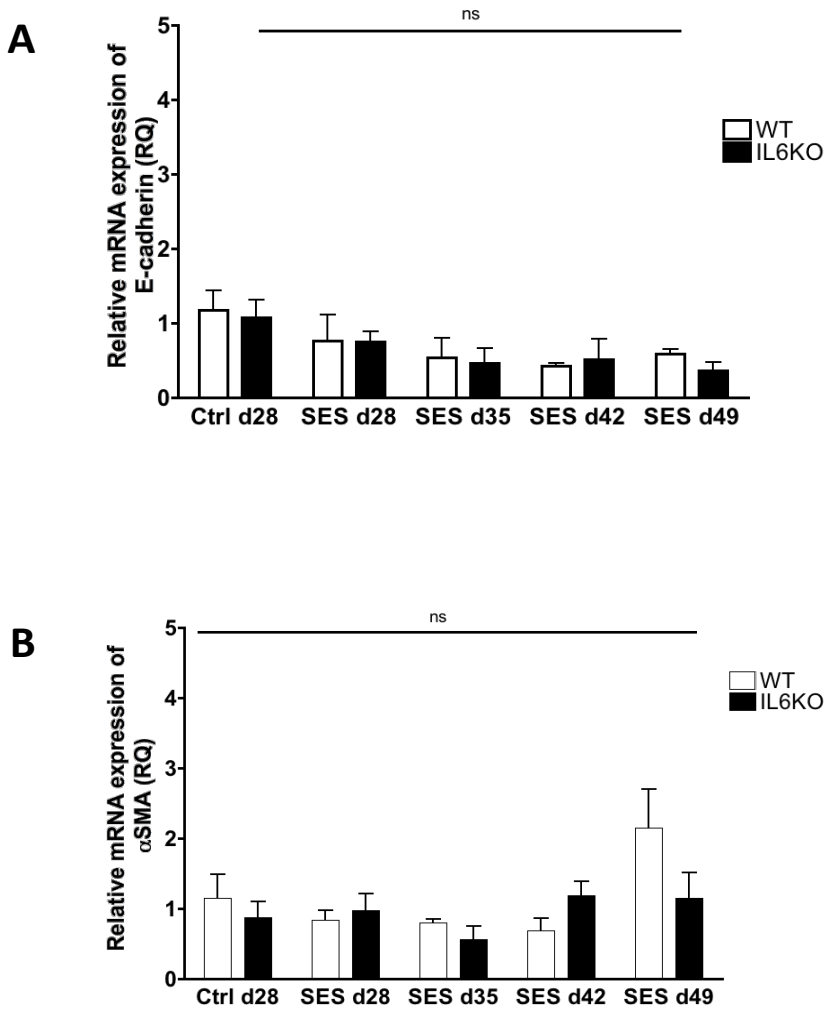

Figure 3.3 No significant difference in mRNA expression of E-cadherin and alpha smooth muscle actin between mice genotype

Extraction of total RNA from peritoneal membranes collected from WT and IL6KO mice at day 28-49 was converted to cDNA and analysed using quantitative PCR. The mRNA expression of E-cadherin (A) and alpha smooth muscle actin (B) were determined with RN-18S used as an endogenous control. The results shown are from cDNA prepared from ≥3 different mice per time point and genotype, expressed relative to WT control, statistically analysed using 2-way ANOVA followed by Bonferonni post-test. A p value of less than 0.05 was deemed statistically significant

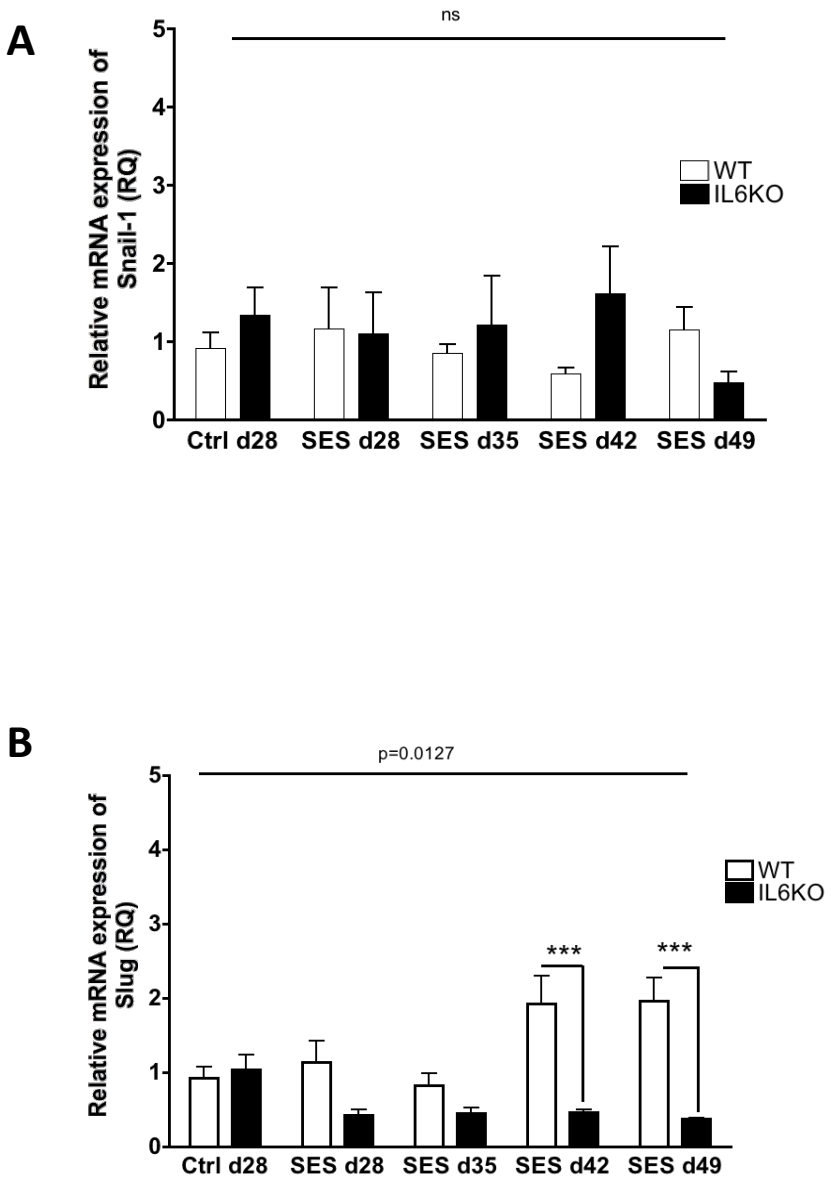

Figure 3.4 Variation in the expression of the E-box repressors between mice genotypes

RNA was extracted from peritoneal membrane samples collected from WT and IL6KO mice at day 28-49 and converted to cDNA. The mRNA expression of Snail-1 (A) and Slug (B) were determined using quantitative PCR, with RN-18S used as an endogenous control. Results shown were generated using cDNA prepared from ≥3 different mice per time point and genotype, expressed relative to WT control. Statistical analysis was performed using 2-way ANOVA followed by Bonferroni post-test ($p<0.0005$ ***).

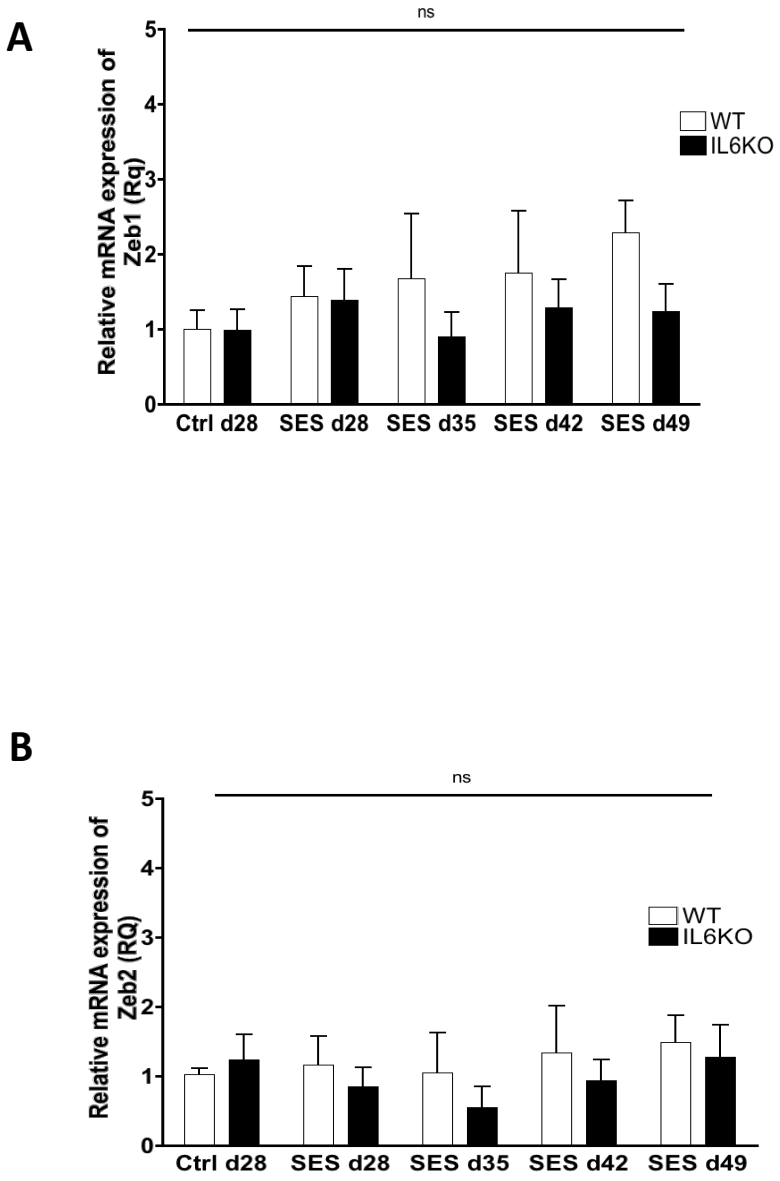

Figure 3.5 Expression of Zeb 1 and 2 does not differ between mouse genotypes
The relative mRNA expression of Zeb1 (A) and Zeb2 (B) was measured in WT and IL6KO mice using quantitative PCR. RNA was extracted from peritoneal membrane samples collected from both mice genotypes from d28-49 and converted to cDNA by reverse transcription. The results shown were generated from cDNA prepared from ≥3 different mice per time point and genotype, expressed relative to WT control. RN-18S was used as an endogenous control gene. Statistical analysis was performed using 2-way ANOVA with Bonferronni post-test.

3.2.3 SES treatment results in greater production of matrix in WT mice

The results of Fielding et al (2014) showed that following SES treatment, there was a greater deposition of collagen within peritoneal sections collected from WT compared to IL6KO (Figure 3.1 B)[265]. I confirmed this at the mRNA level using qPCR to measure col1a1 (A) and col1a2 (B) (Figure 3.6). I found a significant difference in the expression of col1a1 between genotypes, with WT mice expressing 2.5 fold more col1a1 at day 49 compared to IL6KO. Although no significant difference was found in col1a2 expression, there is a trend to suggest that WT mice produce more at the mRNA level.

I examined other matrix components including fibronectin (Figure 3.6 C) and hyaluronic acid production by measuring hyaluronic acid synthase 2 and 3 (HAS 2/3) (figure 3.7). I found significant differences between mouse genotypes in fibronectin and HAS 2 (Figure 3.7 A), with WT mice producing 2 fold more fibronectin and 3 fold more HAS2.

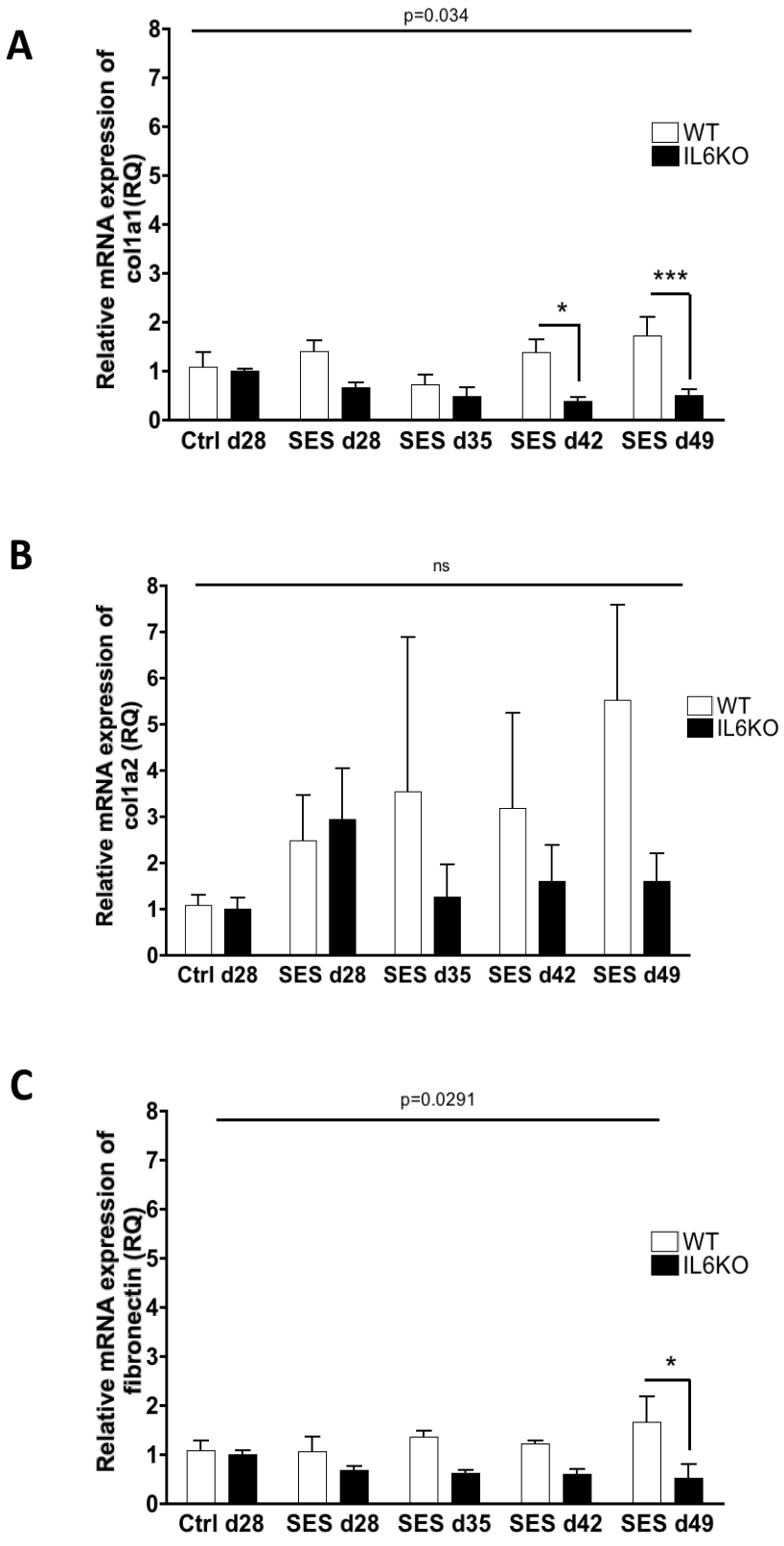

Figure 3.6 WT mice express greater mRNA levels of key matrix components
RNA was extracted from peritoneal membrane samples collected from WT and IL6KO mice from day 28-49 and converted into cDNA. The relative mRNA expression of col1a1 (A), col1a2 (B) and fibronectin (C) were determined using quantitative PCR with RN-18S used as an endogenous control. Results were normalised to WT control samples. The results shown were generated from cDNA prepared from ≥3 different mice per time point and genotype, expressed relative to WT control. Statistical analysis consisted of 2-way ANOVA with Bonferroni post-test ($p<0.05$*, $p<0.0005$). Error bars represent SEM.

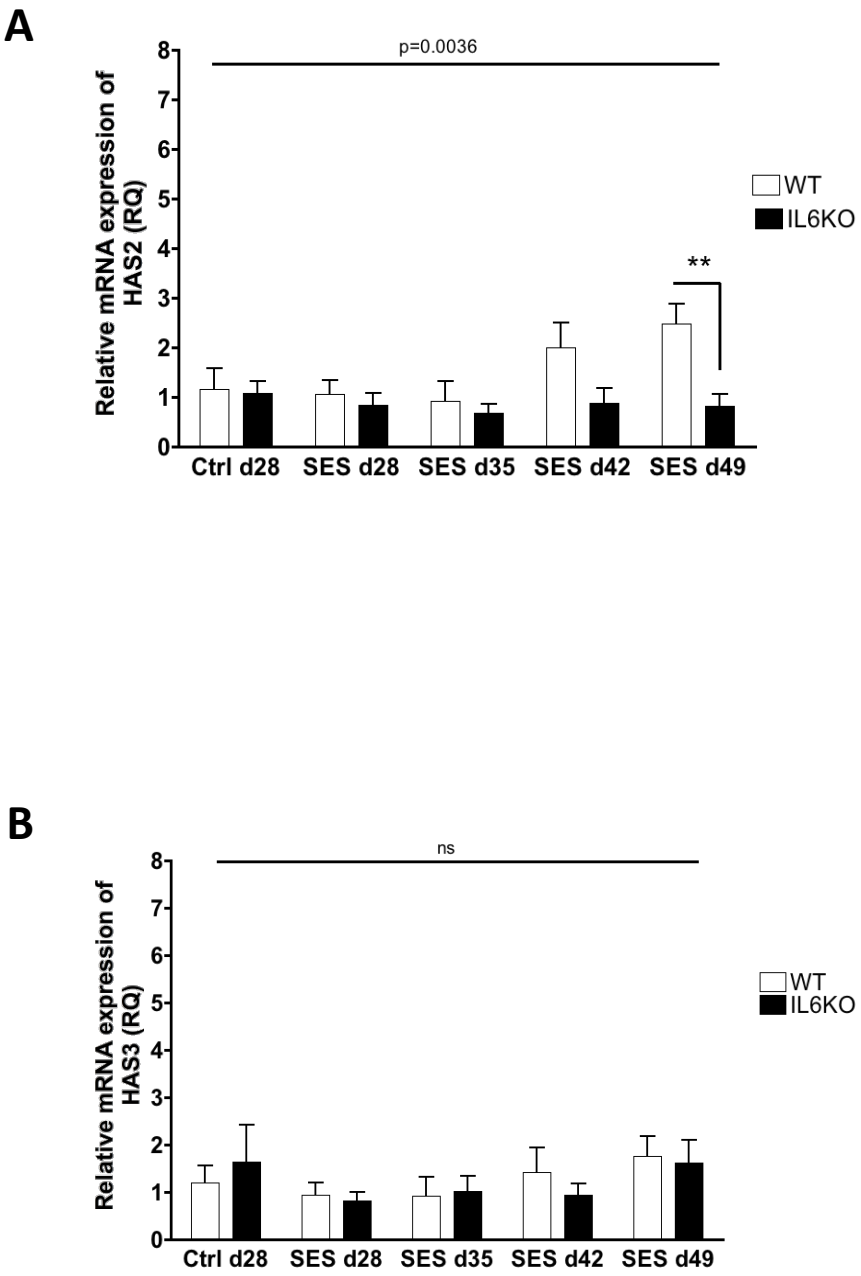

Figure 3.7 Variation in HAS mRNA expression between mice genotypes
RNA was extracted from peritoneal membrane samples collected from WT and IL6KO mice from day 28-49 and converted into cDNA. The relative mRNA expression of HAS 2 (A) and HAS3 (B) were determined using quantitative PCR with RN-18S used as an endogenous control. Results were normalised to each genotype day 28 control samples. The results shown were generated from cDNA prepared from ≥3 different mice per time point and genotype, expressed relative to WT control. Statistical analysis consisted of 2-way ANOVA with Bonferroni post-test ($p<0.05$*, $p<0.005$**)

3.2.4 IL6KO mice display greater matrix degradation at the mRNA level

Fibrosis is characterised by an excessive deposition of ECM, which occurs through enhanced synthesis of ECM components and inhibition of ECM degradation. As described in Section 3.2.3 WT mice produced greater ECM mRNA in response to SES treatment compared to IL6KO mice. This led me to investigate whether matrix degradation differed between mice genotypes (Figure 3.8 and Figure 3.9). IL6KO mice had a 12-fold increase in MMP3 and MMP10 expression at day 42 compared to WT mice, with a significant difference between genotypes across the time course. This result was further supported when I examined the mRNA expression of TIMP1, an inhibitor of MMPs. WT mice had significantly greater mRNA levels of TIMP1 compared to IL6KO, with peak expression at day 35-42. I then determined the ratio of MMP3 and MMP 10 to TIMP1 expression in WT and IL6KO mice, by normalising MMP expression to TIMP1 (Figure 3.9). This showed that IL6KO mice have significantly greater matrix degradation compared to WT mice at the mRNA level, particularly at day 49 when scarring became histologically apparent.

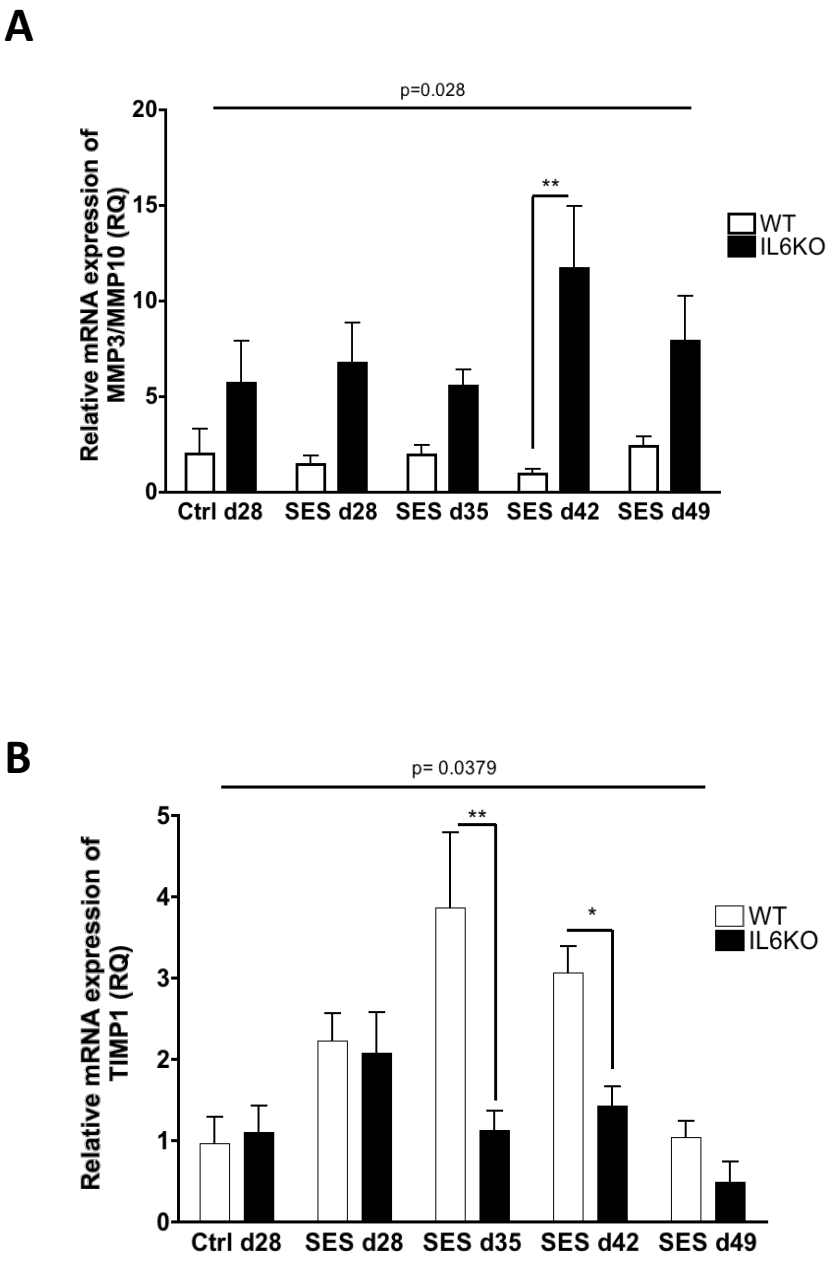

Figure 3.8 Changes in matrix turnover at the mRNA level between mice genotypes
To determine changes in matrix turnover at the mRNA level, RNA was extracted from pertioneal membranes and measured using quantitative PCR. The expression of MMP3 (A) and TIMP1(B) were analysed in WT and IL6KO mice from day 28 to day 49. Results shown are representative of cDNA prepared from ≥3 different mice per time point and genotype, expressed relative to WT control. Statistical analysis was performed using 2-way ANOVA followed by Bonferroni post-test ($p<0.05$*, $P<0.005$**)

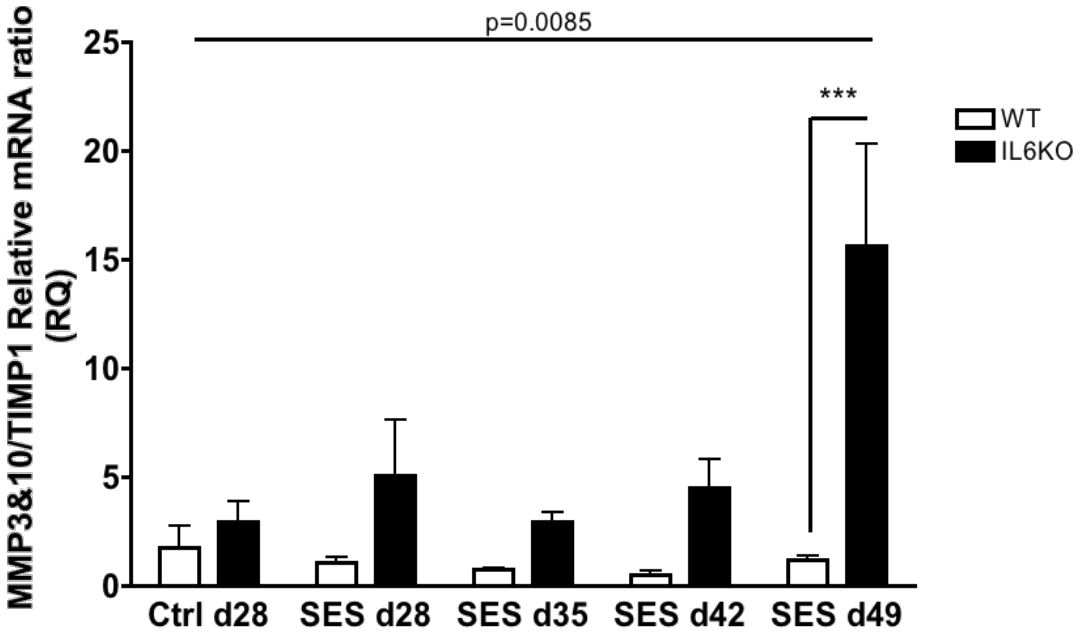

Figure 3.9 Significant difference in MMP:TIMP mRNA ratio between mice genotypes
To determine the overall balance in matrix turnover the ratio of MMP3 and MMP10 was calculated using quantitative PCR. The expression of MMP was normalised to the measurements of TIMP1 in WT and IL6KO between day 28 to day 49. Results shown are from cDNA prepared from ≥ 3 different mice per time point and genotype, expressed relative to WT control. Results show mean values with error bars representing SEM. Statistical analysis was performed using 2-way ANOVA with Bonferronni post-test. A p value of <0.05 was deemed statistically significant (P<0.0005***).

3.3 Discussion

Inflammation is a fundamental bodily response, required for the promotion of wound healing and clearance of infection. The majority of inflammatory processes initiated are transient and self-limiting, however in the presence of a persistent noxious stimuli or deregulation of this process can result in a chronic inflammatory response, which ceases to be beneficiary to the host and becomes detrimental[323]. This chronic response may result in the destruction of tissue, leading to scar formation and fibrosis. The peritoneum of PD patients is persistently exposed to various stimuli such as glucose within the PD effluent and the occurrence of peritonitis infections. This may contribute to a chronic inflammatory state[116]. How chronic inflammation within the peritoneum leads to technique failure and fibrosis still requires further elucidation.

The murine SES model adapted by Fielding et al (2014), attempted to represent recurrent episodes of inflammation that occur within long-term PD patients, to try and identify how inflammation can lead to technique failure and fibrotic changes within the peritoneum. IL6 and IFNγ were identified as key mediators of the inflammatory mediated fibrosis present within this model[265]. The role of TGF-β1, a cytokine central to the fibrotic process and an inducer of fibrotic changes to the peritoneum was not investigated by Fielding et al (2014) hence the work of this chapter was to characterise the TGF-β1 response in the murine model.

Peritoneal biopsies collected from WT and IL6KO at day 28,35, 42 and 49 were used for RNA extraction to measure changes in the mRNA expression of TGF-β1 and

downstream mediators of TGF-β1 fibrotic effects (Figure 3.2). The characterisation of the TGF-β1 response within the murine model revealed a significant difference in TGF-β1 expression between the mouse genotypes, with WT SES treated mice showing a two-fold increase at day 35 and a significant increase at day 42 compared to control and IL6KO mice. This increase in TGF-β1 mRNA expression occurred 14 days before scarring became histologically apparent within these animals, suggesting that an enhanced production of TGF-β1 within the WT animals may account for the difference in fibrotic response.

Analysis of the expression of TGF-β1 inducible genes PAI-1 and CTGF showed no difference between mice genotypes at the mRNA level across the time course. In other systems both PAI-1 and CTGF mRNA and protein expression are significantly induced in the presence of TGF-β1[324, 325]. This may represent failure of induction of these genes by TGF-β1 in this context, or a transient change in expression may have been missed by my experimental approach. TGF-β1 induction of PAI-1 and CTGF mRNA can occur quickly and transiently in some systems, whilst persisting in others. However, the time course I have evaluated demonstrates sustained induction of TGF-β, maximal at day 35 and extending to day 49, suggesting the experimental approach is sufficiently comprehensive to capture the most important gene expression changes.

TGF-β1 is shown to be a potent inducer of EMT within numerous cell types. EMT is often observed as a hallmark of the fibrotic process[145]. Within PD research various studies have reported the conversion of mesothelial cells to fibroblasts[122].

Fibroblasts are central to tissue repair during wound healing, becoming activated and differentiating into myofibroblasts that results in production and deposition of ECM. As the tissue is repaired the myofibroblasts are lost via apoptosis. However, during the fibrotic process these cells persist contributing to excessive matrix deposition contributing to organ failure. Similar mRNA levels of EMT markers were observed between the mouse genotypes except for Slug1 which was significantly greater in WT mice compared to IL6KO mice (Figure 3.3, 3.4 and 3.5). Slug1 may therefore represent a promising candidate for future evaluation and a possible therapeutic target in peritoneal fibrosis. These results suggest that EMT does not appear to be present within the mouse model. In this model significant fibrosis may occur without profound peritoneal EMT. This does not exclude EMT playing an important role in peritoneal fibrosis overall, but may have important implications for mechanisms underlying infection driven peritoneal fibrosis.

A key component of the fibrotic process is the excess deposition of ECM. The ECM consists of various components including proteins that provide structural support such as collagen, glycoproteins including fibronectin and glycosaminoglycans such as hyaluronic acid[326]. The induction of ECM production is stimulated by various cytokines and mechanical signals resulting in intracellular synthesis followed by deposition outside of the cell[327]. TGF-β1 is again centrally involved in this process, contributing to the activation of fibroblasts and stimulating the production of ECM in myofibroblasts. The histological findings of Fielding et al (2014) showed that WT mice displayed greater staining for collagen in peritoneal membrane biopsies, coupled with thickening of the SMC[265]. My work in this chapter supports the

findings of Fielding et al (2014)[265] by demonstrating that WT mice express greater mRNA levels of key matrix components col1a1, fibronectin and hyaluronic acid synthase 2 (HAS2), particularly at the time of scarring (day 49).

Hyaluronic acid (HA) is deemed a marker of inflammation within peritoneal dialysis, with serum levels of HA shown to predict mortality and morbidity in PD patients[328, 329]. Increased production of HA may also contribute to the fibrotic process, mediating the induction of matrix proteins such as fibronectin. Therefore the increased mRNA expression of HAS2 supports the greater fibrotic response within WT mice. HAS2 is upregulated by TGF-β1 in dermal fibroblasts, contributing to the differentiation process of fibroblasts to myofibroblasts[330]. My data suggests that the enhanced HAS2 expression in WT mice may be the result of increased TGF-β1 production, which may attribute to the enhanced matrix production and scarring in WT mice.

The regulation of ECM homeostasis involves a balance between production and degradation. During the fibrotic process there is excessive synthesis and decreased degradation of ECM leading to overall accumulation in ECM deposition[55]. The enzyme family known as matrix metalloproteinases (MMP) and their natural inhibitors tissue inhibitors of metalloproteinases (TIMP) regulates the degradation turnover of ECM. Disruption in the MMP to TIMP ratio can lead to various pathologies, including arthritis and cancer[331, 332]. In the context of wound healing, decreased levels of MMP, particularly MMP3 are associated with impaired healing and wound contraction[333]. My data shows that WT mice express greater

levels of TIMP1 mRNA at day 35 and 42, suggesting that prior to formation of scar tissue there is inhibition of matrix degradation. This is in contrast to IL6KO mice which display low TIMP1 mRNA but enhanced MMP3:MMP10 mRNA expression, potentially indicative of greater matrix degradation.

TIMP1 is shown to be a significant mediator of the fibrotic process particularly within the liver, with one study indicating the potential of TIMP1 as a biomarker for the degree of fibrosis in chronic hepatitis B patients[334, 335]. Inflammation and TIMP1 are reported to be associated in various studies, with TIMP1 correlating to the degree of hepatic inflammation and inhibition of inflammatory cytokines such as IFN-γ leading to suppression of TIMP1 levels and attenuation of fibrosis[336, 337]. The TIMP1 data collected from the mice samples supports an increased inflammatory and fibrotic response within the WT animals that is not present in the IL6KO samples.

The enhanced MMP response and low levels of TIMP1 in the IL6KO animals may potentially explain the absence of scarring and fibrosis within these animals when challenged with persistent inflammation. The ratio of MMP:TIMP is greater in IL6KO animals indicating at the mRNA level a potential increase in overall matrix degradation. Within models of fibrosis, matrix accumulation through the suppression of MMPs is commonly reported[338, 339]. Enhanced MMP activity may potentially provide an anti-fibrotic effect, with studies reporting increased MMP expression in scarless wound healing models[340, 341].

Overall my results show a significant difference in the fibrotic response between WT and IL6KO mice. The data suggests that an important component is a significant increase in TGF-β1 production compared to IL6KO mice, suggesting that the inflammatory response may promote TGF-β1 production. I have identified further differences in subsequent gene expression responses between WT and IL6KO genotypes, most particularly and apparent repression of matrix remodelling in WT animals in response to repeated inflammatory stimulation. In my subsequent work I examine the mechanisms underlying these observations.

Chapter 4: The interaction of TGF-β1 and IFN-γ on HPMC responses

4.1 Introduction

The results from the previous chapter have highlighted key differences between WT and IL6KO mice in terms of the fibrotic response at the mRNA level. WT mice expressed greater TGF-β1 and matrix component mRNA coupled with reduced MMP3 expression. The modulation in matrix turnover observed may be the result of inflammation causing an increase in TGF-β1 production alone, or the result of modulation of TGF-β1 responses through increased production of pro-inflammatory cytokines.

Studies have shown an association between inflammation and fibrosis in various systems. Within the peritoneum, persistent inflammation through bio-incompatible dialysate fluid and recurrent peritonitis infections is a key factor in driving fibrosis[57]. Interactions between TGF-β1 and inflammatory cytokines cause agonistic and antagonistic effects. This department reported augmentation of the TGF-β1 response by IL6 in proximal tubular cells (PTC). Interleukin 1 beta (IL1β) exposure had a biphasic effect on TGF-β1 signalling. Short term IL1β exposure of PTC caused inhibition of TGF-β1 signalling, whereas long term exposure results in augmentation of the TGF-β1 SMAD pathway[342]. In other studies inflammation is shown to directly increase TGF-β1 production. Peritonitis episodes are shown to enhance TGF-β1 production[264, 343]. Mlambo et al (1999) found increased levels of TGF-β1 in dialysate fluid of patients suffering with peritonitis infection compared to non-infected. The study also reported that following resolution of peritonitis TGF-β1

levels remained elevated and suggested this could be an indicator of fibrotic changes within the peritoneum[264].

Fielding et al (2014) results from the SES murine model suggested that although IL6 is necessary for the fibrotic process, it was the release of the pro-inflammatory cytokine IFN-γ that caused the scarring within the SES model[265]. This is a novel finding as within other systems IFN-γ is found to exert anti-fibrotic effects, specifically through inhibition of TGF-β1 production and responses. This led me to select IFN-γ as the pro-inflammatory stimulus and determine its impact on TGF-β1 responses.

Research into the role of IFN-γ within the peritoneum has centred mainly on the cytokine's involvement in peritoneal inflammation. Previous studies have highlighted a role of IFN-γ in regulating inflammatory cells within the peritoneum including its production by peritoneal macrophages and key roles in recruitment and clearance of neutrophils within the peritoneal cavity[312]. How this cytokine is involved in peritoneal fibrosis has not been researched, only the findings from Fielding et al (2014) have highlighted the potential fibrotic effect of IFN-γ in this system[265]. HPMC have a focal role in regulating the inflammatory response within the peritoneum and are central regulators of the fibrotic process producing TGF-β1 in response to continued peritoneal dialysis and infection[131, 344].

The purpose of the work detailed in this chapter is to examine the effects of TGF-β1 and IFN-γ on HPMC within an *in vitro* system. The main aims being:

- To determine whether TGF-β1 in sufficient dose is able to induce changes in matrix remodelling and therefore account for the fibrotic effects documented within the SES model in the previous chapter
- To determine how IFN-γ may modify responses of HPMC to TGF-β1 and thus promote fibrosis

4.2 Results

4.2.1 Assessment of optimal HPMC stimulation with TGF-β1 and IFN-γ

The initial work for this chapter involved examining the effect of TGF-β1 stimulation within HPMC. An *in vitro* system of HPMC were stimulated with TGF-β1 alone or in combination with IFN-γ for varying time points to observe peak changes in mRNA expression. My experiments involved measuring changes in the transcription of TGF-β1 dependent genes following culture of HPMC with 1 ng/ml TGF-β1 alone or in combination with 10 ng/ml of IFN-γ from 12 hours to 48 hours (Figure 4.1 and 4.2), thus determining whether TGF-β1 stimulation alone was sufficient to elicit fibrotic changes or whether modulation of TGF-β1 responses by IFN-γ accounted for the fibrogenic effects observed in the SES mouse model.

Changes in transcription of TGF-β1 dependent responses in HPMC were measured using quantitative PCR from cDNA generated from two separate omental donors. The expression of TGF-β1 and PAI-1 mRNA was induced by 1 ng/ml of TGF-β1 following 12 and 24 hour stimulation respectively (Figure 4.1 A and B). This transcriptional induction was maintained when HPMCs were cultured in the presence of TGF-β1 and IFN-γ. Transcription of MMP3, TIMP1 (Figure 4.1), Fibronectin and MMP1 (Figure 4.2) were induced by TGF-β1, with peak expression at 48h. Exposure to TGF-β1 and IFN-γ produced similar mRNA level expression of TIMP1, Fibronectin and MMP1 as when HPMC were exposed to TGF-β1 alone, suggesting that many gene responses were elicited by TGF-β1 alone and were not modified by IFN-γ. However when HPMC were exposed to TGF-β1 and IFN-γ an inhibitory effect on MMP3 expression was observed.

Acute stimulation (6h) of HPMC with TGF-β1 and IFN-γ (Figure 4.3) revealed early transcriptional changes in PAI-1, MMP3 and TIMP1 expression (B and C). There was a significant induction of PAI-1 and TIMP1 mRNA expression following exposure of HPMC to TGF-β1 and this was not affected by IFN-γ. MMP3 expression was induced in HPMC exposed to TGF-β1, with this induction inhibited in the presence of IFN-γ. There was no change in the expression of TGF-β1. Thus coupled with the time course stimulation experiments (Figure 4.1 and 4.2) changes at the mRNA level were observed between 24-48h of stimulation.

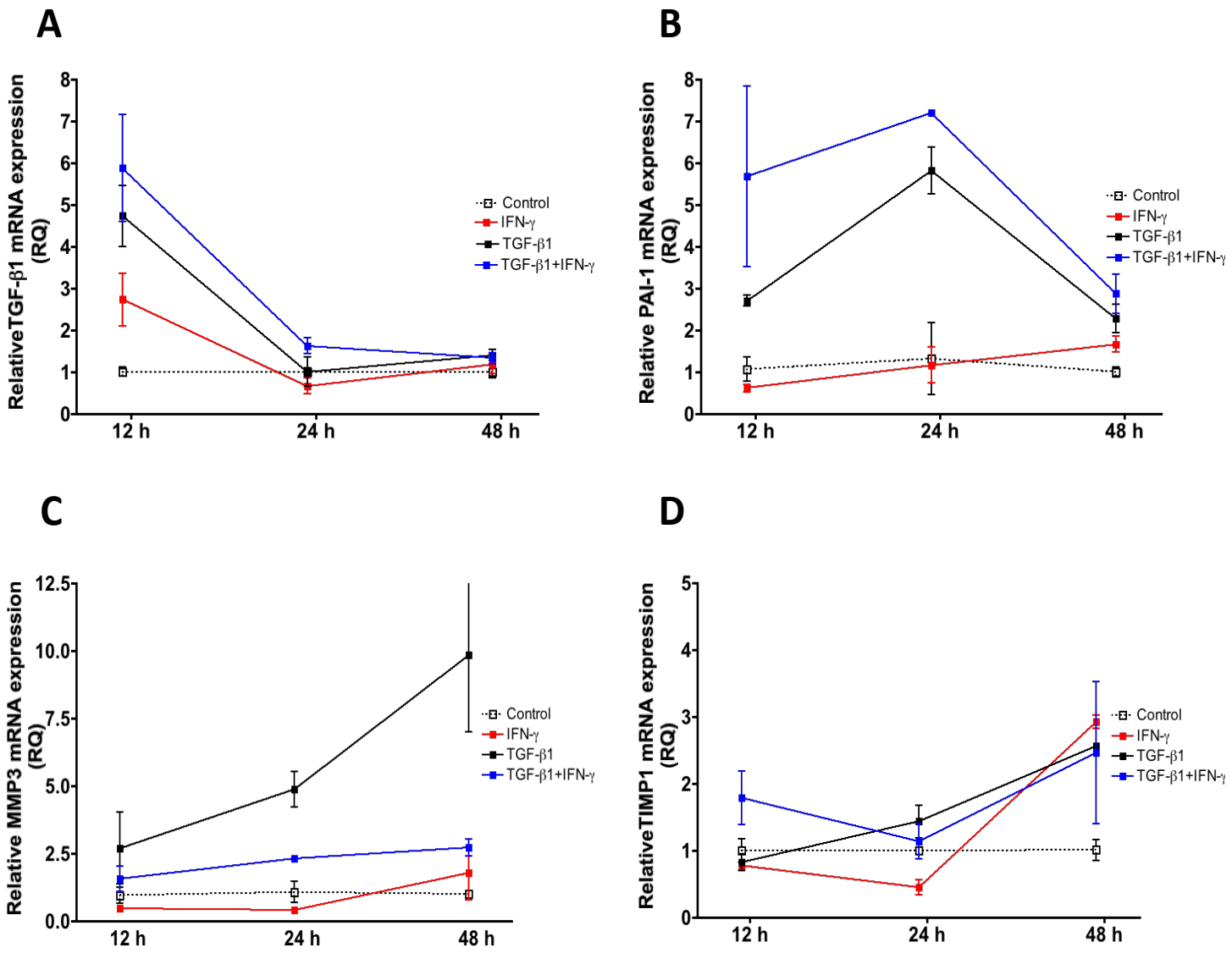

Figure 4.1 Time course of transcriptional activation of HPMC stimulated with TGF-β1 and IFN-γ

Confluent monolayers of HPMC were growth arrested for 24h then stimulated with TGF-β1 (1ng/ml) +/- IFN-γ (10ng/ml) for 12-48h. Following stimulation RNA was extracted and transcription of TGF-β1 (A), PAI-1 (B), MMP3 (C) and TIMP1 (D) was determined using quantitative PCR from cDNA generated (n=2). All data was normalised to control values at 12h. Ribosmoal (r)RNA was used as an endogenous control. Results shown are from 2 omental donors with mean values plotted and error bars representing SEM (n=2).

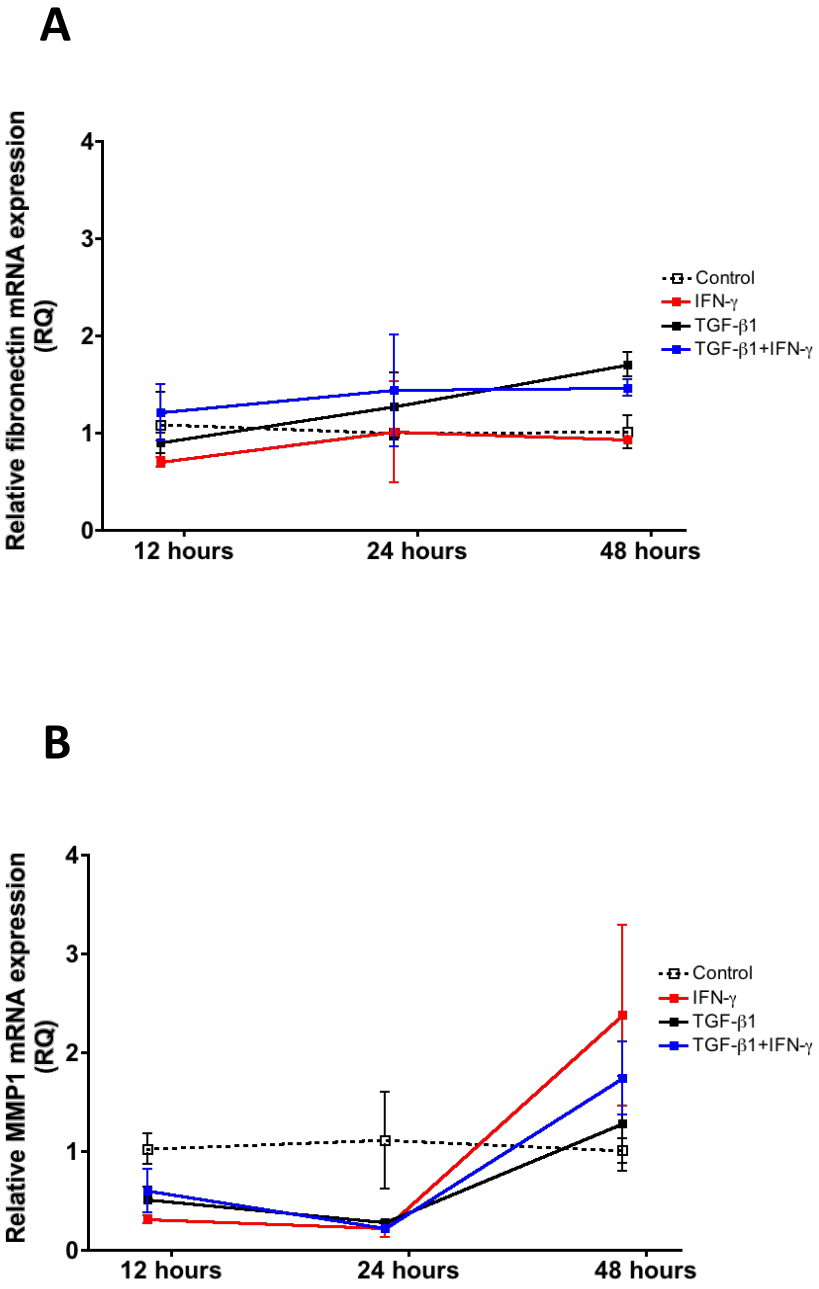

Figure 4.2 Time course of matrix and epithelial-mesenchymal mRNA expression in HPMC exposed to TGF-β1 and IFN-γ

Confluent (80%) monolayers of primary HPMC were growth arrested in serum free medium for 24h. The medium was replaced with medium containing 1ng/ml of TGF-β1 (black line) or 10ng/ml IFN-γ (red line) or combination (blue line) or without (dotted line) for 12-48h. Following stimulation RNA extraction was extracted and mRNA expression of MMP1 (A) and fibronectin (B) were calculated using quantitative PCR. 18S rRNA was used as an endogenous control. Data was normalised to control values at 12h. Results shown are from two omental donors (n=2).

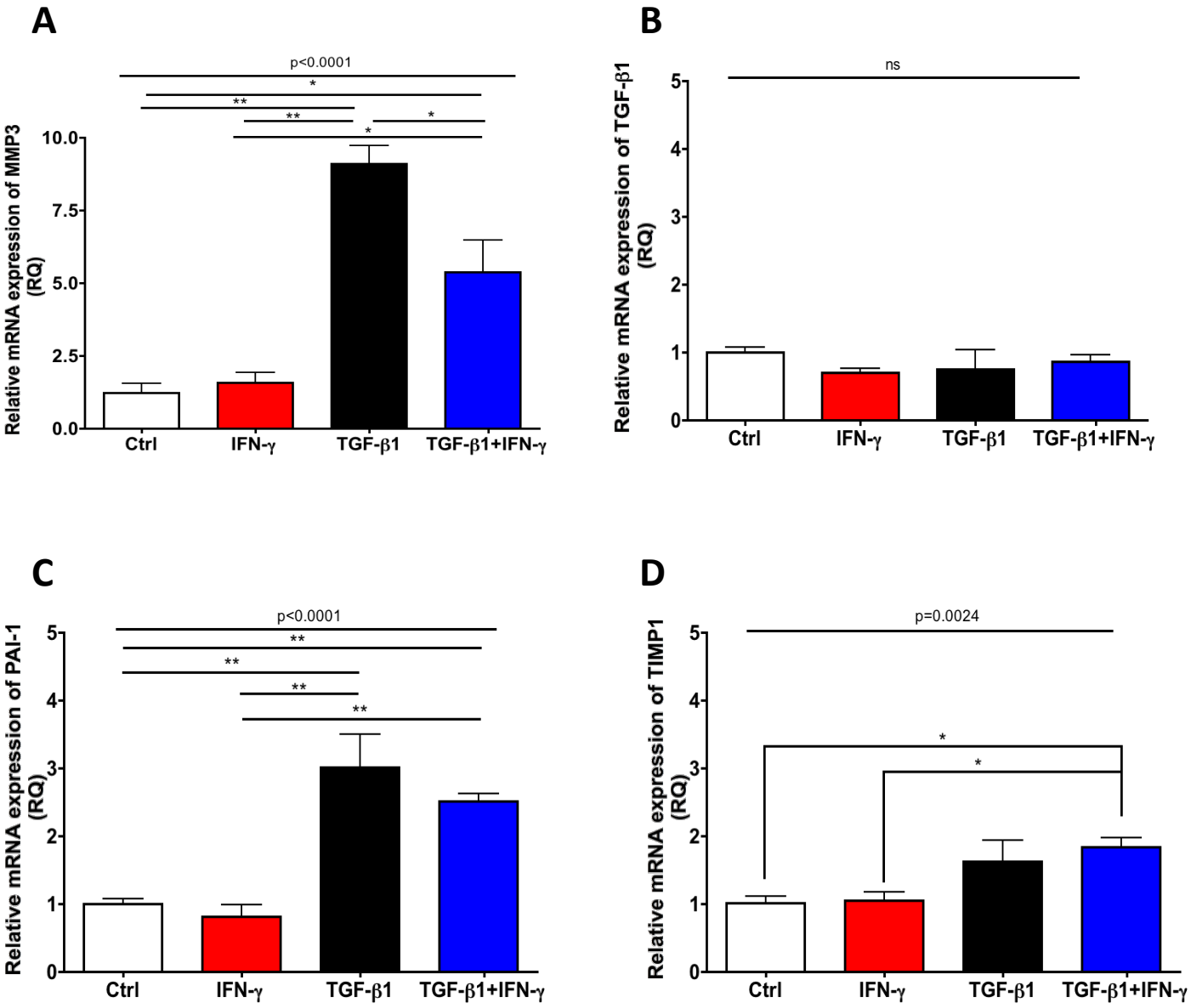

Figure 4.3 Acute effects of stimulation on HPMC transcription
Confluent (80%) monolayers of primary HPMC collected from 3 omental donors were growth arrested in serum free medium for 24 h (n=3). The medium was aspirated and replaced with serum free medium alone (white bars) or serum free medium containing either 10 ng/ml IFN-γ (red bars), 1 ng/ml of TGF-β1 (black bars) or combination of both (blue bars) for 6h. RNA was extracted and converted to cDNA by reverse transcription. Relative mRNA expression of TGF-β1 (A), PAI-1 (B), MMP3 (C) and TIMP-1 (D) were determined using quantitative PCR with rRNA measured as an endogenous control. Data was normalised to control values. Mean values are plotted with error bars representing SEM. The data was statistically analysed using a one-way ANOVA followed by Bonferroni post tests with a p value of <0.05 being deemed significant (p<0.05*, p<0.005**)

4.2.2 IFN-γ does not affect the induction of fibrotic mediators and matrix components by TGF-β1 at the mRNA level

The above data demonstrated gene expression changes following stimulation with TGF-β1 alone combined with an apparent specific effect on MMP3 expression, which is inhibited in the presence of IFN-γ. TGF-β1 has pleiotropic effects and different responses are reported in a dose dependent fashion secondary to differential TGF-β1 receptor recruitment. Therefore I studied TGF-β1 responses in HPMC following exposure to 0.1 – 10ng/ml of TGF-β1 and modifications of these gene expression responses by IFN-γ for 24h. This also determined the optimal doses of cytokines required to produce a maximal response, using quantitative PCR (Figure 4.4 to Figure 4.6). Changes in the mRNA expression of TGF-β1 and PAI-1 (Figure 4.4) peaked following stimulation with 1 ng/ml of TGF-β1 and IFN-γ did not affect mRNA expression of either gene.

TGF-β1 stimulates ECM production. To determine the dose required for maximal ECM mRNA induction and to assess whether IFN-γ affected this process, I measured col1a1, col1a2, and Hyaluronan Synthases 1 to 3 (HAS1-HAS3) (Figure 4.5 and Figure 4.6). As with TGF-β1 and PAI-1, maximal induction of mRNA occurred following stimulation with 1 ng/ml of TGF-β1. No significant difference in col1a1 and col1a2 mRNA expression was observed between HPMC treated with TGF-β1 alone or in combination with 10 ng/ml IFN-γ. The results for HAS1 and HAS2 were also the same, with no difference detected between the TGF-β1 treated and the TGF-β1 + IFN-γ treated. Interestingly IFN-γ had a significant stimulatory effect on HAS3 mRNA expression.

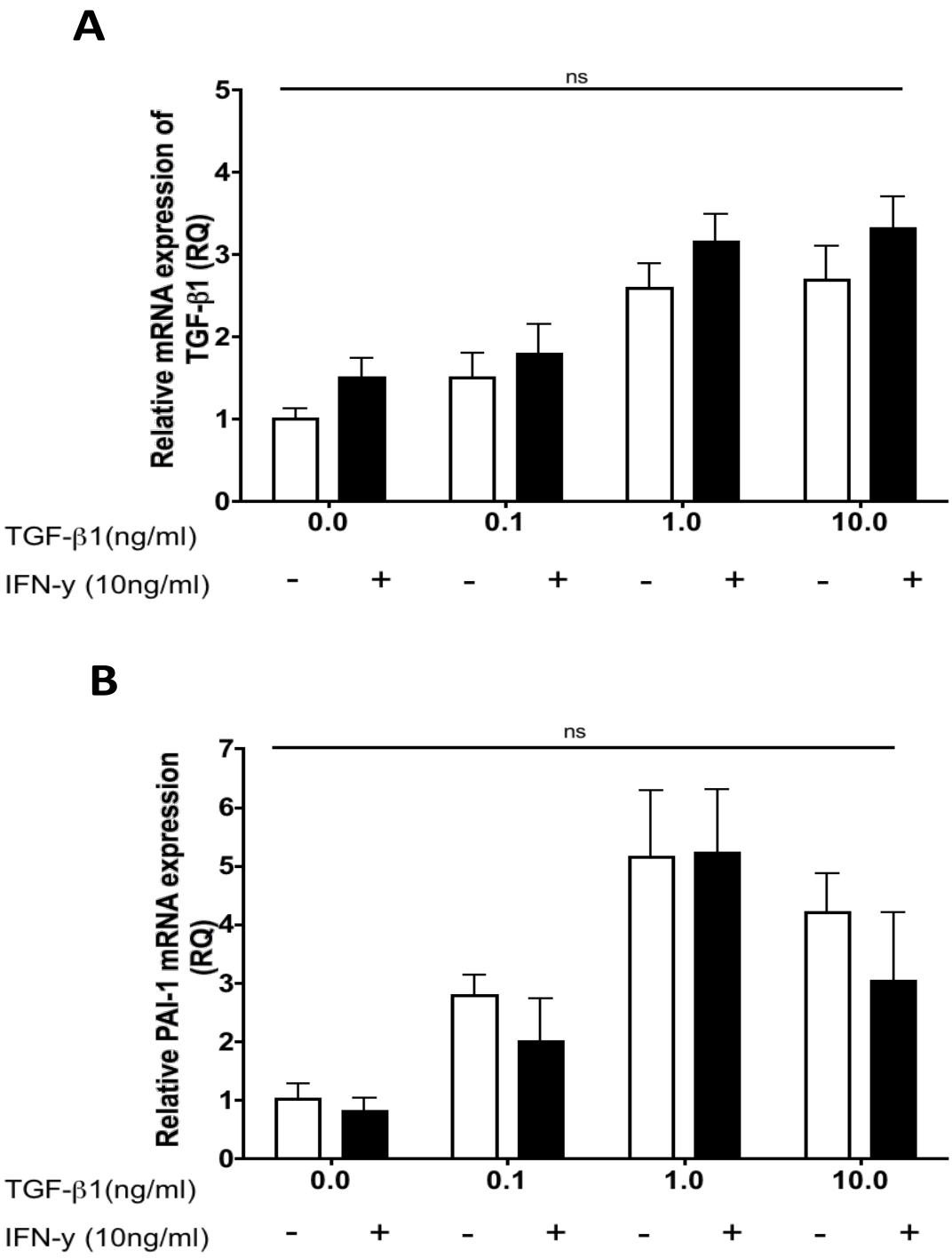

Figure 4.4 Dose response of TGF-β1 stimulation in HPMC
Confluent (80%) monolayers of primary HPMC collected from 3 omental donors were growth arrested for 24 h (n=3). The cells were then stimulated with a range of TGF-β1 doses (0.1 ng/ml- 10 ng/ml) alone (white bars) or in combination with 10 ng/ml IFN-γ (black bars) for 24 h. RNA was extracted and and relative mRNA expression of TGF-β1 (A) and PAI-1 (B) were determined using quantitative PCR with rRNA measured as an endogenous control. Data was normalised to control values of 0ng/ml of TGF-β1. Mean values were plotted with error bars representing SEM. The data was statistically analysed using a 2-way ANOVA followed by Bonferroni post tests with a p value of <0.05 being deemed significant.

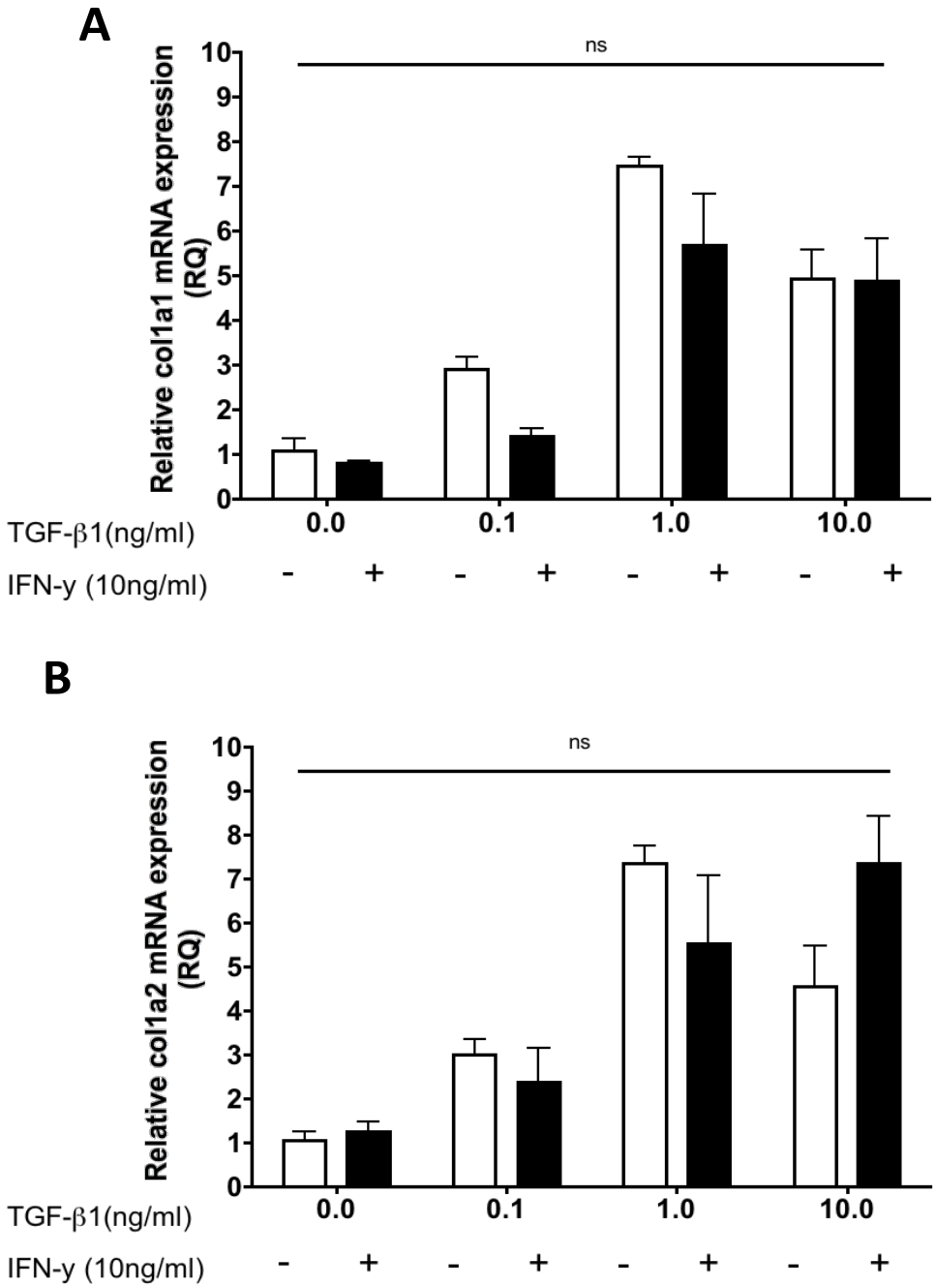

Figure 4.5 TGF-β1 dependent up-regulation of collagen I mRNA is not affected by the presence of IFN-γ

Confluent (80%) monolayers of primary HPMC collected from 3 omental donors were growth arrested for 24 h (n=3). The cells were then stimulated with a range of TGF-β1 doses (0.1 ng/ml- 10 ng/ml) alone (white bars) or in combination with 10 ng/ml IFN-γ (black bars) for 24 h. RNA was extracted and and relative mRNA expression of col1a1 (A) and col1a2 (B) calculated using quantitative PCR with rRNA measured as an endogenous control. Data was normalised to control values of 0ng/ml of TGF-β1 . The data was statistically analysed using a 2-way ANOVA followed by Bonferroni post tests with a p value of <0.05 being deemed significant.

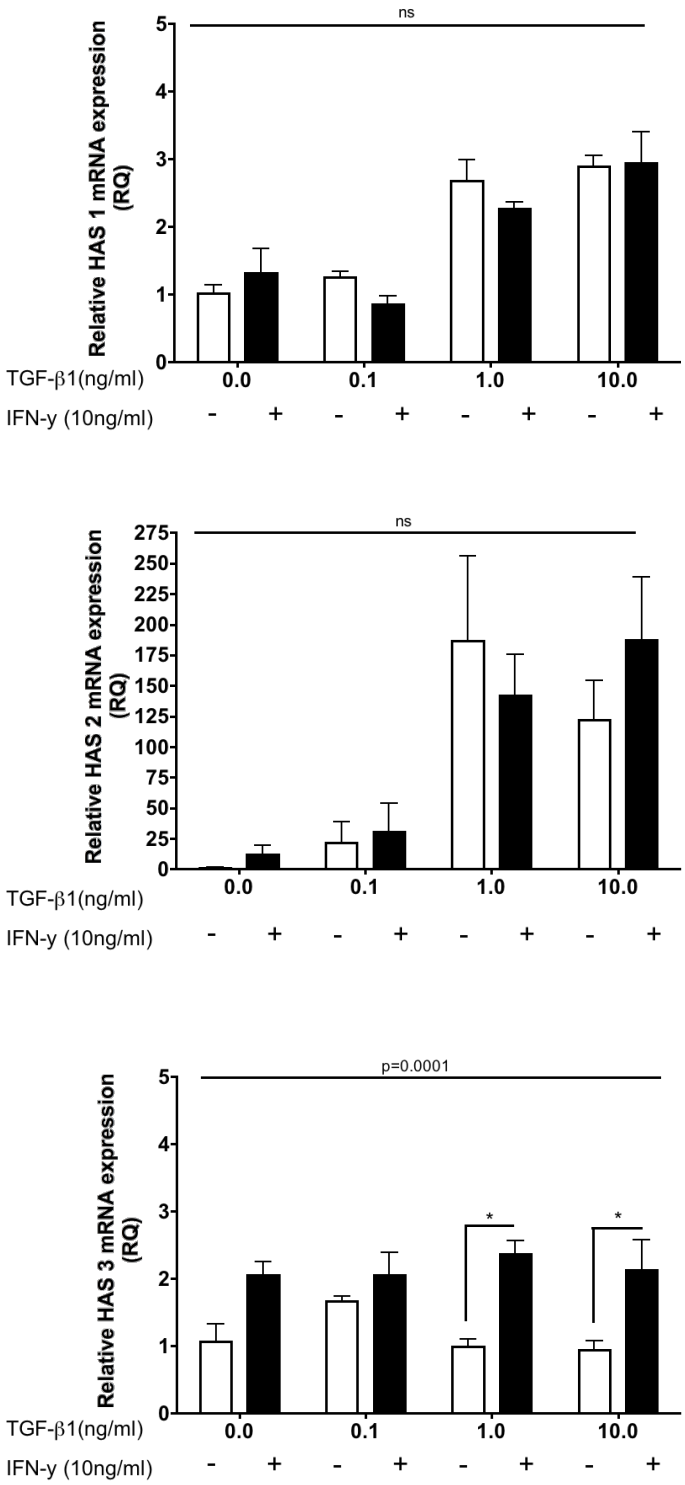

Figure 4.6 TGF-β1 dependent up-regulation of Hyaluronic acid synthase mRNA in HPMC is not affected by IFN-γ

Confluent (80%) monolayers of primary HPMC collected from 3 omental donors were growth arrested for 24 h (n=3). The cells were then stimulated with a range of TGF-β1 doses (0.1 ng/ml- 10 ng/ml) alone (white bars) or in combination with 10 ng/ml IFN-γ (black bars) for 24 h. RNA was extracted and and relative mRNA expression of HAS1 (A) HAS2 (B) and HAS3 (C) calculated using quantitative PCR with rRNA measured as an endogenous control. Data was normalised to control values of 0ng/ml of TGF-β1 . The data was statistically analysed using a 2-way ANOVA followed by Bonferroni post tests with a p value of <0.05 being deemed significant ($p<0.05$*)

4.2.3 IFN-γ significantly inhibits mRNA expression of MMP3

Previous research has reported that IFN-γ can inhibit various members of the matrix metalloproteinase (MMP) family of enzymes[345-347]. Within the previous chapter my data collected from the SES mouse model shows that the absence of pro-inflammatory signalling increased mRNA expression of MMP3. Therefore I decided to examine whether there was an effect on MMP3 production in HPMC treated with TGF-β1 and whether IFN-γ inhibited this.

Following stimulation of HPMC for 24h with the various doses of TGF-β1 there was a substantial increase in MMP3 mRNA expression, approximately 1000-fold following 1 ng/ml (Figure 4.7 A). There was no change in the TGF-β1 response when the dose of TGF-β1 was increased to 10ng/ml, thus suggesting optimal response occurred at 1ng/ml. MMP3 induction was significantly inhibited in the presence of 10ng/ml IFN-γ. The repression of MMP3 by IFN-γ occurred following exposure to the higher dose of TGF-β1. Examining the dose of IFN-γ (1-30 ng/ml Figure 4.7 B) suggested that the optimal dose was 10 ng/ml of IFN-γ. The mRNA expression of MMP3 was measured following 72 h stimulation with TGF-β1 (1 ng/ml) and IFN-γ alone or in combination (Figure 4.8). The induction of MMP3 by TGF-β1 was maintained and was significantly inhibited in the presence of IFN-γ, showing that this specific inhibition is not transient.

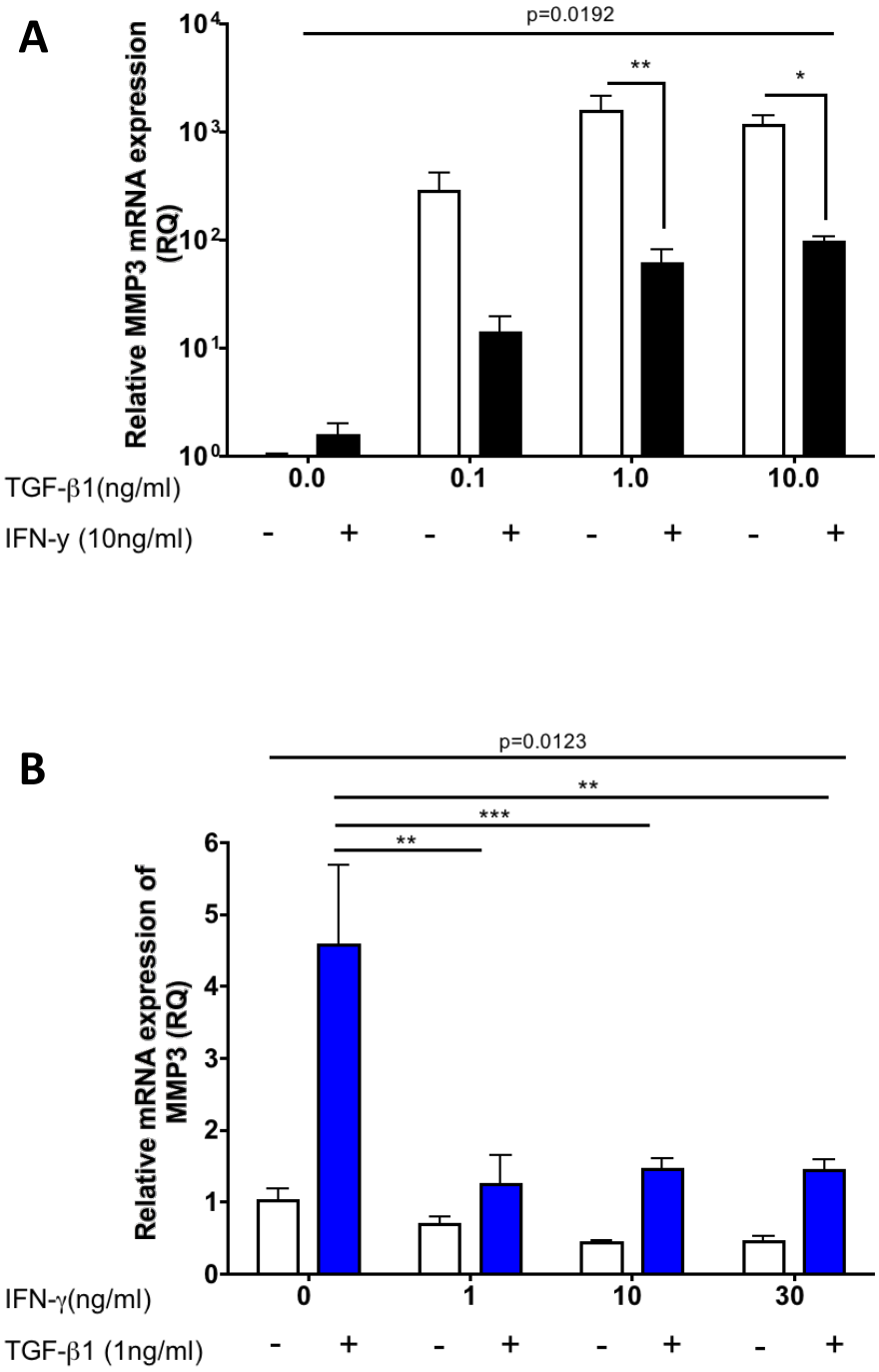

Figure 4.7 TGF-β1 induces MMP3 mRNA expression which is inhibited in the presence of IFN-γ

Confluent (80%) monolayers of primary HPMC collected from 3 omental donors were growth arrested for 24 h (n=3). The cells were then stimulated with medium containing either: (A) TGF-β1 (white bars) in doses ranging from 0.1 ng/ml- 10 ng/ml alone or in combination with 10 ng/ml IFN-γ (black bars) or (B) IFN-γ (white bars) doses ranging from 1 ng/ml to 30 ng/ml alone or in combination with 1 ng/ml TGF-β1 (blue bars) for 24 h. RNA was extracted and and relative mRNA expression calculated using quantitative PCR with rRNA measured as an endogenous control. Data was normalised to control values of 0 ng/ml of TGF-β1 (A) and 0 ng/ml of IFN-γ (B) respectively. The data was statistically analysed using a 2-way ANOVA followed by Bonferroni post tests with a p value of <0.05 being deemed significant ($p<0.05$*, $p<0.005$**, $p<0.0005$***)

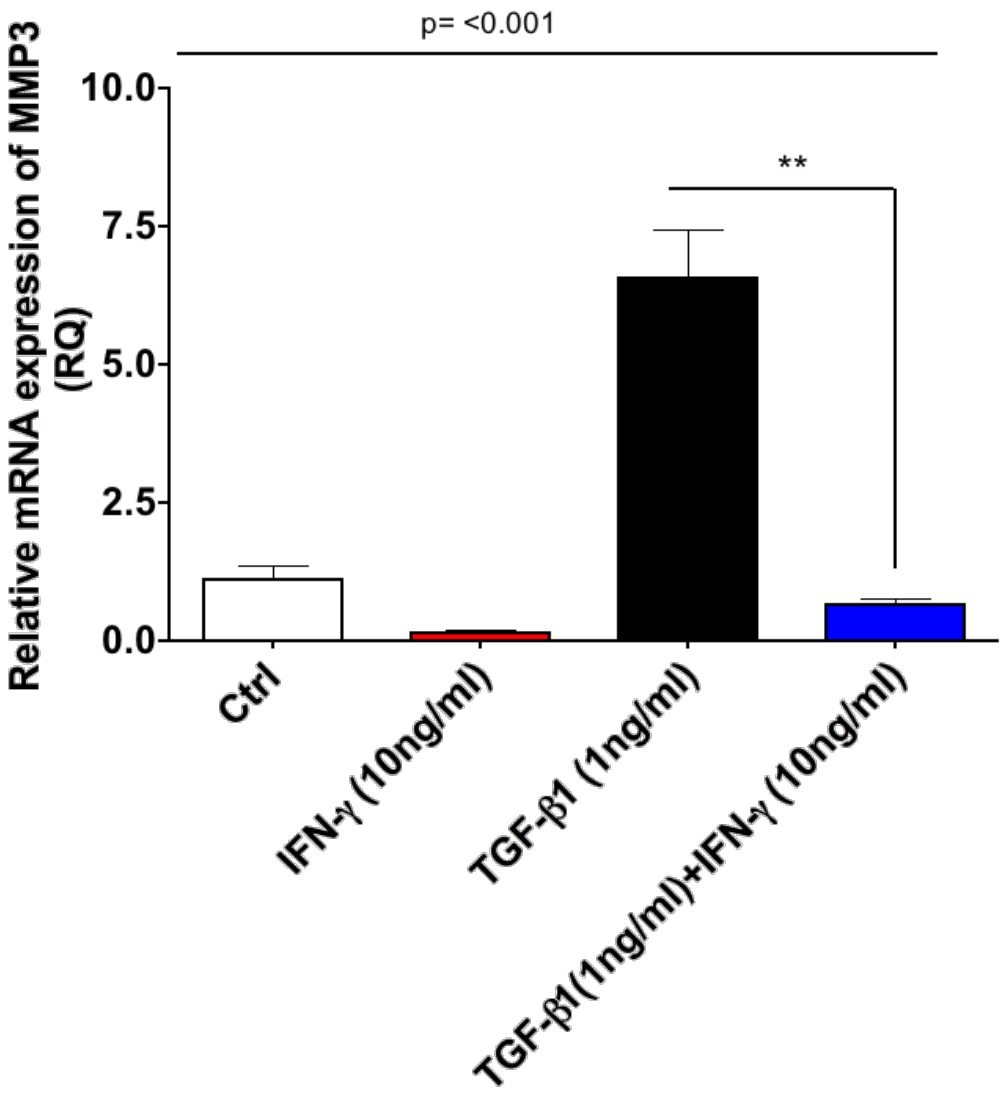

Figure 4.8 The effects of TGF-β1 and IFN-γ on MMP3 expression following 72 h stimulation

Confluent (80%) monolayers of primary HPMC collected from 3 omental donors were growth arrested in serum free medium for 72 h (n=3). The medium was aspirated and replaced with serum free medium alone (white bars) or serum free medium containing either 10 ng/ml IFN-γ (red bars), 1 ng/ml of TGF-β1 (black bars) or combination of both (blue bars) for 6h. RNA was extracted and converted to cDNA by reverse transcription. Relative mRNA expression of MMP3 was determined using quantitative PCR with rRNA measured as an endogenous control. Data was normalised to control values. Mean values are plotted with error bars representing SEM. The data was statistically analysed using a one-way ANOVA followed by Bonferroni post tests with a p value of <0.05 being deemed significant ($p<0.05$*, $p<0.005$**)

4.2.4 Combined stimulation of HPMC with TGF-β1 and IFN-γ caused increased TIMP1 mRNA expression

MMP activity is regulated through natural antagonists referred to as the Tissue Inhibitors of metalloproteinases (TIMPs). In various systems it is reported that TGF-β1 promotes fibrosis through induction of TIMP expression, resulting in increased accumulation of matrix. Therefore I measured the mRNA expression of TIMP1 in HPMC stimulated with a range of TGF-β1 doses alone or in combination with IFN-γ (Figure 4.9 A) The results showed that, compared to control, exposure of HPMC to TGF-β1 did not affect TIMP1 mRNA expression.

Exposure of HPMC to TGF-β1 and IFN-γ resulted in a significant stimulatory effect on TIMP1 mRNA. To determine if IFN-γ was responsible for the induction in TIMP1 mRNA, I used cDNA collected from HPMC stimulated for 24 h with varying doses of IFN-γ +/- TGF-β1 (1ng/ml) and measured TIMP1 mRNA expression using qPCR (Figure 4.9 B). Results were similar to those observed in the TGF-β1 dose response (A). Alone IFN-γ did not affect TIMP1 mRNA expression. However HPMC exposed to both cytokines produced significantly more TIMP1 mRNA. Coupled with the matrix and MMP3 qPCR data, this suggests IFN-γ may promote fibrosis by modulating responses to TGF-β1 and enhancing matrix accumulation.

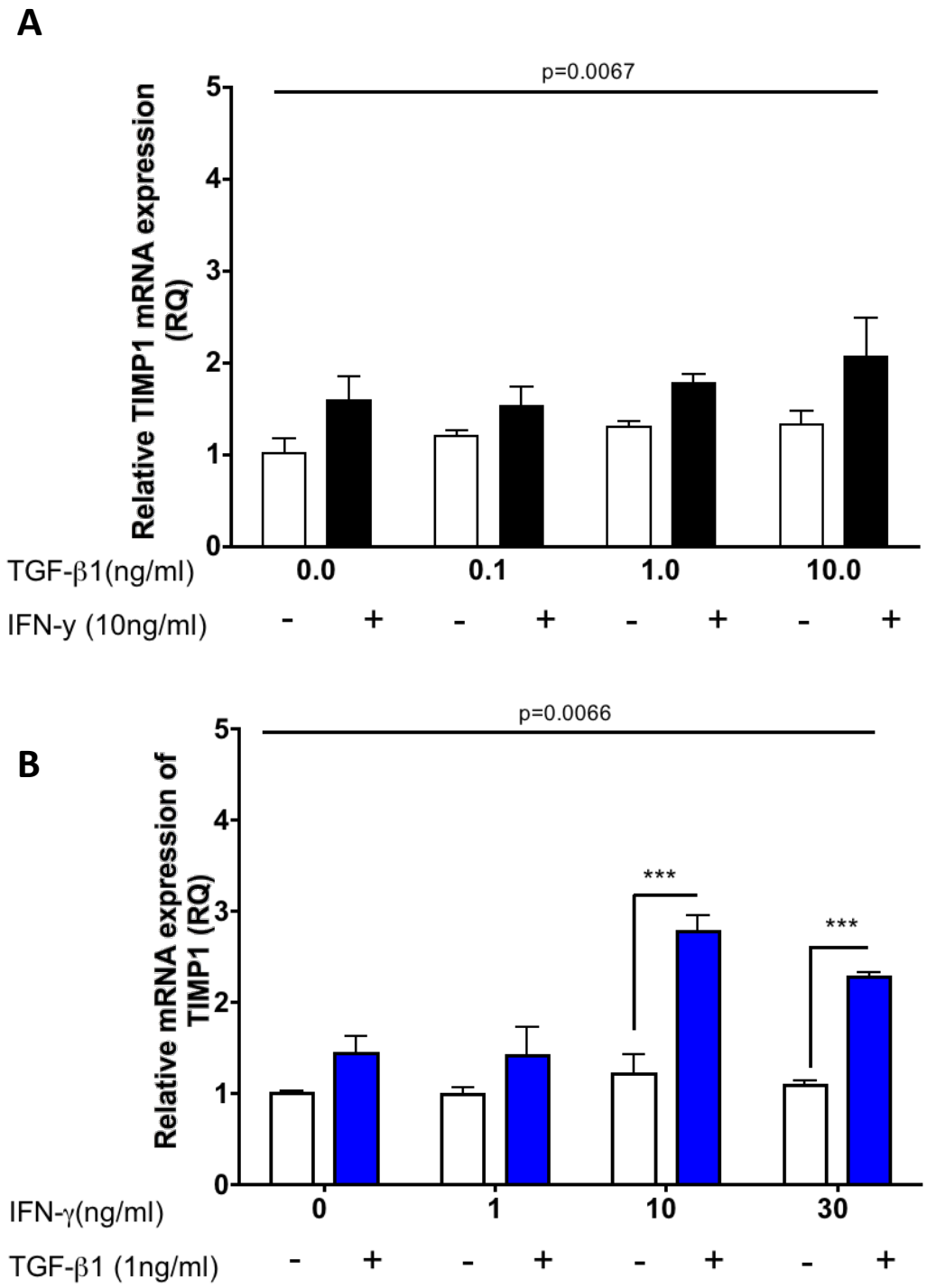

Figure 4.9 IFN-γ increases the expression of TIMP1 mRNA in HPMC
Confluent (80%) monolayers of primary HPMC collected from 3 omental donors were growth arrested for 24 h (n=3). The cells were then stimulated with medium containing either: (A) TGF-β1 (white bars) in doses ranging from 0.1 ng/ml- 10 ng/ml alone or in combination with 10 ng/ml IFN-γ (black bars) or (B) IFN-γ (white bars) doses ranging from 1 ng/ml to 30 ng/ml alone or in combination with 1 ng/ml TGF-β1 (blue bars) for 24 h. RNA was extracted and and relative mRNA expression calculated using quantitative PCR with rRNA measured as an endogenous control. Data was normalised to control values of 0 ng/ml of TGF-β1 (A) and 0 ng/ml of IFN-γ (B) respectively. The data was statistically analysed using a 2-way ANOVA followed by Bonferroni post tests with a p value of <0.05 being deemed significant (p<0.05*, p<0.005**, p<0.0005***)

4.2.5 IFN-γ significantly inhibits MMP3 expression at the protein level

The effect of TGF-β1 and IFN-γ on MMP3 was examined at the protein level using immunoblotting, which measured the total amount of MMP3 protein in HPMC following 72 h stimulation (Figure 4.10). Densitometry analysis showed that IFN-γ significantly inhibited TGF-β1-dependent MMP3 expression ($P<0.05$).

A limitation with this technique is the inability to distinguish between active and latent enzyme. Therefore I also measured catalytic activity of the MMP3 secreted by HPMC, by fluorogenic substrate assay M-2300 (Bachem (Figure 4.11-Figure 4.13). Supernatant was collected from HPMC serum starved for 24h then stimulated with TGF-β1 and IFN-γ alone or in combination for 24-48 h. Optimisation of the assay was undertaken initially, to determine how long to incubate the substrate with supernatant collected from HPMC stimulated for 48 h (Figure 4.11). Equal volumes of substrate and supernatant were incubated for 15 minutes to 72 h with fluorescent readings measured accordingly. Results showed that optimal measurements occurred following 9 h of incubation with the substrate, hence subsequent experiments the substrate was incubated with the HPMC supernatant overnight at 37°C.

Following optimisation of the incubation time, I stimulated HPMC from three different omental donors for 24-72 h to determine the effects of TGF-β1 and IFN-γ stimulation on MMP3 activity (Figure 4.12). All three donors had a similar response to the combination of stimuli. TGF-β1 induced a significant induction in MMP3 activity, which was inhibited in the presence of IFN-γ. Following the time course

experiment I performed 48h stimulation experiments on HPMC collected from 9 different omental donors (Figure 4.13). The individual results support the data collected from the time course experiments that TGF-β1 induces the activity of MMP3 and that IFN-γ inhibits this enzyme. Interestingly, donor specific effects were observed that did not show the inhibition of TGF-β1 induced MMP3 activity in the presence of IFN-γ (4.13 A). When the results were pooled the inhibition of MMP3 activity by IFN-γ was clearly indicated in the overall population of donors studied (Figure 4.13 B).

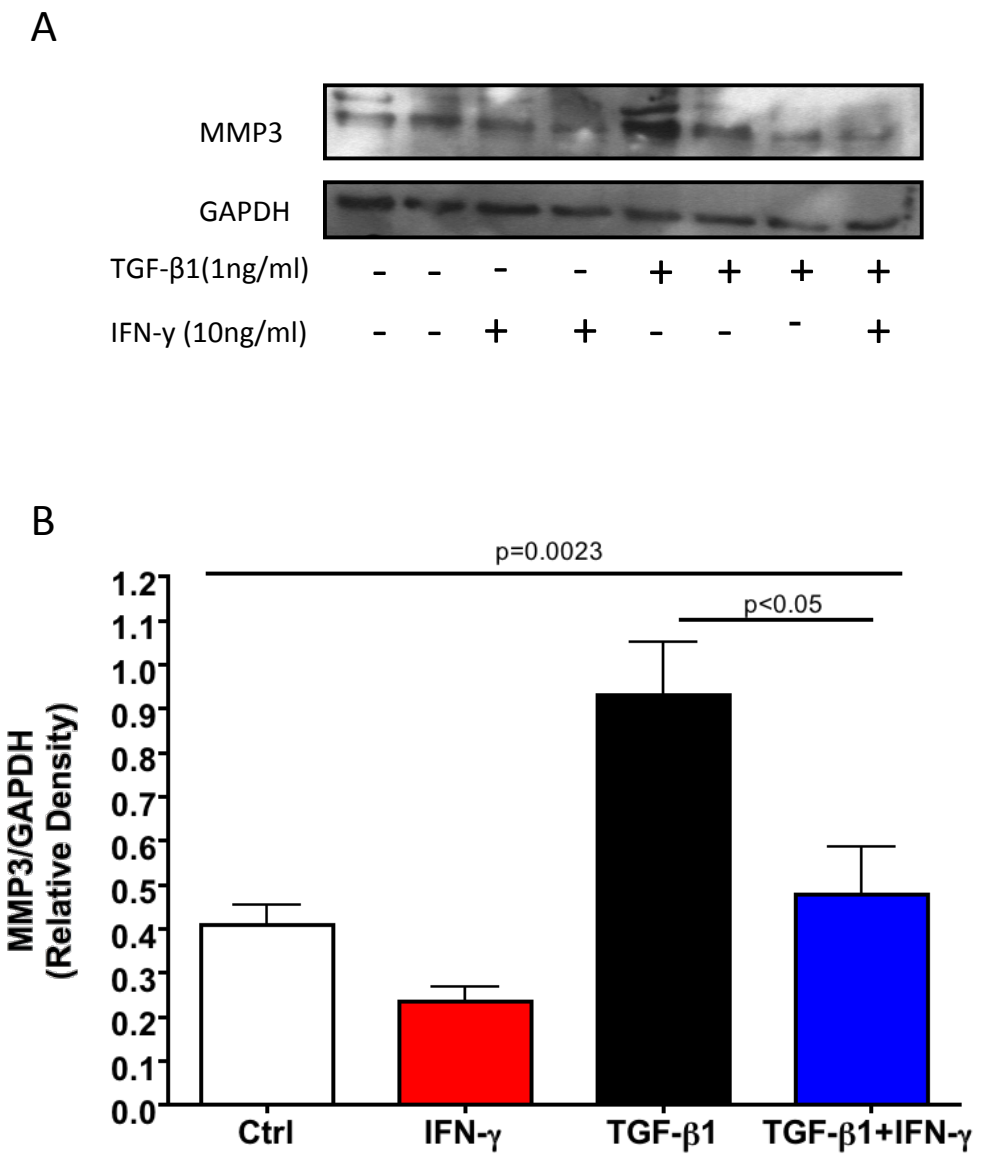

Figure 4.10 Immunoblot analysis of MMP3 expression in HPMC

HPMC were cultured in 6 well plates and growth arrested for 24h in serum free medium. The medium was then replaced with serum free medium only or in presence of 1 ng/ml of TGF-β1 +/- 10 ng/ml of IFN-γ for 72 h. Protein was extracted using PBS and RIPA lysis buffer. Protein concentration was determined using Bradford Assay. 30μg of protein was loaded onto 7.5% PAGE gel and expression determined by immunblot with GAPDH expression measured as a loading control (A). Results in A show one experiment of three separate experiments from 4 omental donors (n=4). Combined densitometry generated from the three experiments calculated from mean MMP3/GAPDH (B).

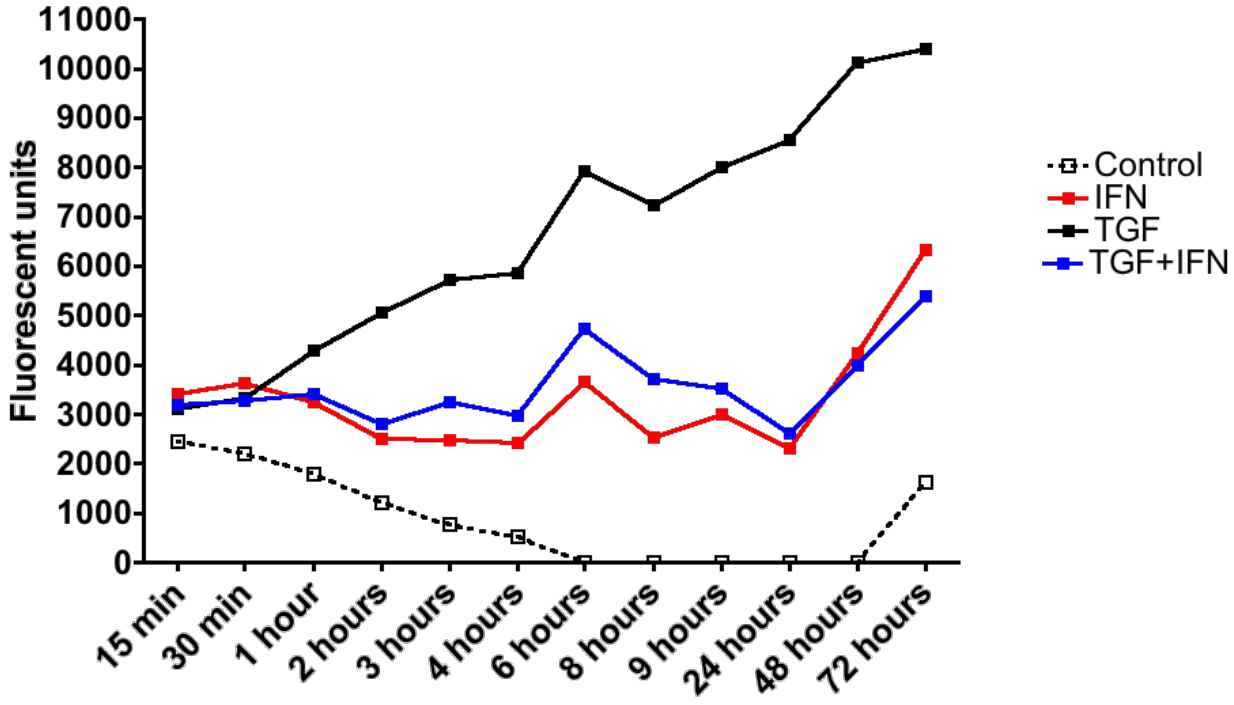

Figure 4.11 Determining incubation time of fluorogenic MMP3 substrate for optimisation of assay

Confluent (80%) monolayers of HPMC were growth arrested with serum free medium for 24 h. The medium was then replaced with medium containing 1 ng/ml of TGF-β1 (black line) or 10 ng/ml of IFN-γ (red line) or in combination (blue line) or cytokine free medium (dotted line) for 48 h. During this time cells were frequently observed to check for any evidence of damage or death. Prior to the collection of supernatant cells numbers were comparable for all conditions. Cell free supernatant was collected following stimulation and 50µl of supernatant was incubated with 50µl M-2300 substrate for 15 min – 72 h at which point MMP3 activity was determined by measuring relative fluorescence.

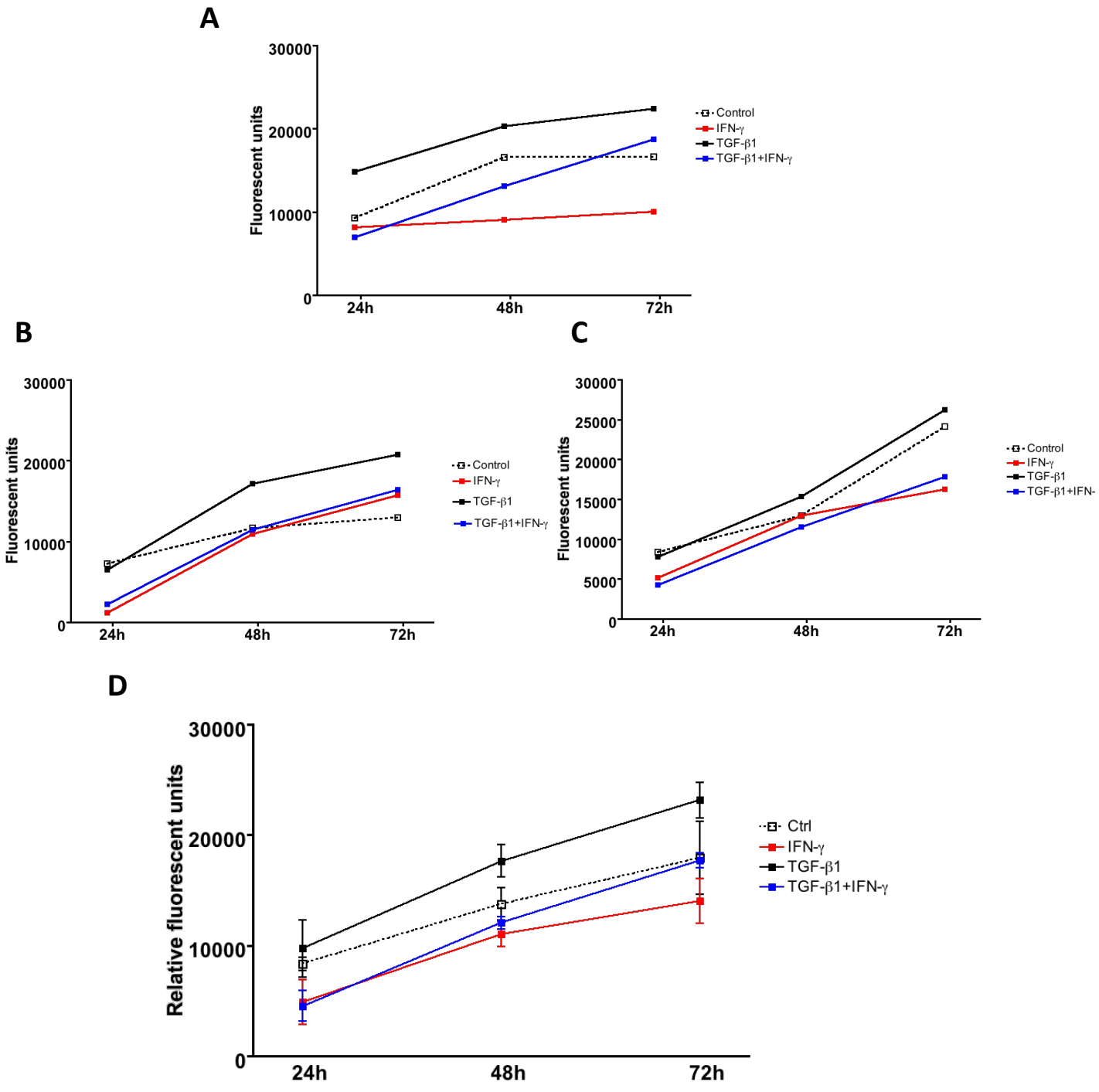

Figure 4.12 Time course of MMP3 activity in HPMC stimulated with TGF-β1 +/- IFN-γ

Confluent (80%) monolayers of HPMC were growth arrested with serum free medium for 24 h. The medium was then replaced with medium containing 1 ng/ml of TGF-β1 (black line) or 10 ng/ml of IFN-γ (red line) or in combination (blue line) or cytokine free medium (dotted line) for 48 h. Supernatant was collected following stimulation and 50µl of supernatant was incubated with 50µl M-2300 substrate overnight. Activity was quantified by measuring fluorescence relative to control sample of serum free medium that has not been placed on cells. Results shown are from 3 omental donors with each omental donor response shown separately (A-C) and the combined result shown in D.

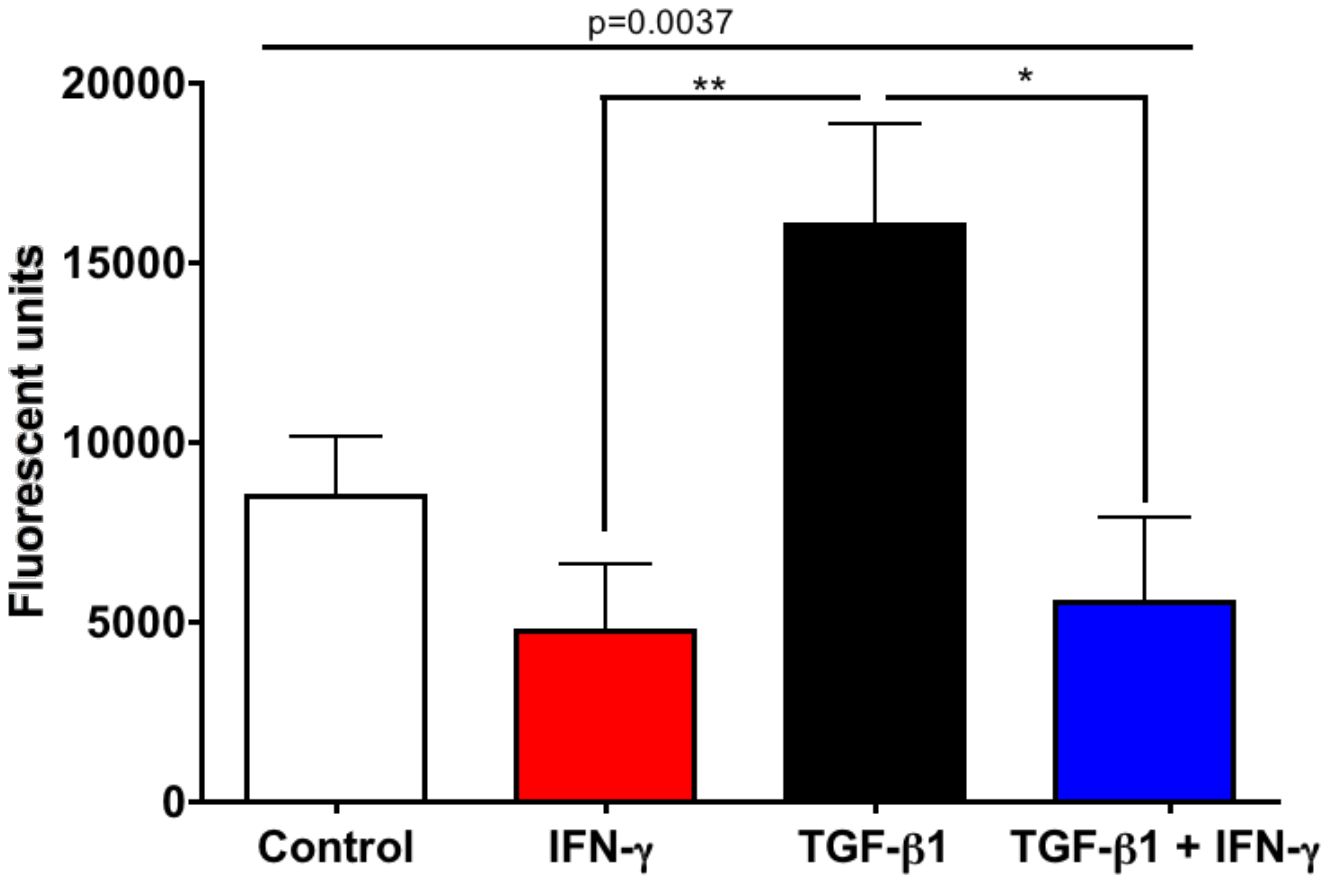

Figure 4.13 TGF-β1 induces a significant increase in MMP3 activity which is inhibited in the presence of IFN-γ

Confluent monolayers of primary HPMC collected from 9 omental donors (n=9) were cultured in T75 flasks and growth arrested for 24 h in serum free medium. The medium was then replaced with fresh serum free medium alone (white bars) or serum free medium containing either 10 ng/ml IFN-γ (red bars), 1 ng/ml of TGF-β1 (black bars) or combination of the two cytokines (blue bars) for 48h. Cell free supernatant was collected following stimulation. 50μl of supernatant was incubated with 50μl M-2300 MMP3 substrate overnight. Relative MMP3 activity was calculated by measuring fluorescence and nomalising data to blank sample containing uncultured serum free medium. Statistical analysis was performed using one-way ANOVA with Bonferroni post test. A p value of <0.05 was deemed statistically significant ($p<0.05$*, $p<0.005$**)

4.2.6 The inhibition of MMP3 expression in HPMC exposed to TGF-β1 and IFN-γ does not result in enhanced fibronectin production

Increased deposition of matrix is a fibrotic effect that has been attributed to TGF-β1. Previous studies have shown that stimulation of HPMC with TGF-β1 results in increased expression of matrix proteins collagen I, collagen III and fibronectin. Within this chapter my qPCR data has shown that TGF-β1 stimulation caused increased expression of col1a1, col1a2 and a modest increase in fibronectin mRNA. Fibronectin is a substrate of MMP3. Thus I examined the hypothesis that the inhibition of MMP3 by IFN-γ results in increased matrix accumulation, enhancing the fibrotic effect.

My qPCR data (Figure 4.2 B) showed a modest induction of fibronectin mRNA in HPMC following exposure to TGF-β1, with no apparent augmentation when HPMC were exposed to TGF-β1 and IFN-γ. Protein expression of fibronectin was examined using immunoblotting (Figure 4.14) and immunohistochemistry (Figure 4.15). Exposure of HPMC to TGF-β1 for 72h resulted in a three-fold induction in fibronectin expression relative to HPMC that were not stimulated or stimulated only with IFN-γ (Figure 4.14 B). Exposure of HPMC to both TGF-β1 and IFN-γ produced similar protein levels of fibronectin to HPMC exposed to TGF-β1 only, thus suggesting that IFN-γ does not augment fibronectin accumulation. This was further confirmed with immunohistochemistry, which measured fibronectin deposition in HPMC exposed for 24-72 h (Figure 4.15). Deposition of fibronectin peaked at 72 h stimulation with TGF-β1, with no apparent increase when HPMC were exposed to both stimuli.

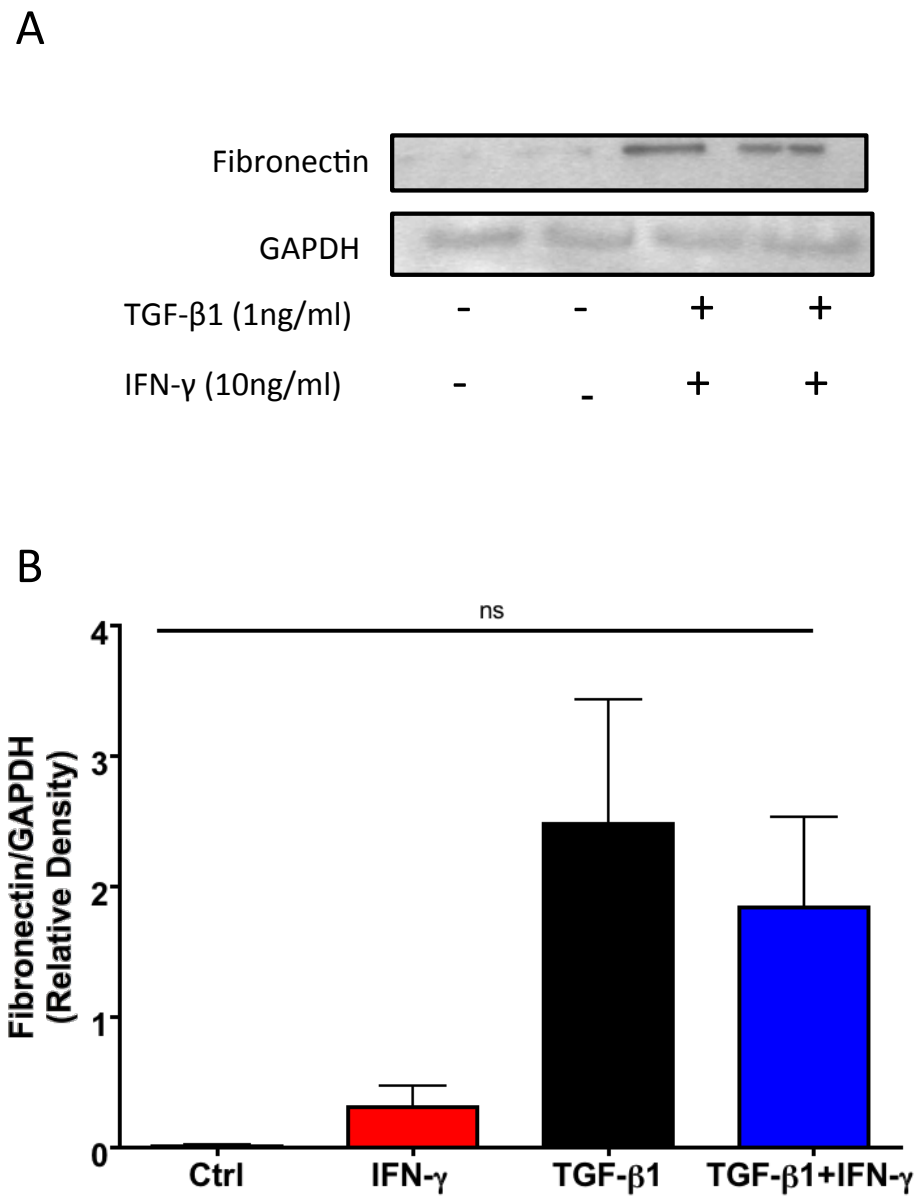

Figure 4.14 The effect of TGF-β1 and IFN-γ on MMP3 substrate fibronectin
HPMC were cultured in 6 well plates and growth arrested for 24 h in serum free medium. The medium was then replaced with serum free medium only, or in the presence of 1 ng/ml TGF-β1 +/- 10 ng/ml IFN-γ for 72 h. Protein was extracted using PBS and RIPA lysis buffer. Protein concentration was determined using Bradford assay. 30μg of protein was loaded onto 7.5% PAGE gel and expression determined by immunoblot with GAPDH expression measured as a loading control (A). Results show one experiment of three separate experiments generated from 3 omental donors (n=3). Combined densitometry results generated from the three experiments of mean fibronectin/GAPDH is plotted (B). Statistical analysis was performed using one-way ANOVA with Bonferroni post test and significance was determined as a p value of < 0.05

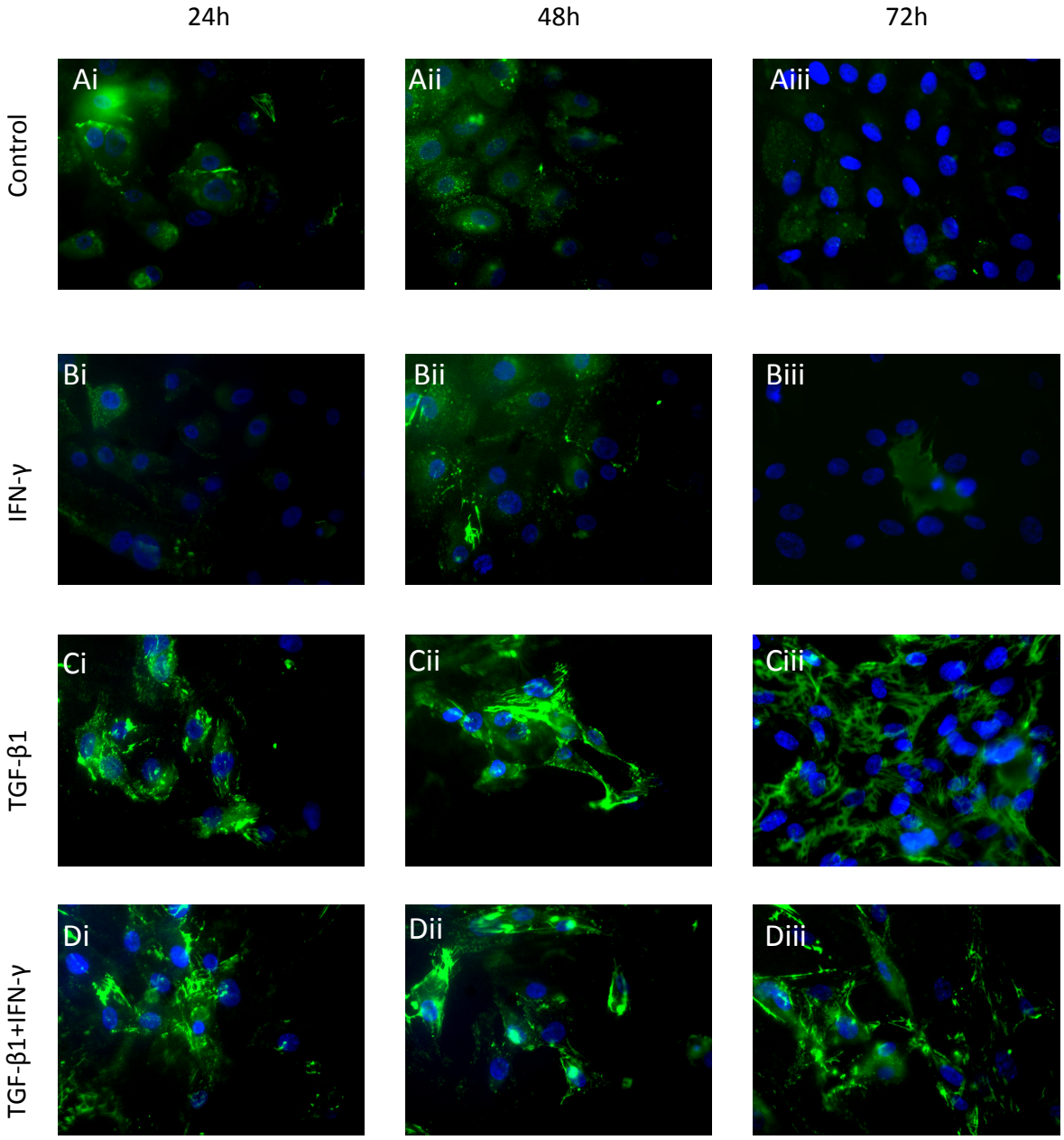

Figure 4.15 IFN-γ does not affect TGF-β1 induction of fibronectin production in HPMC

60% confluent monolayer of primary HPMC were growth arrested in serum free medium for 24h. Cells were then fixed and permeabilised using 4.5% paraformaldehyde and blocked with 1% BSA before incubation with primary antibody overnight. Cells were then incubated at room temperature with secondary antibody before staining of nuclei with Hoechst (blue stain). Cells were then mounted and immunofluorescent localisation of fibronectin (green) detected in cells untreated (A), IFN-γ treated (B), TGF-β1 treated (C) and TGF-β1 and IFN-γ treated cells.

4.2.7 The effect of IL6 on TGF-β1-dependent responses and matrix turnover

The *in vivo* SES murine model highlighted the necessity of IFN-γ in driving fibrosis. However, the release of IFN-γ required the presence of interleukin 6 (IL6) as demonstrated in the IL6KO animals, which do not release IFN-γ following the 4 hits of SES[265]. IL6 is produced by an array of cells within the body and the signal of this cytokine is propagated through a dimeric receptor complex. This receptor complex consists of a cognate receptor subunit (IL6R) and a signal-transducing element, the glycoprotein gp130[348]. The expression of gp130 is extensive and widespread through the body compared to the limited expression of IL6R, which is restricted to hepatocytes and leukocyte subsets[349]. In order for cells to respond to IL6, IL6 must bind to the receptor subunit. Arguably this would mean that only cells expressing IL6R could respond to IL6, however a soluble IL6 receptor (sIL6) was isolated in human serum and urine[350, 351]. The sIL6R binds to IL6 with high affinity and enables cells to respond to IL6 by interacting with gp130 at the membrane. Hurst et al (2001) did not detect the expression of membrane bound IL6R on HPMC (data not shown), thus suggesting that HPMC require the presence of sIL6R to respond to IL6[266].

Therefore to assess how IL6 may influence HPMC responses to TGF-β1 I measured changes in the mRNA expression of HPMC stimulated with IL6 +/- sIL6R using cDNA kindly donated by Christopher Rice (Figure 4.16). HPMC were isolated from three omental donors and cultured according to methods described in chapter two. When cells reached experimental passage (P2) HPMC were growth arrested for 24 h and then cultured in serum free medium alone or in the presence of IL6 (10 ng/ml) alone

or in combination with sIL6R (50 ng/ml) for 0h and 12 h respectively. RNA was extracted from stimulated HPMC and cDNA generated using methods detailed in chapter 2. Using qPCR I measured changes in the mRNA expression of TGF-β1 and PAI-1 within HPMC stimulated for 0 and 12h (A and B). Stimulation of HPMC for 12h in the presence of IL6+sIL6R resulted in a 10 fold increase in TGF-β1 mRNA and a 15 fold increase in PAI-1 mRNA, thus supporting the findings of the *in vivo* model that IL6 is required for the fibrotic process. I also measured the mRNA expression of MMP3 and TIMP1 following stimulation with IL6 +/- sIL6R (C and D). Interestingly, IL6+ sIL6R induced a trend to increase in MMP3, but significantly upregulated the mRNA expression of TIMP1. This suggests that IL6 may promote fibrosis by contributing to matrix accumulation through an additional novel mechanism of augmenting the inhibition of matrix degradation.

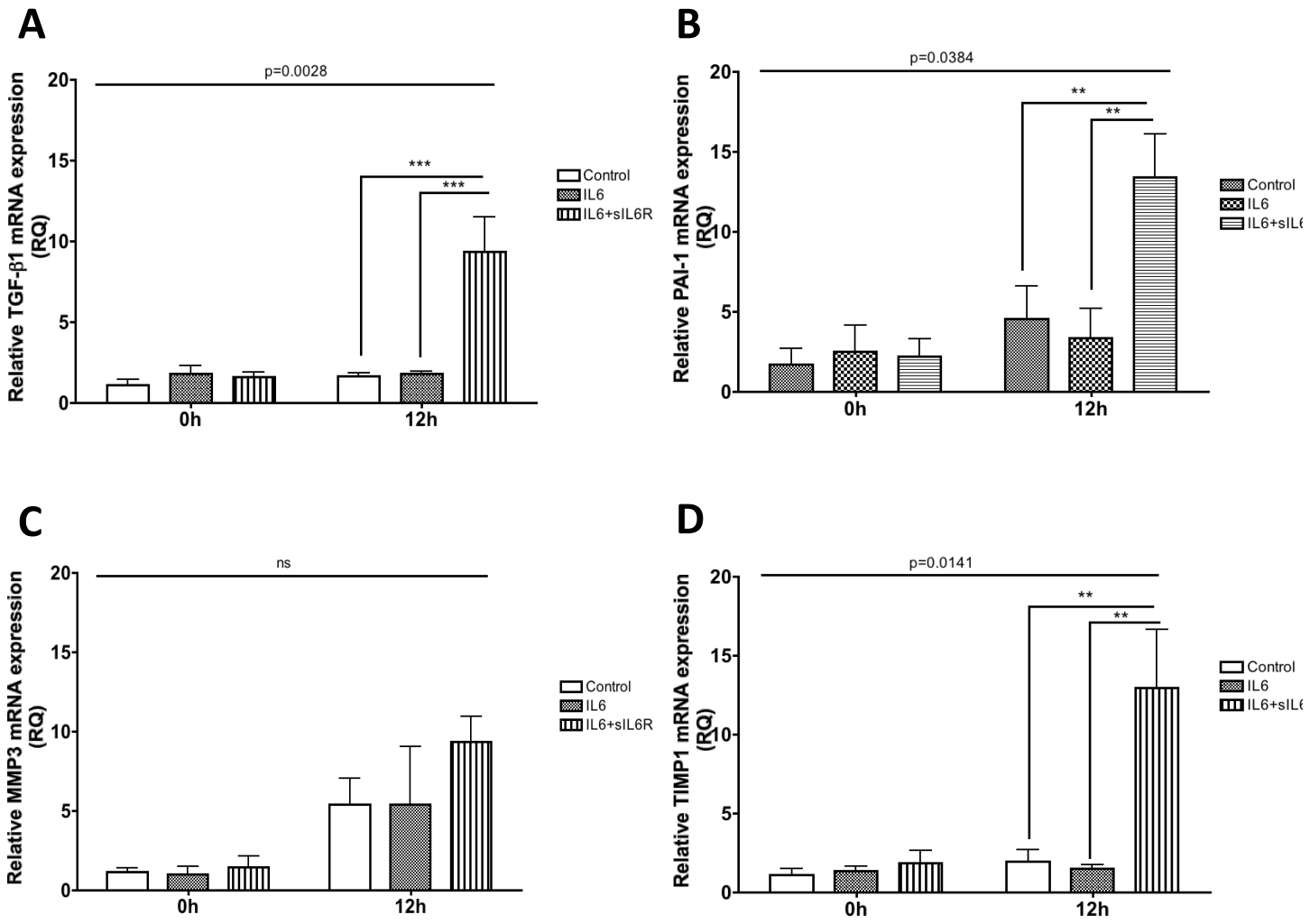

Figure 4.16 Stimulation of HPMC with Il6 enhances mRNA expression of fibrotic mediators

The cDNA for this experiment was kindly donated by Christopher Rice. HPMC were cultured in 6 well plates and growth arrested in serum free medium for 24 h. HPMC were then stimulated for 0 – 12 h with Il6 (10 ng/ml) +/- sIL6R (50 ng/ml). The relative mRNA expression of TGF-β1 (A), PAI-1 (B), MMP3 (C) and TIMP1 (D) were determined using quantitative PCR with rRNA used as an endogenous control. Results were normalised to time 0h control samples. The cDNA was generated from 3 different omental donors(n=3). Results were statistically analysed using 2-way ANOVA with Bonferroni post tests. A p value of < 0.05 was deemed significant ($p<0.05$*, $p<0.005$**, $p<0.0005$***)

4.3 Discussion

Peritoneal fibrosis is the leading cause of treatment failure for patients receiving PD. The development of fibrosis is linked to bio-incompatible dialysis fluid and recurrent infections leading to a state of chronic inflammation[57]. TGF-β1 is a central mediator of the fibrotic process, acting as a potent inducer of matrix production. *In vitro* studies have shown increased expression of TGF-β1 and matrix components by HPMC exposed to high glucose and transient over-expression of inflammatory cytokines[124, 352]. In this institute, Fielding *et al.* (2014) found that repeated episodes of circumscribed inflammation in response to SES led to peritoneal fibrosis, thickening of the submesothelial compact zone and deposition of collagen[265]. These fibrotic changes were concluded to be the result of an IL6 dependent release of IFN-γ.

IL6 and IFN-γ have been studied extensively in relation to peritoneal inflammation. Both cytokines are expressed at high levels during episodes of peritonitis[266, 310]. HPMC are the main source of IL6 within the peritoneum, producing IL6 in response to inflammatory stimuli, whereas NK and T cells predominantly produce IFN-γ[353]. Key roles were identified for both cytokines in regulation of neutrophil recruitment and clearance within the peritoneum and IFN-γ is shown to enhance bacterial clearance within the peritoneum[309, 312]. This suggests that both cytokines are important in control and resolution of the inflammatory response. Failure to resolve the inflammatory response leads to damage to host tissue and fibrosis. How these cytokines modulate TGF-β1 signalling within the peritoneum has not previously been investigated.

The conclusion of Fielding's et al study (2014) that IFN-γ was the main mediator of the fibrotic effects observed led me to examine how IFN-γ may affect HPMC responses to TGF-β1. Typically IFN-γ is reported to be anti-fibrotic in various systems, inhibiting collagen synthesis in human dermal fibroblasts and suppressing αSMA and fibronectin in renal interstitial fibroblasts[354, 355]. Direct inhibition of TGF-β1 signalling by IFN-γ was shown in proximal tubular epithelial cells with suppression of PAI-1 and fibronectin expression[356]. My results differ from these reports, as I found that induction of PAI-1 and fibronectin in HPMC by TGF-β1 was not affected by the presence of IFN-γ. This was also the case for other matrix components, suggesting that IFN-γ does not affect TGF-β1 induction of matrix within HPMC. This suggests a highly specific interaction of IFN-γ, the mechanism of which I try to elucidate in the subsequent chapter.

Matrix homeostasis is a balance between degradation and synthesis. ECM components are degraded by various enzymes, which include the matrix metalloproteinase (MMP) family. Regulating these enzymes are specific inhibitors known as the Tissue Inhibitors of Metalloproteinases (TIMP). The balance between these proteins contributes to the homeostasis of the ECM. In fibrosis the balance is shifted to favour matrix accumulation.

Previous studies have shown that TGF-β1 augments matrix accumulation through stimulation of matrix production and also through modulation of the MMP and TIMP balance[357]. Within an *in vivo* model overexpression of TGF-β1 produced

myocardial fibrosis through increased production of matrix proteins and enhanced expression of TIMP1, 2 and 4 resulting in a decrease in matrix degradation activity[358]. IFN-γ is shown to have an effect on matrix turnover. Within models of early inflammatory arthritis IFN-γ is shown to inhibit induction of MMP1 and MMP3, thus potentially offering protection against cartilage destruction[347]. This was also shown by Fielding et al (2014), which revealed a similar inhibition of IL1-β driven MMP3 by IFN-γ within HPMC.

The lack of effect on TGF-β1 dependent matrix production led me to investigate whether IFN-γ changes ECM homeostasis. I examined the mRNA expression of MMP1 and 3, finding no difference in MMP1 but significant changes in MMP3 expression. When HPMC were exposed to TGF-β1 only, a substantial increase in MMP3 mRNA was observed, which was inhibited when HPMC were exposed to both TGF-β1 and IFN-γ. This effect was detected following 6, 12, 24, 48 and 72h of exposure and at various doses of both cytokines. Importantly a high dose of TGF-β1 was not sufficient to demonstrate this response, suggesting that TGF-β1 may be necessary but not sufficient to induce inflammation driven peritoneal fibrosis.

Further to this change, I found that exposure of HPMC to TGF-β1 or IFN-γ alone resulted in a minimal induction of TIMP1 mRNA. However, when cells were exposed to the combined stimuli this resulted in a significant augmentation of TIMP1 expression. This suggests that the overall ratio of MMP and TIMP is drastically altered by the continued effect of TGF-β1 and IFN-γ. IFN-γ appears to promote matrix accumulation through repression of MMP3 leading to inhibition of matrix

degradation. IFN-γ significantly reduced the TGF-β1 dependent induction of MMP3, resulting in a decrease in total and active enzyme. These results support the findings from the previous chapter, indicating a change in MMP3 and TIMP1 balance underlies IFN-γ promotion of the fibrotic effects of TGF-β1 in inflammation-driven fibrosis.

As a follow on from this experimental work I investigated the effects of IL6 stimulation on HPMC. I found IL6 significantly enhanced the production of TGF-β1 and PAI-1 and suggested a trend in increased MMP3 mRNA. Interestingly following 12 h of stimulation IL6+sIL6R resulted in a significant increase in HPMC TIMP1 production. These results further suggest contributable effects of IL6 and IFN-γ on matrix remodelling augmenting the fibrotic response of TGF-β1.

Taken together, the results of this chapter have shown a specific opposing interaction of TGF-β1 and IFN-γ on the enzyme MMP3. MMP3 is a stromelysin enzyme involved in the degradation of proteoglycans, fibronectin, laminin and collagen IV. In the next chapter I examine the mechanism underlying the regulation of this enzyme by these cytokines. Despite an apparent change in the MMP3 and TIMP1 balance within this system, there does not appear to be an augmentation in all matrix components following exposure of HPMC to TGF-β1 and IFN-γ. However combined with the data obtained from IL6 stimulation of HPMC, these findings further highlight that a change in the MMP3 and TIMP1 balance may be a significant contributor to inflammation-driven fibrosis.

Chapter 5: The mechanism of MMP3 regulation within HPMC

5.1 Introduction

In the previous results chapters, my findings indicate a significant difference in the expression of MMP3, suggesting that MMP3 regulation may be a key point of the interaction for TGF-β1 and pro-inflammatory signalling in peritoneal fibrosis. In the SES murine samples MMP3 expression is significantly greater in the IL6KO mice compared to WT samples. The HPMC system examined in chapter 4 indicates an induction of MMP3 expression when HPMC are stimulated with TGF-β1, which is inhibited when IFN-γ is present. This indicates that IFN-γ promotes fibrosis through inhibition of matrix degradation, potentially resulting in an accumulation of ECM. The opposite effects of these two cytokines on MMP3 expression led to the aim of this chapter to examine the mechanism of MMP3 regulation by TGF-β1 and IFN-γ.

5.1.2 Matrix metalloproteinases

The MMPs consist of a family of 23 zinc-dependent endopeptidases in humans that share similarities in function and structure[359, 360]. The main function of this enzyme family is the regulation of ECM composition through cleavage of various ECM and non-ECM components. These enzymes are therefore involved in various physiological and pathological processes such as embryo development, wound healing, angiogenesis, tissue remodelling, inflammation, cancer, autoimmune diseases and arthritis[359, 361].

5.1.3 Regulation of MMP expression

5.1.3.1 Activation

MMPs exhibit tightly controlled tissue specific expression and activity at numerous levels[362]. MMPs are synthesised as inactive pro-zymogens[363]. All mammalian MMPs possess a conserved domain structure that is composed of a catalytic domain and an inhibitory pro-domain. The pro-zymogen is maintained in a latent state though conserved cysteine residue in the pro-domain that inhibits binding and catalysis of the substrate by blocking the active site zinc ion[364, 365]. This mechanism first described by Hal Van Wart and Henning Birkedal-Hansen is known as the "cysteine switch" mechanism[366].

The latent zymogens become activated under physiological conditions through multiple mechanisms that result in disruption to the cysteine leading to destabilisation or removal of the pro-domain[364, 365]. This ensures the active site becomes available to catalyse substrates. Activators of MMPs include plasmin, urokinase type plasminogen activator (uPA), tissue-type plasminogen activator (tPA) and other serine proteases and MMPs[367, 368]. Chemical disruption through amino phenyl mercuric acid (APMA) is also reported to result in activation[369].

5.1.3.2 Inhibitory regulation

MMP activity is regulated at the cellular level being inhibited by general protease inhibitor α2-macroglobulin and thrombospondin-2, which promote their removal from the extracellular environment. MMPs are also regulated by a family of four natural endogenous inhibitors known as tissue inhibitiors of metalloproteinases

(TIMPS 1-4). As with MMPs the TIMP proteins ranging from 21-30kDa in size are homologous in structure and function sharing 41-52% sequence identity[370], however they do have distinctive structural and biochemical properties as well as differences in expression patterns[371]. The TIMPs are promiscuous in function and are shown to inhibit all MMPs *in vivo*[372]. TIMPs act as inhibitors by forming 1:1 complexes with the catalytic zinc ion in the active site of the MMP enzyme. This prevents substrate binding to the active site thus inhibiting cleavage and catalysis[369, 373]. This is an important regulator of MMP activity, with the balance between MMP:TIMP determining overall matrix homeostasis.

5.1.3.3 Signalling pathways

MMP expression is shown to change in response to various cellular signalling pathways. This occurs through activation of transcription factors and binding to the promoter sequence resulting in changes to MMP transcription. These signalling pathways that regulate MMP expression are at present still incompletely defined.

The MAPK pathway is known to be involved in cytokine regulation of MMP expression. Induction of MMP-1 by IL-1 and TNF-α is mediated through activation of p38 and ERK pathways[374]. TGF-β1 signals predominantly through SMAD transcription factor pathway, however activation of MAPK is also reported to occur in co-ordination and independently of SMAD. Inhibition of both Smad and MAPK resulted in a suppression of MMP-1 and MMP-2 by TGF-β1[375]. Both these pathways may be involved in TGF-β1 induction of MMP3 within this system.

The JAK/STAT signalling pathway is also implicated in regulation of MMP expression. In chondrocytes blockade of JAK2 and STAT1/2 resulted in inhibition of IL-1β induced MMP13 expression[376]. In another study STAT3 is shown to induce MMP-2 activation in response to TNF-α in proximal tubule cells[377]. The STAT pathway may be involved in the IFN-γ mediated inhibition of MMP3 reported within this thesis. Previous research has shown induction of STAT1 by IFN-γ results in suppression of MMP transcription such as MMP9 in human atroglioma and human fibrosarcoma cell lines[346, 378].

5.1.3.4 Transcriptional regulation

The MMP genes are reported to be "inducible" in nature, responding to various stimuli that includes growth factors, cytokines, mechanical stress and chemical agents such as phorbol ester[363]. Induction or inhibition of MMP transcription by cytokines can result in 20-50 fold changes in mRNA and protein expression[361]. Studies have shown stimulation of MMP3 in response to IL-1β and TNF-α[379]. Within my *in vitro* system MMP3 mRNA is significantly increased in the presence of TGF-β1.

Within the promoter sequence of MMP genes resides numerous cis-regulatory elements that enable binding of specific transcription factors, which can both induce and repress transcription. This also provides a high degree of control of cell specific expression. There is a high degree of homology between MMP genes and the cis-elements they contain, which explains the co-expression of MMPs in response to stimuli. Highly conserved cis-elements include the TATA boxes found at around

-30bp and the activator protein-1 (AP-1) binding site at -70bp. In the review from Yan and Boyd (2007), MMP genes are divided into three categories depending on the promoter confirmation containing TATA box and AP-1 site, TATA box and no AP-1 site and no TATA box nor AP-1 site[359]. Further studies have identified other functional cis-elements within MMP promoters, which include polymavirus enhancer A-binding protein-3 site (PEA3), STAT binding element, TGF-β1 inhibitory element (TIE). The MMP3 promoter contains the TATA box, the proximal AP-1 site (-70bp), two PEA3 binding sites and a stromelysin-1 PDGF responsive element (SPRE)[359].

5.1.4 Activator protein-1

The AP-1 binding site at approximately -70bp appears to be a major regulatory site of various MMP genes. The AP-1 complex that binds to this site, is a heterodimer composed of proteins from the Jun protein family and the Fos protein family. The proteins within this complex all contain a leucine zipper region that enables dimerization and binding to the AP-1 consensus DNA sequence (5'-TGAG/CTCA-3')[380].

Within the MMP3 promoter the AP-1 site appears to be essential for basal transcription, as mutations to the site caused a reduction in promoter activity. However, a similar reduction in basal activity was observed when either of the two PEA3 site within the MMP3 promoter were mutated. This suggests that AP-1 site is not solely responsible for basal activity in the MMP3 promoter.

The AP-1 complex is shown to mediate the induction of MMP3 by certain stimuli such as IL-1α in Human Trabecular Meshwork Cells[381]. Decreased binding to the AP-1 site is also shown to suppress MMP3 transcription. Human fibroblasts treated with IFN-γ displayed decreased AP-1 specific binding in gel shift assays[382]. The DNA binding and activation of transcription factors through AP-1 can be regulated through MAPK signalling pathway, with various studies highlighting the involvement of this pathway in the induction of MMP3[383, 384]. The MAPK pathway is shown to augment the AP-1 response through induction and phosphorylation of c-jun and c-fos. The p38 branch can also enhance the AP-1 response through induction of transcription factors such as ATF-2 and Elk-1 that cause an increase in the promoter activity of of c-jun and c-fos[385]

In conclusion the aims of this chapter will be:

- To characterise the mechanism of MMP3 induction by TGF-β1
- To determine the mechanism of how IFN-γ suppresses the TGF-β1 dependent induction of MMP3

5.2 Results

5.2.1 Examination of potential transcription factors potentially contributing to MMP3 regulation

Within the previous chapter I have demonstrated a significant effect of TGF-β1 and IFN-γ on the mRNA level of MMP3, suggesting the effects of these cytokines occurs at the level of transcription. Examination of the transcription factor Zinc Binding Protein-89 (ZBP-89), a protein shown to enhance MMP3 promoter activity revealed a significant difference in the *in vivo* system with 2 fold difference in mRNA expression between the genotypes (Figure 5.1 A). Similar levels of mRNA expression were detected within the *in vitro* system, however there was no difference in ZBP-89 mRNA expression between TGF-β1 and IFN-γ treated HPMC alone or in combination.

IFN-γ is reported to inhibit TGF-β1 signalling through induction of the inhibitory SMAD 7[386, 387]. Therefore I examined mRNA expression of SMAD 7 in both the *in vivo* (Figure 5.1 B) and *in vitro system* (Figure 5.2 B). WT mice expressed greater levels of SMAD 7 compared to IL6KO mice, with maximal expression occurring at day 42 and 49 when scarring became histologically apparent. Within the *in vitro* system HPMC stimulated with increasing doses of TGF-β1 resulted in increased expression of SMAD 7 that was not affected in the presence of IFN-γ. Peak expression occurred when HPMC were stimulated with 1 ng/ml of TGF-β1 and IFN-γ did not affect the mRNA expression, suggesting this is not the mechanism through IFN-γ inhibition of MMP3 induction by TGF-β1.

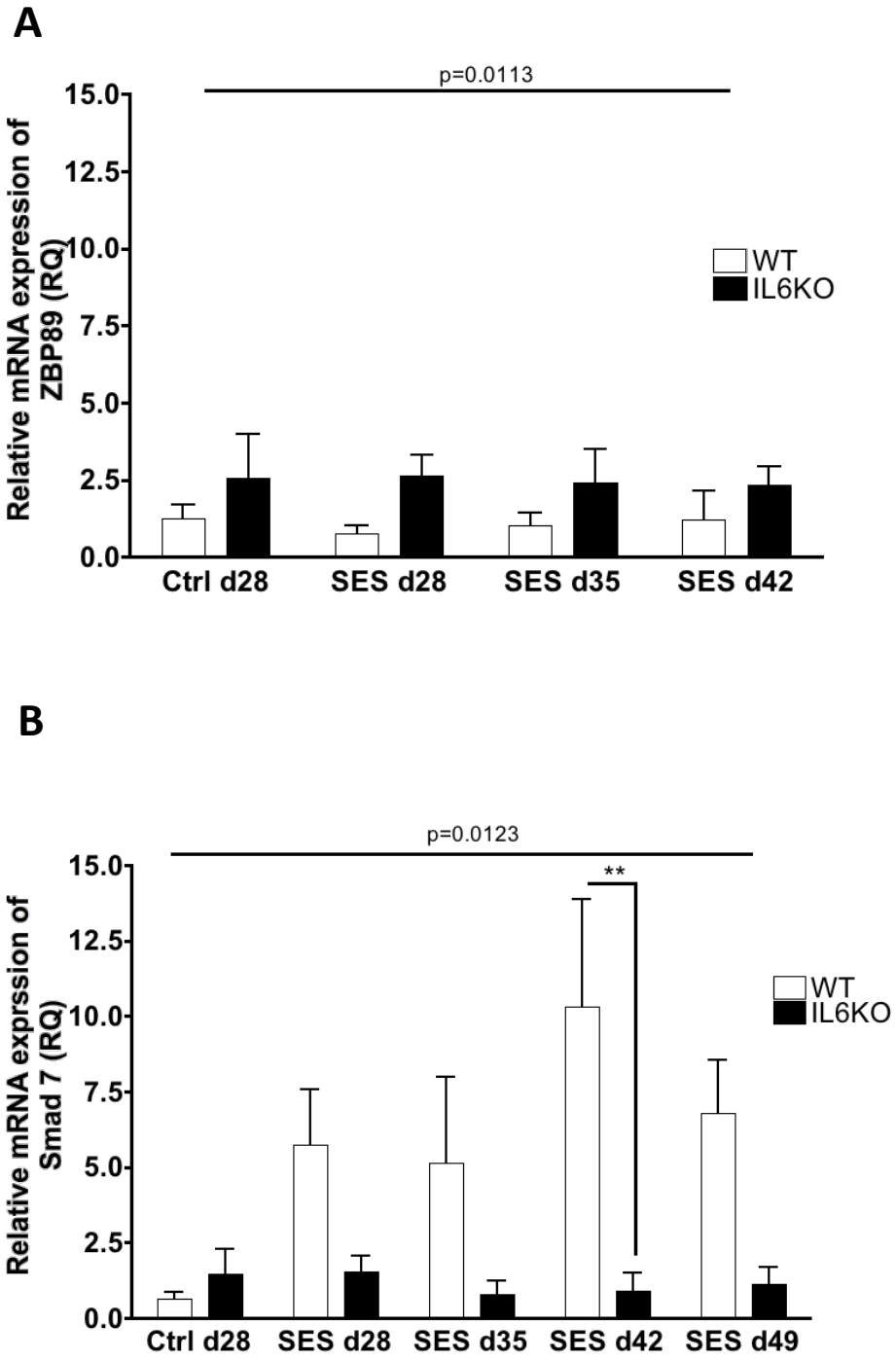

Figure 5.1 Transcription factor mRNA variation between WT and IL6KO
Quantitative PCR was used to analyse the mRNA expression of potentially fibrotic transcription factors using RNA extracted from peritoneal membranes. ZBP89 (A) and Smad7 (B) were compared between mice genotypes (WT and IL6KO) from day 28 to day 49. Results shown are representative of cDNA prepared from ≥3 different mice per time point and genotype, expressed relative to WT control. Results shown are mean values with error bars representing SEM. Statistical analysis was performed using 2-way ANOVA followed by Bonferroni post-test a p value of <0.05 was deemed significant ($p<0.05$*, $p<0.005$**).

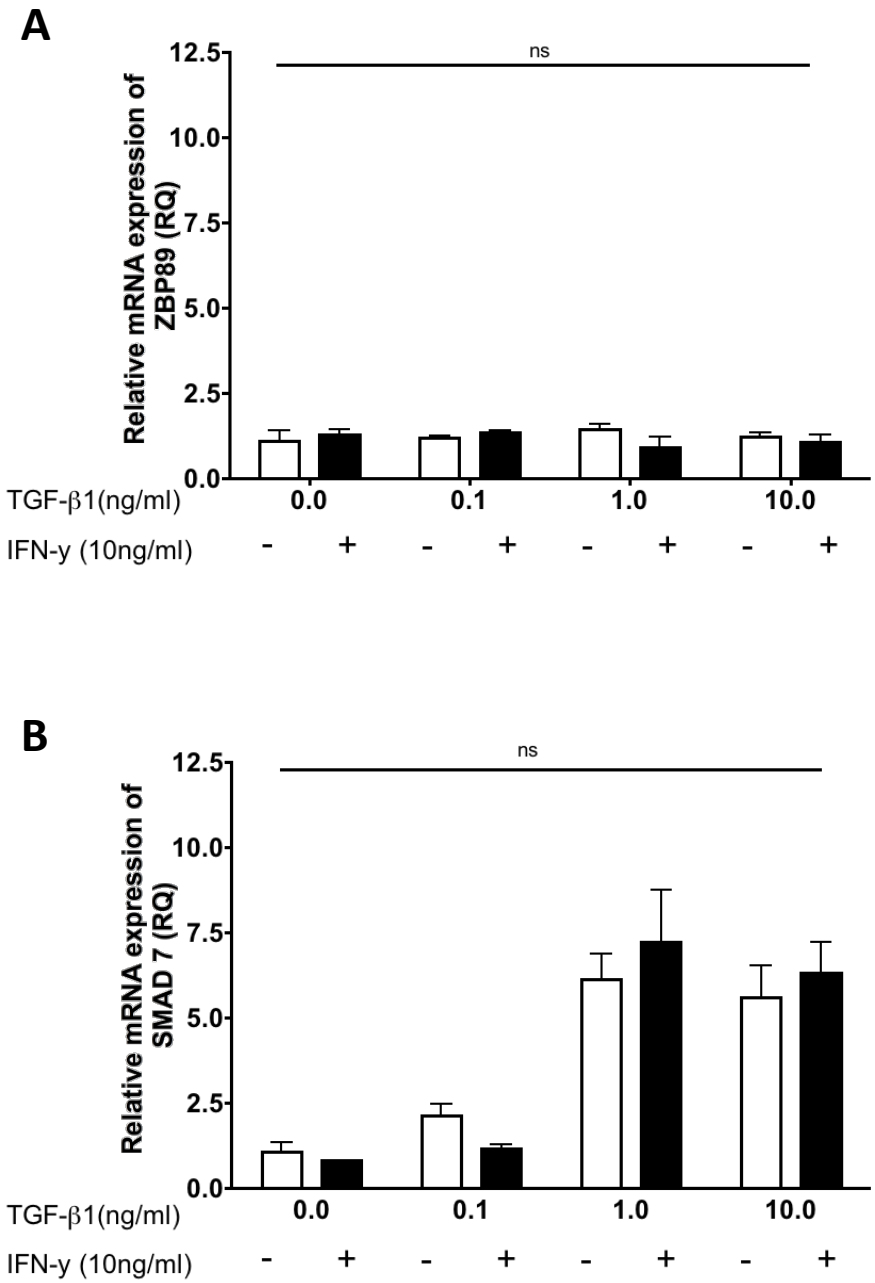

Figure 5.2 Effect of TGF-β1 and IFN-γ on the mRNA expression of various transcription factors

Confluent (80%) monolayers of primary HPMC were growth arrested with serum free medium for 24h. The medium was replaced with medium containing TGF-β1 (white bars) in doses ranging from 0-10ng/ml alone or in combination with 10ng/ml IFN-γ (black bars) for 24h. Total RNA was extracted and relative expression of ZBP89 (A) and SMAD7 (B) were calculated using quantitative PCR. 18S rRNA was used as an endogenous control and data were normalised to 0ng/ml TGF-β1 treated samples. Results shown are generated from 3 different omental donors (n=3). Statistical analysis was performed using a 2-way ANOVA followed by Bonferonni post tests to determine difference between treatments across the dose range. A p value of <0.05 was deemed significant

5.2.2 Blockade of SMAD3 signalling results in inhibition of MMP3 induction and significant effect on cell viability

The primary signalling pathway through which TGF-β1 exerts cellular effects occurs predominantly through the SMAD transcription factors. To determine whether the TGF-β1 dependent induction of MMP3 occurred through this pathway I used a selective Smad3 inhibitor SIS3 shown to diminish phosphorylation of SMAD 3 within fibroblasts[388]. I measured the effect of SIS3 at the level of transcription (Figure 5.3) using qPCR to measure both PAI-1 (A) and MMP3 (B) in HPMC stimulated for 24 and 48 h with TGF-β1. The blockade of SMAD3 with SIS3 resulted in a significant reduction in both PAI-1 and MMP3 mRNA expression particularly at 48 h when expression in both MMP3 and PAI-1 peaked.

To determine if the SIS3 inhibitor had an effect on the phosphorylation of the SMAD 3 protein HPMC stimulated for 1 h with TGF-β1 +/- SIS3 (3 μM) pre-treatment for 1h then underwent cellular protein extraction. I measured phosphorylated SMAD3 (pSMAD3) expression using immunoblotting (Figure 5.4). The data indicates that following 1 h stimulation there was no reduction in pSMAD3 expression following treatment with SIS3, suggesting that the inhibitor was not exhibiting a suppression of pSMAD3 under these experimental conditions.

To try and inhibit phosphorylation of SMAD3 I increased the dose from 3 μM to 5 μM and 7.5 μM respectively (Figure 5.5). Increasing the dose to 5 μM resulted in further suppression of TGF-β1 induced MMP3 mRNA expression, however increasing the dose beyond 3 μM resulted in a significant effect on cell viability assessed using

Alamar Blue. Therefore the data showed that treatment with SIS3 for 24 h and 48 h does cause pSMAD3 suppression, which leads to inhibition of the induction of MMP3 by TGF-β1 suggesting a potential role for SMAD pathway in this mechanism.

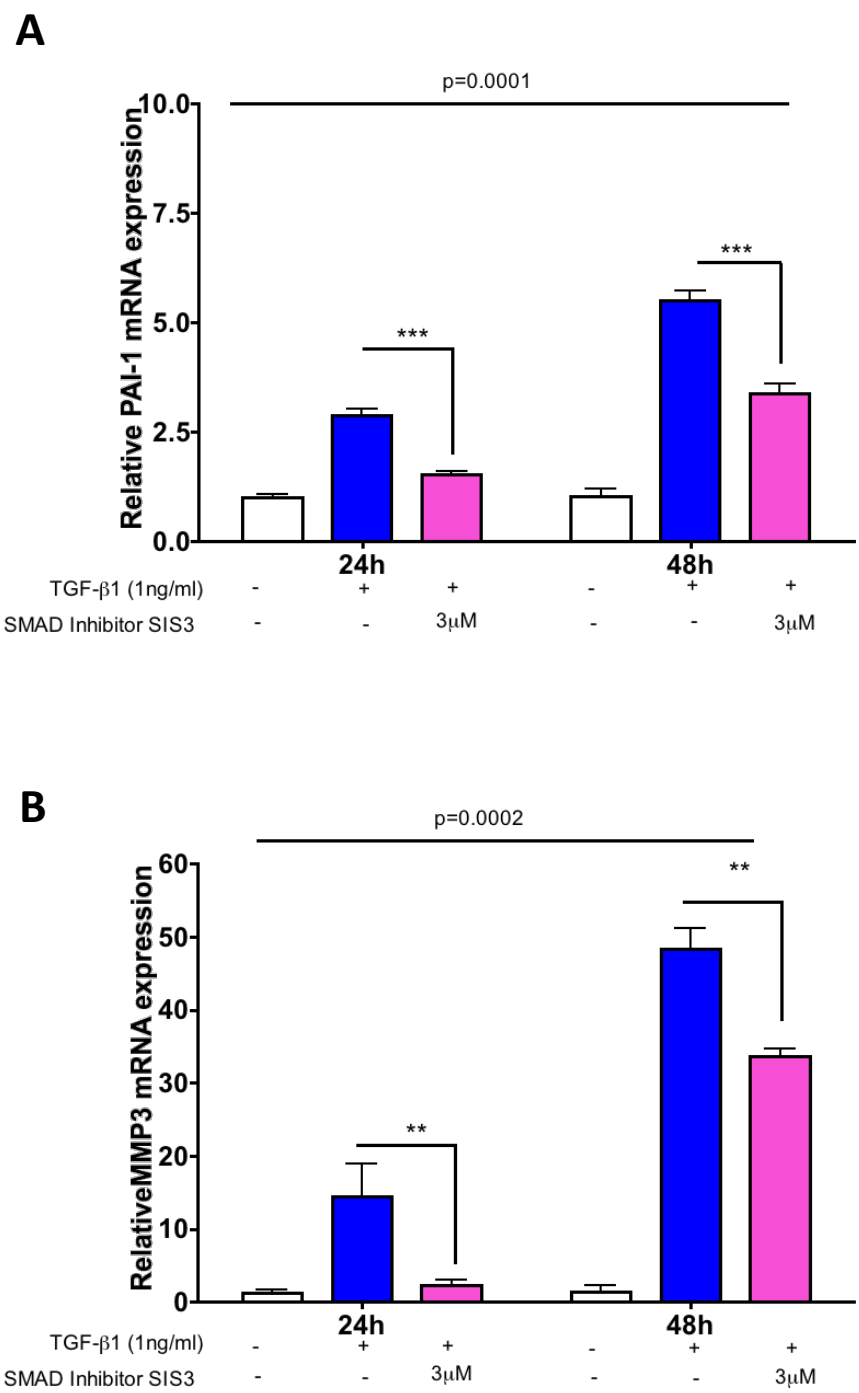

5.3 Up-regulation of PAI-1 and MMP3 mRNA expression in HPMC by TGF-β1 is significantly attenuated by SMAD3 inhibitor SIS3

Confluent (80%) monolayers of primary HPMC were growth arrested in serum free medium for 48h. The medium was replaced with medium containing 1ng/ml TGF-β1 (blue bars) in the absence or presence (pink bars) of 3μM of SIS3 or absence of both (white bars). RNA was extracted following 24h stimulation and relative expression of PAI-1 (A) and MMP3 (B)were determined using quantitative PCR. rRNA expression was used as an endogenous control and data were normalised to control samples at 24h time point. Results were generated from 3 different omental donors (n=3) with mean values plotted and error bars representing SEM. Statistical analysis was performed using 2-way ANOVA with Bonferroni post tests. A p value of < 0.05 was deemed significant($P<0.005$**, $P<0.0005$***).

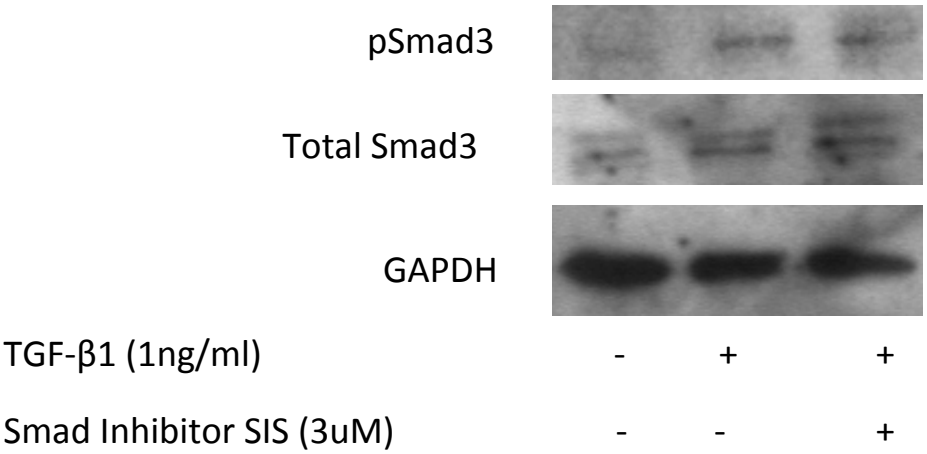

Figure 5.4 Western analysis of inhibitor SIS3 shows no inhibition of SMAD3 phosphorylation

Confluent (80%) primary HPMC were growth arrested in serum free medium for 24h after which medium was replaced with fresh serum medium only or medium containing 1ng/ml TGF-β1 alone or in the presence of 3μM SIS3. Cells were incubated with the stimuli for 1h and then protein was extracted using RIPA lysis buffer. Protein concentration was determined using Bradford assay and 30μg of protein was loaded onto a PAGE gel and amount determined by immunoblot using GAPDH expression as a measurement of loading control.

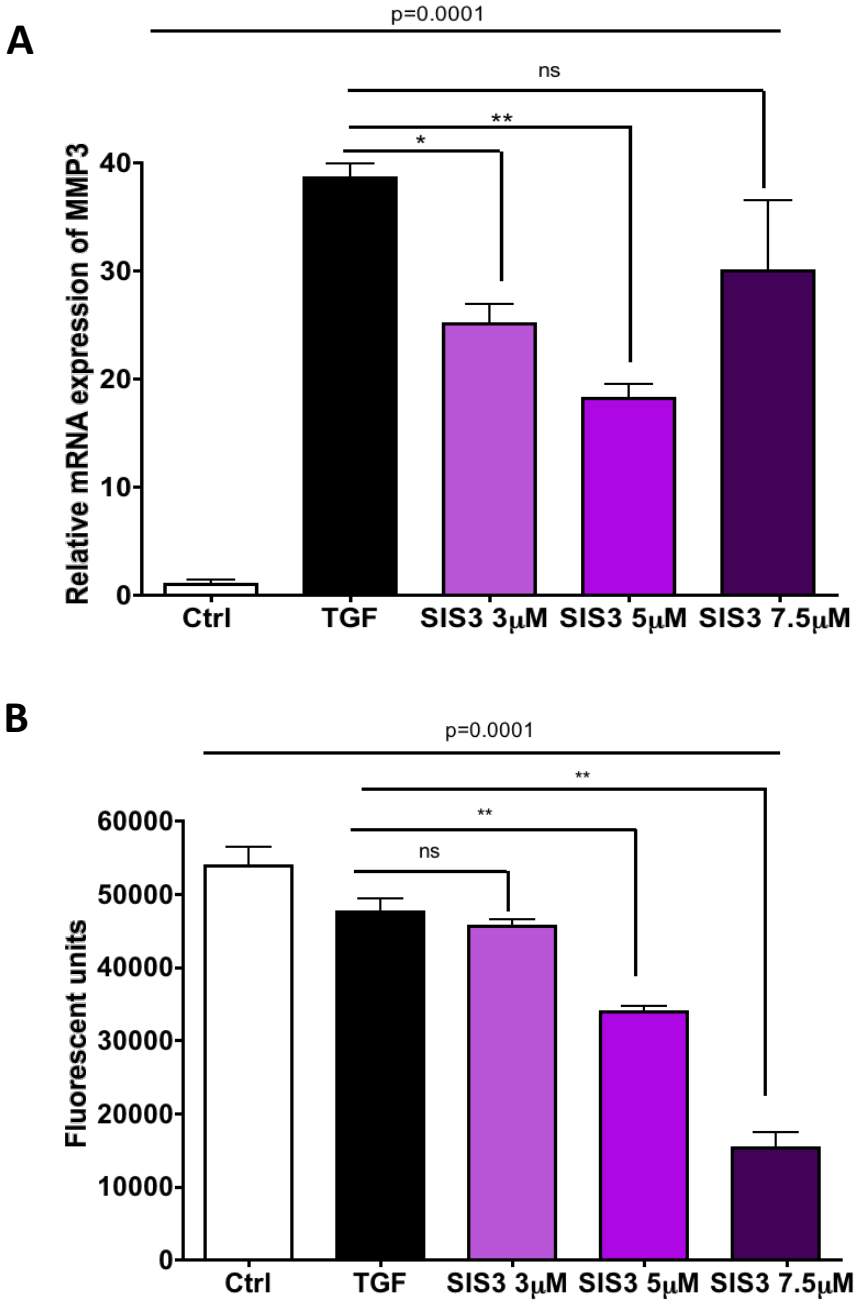

Figure 5.5 Increased concentration of SIS inhibits the TGF-β1 dependent increase in MMP3 but with a significant effect on cell viability

Confluent monolayers of primary HPMC were cultured in 12 well plates. Cells were starved of serum for 24h before incubation with SIS inhibitor at concentrations 3μM, 5μM and 7.5μM for 48h or in fresh serum free medium only. Proliferation was determined using alamar blue assay, which involved adding 10% alamar substrate to medium for 1h following 48h of incubation before cell supernatant was collected. Activity was determined by measuring fluorescence. Results show 3 experiments generated from 3 different omental donors performed in triplicate (n=3). Statistical analysis was performed using one-way ANOVA with Bonferroni post tests. A p value of <0.05 was deemed significant ($p<0.005$**, $p<0.0005$***).

5.2.3 IFN-γ does not inhibit TGF-β1 induced SMAD3 signalling

The role of SMADS in the induction of MMP3 by TGF-β1 resulted in my examination of SMAD3 signalling in HPMC cultured with TGF-β1 +/- IFN-γ. This investigation was to determine whether IFN-γ inhibited the induction of MMP3 through modulation of SMAD3 signalling. I assessed SMAD3 signalling with immunoblotting measuring pSMAD3 expression in cellular protein collected from HPMC stimulated with TGF-β1 and IFN-γ alone or in combination at time intervals up to 6 hours with protein levels of GAPDH measured as an endogenous control (Figure 5.6).

Peak expression of pSMAD3 occurred following 30 min to 1 h of stimulation with TGF-β1. The signal from immunoblotting began to decrease following 3 h of stimulation before returning to control levels after 6 h of stimulation. Stimulation of HPMC with IFN-γ alone did not cause an induction in pSMAD3 expression, with levels remaining similar to the control sample. The induction of pSMAD3 by TGF-β1 was not affected when HPMC were stimulated with combination of TGF-β1 and IFN-γ throughout the time course, with expression levels remaining similar to HPMC treated with TGF-β1 only.

Further confirmation of the above data occurred through subsequent transfection experiments of transformed mesothelial cells from the cell line Met5A with the SMAD responsive reporter vector CAGA. Following transfection, Met5A cells were stimulated with TGF-β1 and IFN-γ alone or in combination for 24h. Basal Smad3 reporter activity was significantly increased in the presence of TGF-β1 and this increase was not significantly altered in the presence of IFN-γ.

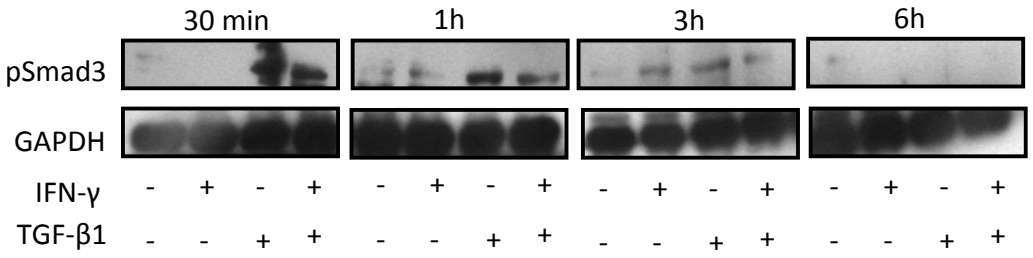

Figure 5.6 Western analysis shows IFN-γ has no effect on TGF-β1 dependent phosphorylation of SMAD 3

Confluent (80%) monolayers of primary HPMC were growth arrested in serum free medium for 24h. Medium was then aspirated and replaced with fresh serum free medium only or medium containing TGF-β1 (1ng/ml) or IFN-γ (10ng/ml) alone or in combination for 30 min – 6h. RIPA lysis buffer was then used to extract protein, protein expression of pSMAD3 was determined using immunoblotting with GAPDH expression as a measurement of loading control. One representative experiment of three separate experiments shown

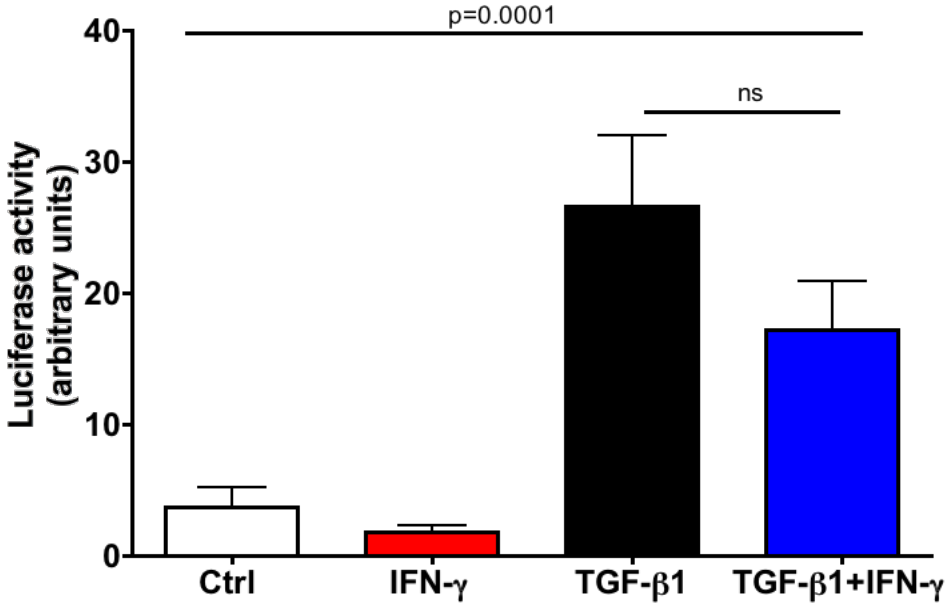

Figure 5.7 Transfection of met5a with SMAD responsive pGL3 vector (CAGA) confirms IFN-γ does not affect TGF-β1 dependent SMAD signalling

Met5a cells were transfected with CAGA pGL3 plasmid and renilla before incubation for 24h with control serum free medium, 10ng/ml of IFN-γ, 1ng/ml TGF-β1 and combination of TGF-β1 and IFN-γ. Ratio of firefly to renilla luciferase activity is shown, normalised to control cells. Three experiments shown performed in triplicate (n=3). Statistical analysis performed using one-way ANOVA followed by Bonferroni post test. A p value of <0.05 was deemed statistically significant.

5.2.4 Blockade of ERK signalling results in suppression of TGF-β1 induced MMP3 mRNA induction

To gain further understanding of the mechanism through which TGF-β1 regulates MMP3 expression within HPMC I examined the role of the MAPK pathway, which is shown to be involved in both TGF-β1 signalling and MMP regulation. Within arthritis research, blockade of the ERK MAPK resulted in significant inhibition of MMP3 induction by IL-1β[389]. The initial investigation of MAPK pathway involved examining the role of ERK specifically.

I examined the effect of ERK blockade on MMP3 expression at the level of transcription. The MAPK Kinase (MEK) 1/2 inhibitor PD98059 was chosen as MEK is upstream from ERK and ERK is the only known substrate of MEK. Therefore inhibiting MEK prevents the phosphorylation and activation of ERK. HPMC were stimulated with TGF-β1 for 24 and 48h alone or in combination with MEK inhibitor PD98059 (10μM) before RNA was extracted and expression of PAI-1 and MMP3 determined using qPCR (Figure 5.8).

Blockade of ERK did not affect TGF-β1 induction PAI-1 expression in HPMC, with mRNA expression increasing 22 fold in both TGF-β1 +/- MEK inhibitor PD98059 following 48h of stimulation. Blockade of ERK signalling did cause a significant reduction in MMP3 mRNA expression following TGF-β1 treatment, with a reduction of approximately 50% in MMP3 mRNA expression. To ensure that the MMP3 data generated was not the result of an effect on cell viability, I cultured HPMC for 24h with MEK inhibitor PD98059 at 10μM and 30μM then assessed cell viability using

Alamar Blue (Figure 5.9). The results showed that even at 30µM the MEK inhibitor PD98059 has no impact on cell viability indicating that ERK has a significant role in the induction of MMP3 by TGF-β1.

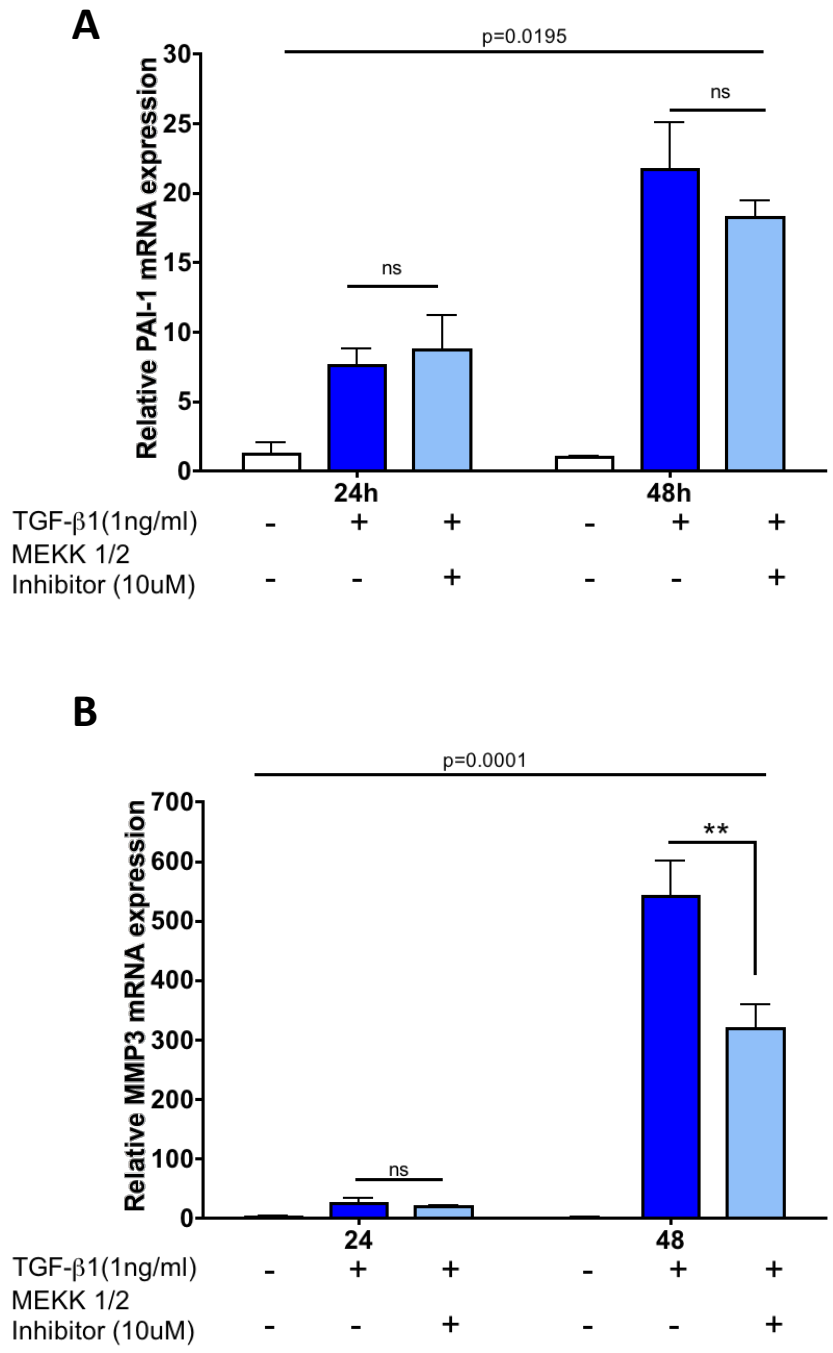

Figure 5.8 Up-regulation of MMP3 mRNA expression by TGF-β1 in HPMC is attenuated by ERK inhibitor PD98059

Confluent (80%) monolayers of primary HPMC were growth arrested for 24h in serum free medium. The medium was replaced with medium containing 1ng/ml TGF-β1 (dark blue bars) in the absence or presence (light blue bars) of 10μM of PD98059 or absence of both (white bars). RNA was extracted following 24h and 48h stimulation and relative expression of PAI-1 (A) and MMP3 (B)were determined using quantitative PCR. rRNA expression was used as an endogenous control and data were normalised to control samples at 24 h time point. The results were generated from 3 omental donors and show 3 experiments (n=3). Statistical analysis was performed using 2-way ANOVA with Bonferroni post tests. A p value of < 0.05 was deemed significant(<0.05*, $p<0.005$**, $p<0.0005$***).

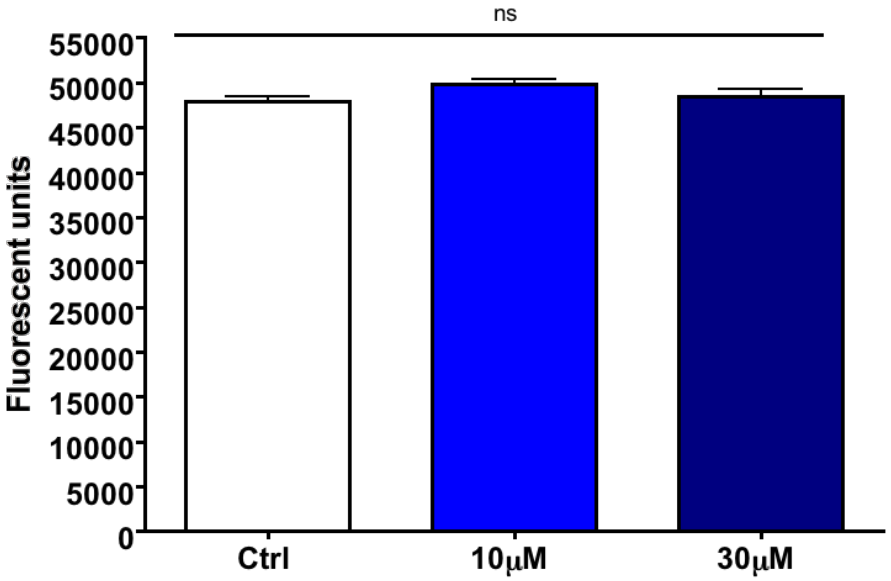

Figure 5.9 Effect of PD98059 MEK 1/2 Inhibitor on HPMC proliferation
Confluent monolayers of primary HPMC were growth arrested for 24h before incubation with MEK 1/2 inhibitor PD98059 at concentrations of 10μM and 30μM for 48h or in fresh serum free medium only. Cellular proliferation was determined using Alamar Blue assay, adding 10% Alamar Blue substrate to medium for 1h following treatment. Activity was determined by measuring fluorescence. Results shown are three separate experiments generated from 3 omental donors performed in triplicate (n=3).

5.2.5 ERK signalling in HPMC does not change in the presence of IFN-γ

The previous data supports the involvement of ERK in the TGF-β1 induction of MMP3. This led to examination of ERK signalling in HPMC stimulated with TGF-β1 +/- IFN-γ, to determine whether IFN-γ inhibits MMP3 expression through modulation of the ERK signalling pathway. To examine this HPMC were stimulated with TGF-β1 and IFN-γ alone or in combination for designated times (30min-6h). Following stimulation HPMC underwent cell lysis and cellular protein was collected, with phosphorylated ERK (pERK) measured using immunoblotting (Figure 5.9).

The protein expression of pERK appeared maximal following 30min of stimulation with TGF-β1. The protein expression of pERK was not affected in HPMC treated with both TGF-β1 and IFN-γ, thus suggesting that IFN-γ does not inhibit MMP3 through modulation of the ERK pathway. HPMC stimulated with IFN-γ alone did not result in an induction in pERK until 6h of stimulation, at which point induction of pERK by TGF-β1 had returned to basal level.

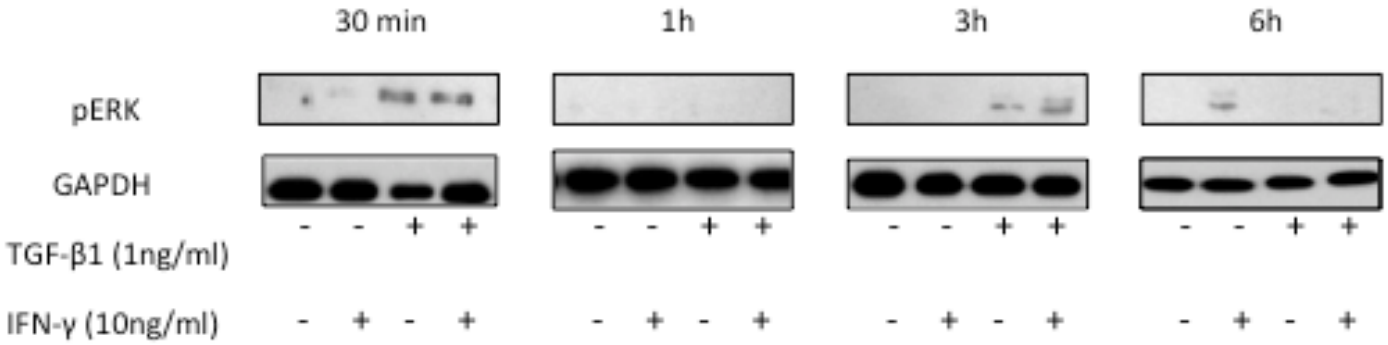

Figure 5.10 TGF-β1 induces ERK signalling in HPMC that is not affected in the presence of IFN-γ

Protein extracted from HPMC growth arrested for 24h and subsequently treated with TGF-β1 and IFN-γ alone or in combination for 30min-6h was analysed by immunoblotting for pERK. GAPDH expression was used as measurement of loading control. One experiment shown of three experiments performed from 3 omental donors (n=3).

5.2.6 Blockade of p38 MAPK signalling results in significant inhibition of TGF-β1 MMP3 expression

To further elucidate the mechanism of TGF-β1 induction of MMP3 I examined whether p38 MAPK signalling pathway was involved. The p38 MAPK signalling pathway is implicated in the mechanism of TGF-β1 induction of MMP2 and MMP9 within human breast epithelial cells and is also reported to be the pathway involved in IL-1β induction of MMP3 within preadipocytes[390, 391]. The role of p38 MAPK signalling was determined using the p38 specific inhibitor SB203580.

HPMC were treated with TGF-β1 alone or in combination with p38 inhibitor SB203580 (300ng/ml) for 24 and 48h respectively. Following stimulation RNA was extracted from the cells and PAI-1 and MMP3 mRNA expression determined using qPCR (Figure 5.10). Following 48h of stimulation maximal expression of both PAI-1 (A) and MMP3 (B) was measured following treatment with TGF-β1. The mRNA expression of PAI-1 was not affected with treatment of the p38 inhibitor SB203580. MMP3 mRNA expression was significantly reduced in HPMC treated with both TGF-β1 and the p38 inhibitor SB203580 following 48h of treatment. The mRNA expression was suppressed by approximately 75% compared to HPMC treated with only TGF-β1.

As with the previous experiments within this chapter, the effect of the SB203580 inhibitor on cell viability was assessed using Alamar Blue (Figure 5.11). HPMC were treated for 48h with 300ng/ml and 3μg/ml respectively, before cells viability was determined through measuring fluorescence omitted by the Alamar Blue substrate.

The SB203580 inhibitor had no impact on cell viability with both doses displaying similar fluorescent measurements to those of untreated cultured HPMC. This indicated that the effect of the SB203580 inhibitor on MMP3 mRNA expression was due to the involvement of the p38 signalling pathway in the induction of MMP3 through TGF-β1.

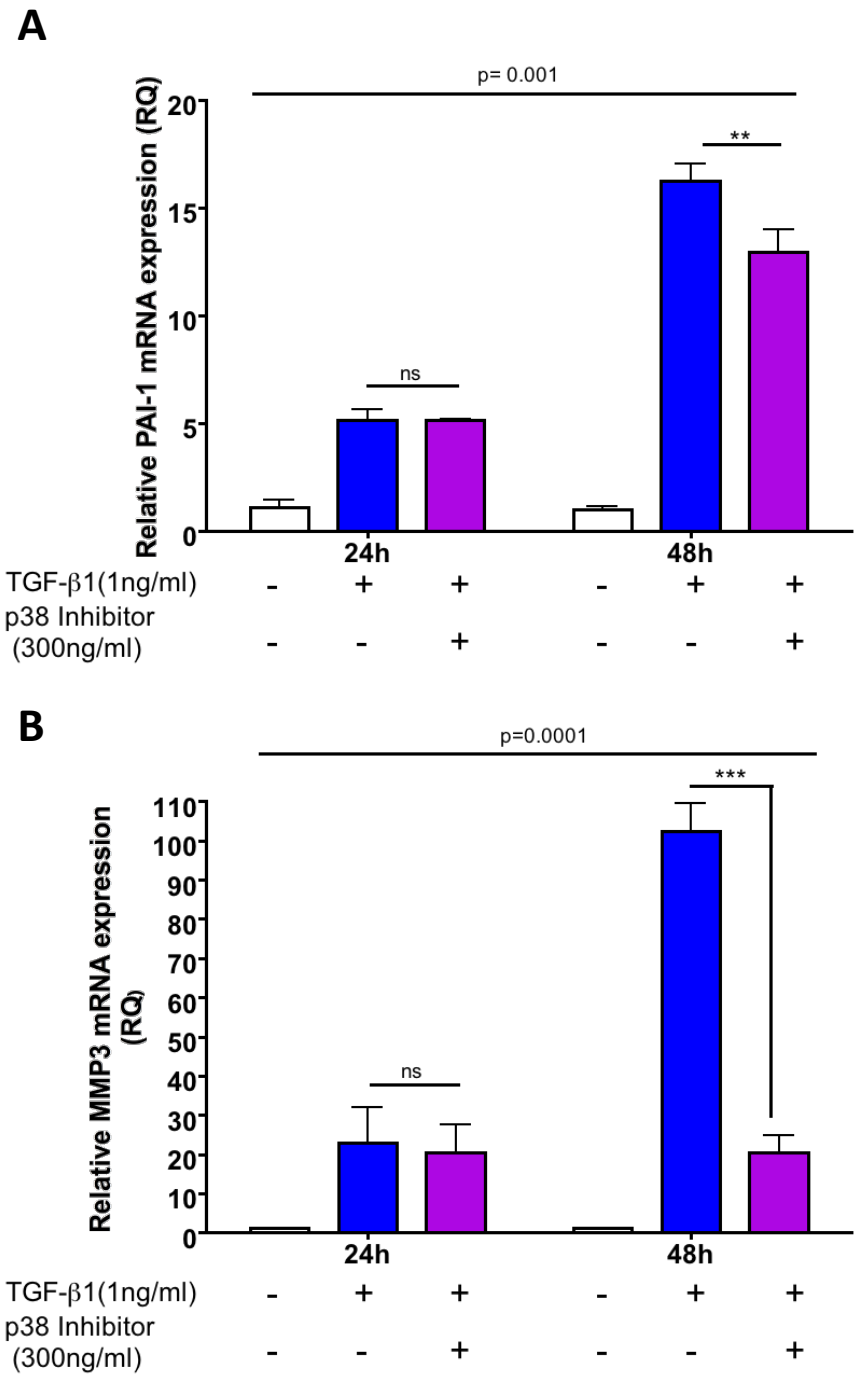

Figure 5.11 Up-regulation of MMP3 mRNA expression by TGF-β1 is significantly attenuated by p38 inhibitor SB203580

Confluent (80%) monolayers of primary HPMC were growth arrested for 24h in serum free medium. The medium was replaced with medium containing 1ng/ml TGF-β1 (blue bars) in the absence or presence (purple bars) of 300ng/ml of SB203580 or absence of both (white bars). RNA was extracted following 24h stimulation and relative expression of PAI-1 (A) and MMP3 (B)were determined using quantitative PCR. rRNA expression was used as an endogenous control and data were normalised to control samples at 24h time point. The results show 3 experiments generated from 3 omental donors (n=3). Statistical analysis was performed using 2-way ANOVA with Bonferroni post tests. A p value of <0.05 was deemed significant (p<0.05*, p<0.005**, p<0.0005***)

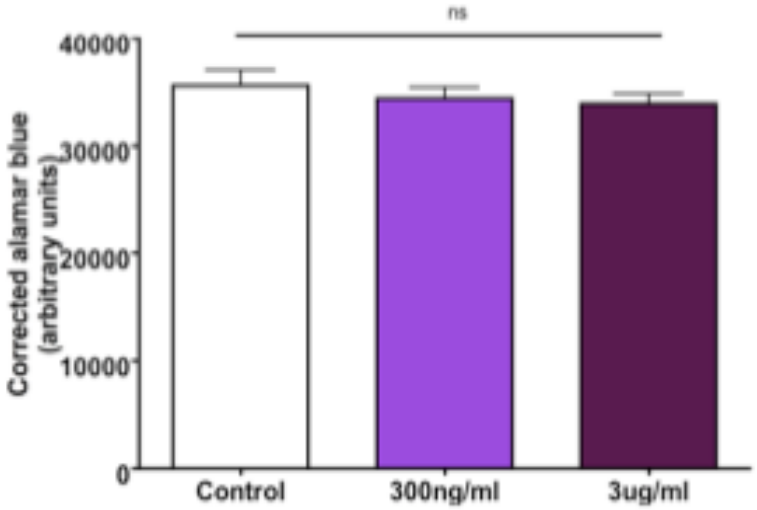

Figure 5.12 Effect of p38 inhibitor SB203580 on HPMC proliferation
Confluent monolayers of primary HPMC were cultured in 12 well plates. Cells were starved of serum for 24h before incubation with p38 inhibitor SB203580 at concentrations 300ng/ml and 3µg/ml for 48h or in fresh serum free medium only. Proliferation was determined using Alamar Blue assay, which involved adding 10% Alamar Blue substrate to medium for 1h following 47h of incubation before cell supernatant was collected. Activity was determined by measuring fluorescence. Results show 3 experiments generated from 3 omental donors (n=3) performed in triplicate. Statistical analysis was performed using a 1-way ANOVA with Bonferroni post tests a p value of <0.05 was deemed significant.

5.2.7 Stimulation of HPMC with TGF-β1 and IFN-γ induces p38 signalling

The p38 inhibitor studies in HPMC suggested that p38 signalling is involved in the induction of MMP3 by TGF-β1 at the level of transcription. This led to the examination of p38 signalling at the protein level to determine if the mechanism of IFN-γ suppression of MMP3 was through modulation of the p38 pathway.

Following stimulation of HPMC for a time course of 30min-6h, samples underwent cellular lysis and protein extraction. Protein levels of phosphorylated p38 (pp38) were determined using immunoblotting (Figure 5.13). Following 30 min of

stimulation with TGF-β1 and IFN-γ alone or in combination detection of pp38 was observed. Expression levels of pp38 peaked in samples collected following 1h of stimulation with the cytokines, with TGF-β1 treated samples expressing the greatest levels. Levels of pp38 protein were present following 3h of stimulation before returning to basal level after 6h of stimulation. The levels of pp38 in samples stimulated with both TGF-β1 and IFN-γ were similar to those observed in TGF-β1 treated samples. IFN-γ treatment in HPMC also resulted in induction of pp38 protein although at lower levels then that detected in TGF-β1 treated HPMC. This suggests that the p38 pathway is not modulated by IFN-γ and therefore not involved in the IFN-γ dependent suppression of MMP3.

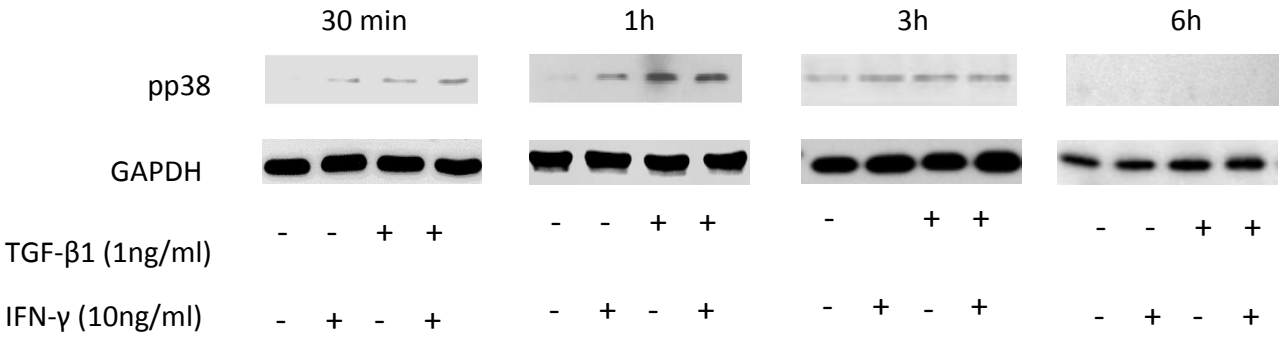

Figure 5.13 TGF-β1 induces p38 signalling in HPMC that is not affected in the presence of IFN-γ
Protein extracted from HPMC growth arrested for 24h and subsequently treated with TGF-β1 and IFN-γ alone or in combination for 30min-6h was analysed by immunoblotting for pp38. GAPDH expression was used as measurement of loading control.

5.2.8 TGF-β1 treatment increases MMP3 promoter activity in transfected Met-5a cells

The previous results suggest that both SMAD and MAPK signalling pathways are involved in the induction of MMP3 following TGF-β1 treatment in HPMC. Previous research has characterised the promoter of MMP3 indicating various *cis*-elements within the promoter involved in transcription factor binding and hence regulation of MMP3 expression. Therefore this led to investigation of which regions of the MMP3 promoter were responsive to TGF-β1 treatment.

Promoter constructs were generated using the software PRIMER BLAST, which designed primers ranging from 18bp-24bp corresponding to complementary bases within the promoter. The primers were amplified using PCR, which led to the formation of promoter constructs ranging from 0.1kb to 1.5kb (Figure 5.14). Following the PCR generation of the constructs, each promoter construct was loaded onto a 1.5% agrose gel and underwent electrophoresis that enabled the separation of the promoter fragments according to size (B). The constructs were then purified and ligated into a pGL3-luciferase reporter vector, transformed into E.coli cells before transfection into transformed mesothelial cell line Met-5A. Following transfection the Met-5a cells were stimulated with TGF-β1 for 24 h (Figure 5.15).

Stimulation of the transfected Met-5A with TGF-β1 led to an overall significant increase in promoter activity when compared to untreated samples (A). Further investigation into the effects of TGF-β1 treatment on each individual promoter

fragment showed a trend in all the promoter constructs except for 0.1 kb for increased promoter activity following TGF-β1 treatment. Significant changes were observed in the Met-5a cells transfected with the 0.9 kb, 1.2 kb and 1.5 kb promoter construct, suggesting a TGF-β1 responsive element upstream in the promoter region.

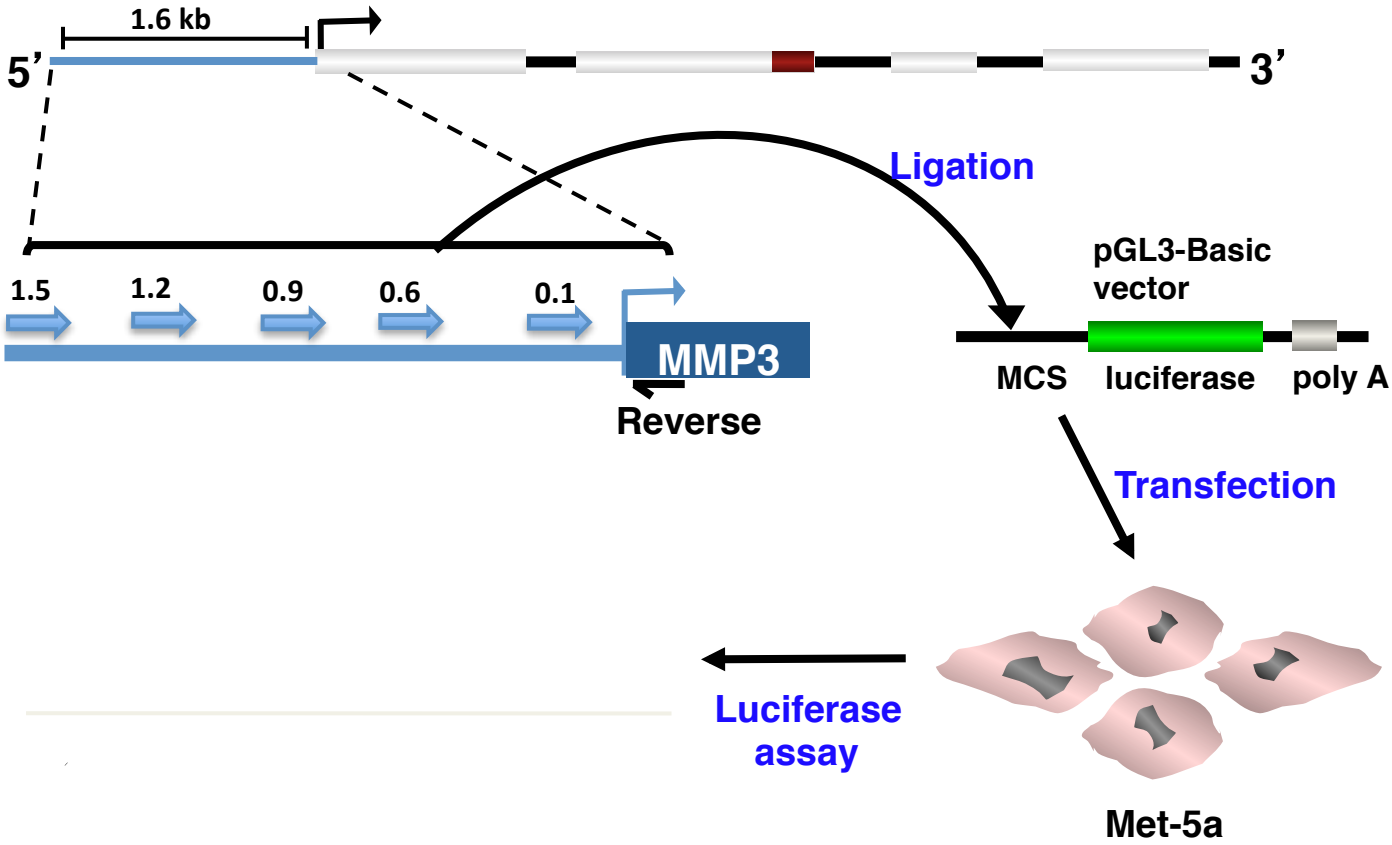

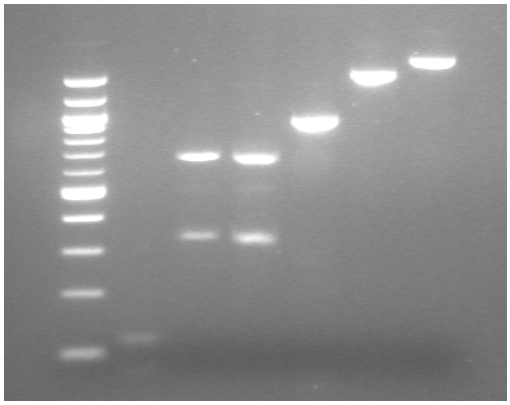

Figure 5.14 MMP3 promoter region showing PCR amplification primers
The region upstream of the MMP3 transcription start site was identified using http: // genome. ucsc.edu/. Primers were designed to be 18-24bp (shown in red) in length using Primer-BLAST design software. (www.ncbi.nlm.nih.gov/tools/**primer-blast/**). The primers amplified regions of the mmp3 promoter ranging from 0.1kb to 1.6kb. Sequence validation of promoter constructs were undertaken using DNA sequencing Core at Cardiff University.

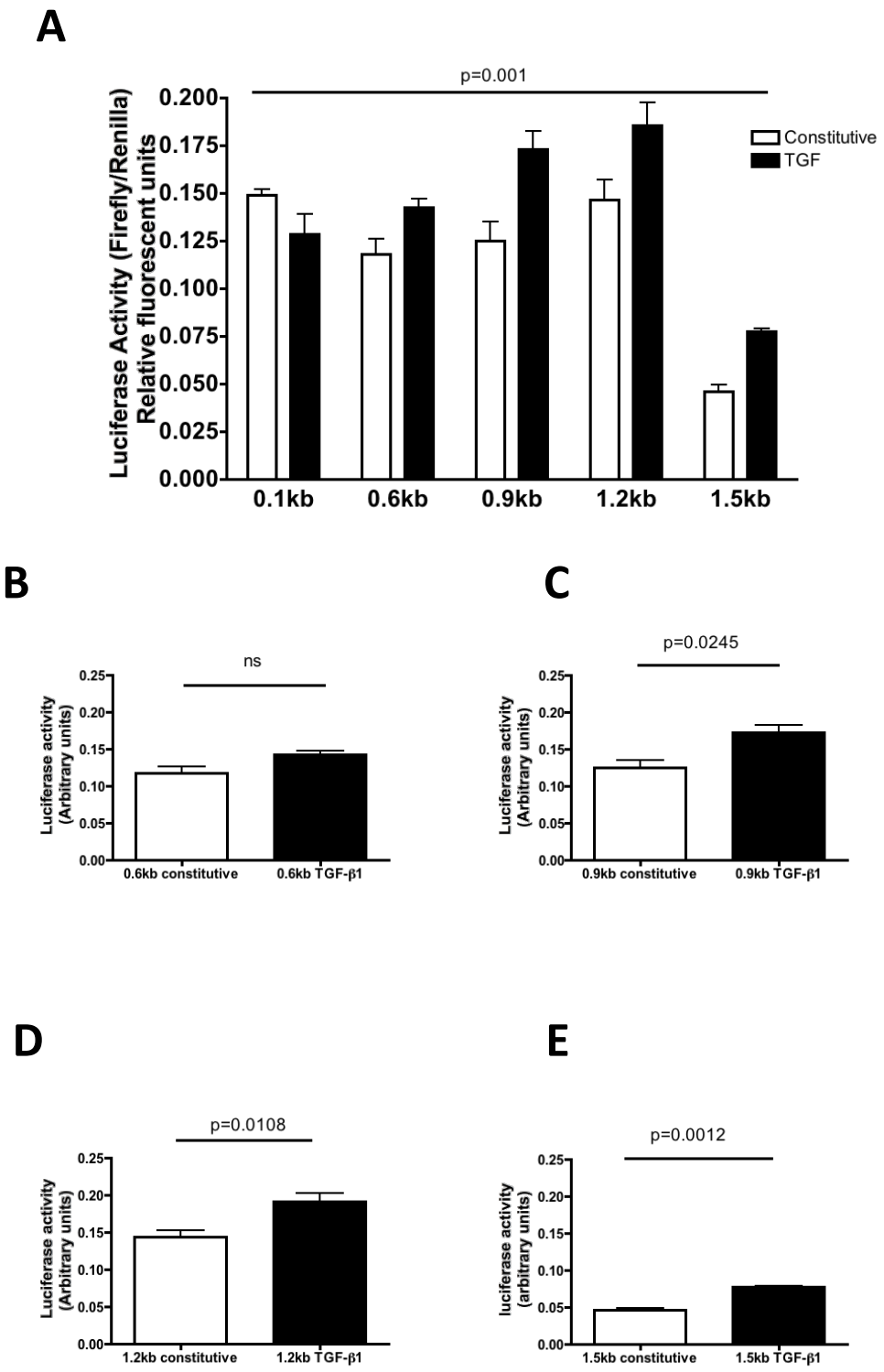

Figure 5.15 TGF-β1 increases MMP3 promoter activity in transfected Met5a cells
Met5a cells were growth arrested for 24h before transfection with MMP3 promoter pGL3 vector constructs ranging from 0.1kb to 1.5kb (A) and renilla. Transfected Met5a were then treated with TGF-β1 for 24h (Black bars) or in serum free medium only (white bars). Luciferase activity was measured using ratio of firefly to renilla normalised to control cells. Three experiments shown (n=3). Statistical analysis was performed using 2-way ANOVA followed by Bonferroni post tests the results of which are shown in figures B-E. A p value of less than 0.05 was deemed significant

by stimulation with TGF-β1 but is slightly reduced following IFN-γ stimulation

The MMP3 promoter contains an AP-1 site located at -70bp within the sequence. This AP-1 site is shown in previous research to be important in the induction of MMP3 expression by various stimuli and blockade of this site results in suppression of MMP3. Therefore I investigated whether the AP-1 site was involved in the TGF-β1 dependent induction of MMP3 and also if suppression of MMP3 by IFN-γ was mediated through suppression of AP-1 activity.

First I examined the time course of AP-1 activation in TGF-β1 treated HPMC using non-radioactive electrophoretic mobility shift assay (EMSA) (Figure 5.16). Following 30 min of TGF-β1 treatment probe retardation was detected and this was maintained for 48h of treatment. Competitor experiments were performed to ensure binding specificity of the probe and confirm AP-1 binding (Figure 5.17). Unlabelled consensus AP-1 oligonucleotide was used in excess with HPMC collected following 24h of experimental conditions, which resulted in the loss of the retarded probe. Comparisons of TGF-β1 treated HPMC protein with untreated control HPMC samples appeared to show no difference in AP-1 activity. IFN-γ treated HPMC samples appear to have a reduction in AP-1 activity compared to untreated control and TGF-β1 treated samples. However, samples treated with both TGF-β1 and IFN-γ displayed similar AP-1 activity to that of untreated and TGF-β1 treated samples, suggesting that IFN-γ does not suppress MMP3 expression through modulation of AP-1 activity.

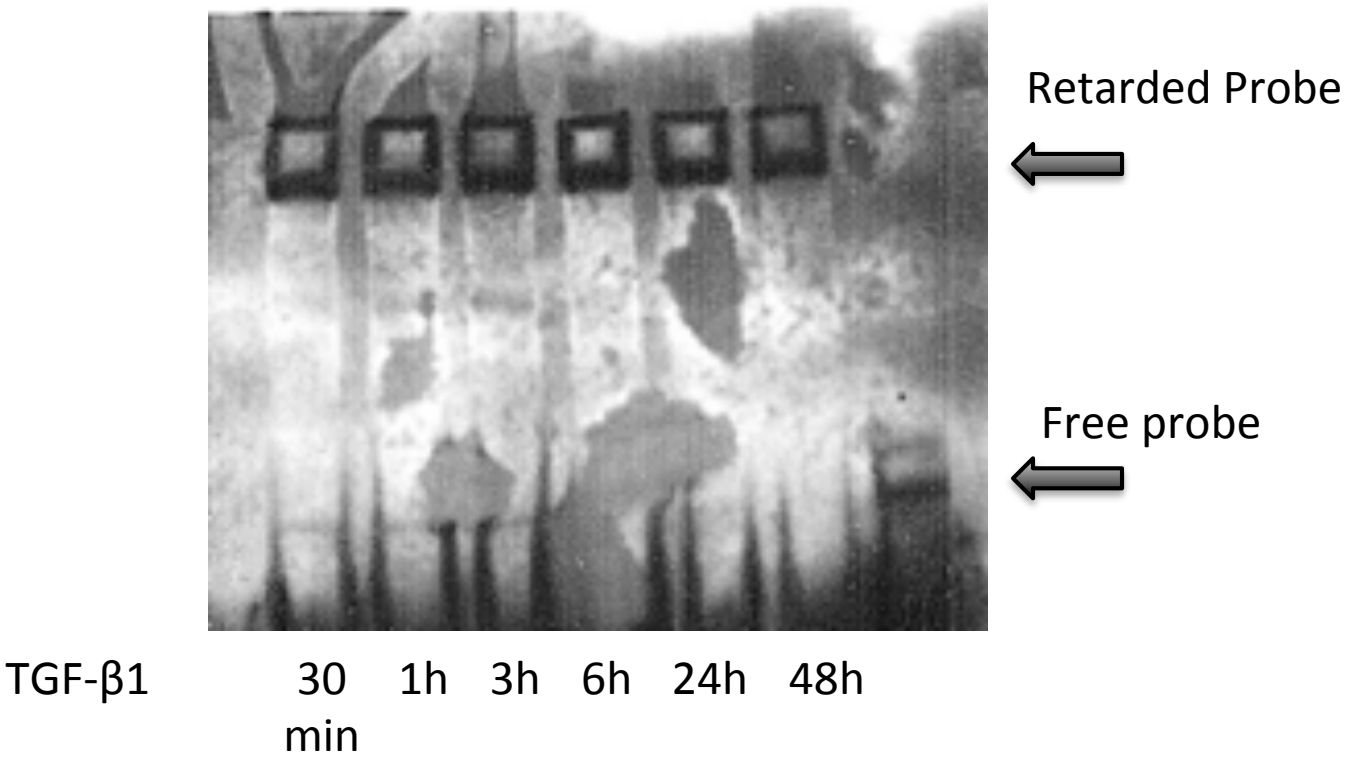

Figure 5.16 Time course of AP-1 activation by TGF-β1 in primary HPMC
AP-1 Non-Radioactive Electrophoretic mobility shift assay. HPMC were stimulated with 1ng/ml TGF-β1 from 30 min to 48h before nuclear protein extraction and electrophoretic mobility shift assay with consensus AP-1 biotinylated labelled probe. Retarded probe and free probe indicated. One gel showing one of three experiments obtained from three different omental donors (n=3).

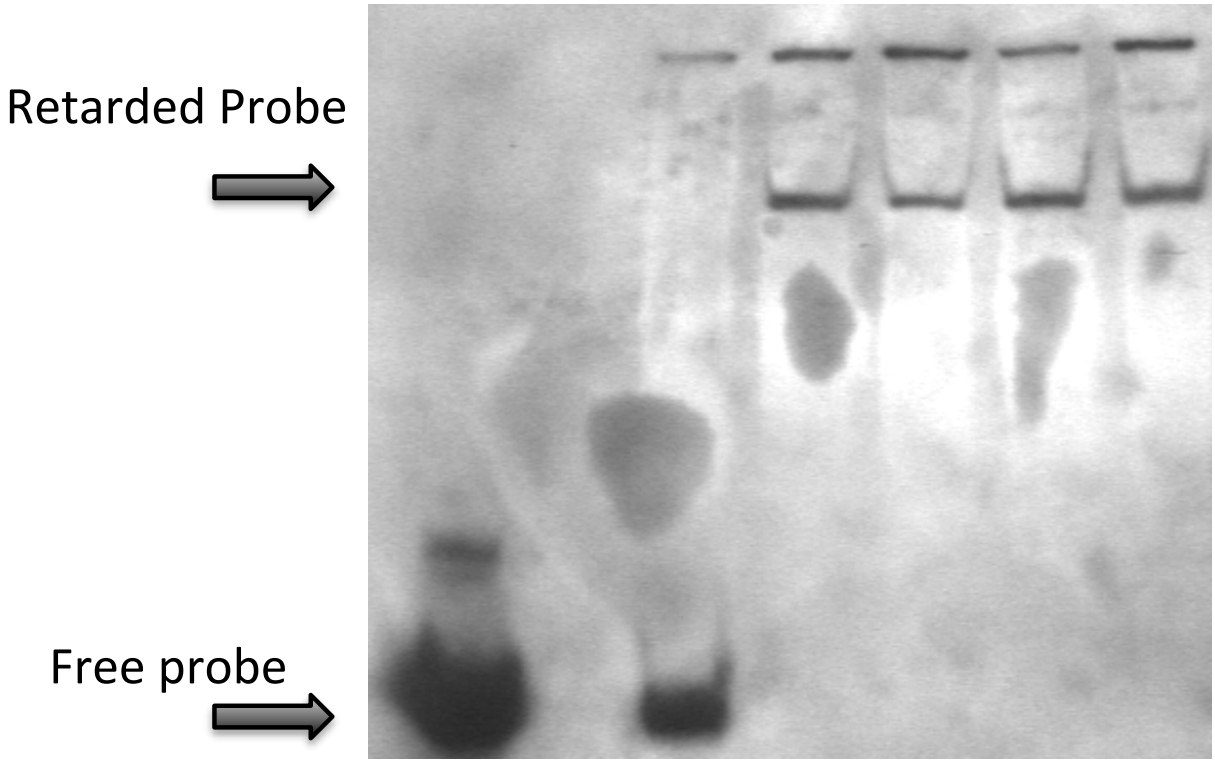

TGF-β1 (1ng/ml)	-	-	-	+	+
IFN-γ (10ng/ml)	-	-	+	-	+
AP-1 competitor oligo	+	-	-	-	-

Figure 5.17 AP-1 activation in HPMC following 24h stimulation with TGF-β1 +/- IFN-γ

HPMC were stimulated for 24h with TGF-β1 and IFN-γ alone or in combination. Nuclear protein was then extracted and AP-1 activation measured by EMSA. Confirmation of AP-1 binding was obtained using a consensus AP-1 unlabelled oligonucleotide probe. Retarded probe and free probe are indicated. One gel showing one experiment of two experiments generated from two omental donors(n=2).

5.3 Discussion

5.3.1 Overview

The previous chapters reported significant changes observed in MMP3 expression in both the *in vivo* SES murine model and the HPMC *in vitro* system. Numerous transcription factors are reported to be involved in the induction and suppression of MMPs within various systems, which require the use of signalling pathways to convey the message to the nucleus of the cell. The data from the previous chapters demonstrated significant changes particularly in the mRNA expression of MMP3, suggesting that the effect of TGF-β1 and IFN-γ on MMP3 expression occurred at the level of transcription. Therefore the main focus of this chapter was to determine the mechanism of MMP3 regulation through identification of transcription factors and signalling pathways utilised by TGF-β1 and IFN-γ and examine regions within the MMP3 promoter regulated by these factors.

5.3.2 The transcription factors ZBP-89 is not involved in the regulation of MMP3 by TGF-β1 and IFN-γ

My initial investigations involved examination of Zinc Binding protein-89 (ZBP-89) within both the *in vivo* and *in vitro* system. ZBP-89 is a ubiquitously expressed Krüppel-type zinc-finger transcription factor involved in various processes including cell growth arrest, cell apoptosis and regulation of several genes[392-395]. Importantly ZBP-89 is shown to increase the promoter activity of MMP3, binding to a region in the MMP3 promoter deemed the stromelysin IL-1 responsive element (SIRE) at -1626bp to -1599bp[396, 397]. This combined with previous research

showing that ZBP-89 mRNA is induced by TGF-β1 led me to examine mRNA expression of ZBP-89 in my *in vivo* and *in vitro* system[398].

The data from this chapter shows that within the SES murine system significant differences in ZBP-89 mRNA were observed between the mouse genotypes, with greater expression detected in IL6KO mice. This was not the case within the HPMC system with neither TGF-β1 nor IFN-γ having an effect on ZBP-89 mRNA expression, although relative expression levels of ZBP-89 mRNA were similar in both systems. The HPMC results corroborates results from recent research showing no effect of TGF-β1 on ZBP-89 mRNA within WI-38 normal human fibroblasts. Interestingly within this same study ZBP-89 was shown to be significantly inhibited by pro-inflammatory cytokines, specifically IL-1β[399].

The difference in ZBP89 expression between the two systems may be due to the absence of inflammatory stimuli within the HPMC system. The murine model was exposed to inflammatory insult, leading to the release of numerous pro-inflammatory cytokines. Research has shown that STAT3 a mediator of IL6 can compete and inhibit the repression of vimentin expression by ZBP-89[400]. This may potentially explain why IL6KO mice, which were shown to have a reduction in STAT3 activity may express higher levels of ZBP-89. This may also account for the increased MMP3 expression shown in IL6KO mice. To confirm this further analysis would be required, such as the use of ZBP-89 immunoblots and EMSAs within murine protein samples. Despite this the HPMC system confirms that ZBP-89 is not involved in the TGF-β1 and IFN-γ dependent regulation of MMP3.

5.3.3 TGF-β1 induction of MMP3 requires SMAD and MAPK signalling pathways

Within chapter one I described the basis of TGF-β1 signalling, which mainly propagates through the SMAD transcription factor pathway. Following receptor activation phosphorylation of either SMAD2 or SMAD3 occurs, which then forms a homodimer with SMAD4 before translocation to the nucleus. Several studies have identified distinct roles for SMAD2 and SMAD3 in TGF-β1 signalling[401-403], with one study reporting that SMAD3 is the essential mediator of TGF-β1 signalling and SMAD2 and SMAD independent pathways acting as modulators[404].

Examination of the role of SMAD3 in the induction of MMP3 through use of the selective SMAD3 SIS3 inhibitor showed a significant reduction in both PAI-1 and MMP3 mRNA expression. Immunoblots revealed that at the protein level the SIS3 at 3μM did not exert a suppression of SMAD3 phosphorylation. I attempted to inhibit phosphorylation of SMAD3 through increasing the dose of SIS3, which reduced mRNA expression of both PAI-1 and MMP3 further but had a detrimental effect on cell viability, suggesting that the reduction in mRNA was through loss of cells and not blockade of pSMAD3.

The results suggest that SMAD3 is involved in the TGF-β1 dependent induction of MMP3. This concurs with previous work, which shows knockdown of SMAD3 results in attenuation of TGF-β1 induction of MMP-2 in mesangial and endothelial cells[405]. The same study however also reported that TGF-β1 induction of MMP-2 expression was SMAD3 independent *in vivo* when analysing the total renal MMP-2 mRNA. This implies differential regulation in MMP expression within different cell

types and systems. The role of SMAD2 in MMP3 induction within this system cannot be ruled out. Within models of peritoneal fibrosis, SMAD 2 deletion is shown to abrogate the fibrotic effect whereas SMAD3 deletion protects mice from peritoneal fibrosis[406, 407].

Previous research has shown the involvement of the MAPK signalling pathway in regulation of MMP3 expression. The MAPK pathway is also involved in TGF-β1 signalling acting independently or in co-ordination with SMAD signalling. Blockade of ERK and p38 significantly suppressed the mRNA expression of MMP3 following TGF-β1 stimulation. There was no effect of the specific inhibitors on cell viability confirming a genuine effect of MAPK blockade on MMP3 expression. This supports previous research that has shown the involvement of both ERK and p38 in MMP3 regulation following activation from various stimuli within other systems[408, 409]. The data therefore implies the involvement of both SMAD and MAPK signalling in the induction of MMP3 by TGF-β1.

5.3.4 IFN-γ does not inhibit MMP3 through modulation of SMAD and MAPK signalling pathways

The involvement of SMAD and MAPK signalling in the TGF-β1 induction of MMP3 led to the examination of IFN-γ mediated suppression. IFN-γ is shown to inhibit the actions of TGF-β1 in various cellular environments. One mechanism, which is frequently reported, is the induction of SMAD7 by IFN-γ. However my data within the HPMC system does not support this in this context. Stimulation with increasing doses of TGF-β1 resulted in increased SMAD7 mRNA expression, which was not

augmented or suppressed in the presence of IFN-γ. Within the SES system WT animals showed significantly greater expression of SMAD7 compared to IL6KO mice. Combining the results this suggests the induction of SMAD7 is mediated through TGF-β1. This is supported in various studies that show SMAD7 is responsive to TGF-β1 stimulation, potentially as part of a negative feedback loop[410, 411]. The increase in SMAD7 peaking at day 42 within the *in vivo* system may indicate the negative feedback to TGF-β1 response within the WT animals.

Further investigation into the effect of IFN-γ on SMAD signalling revealed no difference in SMAD3 signalling in HPMC treated with TGF-β1 +/- IFN-γ. This is in contrast to the findings from Ulloa *et al* (1999) that found IFN-γ inhibited TGF-β1-induced phosphorylation of SMAD3, although the mechanism was through SMAD7, which does not change within my system[386]. Higashi *et al* (2003) also reported IFN-γ inhibits TGF-β1 induction of COL1A2 through the transcription factor YB-1, which interacts with SMAD3 itself and binds to p300 thus modulating the TGF-β1 SMAD3 signalling cascade[412]. This variation in IFN-γ action may be the result of cell specific interactions, in which HPMC SMAD signalling is not affected by stimulation with IFN-γ.

Similar results were also observed when I examined MAPK signalling in HPMC with no change in phosphorylation of either ERK or p38 following treatment with TGF-β1 and IFN-γ. Some research has shown that IFN-γ can suppress MMP3 through inhibition of p38 activation[413]. However, other research has shown no effect of IFN-γ stimulation on p38 activity within MMP regulation, thus again suggesting the

effects of IFN-γ differ depending on cell specificity and environment[414]. ERK signalling is shown in several cell types to be necessary for the induction of various MMPs, however IFN-γ does not appear to modulate MMP expression through the ERK pathway. One study reported that IFN-γ had differential effects on MMP-1 and MMP-9 in monocytes depending on the presence of other stimuli, which also affected both p38 and ERK pathways in MMP regulation. In other contexts IFN-γ does utilise the MAPK signalling pathway, particularly in the immune response. However, my results concur with the current research that IFN-γ does not suppress MMP3 expression through modulation of the MAPK pathway.

5.3.5 The AP-1 site within the MMP3 promoter does not appear to be involved in the regulation of MMP3 expression by TGF-β1 and IFN-γ

The MMP3 promoter region contains a number of transcription factor binding sites that are important in the regulation of MMP3 expression. With the use of the transformed mesothelial cell line Met-5a, I transfected regions of the MMP3 promoter ranging from 0.1kb to 1.5kb in size. I then measured the activity in untreated and TGF-β1 treated transfected samples using dual reporter luciferase assay. The data showed significant increase in promoter activity following TGF-β1 treatment within the majority of the constructs, suggesting a potential TGF-β1 responsive element.

The AP-1 binding site located at -70bp is present within construct 0.3kb - 1.5kb. Previous research has shown the importance of this site in basal expression and induction of MMP3. The AP-1 site in previous work is shown to be involved in TGF-

β1 induction of MMP2 and IFN-γ is also shown to act on this site. Examination of the AP-1 site using non-radioactive EMSA revealed no difference in activity between control HPMC and HPMC treated with TGF-β1 and IFN-γ alone or in combination. The data suggests that the AP-1 site is constitutively active as untreated HPMC nuclear extracts collected following 24h of experimental conditions show a measurable degree of binding. This concurs with previous research that the AP-1 site is mainly involved in basal regulation of the enzyme. The TGF-β1 responsive element observed in the promoter construct reporter analysis requires further work to be identified.

5.3.6 Conclusions of the chapter

In conclusion the data from this chapter has revealed that the induction of MMP3 by TGF-β1 in HPMC requires both the SMAD signalling pathway and the p38 and ERK branches of the MAPK signalling pathway. Neither of these signalling pathways are affected when HPMC are stimulated with both TGF-β1 and IFN-γ, suggesting this is not how IFN-γ suppresses MMP3. The MMP3 promoter activity increases significantly following stimulation with TGF-β1. Analysis of the AP-1 site located at -70bp in the MMP3 promoter revealed that this is not involved in the TGF-β1 dependent induction of MMP3 and IFN-γ does not reduce activity. This transcription factor-binding site appears to be involved in regulation of basal expression of MMP3. Further research is required to elucidate the mechanism of IFN-γ mediated suppression of MMP3 and determine the location of the site within the MMP3 promoter involved in the induction and suppression of this enzyme in HPMC.

Chapter 6: General Discussion

6.1 Previous work

Peritoneal dialysis (PD) provides renal replacement therapy for approximately 20% of the UK dialysis population[15]. The increasing use of this technique can be attributed to the notable advantages of greater mobility, independence, simplicity in administration and the ability to administer dialysis within the patients' home[17]. Despite the advantages of PD therapy a major limitation is the development of membrane failure, which results in the loss of ultrafiltration and the occurrence of fibrotic changes to the membrane. This leads to technique failure and subsequent transfer to haemodialysis. Understanding the mechanisms of peritoneal fibrosis will help develop preventative and therapeutic measures to enable the maintenance of membrane functionality and longevity of therapy.

The development of a mouse murine model of chronic inflammation driven peritoneal fibrosis revealed the important role of pro-inflammatory signalling in driving the fibrotic response to repeat inflammatory stimulation, specifically IL6 and IFN-γ[265]. The pro-fibrotic cytokine TGF-β1 is also a central mediator of the fibrotic process within the peritoneum. Therefore the initial focus of this thesis was to characterise the interaction between pro-inflammatory signalling and TGF-β1 within the *in vivo* SES murine model and also within an *in vitro* system of HPMC.

6.2 The TGF-β1 response within the SES murine *in vivo* system

Since the TGF-β1 response was not investigated within the murine model at the time of commencing my PhD, the initial focus was to investigate any differences in TGF-β1 and TGF-β1 dependent responses between WT and IL6KO mice. Significant differences in the mRNA expression of TGF-β1 and various matrix components were found between genotypes, with greater expression detected in the WT animals. Enhanced ECM deposition is a key fibrotic effect mediated by TGF-β1, thus these results suggest a key involvement of TGF-β1 in driving the fibrotic response observed in WT animals. Fielding et al (2014) showed increased matrix deposition in WT animals at the protein level using collagen staining on membrane sections[265]. Thus my qPCR results concur with these findings.

Fielding et al (2014) later concluded that the SES model of fibrosis is not driven by traditional pro-fibrotic cytokines including TGF-β1. These conclusions were based on data obtained from samples collected acutely following administration of the SES (0-24h)[265]. My samples were collected weeks after the final administration of SES with the earliest sample (28 day) collected 7 days after the administration. The differences between the samples may reflect variation in acute and chronic response. Within human studies levels of TGF-β1 remain elevated for up to 6 weeks following peritonitis infection. Therefore the peak in my results in TGF-β1 mRNA expression at day 35, 1 week before scarring became histologically apparent may indicate the response of the peritoneum to a chronic inflammatory response.

A significant change I observed in the IL6KO mouse samples was greater mRNA expression of the enzymes MMP3 and MMP10 and lower expression of TIMP1 compared to WT animals. This generated an overall ratio favouring increased matrix degradation in the IL6KO animals, which may explain the absence of scarring reported within these animals. The anti-fibrotic function of MMPs is shown in previous studies, with higher ratios of MMP to TIMP expression associated with scarless repair. This anti-fibrotic effect occurs in IL6KO animals that were shown to have an absence in IFN-γ and STAT-1 response, suggesting that IFN-γ may potentially promote the fibrotic response through modulation of matrix turnover.

A limitation of my SES murine *in vivo* data is that it analyses the expression of TGF-β1 and TGF-β1 related products at the level of transcription only. Further work would involve confirming the mRNA findings at the protein level. This would include analysis of the TGF-β1 signalling pathway SMAD through immunoblotting to determine any difference in response between the genotypes. Potentially this would require acute samples used by Fielding et al (2014)[265]. The anti-fibrotic effect of MMP3 and MMP10 could also be investigated further, potentially through blockade of MMP3 or MMP10 in SES treated mice or through administration of agents known to prevent scarring via induction of MMPs such as kynurenic acid[341]. Fielding et al (2014) did demonstrate that use of collagenase-specific MMP inhibitor (Ro32-355) causes fibrosis in IL6KO mice comparable to that shown in WT mice, thus supporting the importance of MMP3 in protection against fibrosis[265].

6.3 The interaction of TGF-β1 and IFN-γ on fibrotic responses within HPMC

The prior findings of the Fielding et al (2014) implicated IFN-γ as the fibrotic mediator within the SES inflammation driven peritoneal fibrosis model[265]. This is in sharp contrast to the majority of the literature, which reports the anti-fibrotic effects of IFN-γ in various systems exerted through modulation and inhibition of TGF-β1 signalling. Therefore I decided to examine the interaction between TGF-β1 and IFN-γ signalling within HPMC to determine if within this system IFN-γ augments the fibrotic response.

Following stimulation of HPMC for 6-48h increases in the expression of PAI-1, Col1a1, Col1a2, HAS 1-3 and fibronectin were shown following stimulation with TGF-β1. This was expected and supported previous research of PAI-1 as a TGF-β1 responsive component and TGF-β1 as an inducer of ECM accumulation[415]. Stimulation of HPMC with the combination of TGF-β1 and IFN-γ did not result in suppression of any of these components. This is the opposite effect of results obtained in other systems, which report suppression of TGF-β1 induced PAI-1 and ECM components such as Col1a2 in other systems. The difference in the IFN-γ response may be due to a unique reaction within HPMC and the peritoneum. Previous study of TGF-β1 synthesis in HPMC also revealed that IFN-γ had no effect, thus again highlighting the specific interaction or lack of between these cytokines in this system[125].

Of interest within this system was the significant augmentation of HAS3 mRNA expression following combined stimulation with TGF-β1 and IFN-γ. The HAS isoforms

synthesis hyaluronic acid (HA). HA is a glycosaminoglycan molecule found throughout human tissue as a key component of ECM. During wound healing HA accumulates at the wound site and is involved in the induction of the inflammatory response and signalling fibroblast proliferation. HA is deemed a marker of inflammation and tissue remodelling within PD patients, with HA levels increasing with time on PD[328, 416]. Whether the increase in HAS3 via IFN-γ leads to greater HA production in HPMC and augments the fibrotic response would be further work to consider. This could be achieved through examination of HA production in HPMC using ELISA. However determining the contribution of HA production through HAS3 would be difficult to quantify unless selective knockouts of HAS1 and HAS2 were generated.

The main finding within the HPMC *in vitro* system concerned the enzyme MMP3. As described previously ECM homeostasis is a balance between matrix synthesis and matrix degradation. Within this system I found a significant increase in MMP3 expression at the mRNA and protein level following stimulation with TGF-β1. This increase in MMP3 was significantly suppressed when HPMC were stimulated with TGF-β1 and IFN-γ. This result is supported by previous research that has shown IFN-γ has an inhibitory effect on MMP expression.

I infer from my data that IFN-γ promotes the fibrotic effect of TGF-β1 through suppressing matrix degradation and favouring matrix accumulation. This was supported when I examined TIMP1 expression and the data showed a significant augmentation in TIMP1 mRNA expression following combined treatment with TGF-

β1 and IFN-γ again suggesting an increase in matrix accumulation. Analysis of fibronectin a substrate of MMP3 revealed no augmentation in protein expression following treatment of HPMC with TGF-β1 and IFN-γ for 72h. This may reflect a need for longer incubation times and examination of other MMP3 substrates such as laminin.

6.4 Regulation of MMP3 expression within HPMC

To determine the mechanism of MMP3 regulation I examined inhibition of SMAD and ERK and p38 MAPK pathways on MMP3 expression following TGF-β1 stimulation. Blockade of each pathway resulted in a significant inhibition of MMP3 mRNA expression, thus suggesting the involvement of SMAD and MAPK in TGF-β1 regulation of MMP3. This is supported in the literature with SMAD3 being required for TGF-β1 induction of MMP13 in squamous cell carcinoma cells and ERK signalling involved in TGF-β1 induction of MMP9[417]. A study investigating MMP-13 induction by TGF-β1 in fibroblasts also showed co-operation between p38 and SMAD signalling in the induction of MMP13.

Stimulation of HPMC with TGF-β1 and IFN-γ for 30min-6h did not cause a change in protein expression of pSMAD3, pERK or p38 expression, thus suggesting that IFN-γ does not suppress MMP3 through modulation of these pathways. Some studies have reported a modulation by IFN-γ in MAPK signalling thus causing an effect on MMP expression. Another mechanism of IFN-γ suppression of TGF-β1 effects is through induction of SMAD7[387]. My qPCR data shows that although SMAD7 mRNA expression is greater in IFN-γ producing WT animals, this is probably an effect

mediated by TGF-β1. In the HPMC *in vitro* system TGF-β1 stimulation increased SMAD 7 expression and this was not augmented in the presence of IFN-γ. Thus IFN-γ does not suppress MMP3 via induction of SMAD7.

The MMP3 promoter contains various *cis-elements* that are shown to mediate induction and suppression of MMP3 expression[361]. I confirmed that following TGF-β1 stimulation HPMC transfected with reporter gene constructs of the MMP3 promoter resulted in increased promoter activity. Analysis of the promoter constructs revealed an AP-1 site at -70bp and my data demonstrates that the constructs containing this site showed increased promoter activity. The AP-1 site is shown in previous research to be important in both basal transcription and induction of MMP3 to various stimuli[381, 418]. TGF-β1 is also shown to induce expression of MMP-1 via activation of AP-1[419]. Within HPMC AP-1 activity was not affected by stimulation with TGF-β1 or IFN-γ. Untreated HPMC at 24h showed AP-1 activity thus suggesting this site is primarily involved in basal MMP3 expression[420].

Further work is required to identify the elements in the promoter responsible for MMP3 induction by TGF-β1 and the mechanism of IFN-γ suppression. Within the MMP3 promoter there are further transcription factor binding sites upstream including another AP-1 site, two PEA3 sites and a stromelysin-1 PDGF responsive element (SPRE)[359, 418]. Research has shown that MMP3 activity may require co-operation between various sites[421]. In the case of TGF-β1 induction of MMP13 both the AP-1 and PEA3 sites were required[422]. Further work could investigate the activity of this promoter site and determine if TGF-β1 stimulation has an effect.

Research investigating the effects of IFN-γ on MMP expression has shown the involvement of the JAK/STAT pathway. In monocytes IFN-γ suppresses MMP-1 through STAT1 dependent mechanisms and other studies have shown suppression of MMP13 through STAT1 sequestration of the co-activators CBP/p300 complex thus preventing transcription[423, 424]. Fielding et al (2014) also showed that transfection of HPMC with a constitutively active form of STAT1 suppressed MMP3 induction by IL-1β[265]. Therefore further work could examine the role of STAT signalling within this system through use of STAT inhibitors and examination of the MMP3 promoter to determine if STAT1 directly binds to the MMP3 promoter and thus represses MMP3 transcription directly.

6.5 Summary

The data from this thesis demonstrates a unique interaction between TGF-β1 and IFN-γ that occurs within an *in vivo* SES murine model and a HPMC *in vitro* system of peritoneal fibrosis. In contrast to findings in other contexts IFN-γ does not inhibit the fibrotic effect of TGF-β1 such as PAI-1 and ECM generation. Instead there is a specific reaction on matrix turnover involving the enzyme MMP3. IFN-γ suppresses the induction of MMP3 by TGF-β1 appearing to favour matrix accumulation a key hallmark of the fibrotic process. The mechanism of this suppression still remains to be elucidated, however the induction of this enzyme involves both SMAD and MAPK signalling pathways. MMP3 appears to be a promising target for protection against fibrosis. Further understanding of its regulation within PD may provide therapeutics against peritoneal fibrosis and eventually help prevent technique failure.

Chapter 7: References

1. Foundation, N.K., *K/DOQI clinical practice guidelines for chronic kidney disease: evaluation, classification, and stratification.* American journal of kidney diseases : the official journal of the National Kidney Foundation, 2002. **39**(2 Suppl 1): p. S1-266.
2. Roderick, P., M. Roth, and J. Mindell, *Prevalence of chronic kidney disease in England: Findings from the 2009 Health Survey for England.* Journal of epidemiology and community health, 2011. **65**(Suppl 2): p. A12.
3. Coresh, J., et al., *Prevalence of chronic kidney disease in the United States.* JAMA : the journal of the American Medical Association, 2007. **298**(17): p. 2038-47.
4. Kearns, B., H. Gallagher, and S. de Lusignan, *Predicting the prevalence of chronic kidney disease in the English population: a cross-sectional study.* BMC nephrology, 2013. **14**: p. 49.
5. Haroun, M.K., et al., *Risk factors for chronic kidney disease: a prospective study of 23,534 men and women in Washington County, Maryland.* Journal of the American Society of Nephrology : JASN, 2003. **14**(11): p. 2934-41.
6. Wang, Y., et al., *Association between obesity and kidney disease: a systematic review and meta-analysis.* Kidney international, 2008. **73**(1): p. 19-33.
7. Bang, H., et al., *SCreening for Occult REnal Disease (SCORED): a simple prediction model for chronic kidney disease.* Archives of internal medicine, 2007. **167**(4): p. 374-81.
8. Maxwell, M.H., et al., *Peritoneal dialysis. 1. Technique and applications.* J Am Med Assoc, 1959. **170**(8): p. 917-24.
9. Boen, S.T., et al., *Periodic peritoneal dialysis using the repeated puncture technique and an automatic cycling machine.* Trans Am Soc Artif Intern Organs, 1964. **10**: p. 409-14.
10. Popovich, R.P., et al., *Continuous ambulatory peritoneal dialysis.* Annals of internal medicine, 1978. **88**(4): p. 449-56.
11. Diaz-Buxo, J.A., et al., *Continuous cyclic peritoneal dialysis: a preliminary report.* Artificial organs, 1981. **5**(2): p. 157-61.
12. Rabindranath, K.S., et al., *Automated vs continuous ambulatory peritoneal dialysis: a systematic review of randomized controlled trials.* Nephrology, dialysis, transplantation : official publication of the European Dialysis and Transplant Association - European Renal Association, 2007. **22**(10): p. 2991-8.
13. Peppelenbosch, A., et al., *Peritoneal dialysis catheter placement technique and complications.* NDT Plus, 2008. **1**(suppl 4): p. iv23-iv28.
14. Gokal, R. and N.P. Mallick, *Peritoneal dialysis.* Lancet, 1999. **353**(9155): p. 823-8.
15. Ellam, T. and M. Wilkie, *Peritoneal dialysis.* Medicine, 2011. **39**(7): p. 434-437.
16. Rubin, H.R., et al., *Patient ratings of dialysis care with peritoneal dialysis vs hemodialysis.* JAMA : the journal of the American Medical Association, 2004. **291**(6): p. 697-703.
17. Jain, A.K., et al., *Global trends in rates of peritoneal dialysis.* Journal of the American Society of Nephrology : JASN, 2012. **23**(3): p. 533-44.

18. Williams, J.D., et al., *Morphologic changes in the peritoneal membrane of patients with renal disease.* Journal of the American Society of Nephrology : JASN, 2002. **13**(2): p. 470-9.
19. Gandawidjaja, L. and T. Hau, *Anatomic, physiologic, bacteriologic and immunologic aspects of peritonitis.* Acta Chir Belg, 1997. **97**(4): p. 163-7.
20. Melichar, B. and R.S. Freedman, *Immunology of the peritoneal cavity: relevance for host-tumor relation.* Int J Gynecol Cancer, 2002. **12**(1): p. 3-17.
21. Gray, H., *Anatomy of the Human Body: 20th Edition*. 1918: Lea & Febiger. 1825-1861.
22. Patel, R.R. and K. Planche, *Applied peritoneal anatomy.* Clin Radiol, 2013. **68**(5): p. 509-20.
23. Cunningham, R.S., *THE PHYSIOLOGY OF THE SEROUS MEMBRANES.* Physiological Reviews, 1926. **6**(2): p. 242-280.
24. Nagy, J.A. and R.W. Jackman, *Anatomy and Physiology of the Peritoneal Membrane.* Seminars in dialysis, 1998. **11**(1): p. 49-56.
25. Nagy, J.A., *Peritoneal membrane morphology and function.* Kidney international. Supplement, 1996. **56**: p. S2-11.
26. Davila, R.M. and E.C. Crouch, *Role of mesothelial and submesothelial stromal cells in matrix remodeling following pleural injury.* The American journal of pathology, 1993. **142**(2): p. 547-55.
27. Witz, C.A., et al., *Composition of the extracellular matrix of the peritoneum.* J Soc Gynecol Investig, 2001. **8**(5): p. 299-304.
28. Wilkosz, S., et al., *A comparative study of the structure of human and murine greater omentum.* Anat Embryol (Berl), 2005. **209**(3): p. 251-61.
29. Whitaker, D., J.M. Papadimitriou, and M.N. Walters, *The mesothelium and its reactions: a review.* Crit Rev Toxicol, 1982. **10**(2): p. 81-144.
30. Mutsaers, S.E., *The mesothelial cell.* The international journal of biochemistry & cell biology, 2004. **36**(1): p. 9-16.
31. Minot, C.S., *A Sketch of Comparative Embryology.* The American Naturalist, 1880. **14**(12): p. 871-880.
32. Louise Odor, D., *Observations of the rat mesothelium with the electron and phase microscopes.* American Journal of Anatomy, 1954. **95**(3): p. 433-465.
33. Baradi, A.F. and J. Hope, *Observations on Ultrastructure of Rabbit Mesothelium.* Experimental cell research, 1964. **34**: p. 33-44.
34. Whitaker, D., J.M. Papadimitriou, and M.N. Walters, *The mesothelium: a histochemical study of resting mesothelial cells.* J Pathol, 1980. **132**(3): p. 273-84.
35. Yung, S., F.K. Li, and T.M. Chan, *Peritoneal mesothelial cell culture and biology.* Peritoneal dialysis international : journal of the International Society for Peritoneal Dialysis, 2006. **26**(2): p. 162-73.
36. Mutsaers, S.E., *Mesothelial cells: their structure, function and role in serosal repair.* Respirology, 2002. **7**(3): p. 171-91.
37. Andrews, P.M. and K.R. Porter, *The ultrastructural morphology and possible functional significance of mesothelial microvilli.* Anat Rec, 1973. **177**(3): p. 409-26.
38. Madison, L.D., et al., *Regulation of surface topography of mouse peritoneal cells. Formation of microvilli and vesiculated pits on omental mesothelial*

cells by serum and other proteins. The Journal of cell biology, 1979. **82**(3): p. 783-97.
39. Mutsaers, S.E., D. Whitaker, and J.M. Papadimitriou, *Changes in the concentration of microvilli on the free surface of healing mesothelium are associated with alterations in surface membrane charge.* J Pathol, 1996. **180**(3): p. 333-9.
40. Ferrandez-Izquierdo, A., et al., *Immunocytochemical typification of mesothelial cells in effusions: in vivo and in vitro models.* Diagn Cytopathol, 1994. **10**(3): p. 256-62.
41. Stylianou, E., et al., *Isolation, culture and characterization of human peritoneal mesothelial cells.* Kidney international, 1990. **37**(6): p. 1563-70.
42. Roth, J., *Ultrahistochemical demonstration of saccharide components of complex carbohydrates at the alveolar cell surface and at the mesothelial cell surface of the pleura visceralis of mice by means of concanavalin A.* Exp Pathol (Jena), 1973. **8**(3): p. 157-67.
43. Dobbie, J.W., et al., *Phosphatidylcholine synthesis by peritoneal mesothelium: its implications for peritoneal dialysis.* Am J Kidney Dis, 1988. **12**(1): p. 31-6.
44. Beavis, J., et al., *Synthesis of phospholipids by human peritoneal mesothelial cells.* Perit Dial Int, 1994. **14**(4): p. 348-55.
45. Heldin, P. and H. Pertoft, *Synthesis and assembly of the hyaluronan-containing coats around normal human mesothelial cells.* Experimental cell research, 1993. **208**(2): p. 422-9.
46. Fedorko, M.E., J.G. Hirsch, and B. Fried, *Studies on transport of macromolecules and small particles across mesothelial cells of the mouse omentum. II. Kinetic features and metabolic requirements.* Experimental cell research, 1971. **69**(2): p. 313-23.
47. Cotran, R.S. and M.J. Karnovsky, *Ultrastructural studies on the permeability of the mesothelium to horseradish peroxidase.* The Journal of cell biology, 1968. **37**(1): p. 123-37.
48. Payne, D.K., G.T. Kinasewitz, and E. Gonzalez, *Comparative permeability of canine visceral and parietal pleura.* J Appl Physiol (1985), 1988. **65**(6): p. 2558-64.
49. Hausmann, M.J., et al., *Accessory role of human peritoneal mesothelial cells in antigen presentation and T-cell growth.* Kidney international, 2000. **57**(2): p. 476-86.
50. Liang, Y. and K. Sasaki, *Expression of adhesion molecules relevant to leukocyte migration on the microvilli of liver peritoneal mesothelial cells.* Anat Rec, 2000. **258**(1): p. 39-46.
51. Cunliffe, W.J. and P.H. Sugarbaker, *Gastrointestinal malignancy: rationale for adjuvant therapy using early postoperative intraperitoneal chemotherapy.* The British journal of surgery, 1989. **76**(10): p. 1082-90.
52. van der Wal, B.C., et al., *Paracrine interactions between mesothelial and colon-carcinoma cells in a rat model.* Int J Cancer, 1997. **73**(6): p. 885-90.
53. Jones, L.M., et al., *Hyaluronic acid secreted by mesothelial cells: a natural barrier to ovarian cancer cell adhesion.* Clin Exp Metastasis, 1995. **13**(5): p. 373-80.

54. Wynn, T.A., *Common and unique mechanisms regulate fibrosis in various fibroproliferative diseases.* The Journal of clinical investigation, 2007. **117**(3): p. 524-9.
55. Mutsaers, S.E., et al., *Mechanisms of tissue repair: from wound healing to fibrosis.* The international journal of biochemistry & cell biology, 1997. **29**(1): p. 5-17.
56. Leask, A. and D.J. Abraham, *TGF-beta signaling and the fibrotic response.* FASEB journal : official publication of the Federation of American Societies for Experimental Biology, 2004. **18**(7): p. 816-27.
57. Margetts, P.J. and P. Bonniaud, *Basic mechanisms and clinical implications of peritoneal fibrosis.* Peritoneal dialysis international : journal of the International Society for Peritoneal Dialysis, 2003. **23**(6): p. 530-41.
58. Lai, K.N., S.C. Tang, and J.C. Leung, *Mediators of inflammation and fibrosis.* Peritoneal dialysis international : journal of the International Society for Peritoneal Dialysis, 2007. **27 Suppl 2**: p. S65-71.
59. Tomino, Y., *Mechanisms and interventions in peritoneal fibrosis.* Clinical and experimental nephrology, 2012. **16**(1): p. 109-14.
60. Braun, N., et al., *Encapsulating peritoneal sclerosis - an overview.* Nephrologie & therapeutique, 2011. **7**(3): p. 162-71.
61. Brown, M.C., et al., *Encapsulating peritoneal sclerosis in the new millennium: a national cohort study.* Clinical journal of the American Society of Nephrology : CJASN, 2009. **4**(7): p. 1222-9.
62. Kawanishi, H., et al., *Encapsulating peritoneal sclerosis in Japan: a prospective, controlled, multicenter study.* American journal of kidney diseases : the official journal of the National Kidney Foundation, 2004. **44**(4): p. 729-37.
63. Rigby, R.J. and C.M. Hawley, *Sclerosing peritonitis: the experience in Australia.* Nephrology, dialysis, transplantation : official publication of the European Dialysis and Transplant Association - European Renal Association, 1998. **13**(1): p. 154-9.
64. Summers, A.M., et al., *Single-center experience of encapsulating peritoneal sclerosis in patients on peritoneal dialysis for end-stage renal failure.* Kidney international, 2005. **68**(5): p. 2381-8.
65. Korte, M.R., E.W. Boeschoten, and M.G. Betjes, *The Dutch EPS Registry: increasing the knowledge of encapsulating peritoneal sclerosis.* The Netherlands journal of medicine, 2009. **67**(8): p. 359-62.
66. Kawaguchi, Y., et al., *Encapsulating peritoneal sclerosis: definition, etiology, diagnosis, and treatment. International Society for Peritoneal Dialysis Ad Hoc Committee on Ultrafiltration Management in Peritoneal Dialysis.* Peritoneal dialysis international : journal of the International Society for Peritoneal Dialysis, 2000. **20 Suppl 4**: p. S43-55.
67. Pollock, C.A., *Diagnosis and management of encapsulating peritoneal sclerosis.* Peritoneal dialysis international : journal of the International Society for Peritoneal Dialysis, 2001. **21 Suppl 3**: p. S61-6.
68. Brown, E.A., et al., *Length of time on peritoneal dialysis and encapsulating peritoneal sclerosis: position paper for ISPD.* Peritoneal dialysis international : journal of the International Society for Peritoneal Dialysis, 2009. **29**(6): p. 595-600.

69. Tarzi, R.M., et al., *Assessing the validity of an abdominal CT scoring system in the diagnosis of encapsulating peritoneal sclerosis.* Clinical journal of the American Society of Nephrology : CJASN, 2008. **3**(6): p. 1702-10.
70. Sampimon, D.E., et al., *Early diagnostic markers for encapsulating peritoneal sclerosis: a case-control study.* Peritoneal dialysis international : journal of the International Society for Peritoneal Dialysis, 2010. **30**(2): p. 163-9.
71. Korte, M.R., et al., *Encapsulating peritoneal sclerosis: the state of affairs.* Nature reviews. Nephrology, 2011. **7**(9): p. 528-38.
72. Sherif, A.M., et al., *Comparison between the pathology of encapsulating sclerosis and simple sclerosis of the peritoneal membrane in chronic peritoneal dialysis.* Therapeutic apheresis and dialysis : official peer-reviewed journal of the International Society for Apheresis, the Japanese Society for Apheresis, the Japanese Society for Dialysis Therapy, 2008. **12**(1): p. 33-41.
73. Garosi, G., F. Cappelletti, and N. Di Paolo, *Fibrosis and sclerosis: different disorders or different stages?* Contributions to nephrology, 2006. **150**: p. 62-9.
74. Summers, A.M., C.M. Hoff, and N. Topley, *How can genetic advances impact on experimental models of encapsulating peritoneal sclerosis?* Peritoneal dialysis international : journal of the International Society for Peritoneal Dialysis, 2008. **28 Suppl 5**: p. S16-20.
75. Honda, K. and H. Oda, *Pathology of encapsulating peritoneal sclerosis.* Peritoneal dialysis international : journal of the International Society for Peritoneal Dialysis, 2005. **25 Suppl 4**: p. S19-29.
76. Lee, H.Y., et al., *Sclerosing encapsulating peritonitis as a complication of long-term continuous ambulatory peritoneal dialysis in Korea.* Nephrology, 2003. **8 Suppl**: p. S33-9.
77. Balasubramaniam, G., et al., *The Pan-Thames EPS study: treatment and outcomes of encapsulating peritoneal sclerosis.* Nephrology, dialysis, transplantation : official publication of the European Dialysis and Transplant Association - European Renal Association, 2009. **24**(10): p. 3209-15.
78. Korte, M.R., et al., *Risk factors associated with encapsulating peritoneal sclerosis in Dutch EPS study.* Peritoneal dialysis international : journal of the International Society for Peritoneal Dialysis, 2011. **31**(3): p. 269-78.
79. Johnson, D.W., et al., *Encapsulating peritoneal sclerosis: incidence, predictors, and outcomes.* Kidney international, 2010. **77**(10): p. 904-12.
80. Hendriks, P.M., et al., *Peritoneal sclerosis in chronic peritoneal dialysis patients: analysis of clinical presentation, risk factors, and peritoneal transport kinetics.* Peritoneal dialysis international : journal of the International Society for Peritoneal Dialysis, 1997. **17**(2): p. 136-43.
81. Yamamoto, R., et al., *Risk factors for encapsulating peritoneal sclerosis in patients who have experienced peritoneal dialysis treatment.* Clinical and experimental nephrology, 2005. **9**(2): p. 148-52.
82. Lambie, M.L., et al., *The peritoneal osmotic conductance is low well before the diagnosis of encapsulating peritoneal sclerosis is made.* Kidney international, 2010. **78**(6): p. 611-8.

83. Yamamoto, R., et al., *High-transport membrane is a risk factor for encapsulating peritoneal sclerosis developing after long-term continuous ambulatory peritoneal dialysis treatment.* Advances in peritoneal dialysis. Conference on Peritoneal Dialysis, 2002. **18**: p. 131-4.
84. Sampimon, D.E., et al., *The time course of peritoneal transport parameters in peritoneal dialysis patients who develop encapsulating peritoneal sclerosis.* Nephrology, dialysis, transplantation : official publication of the European Dialysis and Transplant Association - European Renal Association, 2011. **26**(1): p. 291-8.
85. Rippe, B., *A three-pore model of peritoneal transport.* Peritoneal dialysis international : journal of the International Society for Peritoneal Dialysis, 1993. **13 Suppl 2**: p. S35-8.
86. Krediet, R.T., B. Lindholm, and B. Rippe, *Pathophysiology of peritoneal membrane failure.* Peritoneal dialysis international : journal of the International Society for Peritoneal Dialysis, 2000. **20 Suppl 4**: p. S22-42.
87. Goffin, E., *Peritoneal membrane structural and functional changes during peritoneal dialysis.* Seminars in dialysis, 2008. **21**(3): p. 258-65.
88. Krediet, R.T., *The physiology of peritoneal solute transport and ultrafiltration*, in *Textbook of Peritoneal Dialysis*, R. Gokal, et al., Editors. 2000, Springer Netherlands. p. 135-172.
89. Krediet, R.T., et al., *Neoangiogenesis in the peritoneal membrane.* Peritoneal dialysis international : journal of the International Society for Peritoneal Dialysis, 2000. **20 Suppl 2**: p. S19-25.
90. Kawaguchi, Y., et al., *Issues affecting the longevity of the continuous peritoneal dialysis therapy.* Kidney international. Supplement, 1997. **62**: p. S105-7.
91. Twardowski, Z.j., et al., *PERITONEAL EQUILIBRATION TEST.* Peritoneal Dialysis International, 1987. **7**(3): p. 138-148.
92. Correa-Rotter, R. and A. Cueto-Manzano, *The problem of the high transporter: is survival decreased?* Peritoneal dialysis international : journal of the International Society for Peritoneal Dialysis, 2001. **21 Suppl 3**: p. S75-9.
93. Churchill, D.N., et al., *Increased peritoneal membrane transport is associated with decreased patient and technique survival for continuous peritoneal dialysis patients. The Canada-USA (CANUSA) Peritoneal Dialysis Study Group.* Journal of the American Society of Nephrology : JASN, 1998. **9**(7): p. 1285-92.
94. Davies, S.J., L. Phillips, and G.I. Russell, *Peritoneal solute transport predicts survival on CAPD independently of residual renal function.* Nephrology, dialysis, transplantation : official publication of the European Dialysis and Transplant Association - European Renal Association, 1998. **13**(4): p. 962-8.
95. Szeto, C.C., et al., *Peritoneal transport status correlates with morbidity but not longitudinal change of nutritional status of continuous ambulatory peritoneal dialysis patients: a 2-year prospective study.* American journal of kidney diseases : the official journal of the National Kidney Foundation, 2001. **37**(2): p. 329-36.
96. Rumpsfeld, M., S.P. McDonald, and D.W. Johnson, *Higher peritoneal transport status is associated with higher mortality and technique failure in*

the Australian and New Zealand peritoneal dialysis patient populations. Journal of the American Society of Nephrology : JASN, 2006. **17**(1): p. 271-8.
97. Rumpsfeld, M., et al., *Predictors of baseline peritoneal transport status in Australian and New Zealand peritoneal dialysis patients.* American journal of kidney diseases : the official journal of the National Kidney Foundation, 2004. **43**(3): p. 492-501.
98. Prowant, B.F., et al., *Peritoneal dialysis survival in relation to patient body size and peritoneal transport characteristics.* Nephrology nursing journal : journal of the American Nephrology Nurses' Association, 2010. **37**(6): p. 641-6; quiz 647.
99. Davies, S.J., *Mitigating peritoneal membrane characteristics in modern peritoneal dialysis therapy.* Kidney international. Supplement, 2006(103): p. S76-83.
100. Blake, P.G., et al., *Changes in peritoneal membrane transport rates in patients on long term CAPD.* Advances in peritoneal dialysis. Conference on Peritoneal Dialysis, 1989. **5**: p. 3-7.
101. Davies, S.J., et al., *Longitudinal changes in peritoneal kinetics: the effects of peritoneal dialysis and peritonitis.* Nephrol Dial Transplant, 1996. **11**(3): p. 498-506.
102. Numata, M., et al., *Association between an increased surface area of peritoneal microvessels and a high peritoneal solute transport rate.* Peritoneal dialysis international : journal of the International Society for Peritoneal Dialysis, 2003. **23**(2): p. 116-22.
103. de Lima, S.M., et al., *Inflammation, neoangiogenesis and fibrosis in peritoneal dialysis.* Clinica chimica acta; international journal of clinical chemistry, 2013. **421**: p. 46-50.
104. Coester, A.M., et al., *Longitudinal analysis of peritoneal fluid transport and its determinants in a cohort of incident peritoneal dialysis patients.* Peritoneal dialysis international : journal of the International Society for Peritoneal Dialysis, 2014. **34**(2): p. 195-203.
105. Carmeliet, P., *Angiogenesis in life, disease and medicine.* Nature, 2005. **438**(7070): p. 932-6.
106. Mateijsen, M.A., et al., *Vascular and interstitial changes in the peritoneum of CAPD patients with peritoneal sclerosis.* Peritoneal dialysis international : journal of the International Society for Peritoneal Dialysis, 1999. **19**(6): p. 517-25.
107. Zweers, M.M., et al., *Vascular endothelial growth factor in peritoneal dialysis: a longitudinal follow-up.* The Journal of laboratory and clinical medicine, 2001. **137**(2): p. 125-32.
108. Zweers, M.M., et al., *Growth factors VEGF and TGF-beta1 in peritoneal dialysis.* The Journal of laboratory and clinical medicine, 1999. **134**(2): p. 124-32.
109. Pecoits-Filho, R., et al., *Plasma and dialysate IL-6 and VEGF concentrations are associated with high peritoneal solute transport rate.* Nephrology, dialysis, transplantation : official publication of the European Dialysis and Transplant Association - European Renal Association, 2002. **17**(8): p. 1480-6.

110. Margetts, P.J., et al., *Antiangiogenic and antifibrotic gene therapy in a chronic infusion model of peritoneal dialysis in rats.* Journal of the American Society of Nephrology : JASN, 2002. **13**(3): p. 721-8.
111. Davies, S.J., et al., *Clinical evaluation of the peritoneal equilibration test: a population-based study.* Nephrology, dialysis, transplantation : official publication of the European Dialysis and Transplant Association - European Renal Association, 1993. **8**(1): p. 64-70.
112. Ho-dac-Pannekeet, M.M., et al., *Analysis of ultrafiltration failure in peritoneal dialysis patients by means of standard peritoneal permeability analysis.* Peritoneal dialysis international : journal of the International Society for Peritoneal Dialysis, 1997. **17**(2): p. 144-50.
113. Heimburger, O., et al., *Peritoneal transport in CAPD patients with permanent loss of ultrafiltration capacity.* Kidney international, 1990. **38**(3): p. 495-506.
114. Smit, W., et al., *Analysis of the prevalence and causes of ultrafiltration failure during long-term peritoneal dialysis: a cross-sectional study.* Peritoneal dialysis international : journal of the International Society for Peritoneal Dialysis, 2004. **24**(6): p. 562-70.
115. Devuyst, O., N. Topley, and J.D. Williams, *Morphological and functional changes in the dialysed peritoneal cavity: impact of more biocompatible solutions.* Nephrology, dialysis, transplantation : official publication of the European Dialysis and Transplant Association - European Renal Association, 2002. **17 Suppl 3**: p. 12-5.
116. Devuyst, O., P.J. Margetts, and N. Topley, *The pathophysiology of the peritoneal membrane.* J Am Soc Nephrol, 2010. **21**(7): p. 1077-85.
117. Honda, K., et al., *Morphological changes in the peritoneal vasculature of patients on CAPD with ultrafiltration failure.* Nephron, 1996. **72**(2): p. 171-6.
118. Williams, J.D., et al., *The natural course of peritoneal membrane biology during peritoneal dialysis.* Kidney international. Supplement, 2003(88): p. S43-9.
119. Plum, J., et al., *Peritoneal sclerosis in peritoneal dialysis patients related to dialysis settings and peritoneal transport properties.* Kidney international. Supplement, 2001. **78**: p. S42-7.
120. Witowski, J., et al., *Prolonged exposure to glucose degradation products impairs viability and function of human peritoneal mesothelial cells.* J Am Soc Nephrol, 2001. **12**(11): p. 2434-41.
121. Boulanger, E., et al., *The triggering of human peritoneal mesothelial cell apoptosis and oncosis by glucose and glycoxydation products.* Nephrol Dial Transplant, 2004. **19**(9): p. 2208-16.
122. Margetts, P.J., et al., *Transient overexpression of TGF-{beta}1 induces epithelial mesenchymal transition in the rodent peritoneum.* J Am Soc Nephrol, 2005. **16**(2): p. 425-36.
123. Ha, H. and H.B. Lee, *Effect of high glucose on peritoneal mesothelial cell biology.* Peritoneal dialysis international : journal of the International Society for Peritoneal Dialysis, 2000. **20 Suppl 2**: p. S15-8.
124. Ha, H., M.R. Yu, and H.B. Lee, *High glucose-induced PKC activation mediates TGF-beta 1 and fibronectin synthesis by peritoneal mesothelial cells.* Kidney international, 2001. **59**(2): p. 463-70.

125. Offner, F.A., et al., *Transforming growth factor-beta synthesis by human peritoneal mesothelial cells. Induction by interleukin-1.* Am J Pathol, 1996. **148**(5): p. 1679-88.
126. Cronauer, M.V., et al., *Basic fibroblast growth factor synthesis by human peritoneal mesothelial cells: induction by interleukin-1.* The American journal of pathology, 1999. **155**(6): p. 1977-84.
127. Tekstra, J., et al., *Identification of the major chemokines that regulate cell influxes in peritoneal dialysis patients.* Journal of the American Society of Nephrology : JASN, 1996. **7**(11): p. 2379-84.
128. Haslinger, B., et al., *Hyaluronan fragments induce the synthesis of MCP-1 and IL-8 in cultured human peritoneal mesothelial cells.* Cell and tissue research, 2001. **305**(1): p. 79-86.
129. Bellingan, G.J., et al., *Adhesion molecule-dependent mechanisms regulate the rate of macrophage clearance during the resolution of peritoneal inflammation.* The Journal of experimental medicine, 2002. **196**(11): p. 1515-21.
130. Schilte, M.N., et al., *Factors contributing to peritoneal tissue remodeling in peritoneal dialysis.* Peritoneal dialysis international : journal of the International Society for Peritoneal Dialysis, 2009. **29**(6): p. 605-17.
131. Yanez-Mo, M., et al., *Peritoneal dialysis and epithelial-to-mesenchymal transition of mesothelial cells.* N Engl J Med, 2003. **348**(5): p. 403-13.
132. Strippoli, R., et al., *Epithelial-to-mesenchymal transition of peritoneal mesothelial cells is regulated by an ERK/NF-kappaB/Snail1 pathway.* Dis Model Mech, 2008. **1**(4-5): p. 264-74.
133. Gabbiani, G., *The myofibroblast in wound healing and fibrocontractive diseases.* J Pathol, 2003. **200**(4): p. 500-3.
134. Aroeira, L.S., et al., *Epithelial to mesenchymal transition and peritoneal membrane failure in peritoneal dialysis patients: pathologic significance and potential therapeutic interventions.* Journal of the American Society of Nephrology : JASN, 2007. **18**(7): p. 2004-13.
135. Jimenez-Heffernan, J.A., et al., *Immunohistochemical characterization of fibroblast subpopulations in normal peritoneal tissue and in peritoneal dialysis-induced fibrosis.* Virchows Arch, 2004. **444**(3): p. 247-56.
136. Gabbiani, G., *The cellular derivation and the life span of the myofibroblast.* Pathol Res Pract, 1996. **192**(7): p. 708-11.
137. Yang, A.H., J.Y. Chen, and J.K. Lin, *Myofibroblastic conversion of mesothelial cells.* Kidney Int, 2003. **63**(4): p. 1530-9.
138. Kalluri, R. and R.A. Weinberg, *The basics of epithelial-mesenchymal transition.* The Journal of clinical investigation, 2009. **119**(6): p. 1420-8.
139. Greenburg, G. and E.D. Hay, *Epithelia suspended in collagen gels can lose polarity and express characteristics of migrating mesenchymal cells.* The Journal of cell biology, 1982. **95**(1): p. 333-9.
140. Hay, E.D., *An overview of epithelio-mesenchymal transformation.* Acta Anat (Basel), 1995. **154**(1): p. 8-20.
141. Kalluri, R. and E.G. Neilson, *Epithelial-mesenchymal transition and its implications for fibrosis.* The Journal of clinical investigation, 2003. **112**(12): p. 1776-84.
142. Liu, Y., *Epithelial to mesenchymal transition in renal fibrogenesis: pathologic significance, molecular mechanism, and therapeutic*

intervention. Journal of the American Society of Nephrology : JASN, 2004. **15**(1): p. 1-12.
143. Zeisberg, M., et al., *Fibroblasts derive from hepatocytes in liver fibrosis via epithelial to mesenchymal transition.* The Journal of biological chemistry, 2007. **282**(32): p. 23337-47.
144. Oh, E.J., et al., *Impact of low glucose degradation product bicarbonate/lactate-buffered dialysis solution on the epithelial-mesenchymal transition of peritoneum.* American journal of nephrology, 2010. **31**(1): p. 58-67.
145. Iwano, M., et al., *Evidence that fibroblasts derive from epithelium during tissue fibrosis.* The Journal of clinical investigation, 2002. **110**(3): p. 341-50.
146. Loureiro, J., et al., *Blocking TGF-beta1 protects the peritoneal membrane from dialysate-induced damage.* J Am Soc Nephrol, 2011. **22**(9): p. 1682-95.
147. Sporn, M.B. and A.B. Roberts, *The transforming growth factor-betas: past, present, and future.* Ann N Y Acad Sci, 1990. **593**: p. 1-6.
148. Heldin, C.H., K. Miyazono, and P. ten Dijke, *TGF-beta signalling from cell membrane to nucleus through SMAD proteins.* Nature, 1997. **390**(6659): p. 465-71.
149. Massague, J., *The transforming growth factor-beta family.* Annu Rev Cell Biol, 1990. **6**: p. 597-641.
150. Fujii, D., et al., *Transforming growth factor beta gene maps to human chromosome 19 long arm and to mouse chromosome 7.* Somat Cell Mol Genet, 1986. **12**(3): p. 281-8.
151. Barton, D.E., et al., *Chromosomal mapping of genes for transforming growth factors beta 2 and beta 3 in man and mouse: dispersion of TGF-beta gene family.* Oncogene Res, 1988. **3**(4): p. 323-31.
152. Margetts, P.J., et al., *Gene transfer of transforming growth factor-beta1 to the rat peritoneum: effects on membrane function.* J Am Soc Nephrol, 2001. **12**(10): p. 2029-39.
153. Assoian, R.K., et al., *Transforming growth factor-beta in human platelets. Identification of a major storage site, purification, and characterization.* J Biol Chem, 1983. **258**(11): p. 7155-60.
154. Wu, M.Y. and C.S. Hill, *Tgf-beta superfamily signaling in embryonic development and homeostasis.* Dev Cell, 2009. **16**(3): p. 329-43.
155. Li, M.O., et al., *Transforming growth factor-beta regulation of immune responses.* Annu Rev Immunol, 2006. **24**: p. 99-146.
156. de Caestecker, M.P., E. Piek, and A.B. Roberts, *Role of transforming growth factor-beta signaling in cancer.* J Natl Cancer Inst, 2000. **92**(17): p. 1388-402.
157. Sinha, S., et al., *Cellular and extracellular biology of the latent transforming growth factor-beta binding proteins.* Matrix Biol, 1998. **17**(8-9): p. 529-45.
158. Annes, J.P., J.S. Munger, and D.B. Rifkin, *Making sense of latent TGFbeta activation.* J Cell Sci, 2003. **116**(Pt 2): p. 217-24.
159. Lyons, R.M., J. Keski-Oja, and H.L. Moses, *Proteolytic activation of latent transforming growth factor-beta from fibroblast-conditioned medium.* J Cell Biol, 1988. **106**(5): p. 1659-65.

160. Crawford, S.E., et al., *Thrombospondin-1 is a major activator of TGF-beta1 in vivo.* Cell, 1998. **93**(7): p. 1159-70.
161. Kulkarni, A.B., et al., *Transforming growth factor beta 1 null mutation in mice causes excessive inflammatory response and early death.* Proceedings of the National Academy of Sciences of the United States of America, 1993. **90**(2): p. 770-4.
162. Barnard, J.A., R.M. Lyons, and H.L. Moses, *The cell biology of transforming growth factor beta.* Biochimica et biophysica acta, 1990. **1032**(1): p. 79-87.
163. Reibman, J., et al., *Transforming growth factor beta 1, a potent chemoattractant for human neutrophils, bypasses classic signal-transduction pathways.* Proc Natl Acad Sci U S A, 1991. **88**(15): p. 6805-9.
164. Ma, J., et al., *MCP-1 mediates TGF-beta-induced angiogenesis by stimulating vascular smooth muscle cell migration.* Blood, 2007. **109**(3): p. 987-94.
165. Pakyari, M., et al., *Critical Role of Transforming Growth Factor Beta in Different Phases of Wound Healing.* Adv Wound Care (New Rochelle), 2013. **2**(5): p. 215-224.
166. Gorelik, L. and R.A. Flavell, *Transforming growth factor-beta in T-cell biology.* Nat Rev Immunol, 2002. **2**(1): p. 46-53.
167. Taylor, A., et al., *Mechanisms of immune suppression by interleukin-10 and transforming growth factor-beta: the role of T regulatory cells.* Immunology, 2006. **117**(4): p. 433-42.
168. Gordon, K.J. and G.C. Blobe, *Role of transforming growth factor-beta superfamily signaling pathways in human disease.* Biochimica et biophysica acta, 2008. **1782**(4): p. 197-228.
169. Yamamoto, T., et al., *Expression of transforming growth factor beta is elevated in human and experimental diabetic nephropathy.* Proceedings of the National Academy of Sciences of the United States of America, 1993. **90**(5): p. 1814-8.
170. Gressner, A.M. and R. Weiskirchen, *Modern pathogenetic concepts of liver fibrosis suggest stellate cells and TGF-beta as major players and therapeutic targets.* Journal of cellular and molecular medicine, 2006. **10**(1): p. 76-99.
171. Anscher, M.S., et al., *Transforming growth factor beta as a predictor of liver and lung fibrosis after autologous bone marrow transplantation for advanced breast cancer.* The New England journal of medicine, 1993. **328**(22): p. 1592-8.
172. Margetts, P.J., K.H. Oh, and M. Kolb, *Transforming growth factor-beta: importance in long-term peritoneal membrane changes.* Peritoneal dialysis international : journal of the International Society for Peritoneal Dialysis, 2005. **25 Suppl 3**: p. S15-7.
173. Lin, C.Y., et al., *Persistent transforming growth factor-beta 1 expression may predict peritoneal fibrosis in CAPD patients with frequent peritonitis occurrence.* Am J Nephrol, 1998. **18**(6): p. 513-9.
174. Lai, K.N., et al., *Changes of cytokine profiles during peritonitis in patients on continuous ambulatory peritoneal dialysis.* Am J Kidney Dis, 2000. **35**(4): p. 644-52.
175. Tsukada, T., et al., *The role of human peritoneal mesothelial cells in the fibrosis and progression of gastric cancer.* Int J Oncol, 2012. **41**(2): p. 476-82.

176. Nie, J., et al., *Smad7 gene transfer inhibits peritoneal fibrosis.* Kidney international, 2007. **72**(11): p. 1336-44.
177. Loureiro, J., et al., *BMP-7 blocks mesenchymal conversion of mesothelial cells and prevents peritoneal damage induced by dialysis fluid exposure.* Nephrology, dialysis, transplantation : official publication of the European Dialysis and Transplant Association - European Renal Association, 2010. **25**(4): p. 1098-108.
178. Vargha, R., et al., *Ex vivo reversal of in vivo transdifferentiation in mesothelial cells grown from peritoneal dialysate effluents.* Nephrology, dialysis, transplantation : official publication of the European Dialysis and Transplant Association - European Renal Association, 2006. **21**(10): p. 2943-7.
179. Massague, J., *TGF-beta signal transduction.* Annual review of biochemistry, 1998. **67**: p. 753-91.
180. ten Dijke, P., et al., *Characterization of type I receptors for transforming growth factor-beta and activin.* Science, 1994. **264**(5155): p. 101-4.
181. Derynck, R. and X.H. Feng, *TGF-beta receptor signaling.* Biochim Biophys Acta, 1997. **1333**(2): p. F105-50.
182. Wrana, J.L., et al., *Mechanism of activation of the TGF-beta receptor.* Nature, 1994. **370**(6488): p. 341-7.
183. Wang, X.F., et al., *Expression cloning and characterization of the TGF-beta type III receptor.* Cell, 1991. **67**(4): p. 797-805.
184. Moustakas, A., et al., *The transforming growth factor beta receptors types I, II, and III form hetero-oligomeric complexes in the presence of ligand.* J Biol Chem, 1993. **268**(30): p. 22215-8.
185. Sankar, S., et al., *Expression of transforming growth factor type III receptor in vascular endothelial cells increases their responsiveness to transforming growth factor beta 2.* J Biol Chem, 1995. **270**(22): p. 13567-72.
186. Cheifetz, S. and J. Massague, *Transforming growth factor-beta (TGF-beta) receptor proteoglycan. Cell surface expression and ligand binding in the absence of glycosaminoglycan chains.* The Journal of biological chemistry, 1989. **264**(20): p. 12025-8.
187. Raftery, L.A., et al., *Genetic screens to identify elements of the decapentaplegic signaling pathway in Drosophila.* Genetics, 1995. **139**(1): p. 241-54.
188. Savage, C., et al., *Caenorhabditis elegans genes sma-2, sma-3, and sma-4 define a conserved family of transforming growth factor beta pathway components.* Proceedings of the National Academy of Sciences of the United States of America, 1996. **93**(2): p. 790-4.
189. Massague, J., J. Seoane, and D. Wotton, *Smad transcription factors.* Genes & development, 2005. **19**(23): p. 2783-810.
190. Moustakas, A., S. Souchelnytskyi, and C.H. Heldin, *Smad regulation in TGF-beta signal transduction.* J Cell Sci, 2001. **114**(Pt 24): p. 4359-69.
191. Miyazawa, K., et al., *Two major Smad pathways in TGF-beta superfamily signalling.* Genes Cells, 2002. **7**(12): p. 1191-204.
192. Xiao, Z., et al., *A distinct nuclear localization signal in the N terminus of Smad 3 determines its ligand-induced nuclear translocation.* Proceedings of the National Academy of Sciences of the United States of America, 2000. **97**(14): p. 7853-8.

193. Hata, A., et al., *Mutations increasing autoinhibition inactivate tumour suppressors Smad2 and Smad4.* Nature, 1997. **388**(6637): p. 82-7.
194. Shi, Y. and J. Massague, *Mechanisms of TGF-beta signaling from cell membrane to the nucleus.* Cell, 2003. **113**(6): p. 685-700.
195. Souchelnytskyi, S., et al., *Phosphorylation of Ser465 and Ser467 in the C terminus of Smad2 mediates interaction with Smad4 and is required for transforming growth factor-beta signaling.* The Journal of biological chemistry, 1997. **272**(44): p. 28107-15.
196. Abdollah, S., et al., *TbetaRI phosphorylation of Smad2 on Ser465 and Ser467 is required for Smad2-Smad4 complex formation and signaling.* The Journal of biological chemistry, 1997. **272**(44): p. 27678-85.
197. Wu, R.Y., et al., *Heteromeric and homomeric interactions correlate with signaling activity and functional cooperativity of Smad3 and Smad4/DPC4.* Molecular and cellular biology, 1997. **17**(5): p. 2521-8.
198. Zawel, L., et al., *Human Smad3 and Smad4 are sequence-specific transcription activators.* Mol Cell, 1998. **1**(4): p. 611-7.
199. Shi, Y., et al., *Crystal structure of a Smad MH1 domain bound to DNA: insights on DNA binding in TGF-beta signaling.* Cell, 1998. **94**(5): p. 585-94.
200. Yagi, K., et al., *Alternatively spliced variant of Smad2 lacking exon 3. Comparison with wild-type Smad2 and Smad3.* The Journal of biological chemistry, 1999. **274**(2): p. 703-9.
201. Massague, J. and D. Wotton, *Transcriptional control by the TGF-beta/Smad signaling system.* The EMBO journal, 2000. **19**(8): p. 1745-54.
202. Weisberg, E., et al., *A mouse homologue of FAST-1 transduces TGF beta superfamily signals and is expressed during early embryogenesis.* Mech Dev, 1998. **79**(1-2): p. 17-27.
203. Ghosh, A.K., et al., *Smad-dependent stimulation of type I collagen gene expression in human skin fibroblasts by TGF-beta involves functional cooperation with p300/CBP transcriptional coactivators.* Oncogene, 2000. **19**(31): p. 3546-55.
204. Akiyoshi, S., et al., *c-Ski acts as a transcriptional co-repressor in transforming growth factor-beta signaling through interaction with smads.* The Journal of biological chemistry, 1999. **274**(49): p. 35269-77.
205. Stroschein, S.L., et al., *Negative feedback regulation of TGF-beta signaling by the SnoN oncoprotein.* Science, 1999. **286**(5440): p. 771-4.
206. Moustakas, A. and C.H. Heldin, *Non-Smad TGF-beta signals.* J Cell Sci, 2005. **118**(Pt 16): p. 3573-84.
207. Zhang, Y.E., *Non-Smad pathways in TGF-beta signaling.* Cell Res, 2009. **19**(1): p. 128-39.
208. Bakin, A.V., et al., *Phosphatidylinositol 3-kinase function is required for transforming growth factor beta-mediated epithelial to mesenchymal transition and cell migration.* J Biol Chem, 2000. **275**(47): p. 36803-10.
209. Mu, Y., S.K. Gudey, and M. Landstrom, *Non-Smad signaling pathways.* Cell Tissue Res, 2012. **347**(1): p. 11-20.
210. Miyazono, K., *Positive and negative regulation of TGF-beta signaling.* J Cell Sci, 2000. **113 (Pt 7)**: p. 1101-9.
211. Ribeiro, S.M., et al., *The activation sequence of thrombospondin-1 interacts with the latency-associated peptide to regulate activation of latent transforming growth factor-beta.* J Biol Chem, 1999. **274**(19): p. 13586-93.

212. Baghy, K., R.V. Iozzo, and I. Kovalszky, *Decorin-TGFbeta axis in hepatic fibrosis and cirrhosis.* J Histochem Cytochem, 2012. **60**(4): p. 262-8.
213. Abreu, J.G., et al., *Connective-tissue growth factor (CTGF) modulates cell signalling by BMP and TGF-beta.* Nat Cell Biol, 2002. **4**(8): p. 599-604.
214. Itoh, S. and P. ten Dijke, *Negative regulation of TGF-beta receptor/Smad signal transduction.* Curr Opin Cell Biol, 2007. **19**(2): p. 176-84.
215. Yan, X., Z. Liu, and Y. Chen, *Regulation of TGF-beta signaling by Smad7.* Acta Biochim Biophys Sin (Shanghai), 2009. **41**(4): p. 263-72.
216. Suzuki, C., et al., *Smurf1 regulates the inhibitory activity of Smad7 by targeting Smad7 to the plasma membrane.* J Biol Chem, 2002. **277**(42): p. 39919-25.
217. Zhang, S., et al., *Smad7 antagonizes transforming growth factor beta signaling in the nucleus by interfering with functional Smad-DNA complex formation.* Mol Cell Biol, 2007. **27**(12): p. 4488-99.
218. Massague, J., *TGF-beta signal transduction.* Annu Rev Biochem, 1998. **67**: p. 753-91.
219. Akhurst, R.J. and A. Hata, *Targeting the TGFbeta signalling pathway in disease.* Nat Rev Drug Discov, 2012. **11**(10): p. 790-811.
220. Freire, M.O. and T.E. Van Dyke, *Natural resolution of inflammation.* Periodontol 2000, 2013. **63**(1): p. 149-64.
221. Tracey, K.J., *The inflammatory reflex.* Nature, 2002. **420**(6917): p. 853-9.
222. Medzhitov, R., *Origin and physiological roles of inflammation.* Nature, 2008. **454**(7203): p. 428-35.
223. Eming, S.A., T. Krieg, and J.M. Davidson, *Inflammation in wound repair: molecular and cellular mechanisms.* J Invest Dermatol, 2007. **127**(3): p. 514-25.
224. Alessandri, A.L., et al., *Resolution of inflammation: mechanisms and opportunity for drug development.* Pharmacol Ther, 2013. **139**(2): p. 189-212.
225. Serhan, C.N. and J. Savill, *Resolution of inflammation: the beginning programs the end.* Nat Immunol, 2005. **6**(12): p. 1191-7.
226. Wang, A.Y., et al., *Is a single time point C-reactive protein predictive of outcome in peritoneal dialysis patients?* Journal of the American Society of Nephrology : JASN, 2003. **14**(7): p. 1871-9.
227. Stenvinkel, P., *Inflammation in end-stage renal failure: could it be treated?* Nephrol Dial Transplant, 2002. **17 Suppl 8**: p. 33-8; discussion 40.
228. Dounousi, E., et al., *Oxidative stress is progressively enhanced with advancing stages of CKD.* Am J Kidney Dis, 2006. **48**(5): p. 752-60.
229. Silverstein, D.M., *Inflammation in chronic kidney disease: role in the progression of renal and cardiovascular disease.* Pediatr Nephrol, 2009. **24**(8): p. 1445-52.
230. Zoja, C., M. Abbate, and G. Remuzzi, *Progression of chronic kidney disease: insights from animal models.* Curr Opin Nephrol Hypertens, 2006. **15**(3): p. 250-7.
231. Stenvinkel, P., et al., *Inflammation and outcome in end-stage renal failure: does female gender constitute a survival advantage?* Kidney international, 2002. **62**(5): p. 1791-8.
232. Wang, A.Y. and K.N. Lai, *The importance of residual renal function in dialysis patients.* Kidney international, 2006. **69**(10): p. 1726-32.

233. Ramos, L.F., et al., *Oxidative stress and inflammation are associated with adiposity in moderate to severe CKD.* Journal of the American Society of Nephrology : JASN, 2008. **19**(3): p. 593-9.
234. Carvalho, L.K., et al., *Annual variation in body fat is associated with systemic inflammation in chronic kidney disease patients Stages 3 and 4: a longitudinal study.* Nephrology, dialysis, transplantation : official publication of the European Dialysis and Transplant Association - European Renal Association, 2012. **27**(4): p. 1423-8.
235. Snaedal, S., et al., *Comorbidity and acute clinical events as determinants of C-reactive protein variation in hemodialysis patients: implications for patient survival.* American journal of kidney diseases : the official journal of the National Kidney Foundation, 2009. **53**(6): p. 1024-33.
236. Schwedler, S., et al., *Inflammation and advanced glycation end products in uremia: simple coexistence, potentiation or causal relationship?* Kidney Int Suppl, 2001. **78**: p. S32-6.
237. Poole, S., et al., *Fate of injected interleukin 1 in rats: sequestration and degradation in the kidney.* Cytokine, 1990. **2**(6): p. 416-22.
238. Bemelmans, M.H., D.J. Gouma, and W.A. Buurman, *Influence of nephrectomy on tumor necrosis factor clearance in a murine model.* J Immunol, 1993. **150**(5): p. 2007-17.
239. Palomar-Fontanet, R., et al., *Markers of inflammation before and during peritoneal dialysis.* Adv Perit Dial, 2011. **27**: p. 28-32.
240. Stenvinkel, P., *Inflammation in end-stage renal disease: the hidden enemy.* Nephrology (Carlton), 2006. **11**(1): p. 36-41.
241. Cho, Y., C.M. Hawley, and D.W. Johnson, *Clinical causes of inflammation in peritoneal dialysis patients.* Int J Nephrol, 2014. **2014**: p. 909373.
242. Carozzi, S., et al., *Peritoneal dialysis effluent, cytokine levels, and peritoneal mesothelial cell viability in CAPD: a possible relationship.* Adv Perit Dial, 1997. **13**: p. 7-12.
243. Cho, Y., et al., *Dialysate interleukin-6 predicts increasing peritoneal solute transport rate in incident peritoneal dialysis patients.* BMC Nephrol, 2014. **15**: p. 8.
244. Beelen, R.H., et al., *A single administration of peritoneal dialysis fluid in the rat induces an acute inflammatory exudate.* Advances in peritoneal dialysis. Conference on Peritoneal Dialysis, 1991. **7**: p. 138-41.
245. Perl, J., S.J. Nessim, and J.M. Bargman, *The biocompatibility of neutral pH, low-GDP peritoneal dialysis solutions: benefit at bench, bedside, or both?* Kidney international, 2011. **79**(8): p. 814-24.
246. Riesenhuber, A., et al., *Peritoneal dialysis fluid induces p38-dependent inflammation in human mesothelial cells.* Peritoneal dialysis international : journal of the International Society for Peritoneal Dialysis, 2011. **31**(3): p. 332-9.
247. Pajek, J., et al., *Short-term effects of a new bicarbonate/lactate-buffered and conventional peritoneal dialysis fluid on peritoneal and systemic inflammation in CAPD patients: a randomized controlled study.* Peritoneal dialysis international : journal of the International Society for Peritoneal Dialysis, 2008. **28**(1): p. 44-52.

248. Williams, J.D., et al., *The Euro-Balance Trial: the effect of a new biocompatible peritoneal dialysis fluid (balance) on the peritoneal membrane.* Kidney international, 2004. **66**(1): p. 408-18.
249. Cho, Y. and D.W. Johnson, *Does the use of neutral pH, low glucose degradation product peritoneal dialysis fluids lead to better patient outcomes?* Current opinion in nephrology and hypertension, 2013.
250. Davies, S.J., et al., *Peritoneal glucose exposure and changes in membrane solute transport with time on peritoneal dialysis.* Journal of the American Society of Nephrology : JASN, 2001. **12**(5): p. 1046-51.
251. Lee, S.K., et al., *High glucose induces MCP-1 expression partly via tyrosine kinase-AP-1 pathway in peritoneal mesothelial cells.* Kidney international, 2001. **60**(1): p. 55-64.
252. Shostak, A., E. Pivnik, and L. Gotloib, *Cultured rat mesothelial cells generate hydrogen peroxide: a new player in peritoneal defense?* Journal of the American Society of Nephrology : JASN, 1996. **7**(11): p. 2371-8.
253. Medcalf, J.F., et al., *Effects of glucose dialysate on extracellular matrix production by human peritoneal mesothelial cells (HPMC): the role of TGF-beta.* Nephrol Dial Transplant, 2001. **16**(9): p. 1885-92.
254. Lee, D.H., et al., *3,4-dideoxyglucosone-3-ene induces apoptosis in human peritoneal mesothelial cells.* Peritoneal dialysis international : journal of the International Society for Peritoneal Dialysis, 2009. **29**(1): p. 44-51.
255. Nakayama, M., et al., *Immunohistochemical detection of advanced glycosylation end-products in the peritoneum and its possible pathophysiological role in CAPD.* Kidney international, 1997. **51**(1): p. 182-6.
256. Honda, K., et al., *Accumulation of advanced glycation end products in the peritoneal vasculature of continuous ambulatory peritoneal dialysis patients with low ultra-filtration.* Nephrology, dialysis, transplantation : official publication of the European Dialysis and Transplant Association - European Renal Association, 1999. **14**(6): p. 1541-9.
257. Boulanger, E., et al., *AGEs bind to mesothelial cells via RAGE and stimulate VCAM-1 expression.* Kidney international, 2002. **61**(1): p. 148-56.
258. Topley, N., *The cytokine network controlling peritoneal inflammation.* Perit Dial Int, 1995. **15**(7 Suppl): p. S35-9; discussion S39-40.
259. Troidle, L., N. Gorban-Brennan, and F.O. Finkelstein, *Outcome of patients on chronic peritoneal dialysis undergoing peritoneal catheter removal because of peritonitis.* Adv Perit Dial, 2005. **21**: p. 98-101.
260. Brown, M.C., et al., *Peritoneal dialysis-associated peritonitis rates and outcomes in a national cohort are not improving in the post-millennium (2000-2007).* Perit Dial Int, 2011. **31**(6): p. 639-50.
261. Mujais, S., *Microbiology and outcomes of peritonitis in North America.* Kidney Int Suppl, 2006(103): p. S55-62.
262. Zemel, D., et al., *Analysis of inflammatory mediators and peritoneal permeability to macromolecules shortly before the onset of overt peritonitis in patients treated with CAPD.* Perit Dial Int, 1995. **15**(2): p. 134-41.
263. Betjes, M.G., et al., *Intraperitoneal interleukin-8 and neutrophil influx in the initial phase of a CAPD peritonitis.* Perit Dial Int, 1996. **16**(4): p. 385-92.
264. Mlambo, N.C., B. Hylander, and A. Brauner, *Increased levels of transforming growth factor beta 1 and basic fibroblast growth factor in patients on*

CAPD: a study during non-infected steady state and peritonitis. Inflammation, 1999. **23**(2): p. 131-9.
265. Fielding, C.A., et al., *Interleukin-6 signaling drives fibrosis in unresolved inflammation.* Immunity, 2014. **40**(1): p. 40-50.
266. Hurst, S.M., et al., *Il-6 and its soluble receptor orchestrate a temporal switch in the pattern of leukocyte recruitment seen during acute inflammation.* Immunity, 2001. **14**(6): p. 705-14.
267. Isaacs, A. and J. Lindenmann, *Virus Interference. I. The Interferon.* Proceedings of the Royal Society of London. Series B - Biological Sciences, 1957. **147**(927): p. 258-267.
268. De Maeyer-Guignard, J. and E. De Maeyer, *Immunomodulation by interferons: recent developments.* Interferon, 1985. **6**: p. 69-91.
269. Ossina, N.K., et al., *Interferon-gamma modulates a p53-independent apoptotic pathway and apoptosis-related gene expression.* The Journal of biological chemistry, 1997. **272**(26): p. 16351-7.
270. Vivo, C., et al., *Control of cell cycle progression in human mesothelioma cells treated with gamma interferon.* Oncogene, 2001. **20**(9): p. 1085-93.
271. Stark, G.R., et al., *How cells respond to interferons.* Annual review of biochemistry, 1998. **67**: p. 227-64.
272. Pestka, S., C.D. Krause, and M.R. Walter, *Interferons, interferon-like cytokines, and their receptors.* Immunological reviews, 2004. **202**: p. 8-32.
273. Schroder, K., et al., *Interferon-gamma: an overview of signals, mechanisms and functions.* Journal of leukocyte biology, 2004. **75**(2): p. 163-89.
274. Katze, M.G., Y. He, and M. Gale, Jr., *Viruses and interferon: a fight for supremacy.* Nature reviews. Immunology, 2002. **2**(9): p. 675-87.
275. Naylor, S.L., et al., *Human immune interferon gene is located on chromosome 12.* The Journal of experimental medicine, 1983. **157**(3): p. 1020-7.
276. Naylor, S.L., P.W. Gray, and P.A. Lalley, *Mouse immune interferon (IFN-gamma) gene is on chromosome 10.* Somat Cell Mol Genet, 1984. **10**(5): p. 531-4.
277. Farrar, M.A. and R.D. Schreiber, *The molecular cell biology of interferon-gamma and its receptor.* Annual review of immunology, 1993. **11**: p. 571-611.
278. Gray, P.W., et al., *Expression of human immune interferon cDNA in E. coli and monkey cells.* Nature, 1982. **295**(5849): p. 503-8.
279. Ealick, S.E., et al., *Three-dimensional structure of recombinant human interferon-gamma.* Science, 1991. **252**(5006): p. 698-702.
280. Bach, E.A., M. Aguet, and R.D. Schreiber, *The IFN gamma receptor: a paradigm for cytokine receptor signaling.* Annual review of immunology, 1997. **15**: p. 563-91.
281. Jung, V., et al., *Human chromosomes 6 and 21 are required for sensitivity to human interferon gamma.* Proceedings of the National Academy of Sciences of the United States of America, 1987. **84**(12): p. 4151-5.
282. Valente, G., et al., *Distribution of interferon-gamma receptor in human tissues.* European journal of immunology, 1992. **22**(9): p. 2403-12.
283. Schindler, C., et al., *Interferon-dependent tyrosine phosphorylation of a latent cytoplasmic transcription factor.* Science, 1992. **257**(5071): p. 809-13.

284. Platanias, L.C., *Mechanisms of type-I- and type-II-interferon-mediated signalling.* Nature reviews. Immunology, 2005. **5**(5): p. 375-86.
285. Leonard, W.J. and J.J. O'Shea, *Jaks and STATs: biological implications.* Annu Rev Immunol, 1998. **16**: p. 293-322.
286. Imada, K. and W.J. Leonard, *The Jak-STAT pathway.* Mol Immunol, 2000. **37**(1-2): p. 1-11.
287. Kiu, H. and S.E. Nicholson, *Biology and significance of the JAK/STAT signalling pathways.* Growth Factors, 2012. **30**(2): p. 88-106.
288. Qu, H.Q., S.P. Fisher-Hoch, and J.B. McCormick, *Molecular immunity to mycobacteria: knowledge from the mutation and phenotype spectrum analysis of Mendelian susceptibility to mycobacterial diseases.* Int J Infect Dis, 2011. **15**(5): p. e305-13.
289. Krause, C.D., et al., *Preassembly and ligand-induced restructuring of the chains of the IFN-gamma receptor complex: the roles of Jak kinases, Stat1 and the receptor chains.* Cell Res, 2006. **16**(1): p. 55-69.
290. Greenlund, A.C., et al., *Ligand-induced IFN gamma receptor tyrosine phosphorylation couples the receptor to its signal transduction system (p91).* EMBO J, 1994. **13**(7): p. 1591-600.
291. Heim, M.H., et al., *Contribution of STAT SH2 groups to specific interferon signaling by the Jak-STAT pathway.* Science, 1995. **267**(5202): p. 1347-9.
292. Igaz, P., S. Toth, and A. Falus, *Biological and clinical significance of the JAK-STAT pathway; lessons from knockout mice.* Inflamm Res, 2001. **50**(9): p. 435-41.
293. Croker, B.A., H. Kiu, and S.E. Nicholson, *SOCS regulation of the JAK/STAT signalling pathway.* Semin Cell Dev Biol, 2008. **19**(4): p. 414-22.
294. Meraz, M.A., et al., *Targeted disruption of the Stat1 gene in mice reveals unexpected physiologic specificity in the JAK-STAT signaling pathway.* Cell, 1996. **84**(3): p. 431-42.
295. Sugawara, I., H. Yamada, and S. Mizuno, *STAT1 knockout mice are highly susceptible to pulmonary mycobacterial infection.* Tohoku J Exp Med, 2004. **202**(1): p. 41-50.
296. Baldridge, M.T., K.Y. King, and M.A. Goodell, *Inflammatory signals regulate hematopoietic stem cells.* Trends Immunol, 2011. **32**(2): p. 57-65.
297. Gil, M.P., et al., *Biologic consequences of Stat1-independent IFN signaling.* Proceedings of the National Academy of Sciences of the United States of America, 2001. **98**(12): p. 6680-5.
298. Blahoianu, M.A., et al., *IFN-gamma-induced IL-27 and IL-27p28 expression are differentially regulated through JNK MAPK and PI3K pathways independent of Jak/STAT in human monocytic cells.* Immunobiology, 2014. **219**(1): p. 1-8.
299. Goh, K.C., S.J. Haque, and B.R. Williams, *p38 MAP kinase is required for STAT1 serine phosphorylation and transcriptional activation induced by interferons.* The EMBO journal, 1999. **18**(20): p. 5601-8.
300. Takaoka, A., et al., *Protein tyrosine kinase Pyk2 mediates the Jak-dependent activation of MAPK and Stat1 in IFN-gamma, but not IFN-alpha, signaling.* The EMBO journal, 1999. **18**(9): p. 2480-8.
301. Gough, D.J., et al., *A novel c-Jun-dependent signal transduction pathway necessary for the transcriptional activation of interferon gamma response genes.* The Journal of biological chemistry, 2007. **282**(2): p. 938-46.

302. Alsayed, Y., et al., *IFN-gamma activates the C3G/Rap1 signaling pathway.* Journal of immunology, 2000. **164**(4): p. 1800-6.
303. Nguyen, H., et al., *Roles of phosphatidylinositol 3-kinase in interferon-gamma-dependent phosphorylation of STAT1 on serine 727 and activation of gene expression.* The Journal of biological chemistry, 2001. **276**(36): p. 33361-8.
304. Deb, D.K., et al., *Activation of protein kinase C delta by IFN-gamma.* Journal of immunology, 2003. **171**(1): p. 267-73.
305. Choudhury, G.G., *A linear signal transduction pathway involving phosphatidylinositol 3-kinase, protein kinase Cepsilon, and MAPK in mesangial cells regulates interferon-gamma-induced STAT1alpha transcriptional activation.* The Journal of biological chemistry, 2004. **279**(26): p. 27399-409.
306. Chang, Y.J., M.J. Holtzman, and C.C. Chen, *Interferon-gamma-induced epithelial ICAM-1 expression and monocyte adhesion. Involvement of protein kinase C-dependent c-Src tyrosine kinase activation pathway.* The Journal of biological chemistry, 2002. **277**(9): p. 7118-26.
307. Chang, Y.J., M.J. Holtzman, and C.C. Chen, *Differential role of Janus family kinases (JAKs) in interferon-gamma-induced lung epithelial ICAM-1 expression: involving protein interactions between JAKs, phospholipase Cgamma, c-Src, and STAT1.* Mol Pharmacol, 2004. **65**(3): p. 589-98.
308. Lamperi, S. and S. Carozzi, *Interferon-gamma (IFN-gamma) as in vitro enhancing factor of peritoneal macrophage defective bactericidal activity during continuous ambulatory peritoneal dialysis (CAPD).* American journal of kidney diseases : the official journal of the National Kidney Foundation, 1988. **11**(3): p. 225-30.
309. Calame, W., et al., *Effect of interferon-gamma in dialysis fluid on peritoneal defence in rats.* Nephrology, dialysis, transplantation : official publication of the European Dialysis and Transplant Association - European Renal Association, 1995. **10**(7): p. 1212-7.
310. Dasgupta, M.K., M. Larabie, and P.F. Halloran, *Interferon-gamma levels in peritoneal dialysis effluents: relation to peritonitis.* Kidney international, 1994. **46**(2): p. 475-81.
311. Robson, R.L., et al., *Differential regulation of chemokine production in human peritoneal mesothelial cells: IFN-gamma controls neutrophil migration across the mesothelium in vitro and in vivo.* Journal of immunology, 2001. **167**(2): p. 1028-38.
312. McLoughlin, R.M., et al., *Interplay between IFN-gamma and IL-6 signaling governs neutrophil trafficking and apoptosis during acute inflammation.* The Journal of clinical investigation, 2003. **112**(4): p. 598-607.
313. Enriquez, J., et al., *Peritonitis in continuous ambulatory peritoneal dialysis: cytokines in peritoneal fluid and blood.* Advances in peritoneal dialysis. Conference on Peritoneal Dialysis, 2002. **18**: p. 177-83.
314. Saed, G.M. and M.P. Diamond, *Effects of interferon-gamma reverse hypoxia-stimulated extracellular matrix expression in human peritoneal and adhesion fibroblasts.* Fertil Steril, 2006. **85 Suppl 1**: p. 1300-5.
315. Saed, G.M., et al., *Modulation of the BCL-2/BAX ratio by interferon-gamma and hypoxia in human peritoneal and adhesion fibroblasts.* Fertil Steril, 2008. **90**(5): p. 1925-30.

316. Kopf, M., et al., *Impaired immune and acute-phase responses in interleukin-6-deficient mice.* Nature, 1994. **368**(6469): p. 339-42.
317. McLoughlin, R.M., et al., *Interplay between IFN-gamma and IL-6 signaling governs neutrophil trafficking and apoptosis during acute inflammation.* J Clin Invest, 2003. **112**(4): p. 598-607.
318. Stylianou, E., et al., *Isolation, culture and characterization of human peritoneal mesothelial cells.* Kidney Int, 1990. **37**(6): p. 1563-70.
319. Topley, N., et al., *Human peritoneal mesothelial cell prostaglandin synthesis: induction of cyclooxygenase mRNA by peritoneal macrophage-derived cytokines.* Kidney Int, 1994. **46**(3): p. 900-9.
320. Reddel, R.R., et al., *Development of tumorigenicity in simian virus 40-immortalized human bronchial epithelial cell lines.* Cancer Res, 1993. **53**(5): p. 985-91.
321. VanSaun, M., et al., *Activation of Matrix Metalloproteinase-3 is altered at the frog neuromuscular junction following changes in synaptic activity.* Dev Neurobiol, 2007. **67**(11): p. 1488-97.
322. Lijnen, H.R., B. Van Hoef, and D. Collen, *Inactivation of the serpin alpha(2)-antiplasmin by stromelysin-1.* Biochim Biophys Acta, 2001. **1547**(2): p. 206-13.
323. Ueha, S., F.H. Shand, and K. Matsushima, *Cellular and molecular mechanisms of chronic inflammation-associated organ fibrosis.* Front Immunol, 2012. **3**: p. 71.
324. Ihn, H., *Pathogenesis of fibrosis: role of TGF-beta and CTGF.* Curr Opin Rheumatol, 2002. **14**(6): p. 681-5.
325. Wickert, L., et al., *Glucocorticoids activate TGF-beta induced PAI-1 and CTGF expression in rat hepatocytes.* Comp Hepatol, 2007. **6**: p. 5.
326. Schultz, G.S. and A. Wysocki, *Interactions between extracellular matrix and growth factors in wound healing.* Wound Repair Regen, 2009. **17**(2): p. 153-62.
327. Boudreau, N.J. and P.L. Jones, *Extracellular matrix and integrin signalling: the shape of things to come.* Biochem J, 1999. **339 (Pt 3)**: p. 481-8.
328. Lipkin, G.W., et al., *Hyaluronic acid metabolism and its clinical significance in patients treated by continuous ambulatory peritoneal dialysis.* Nephrol Dial Transplant, 1993. **8**(4): p. 357-60.
329. Yamagata, K., C. Tomida, and A. Koyama, *Intraperitoneal hyaluronan production in stable continuous ambulatory peritoneal dialysis patients.* Peritoneal dialysis international : journal of the International Society for Peritoneal Dialysis, 1999. **19**(2): p. 131-7.
330. Simpson, R.M., et al., *Age-related changes in pericellular hyaluronan organization leads to impaired dermal fibroblast to myofibroblast differentiation.* Am J Pathol, 2009. **175**(5): p. 1915-28.
331. Burrage, P.S., K.S. Mix, and C.E. Brinckerhoff, *Matrix metalloproteinases: role in arthritis.* Front Biosci, 2006. **11**: p. 529-43.
332. Foda, H.D. and S. Zucker, *Matrix metalloproteinases in cancer invasion, metastasis and angiogenesis.* Drug Discov Today, 2001. **6**(9): p. 478-482.
333. Bullard, K.M., et al., *Impaired wound contraction in stromelysin-1-deficient mice.* Ann Surg, 1999. **230**(2): p. 260-5.

334. Zhu, C.L., et al., *Serum levels of tissue inhibitor of metalloproteinase-1 are correlated with liver fibrosis in patients with chronic hepatitis B.* J Dig Dis, 2012. **13**(11): p. 558-63.
335. Osawa, Y., et al., *Tumor necrosis factor-alpha promotes cholestasis-induced liver fibrosis in the mouse through tissue inhibitor of metalloproteinase-1 production in hepatic stellate cells.* PLoS One, 2013. **8**(6): p. e65251.
336. Boeker, K.H., et al., *Diagnostic potential of circulating TIMP-1 and MMP-2 as markers of liver fibrosis in patients with chronic hepatitis C.* Clinica chimica acta; international journal of clinical chemistry, 2002. **316**(1-2): p. 71-81.
337. Luo, X.Y., et al., *IFN-gamma deficiency attenuates hepatic inflammation and fibrosis in a steatohepatitis model induced by a methionine- and choline-deficient high-fat diet.* Am J Physiol Gastrointest Liver Physiol, 2013. **305**(12): p. G891-9.
338. Gonzalez-Avila, G., et al., *Changes in matrix metalloproteinases during the evolution of interstitial renal fibrosis in a rat experimental model.* Pathobiology, 1998. **66**(5): p. 196-204.
339. Bailey, J.R., et al., *IL-13 promotes collagen accumulation in Crohn's disease fibrosis by down-regulation of fibroblast MMP synthesis: a role for innate lymphoid cells?* PLoS One, 2012. **7**(12): p. e52332.
340. Dang, C.M., et al., *Scarless fetal wounds are associated with an increased matrix metalloproteinase-to-tissue-derived inhibitor of metalloproteinase ratio.* Plast Reconstr Surg, 2003. **111**(7): p. 2273-85.
341. Poormasjedi-Meibod, M.S., et al., *Anti-scarring properties of different tryptophan derivatives.* PLoS One, 2014. **9**(3): p. e91955.
342. Luo, D.D., et al., *Interleukin-1 beta regulates proximal tubular cell transforming growth factor beta-1 signalling.* Nephrology, dialysis, transplantation : official publication of the European Dialysis and Transplant Association - European Renal Association, 2009. **24**(9): p. 2655-65.
343. Lin, C.Y., et al., *Persistent transforming growth factor beta 1 expression may predict peritoneal fibrosis in CAPD patients with frequent peritonitis occurrence.* Advances in peritoneal dialysis. Conference on Peritoneal Dialysis, 1997. **13**: p. 64-71.
344. Ha, H., et al., *Effects of peritoneal dialysis solutions on the secretion of growth factors and extracellular matrix proteins by human peritoneal mesothelial cells.* Peritoneal dialysis international : journal of the International Society for Peritoneal Dialysis, 2002. **22**(2): p. 171-7.
345. Qin, H., et al., *Transcriptional suppression of matrix metalloproteinase-2 gene expression in human astroglioma cells by TNF-alpha and IFN-gamma.* Journal of immunology, 1998. **161**(12): p. 6664-73.
346. Ma, Z., H. Qin, and E.N. Benveniste, *Transcriptional suppression of matrix metalloproteinase-9 gene expression by IFN-gamma and IFN-beta: critical role of STAT-1alpha.* Journal of immunology, 2001. **167**(9): p. 5150-9.
347. Page, C.E., et al., *Interferon-gamma inhibits interleukin-1beta-induced matrix metalloproteinase production by synovial fibroblasts and protects articular cartilage in early arthritis.* Arthritis research & therapy, 2010. **12**(2): p. R49.

348. Taga, T., *IL6 signalling through IL6 receptor and receptor-associated signal transducer, gp130.* Res Immunol, 1992. **143**(7): p. 737-9.
349. Wolf, J., S. Rose-John, and C. Garbers, *Interleukin-6 and its receptors: a highly regulated and dynamic system.* Cytokine, 2014. **70**(1): p. 11-20.
350. Novick, D., et al., *Soluble cytokine receptors are present in normal human urine.* J Exp Med, 1989. **170**(4): p. 1409-14.
351. Rose-John, S., *IL-6 trans-signaling via the soluble IL-6 receptor: importance for the pro-inflammatory activities of IL-6.* Int J Biol Sci, 2012. **8**(9): p. 1237-47.
352. Margetts, P.J., et al., *Inflammatory cytokines, angiogenesis, and fibrosis in the rat peritoneum.* The American journal of pathology, 2002. **160**(6): p. 2285-94.
353. Topley, N., et al., *Human peritoneal mesothelial cells synthesize interleukin-6: induction by IL-1 beta and TNF alpha.* Kidney international, 1993. **43**(1): p. 226-33.
354. Duncan, M.R. and B. Berman, *Gamma interferon is the lymphokine and beta interferon the monokine responsible for inhibition of fibroblast collagen production and late but not early fibroblast proliferation.* The Journal of experimental medicine, 1985. **162**(2): p. 516-27.
355. Strutz, F., et al., *Effects of pentoxifylline, pentifylline and gamma-interferon on proliferation, differentiation, and matrix synthesis of human renal fibroblasts.* Nephrology, dialysis, transplantation : official publication of the European Dialysis and Transplant Association - European Renal Association, 2000. **15**(10): p. 1535-46.
356. Giannopoulou, M., et al., *Distinctive role of Stat3 and Erk-1/2 activation in mediating interferon-gamma inhibition of TGF-beta1 action.* American journal of physiology. Renal physiology, 2006. **290**(5): p. F1234-40.
357. Matrisian, L.M., *Metalloproteinases and their inhibitors in matrix remodeling.* Trends Genet, 1990. **6**(4): p. 121-5.
358. Seeland, U., et al., *Myocardial fibrosis in transforming growth factor-beta(1) (TGF-beta(1)) transgenic mice is associated with inhibition of interstitial collagenase.* European journal of clinical investigation, 2002. **32**(5): p. 295-303.
359. Yan, C. and D.D. Boyd, *Regulation of matrix metalloproteinase gene expression.* J Cell Physiol, 2007. **211**(1): p. 19-26.
360. Massova, I., et al., *Matrix metalloproteinases: structures, evolution, and diversification.* FASEB journal : official publication of the Federation of American Societies for Experimental Biology, 1998. **12**(12): p. 1075-95.
361. Chakraborti, S., et al., *Regulation of matrix metalloproteinases: an overview.* Mol Cell Biochem, 2003. **253**(1-2): p. 269-85.
362. Nissinen, L. and V.M. Kahari, *Matrix metalloproteinases in inflammation.* Biochimica et biophysica acta, 2014. **1840**(8): p. 2571-2580.
363. Nagase, H. and J.F. Woessner, Jr., *Matrix metalloproteinases.* The Journal of biological chemistry, 1999. **274**(31): p. 21491-4.
364. Page-McCaw, A., A.J. Ewald, and Z. Werb, *Matrix metalloproteinases and the regulation of tissue remodelling.* Nature reviews. Molecular cell biology, 2007. **8**(3): p. 221-33.
365. Klein, T. and R. Bischoff, *Physiology and pathophysiology of matrix metalloproteases.* Amino Acids, 2011. **41**(2): p. 271-90.

366. Van Wart, H.E. and H. Birkedal-Hansen, *The cysteine switch: a principle of regulation of metalloproteinase activity with potential applicability to the entire matrix metalloproteinase gene family.* Proceedings of the National Academy of Sciences of the United States of America, 1990. **87**(14): p. 5578-82.
367. Kleiner, D.E., Jr. and W.G. Stetler-Stevenson, *Structural biochemistry and activation of matrix metalloproteases.* Curr Opin Cell Biol, 1993. **5**(5): p. 891-7.
368. Ra, H.J. and W.C. Parks, *Control of matrix metalloproteinase catalytic activity.* Matrix Biol, 2007. **26**(8): p. 587-96.
369. Brinckerhoff, C.E. and L.M. Matrisian, *Matrix metalloproteinases: a tail of a frog that became a prince.* Nature reviews. Molecular cell biology, 2002. **3**(3): p. 207-14.
370. Douglas, D.A., Y.E. Shi, and Q.A. Sang, *Computational sequence analysis of the tissue inhibitor of metalloproteinase family.* J Protein Chem, 1997. **16**(4): p. 237-55.
371. Baker, A.H., D.R. Edwards, and G. Murphy, *Metalloproteinase inhibitors: biological actions and therapeutic opportunities.* J Cell Sci, 2002. **115**(Pt 19): p. 3719-27.
372. Gomez, D.E., et al., *Tissue inhibitors of metalloproteinases: structure, regulation and biological functions.* European journal of cell biology, 1997. **74**(2): p. 111-22.
373. Bode, W., et al., *Insights into MMP-TIMP interactions.* Ann N Y Acad Sci, 1999. **878**: p. 73-91.
374. Reunanen, N., et al., *Enhancement of fibroblast collagenase (matrix metalloproteinase-1) gene expression by ceramide is mediated by extracellular signal-regulated and stress-activated protein kinase pathways.* The Journal of biological chemistry, 1998. **273**(9): p. 5137-45.
375. Asano, K., et al., *Tiotropium bromide inhibits TGF-beta-induced MMP production from lung fibroblasts by interfering with Smad and MAPK pathways in vitro.* Int J Chron Obstruct Pulmon Dis, 2010. **5**: p. 277-86.
376. Lim, H. and H.P. Kim, *Matrix metalloproteinase-13 expression in IL-1beta-treated chondrocytes by activation of the p38 MAPK/c-Fos/AP-1 and JAK/STAT pathways.* Arch Pharm Res, 2011. **34**(1): p. 109-17.
377. Koike, K., et al., *Protective role of JAK/STAT signaling against renal fibrosis in mice with unilateral ureteral obstruction.* Clin Immunol, 2014. **150**(1): p. 78-87.
378. Ma, Z., et al., *Interferon-gamma-activated STAT-1alpha suppresses MMP-9 gene transcription by sequestration of the coactivators CBP/p300.* Journal of leukocyte biology, 2005. **78**(2): p. 515-23.
379. Hosseini, M., et al., *IL-1 and TNF induction of matrix metalloproteinase-3 by c-Jun N-terminal kinase in trabecular meshwork.* Invest Ophthalmol Vis Sci, 2006. **47**(4): p. 1469-76.
380. Hess, J., P. Angel, and M. Schorpp-Kistner, *AP-1 subunits: quarrel and harmony among siblings.* J Cell Sci, 2004. **117**(Pt 25): p. 5965-73.
381. Fleenor, D.L., I.H. Pang, and A.F. Clark, *Involvement of AP-1 in interleukin-1alpha-stimulated MMP-3 expression in human trabecular meshwork cells.* Invest Ophthalmol Vis Sci, 2003. **44**(8): p. 3494-501.

382. Lewis, M., E.P. Amento, and E.N. Unemori, *Transcriptional inhibition of stromelysin by interferon-gamma in normal human fibroblasts is mediated by the AP-1 domain.* J Cell Biochem, 1999. **72**(3): p. 373-86.
383. Park, C.H., et al., *Heat shock-induced matrix metalloproteinase (MMP)-1 and MMP-3 are mediated through ERK and JNK activation and via an autocrine interleukin-6 loop.* J Invest Dermatol, 2004. **123**(6): p. 1012-9.
384. Reunanen, N., et al., *Enhancement of fibroblast collagenase (matrix metalloproteinase-1) gene expression by ceramide is mediated by extracellular signal-regulated and stress-activated protein kinase pathways.* J Biol Chem, 1998. **273**(9): p. 5137-45.
385. Minden, A. and M. Karin, *Regulation and function of the JNK subgroup of MAP kinases.* Biochimica et biophysica acta, 1997. **1333**(2): p. F85-104.
386. Ulloa, L., J. Doody, and J. Massague, *Inhibition of transforming growth factor-beta/SMAD signalling by the interferon-gamma/STAT pathway.* Nature, 1999. **397**(6721): p. 710-3.
387. Weng, H., et al., *IFN-gamma abrogates profibrogenic TGF-beta signaling in liver by targeting expression of inhibitory and receptor Smads.* Journal of hepatology, 2007. **46**(2): p. 295-303.
388. Jinnin, M., H. Ihn, and K. Tamaki, *Characterization of SIS3, a novel specific inhibitor of Smad3, and its effect on transforming growth factor-beta1-induced extracellular matrix expression.* Mol Pharmacol, 2006. **69**(2): p. 597-607.
389. Wang, X., et al., *Effects and relationship of ERK1 and ERK2 in interleukin-1beta-induced alterations in MMP3, MMP13, type II collagen and aggrecan expression in human chondrocytes.* Int J Mol Med, 2011. **27**(4): p. 583-9.
390. Kim, E.S., M.S. Kim, and A. Moon, *TGF-beta-induced upregulation of MMP-2 and MMP-9 depends on p38 MAPK, but not ERK signaling in MCF10A human breast epithelial cells.* Int J Oncol, 2004. **25**(5): p. 1375-82.
391. Gao, D. and C. Bing, *Macrophage-induced expression and release of matrix metalloproteinase 1 and 3 by human preadipocytes is mediated by IL-1beta via activation of MAPK signaling.* J Cell Physiol, 2011. **226**(11): p. 2869-80.
392. Zhang, X., I.H. Diab, and Z.E. Zehner, *ZBP-89 represses vimentin gene transcription by interacting with the transcriptional activator, Sp1.* Nucleic acids research, 2003. **31**(11): p. 2900-14.
393. Remington, M.C., et al., *ZBP-89, a Kruppel-type zinc finger protein, inhibits cell proliferation.* Biochemical and biophysical research communications, 1997. **237**(2): p. 230-4.
394. Zhang, C.Z., G.G. Chen, and P.B. Lai, *Transcription factor ZBP-89 in cancer growth and apoptosis.* Biochimica et biophysica acta, 2010. **1806**(1): p. 36-41.
395. Bai, L., et al., *ZBP-89-induced apoptosis is p53-independent and requires JNK.* Cell Death Differ, 2004. **11**(6): p. 663-73.
396. Ye, S., et al., *Human stromelysin gene promoter activity is modulated by transcription factor ZBP-89.* FEBS letters, 1999. **450**(3): p. 268-72.
397. Borghaei, R.C., G. Gorski, and M. Javadi, *NF-kappaB and ZBP-89 regulate MMP-3 expression via a polymorphic site in the promoter.* Biochemical and biophysical research communications, 2009. **382**(2): p. 269-73.

398. Bai, L., C. Logsdon, and J.L. Merchant, *Regulation of epithelial cell growth by ZBP-89: potential relevance in pancreatic cancer.* Int J Gastrointest Cancer, 2002. **31**(1-3): p. 79-88.
399. Borghaei, R.C. and M. Chambers, *Expression of transcription factor zinc-binding protein-89 (ZBP-89) is inhibited by inflammatory cytokines.* Pathol Lab Med Int, 2009. **1**: p. 7-12.
400. Wu, Y., et al., *Stat3 enhances vimentin gene expression by binding to the antisilencer element and interacting with the repressor protein, ZBP-89.* Oncogene, 2004. **23**(1): p. 168-78.
401. Brown, K.A., J.A. Pietenpol, and H.L. Moses, *A tale of two proteins: differential roles and regulation of Smad2 and Smad3 in TGF-beta signaling.* J Cell Biochem, 2007. **101**(1): p. 9-33.
402. Meng, X.M., et al., *Smad2 protects against TGF-beta/Smad3-mediated renal fibrosis.* Journal of the American Society of Nephrology : JASN, 2010. **21**(9): p. 1477-87.
403. Nakagawa, T., et al., *TGF-beta induces proangiogenic and antiangiogenic factors via parallel but distinct Smad pathways.* Kidney international, 2004. **66**(2): p. 605-13.
404. Yang, Y.C., et al., *Hierarchical model of gene regulation by transforming growth factor beta.* Proceedings of the National Academy of Sciences of the United States of America, 2003. **100**(18): p. 10269-74.
405. Kellenberger, T., et al., *Differential effects of Smad3 targeting in a murine model of chronic kidney disease.* Physiol Rep, 2013. **1**(7): p. e00181.
406. Patel, P., et al., *Smad3-dependent and -independent pathways are involved in peritoneal membrane injury.* Kidney international, 2010. **77**(4): p. 319-28.
407. Duan, W.J., et al., *Opposing Roles for Smad2 and Smad3 in Peritoneal Fibrosis in Vivo and in Vitro.* The American journal of pathology, 2014. **184**(8): p. 2275-84.
408. Alexander, J.P. and T.S. Acott, *Involvement of the Erk-MAP kinase pathway in TNFalpha regulation of trabecular matrix metalloproteinases and TIMPs.* Invest Ophthalmol Vis Sci, 2003. **44**(1): p. 164-9.
409. Kelley, M.J., et al., *p38 MAP kinase pathway and stromelysin regulation in trabecular meshwork cells.* Invest Ophthalmol Vis Sci, 2007. **48**(7): p. 3126-37.
410. Nakao, A., et al., *Identification of Smad7, a TGFbeta-inducible antagonist of TGF-beta signalling.* Nature, 1997. **389**(6651): p. 631-5.
411. Hayashi, H., et al., *The MAD-related protein Smad7 associates with the TGFbeta receptor and functions as an antagonist of TGFbeta signaling.* Cell, 1997. **89**(7): p. 1165-73.
412. Higashi, K., et al., *Interferon-gamma interferes with transforming growth factor-beta signaling through direct interaction of YB-1 with Smad3.* The Journal of biological chemistry, 2003. **278**(44): p. 43470-9.
413. Lockwood, C.J., et al., *Interferon gamma Protects First-Trimester Decidual Cells against Aberrant Matrix Metalloproteinase 1, 3, and 9 Expression in Preeclampsia.* The American journal of pathology, 2014.
414. Rifas, L. and S. Arackal, *T cells regulate the expression of matrix metalloproteinase in human osteoblasts via a dual mitogen-activated*

protein kinase mechanism. Arthritis and rheumatism, 2003. **48**(4): p. 993-1001.
415. Rougier, J.P., et al., *PAI-1 secretion and matrix deposition in human peritoneal mesothelial cell cultures: transcriptional regulation by TGF-beta 1.* Kidney Int, 1998. **54**(1): p. 87-98.
416. Jones, S., et al., *Bicarbonate/lactate-based peritoneal dialysis solution increases cancer antigen 125 and decreases hyaluronic acid levels.* Kidney Int, 2001. **59**(4): p. 1529-38.
417. Santibanez, J.F., et al., *Transforming growth factor-beta1 modulates matrix metalloproteinase-9 production through the Ras/MAPK signaling pathway in transformed keratinocytes.* Biochemical and biophysical research communications, 2002. **296**(2): p. 267-73.
418. Benbow, U. and C.E. Brinckerhoff, *The AP-1 site and MMP gene regulation: what is all the fuss about?* Matrix Biol, 1997. **15**(8-9): p. 519-26.
419. Cheon, H., et al., *Increased expression of pro-inflammatory cytokines and metalloproteinase-1 by TGF-beta1 in synovial fibroblasts from rheumatoid arthritis and normal individuals.* Clinical and experimental immunology, 2002. **127**(3): p. 547-52.
420. Buttice, G., S. Quinones, and M. Kurkinen, *The AP-1 site is required for basal expression but is not necessary for TPA-response of the human stromelysin gene.* Nucleic acids research, 1991. **19**(13): p. 3723-31.
421. Sirum-Connolly, K. and C.E. Brinckerhoff, *Interleukin-1 or phorbol induction of the stromelysin promoter requires an element that cooperates with AP-1.* Nucleic acids research, 1991. **19**(2): p. 335-41.
422. Tardif, G., et al., *Transforming growth factor-beta induced collagenase-3 production in human osteoarthritic chondrocytes is triggered by Smad proteins: cooperation between activator protein-1 and PEA-3 binding sites.* The Journal of rheumatology, 2001. **28**(7): p. 1631-9.
423. Ahmad, R., et al., *Inhibition of interleukin 1-induced matrix metalloproteinase 13 expression in human chondrocytes by interferon gamma.* Ann Rheum Dis, 2007. **66**(6): p. 782-9.
424. Ho, H.H., et al., *Lipopolysaccharide-induced expression of matrix metalloproteinases in human monocytes is suppressed by IFN-gamma via superinduction of ATF-3 and suppression of AP-1.* Journal of immunology, 2008. **181**(7): p. 5089-97.